The Institute of Paper Chemistry

Appleton, Wisconsin

Doctor's Dissertation

An Investigation of Mass Transfer Mechanisms in Ultrafiltration

Daniel R. Trettin

June, 1980

AN INVESTIGATION OF MASS TRANSFER MECHANISMS IN ULTRAFILTRATION

A thesis submitted by

Daniel R. Trettin

B.S.M.E. 1972, Marquette University
M.S. 1974, Lawrence University

in partial fulfillment of the requirements
of The Institute of Paper Chemistry
for the degree of Doctor of Philosophy
from Lawrence University,
Appleton, Wisconsin

June, 1980

TABLE OF CONTENTS

ACKNOWLEDGMENTS

I wish to thank the Board of Trustees and member companies for their support of The Institute of Paper Chemistry and of the graduate studies doctoral program.

The invaluable help of the Thesis Advisory Committee is gratefully acknowledged. Mahendra R. Doshi served as Chairman of the Advisory Committee and provided considerable guidance. His willingness to undertake numerous discussions from day-to-day, and his unique ability to remain optimistic at times when the light at the end of the tunnel was dim is, in no small part, recognized and appreciated. Peter E. Parker and Alexander Babchin, Advisory Committee members, also contributed greatly to the development of theory and interpretation of data.

Special gratitude is extended to Art Webb, George Dubey, and Jacquelyn Kern, who contributed of their valuable time in explaining instrument operation and laboratory techniques. John Carlson is recognized and thanked for providing his expertise in operating the instruments for diffusion coefficient determination. The combined efforts of Mary Block and Hilkka Kaustinen are also acknowledged in providing numerous electron micrographs of membranes.

The efforts of the Plant Engineering Department, in particular, Robert Rae and Lyle Dambruch, are appreciated. Their valuable assistance in the design of the parallel-plate ultrafiltration system contributed greatly. I wish to give special thanks to the team of Paul Van Rossum and Marvin Filz for the timely completion of the experimental ultrafiltration system and the much enjoyable nonpertinent discussion.

Recognition is given to the Editorial Department, in particular Byron Grow and Betty Dorman, for the preparation of the four manuscripts and numerous slides.

Finally, I would like to thank my wife, Diana, for her support, both psychological and financial, over the past three years. Her patience and kindness served as a constant inspiration at times when it was seldom reciprocated.

ABSTRACT

An inherent problem with all membrane separation processes is solute polarization upon the membrane surface. The net buildup of solute molecules in the region of the membrane severely limits permeate flux by thermodynamically decreasing the effective pressure gradient and by forming a gelatinous matrix structure upon the membrane surface when solute concentrations become large enough. This gel layer represents an additional hydraulic resistance to permeate flow and is characteristic of an operating region where flux is pressure independent.

Although more rigorous predictive models exist, the mainstay of the prediction of mass transfer in ultrafiltration continues to center around film theory. With the ultrafiltration of macromolecular solutions in cross flow systems, the prediction of flux rates employing film theory appears questionable. Additionally, when film theory is used in the prediction of colloidal ultrafiltration rates, the experimental flux is often found to be one to two orders of magnitude greater than theoretical prediction. Thus, there is a need to improve our understanding of mass transfer mechanisms in ultrafiltration.

The objectives of this study are:

(1) To determine the validity of the film theory model by comparison with a more exact theory and with experimental data.

(2) To develop a theory which would explain the vast differences between the two apparently similar processes of macromolecular and colloidal ultrafiltration.

(3) To contribute to the basic understanding of the low polarization (pregel) and gel-polarized regions in macromolecular ultrafiltration. The determination of when an ultrafiltration process is osmotic pressure limited and when it is gel limited would be useful.

An integral method solution to the convective diffusion equation was developed for both the unstirred batch cell and cross-flow, parallel-plate (rectangular cross section) geometries. Comparison of predicted values of permeate flux from the closed-form integral method solution was made with the numerical solution to the simplified convective diffusion equation. Agreement was excellent with a difference in predicted flux less than 1%, whereas the widely used film theory deviates considerably from the exact numerical solution.

A well-defined, unstirred batch cell system was used with aqueous bovine serum albumin (BSA) solutions to test the integral method model along with the film theory analogy for the batch cell. Results indicate that the integral method model represents a superior approach to the prediction of permeate flux over that of the film theory model. It is also shown that the assumption of concentration-independent diffusivity is reasonable in such systems. Gel-polarized behavior in the ultrafiltration of BSA was shown to occur only above system pressures of 6.89×10^5 N/m^2 (100 psi).

A unifying model for the batch cell was developed that yielded, in limiting cases, accurate mathematical models for both macromolecular and colloidal ultrafiltration. It was shown that in colloidal ultrafiltration, solvent permeation is dependent upon classical filtration principles where appreciable solute accumulation occurs at the membrane surface and solute back diffusion is negligible. In macromolecular ultrafiltration, the direct opposite is true, and the process is diffusion limited. The model was confirmed experimentally with the ultrafiltration of polymer latex in the unstirred batch cell. The concept was extended to the more practical parallel-plate system, where it was further reinforced that permeate flux indeed follows classical filtration principles for colloidal ultrafiltration.

Through the interpretation of batch cell data for aqueous macromolecular solutions of polyvinyl alcohol, Carbowax 20M (polyethylene oxide), and carboxymethylcellulose, it was shown that the ultrafiltration model which was developed primarily for the gel-polarized region may have definite application to the pregel region as well. Specifically, the assumption of constant wall concentration (an osmotic equivalent) may be reasonable with certain limitations in the pregel region. This broadening of the applicability of the macromolecular ultrafiltration model increases its value greatly as a predictive tool and has contributed additional understanding as to when an ultrafiltration process is gel or osmotic pressure limited. Existing literature data were interpreted in terms of this model, and agreement of theoretically predicted flux to experimental flux was very good for the parallel plate geometry.

Solute-solute and solute-membrane interactions were not considered. It is believed that although phenomena such as solute adsorption upon the membrane surface and solute dimerization may exist, their effect upon the system is secondary. It is suggested that future work along this line be considered to confirm the assumption.

The format of this thesis is organized into seven sections. Section 1 presents a general literature review and an overall definition of the problem. Sections 2 through 5 are four manuscripts detailing the solution to the problem. Section 6 includes a general summary and discussion of results as well as suggestions for future work. Section 7 contains supplementary information in the form of appendixes.

SECTION 1 - GENERAL LITERATURE REVIEW

GENERAL INTRODUCTION

APPLICATIONS OF MEMBRANE SEPARATION PROCESSES

The recognition of the semipermeable nature of certain membranes, both natural and synthetic, has given rise to the utilization of a new separation technique for the chemical process industry. Although the existence of semipermeable membranes can be traced back to their use by Abbé Nollet in 1748 [Dejmek (1975)], large scale industrial use of reverse osmosis membranes was initiated around 1960 with the first high flux membranes developed by Loeb and Sourirajan (1960). The major advantage of reverse osmosis and its closely related sister process of ultrafiltration is that they allow the separation of solutions on a molecular level. An additional attractive feature is that membrane processes facilitate the concentration, purification, or separation of molecular species without relying upon a phase change of the solvent. This aspect represents sizable energy savings and is particularly useful for the treatment of process streams where the product may be temperature sensitive. Membrane separation techniques also offer the unique ability to fractionate process streams on the basis of molecular size to a very high degree of discrimination [Baker (1969)].

The process of reverse osmosis has been studied extensively over the past 20 years and is reasonably well understood. Reverse osmosis is used primarily in the separation of low molecular weight solutions such as sea and brackish water desalination. Ultrafiltration, which differs from reverse osmosis in that solvent permeates through the membrane structure by virtue of pore flow rather than diffusion, lends itself to the separation of chemical species of molecular weight greater than 5000. This is due primarily to the relatively open structure of the porous membrane, and separation is achieved upon the principle of steric exclusion. Separation in reverse osmosis is achieved due to large differences in diffusion rates between

solvent and solute through the membrane. The major difference between ultrafiltration and conventional filtration is the size of the solute or suspended solid material being filtered. The processes of reverse osmosis and ultrafiltration are compared with respect to separation mechanism and solute size range in Fig. 1.

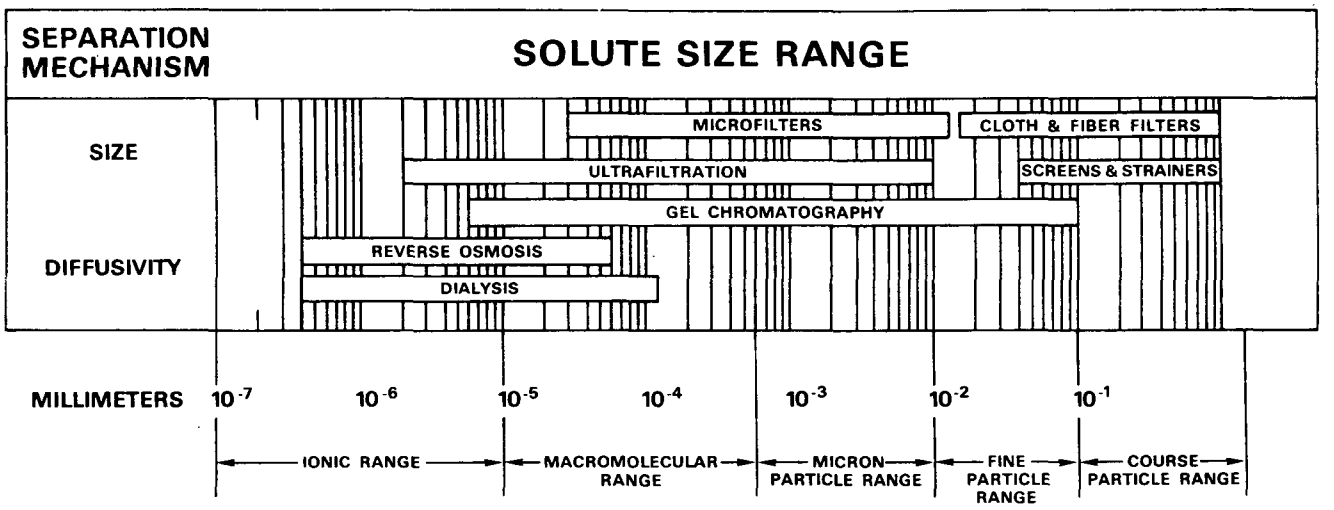

Figure 1. Membrane Separation Processes (Dorr-Oliver, Stamford, Conn., Copyright 1969).

As a molecular solution is pressurized over a selective membrane, solvent permeates through while rejected solute accumulates in the vicinity of the membrane. The net result is a layer of solution adjacent to the membrane surface of substantially greater solute concentration than that of the bulk solution within the cell. The phenomenon is termed "concentration polarization." Concentration polarization always operates to reduce the efficiency of the ultrafiltration process. It does so by thermodynamically decreasing the effective pressure gradient, and when solute concentrations become large enough, by forming a gelatinous matrix structure upon the membrane surface. This gel layer formation corresponds to the attainment of the solubility limit of the solution. The gel layer is effectively an additional hydraulic resistance to solvent flow and represents a region where permeate flux is pressure independent.

The realm of membrane separation techniques that are currently applied to industrial processes is indeed large. With increasing knowledge of transport phenomena in such systems, new and viable applications are found every day. Originally, membranes were cast from cellulose acetate solutions [Sourirajan (1970), Kesting (1977), Merten (1966)]. Cellulose acetate membranes, however, are of limited use due to the chemical properties of the cellulose itself. Cellulose acetate membranes can only be used with aqueous solutions since organic solvents either dissolve or plasticize the membrane to the point of collapse. When cellulose acetate membranes are allowed to dry out, they consolidate and lose their permeability. Operating temperatures above 60°C also facilitate membrane collapse. Because of the chemical nature of cellulose, it is sensitive to hydrolysis at low and high pH and subject to bacterial attack [Michaels (1968)]. Recently, techniques have been developed for manufacturing asymmetric membranes from a variety of synthetic polymers. Materials such as polyamide [Blais (1977)], sulfonated polyphenylene oxide (SPPO) [La Conti (1977)], polybenzimidazole (PBI) [Model, et al. (1977)], and polysulfone-polyethylenimine laminates [Rozelle, et al. (1977)]. Yasuda (1977) has recently performed numerous experiments with composite membranes formed by plasma polymerization. The scope of possible combinations of membrane materials seems only to be limited by the imagination of creative organic chemists. These new synthetic polymer membranes exhibit thermal, chemical, and physical properties far superior to their cellulose acetate predecessors. This added versatility makes the use of membrane separations attractive to many chemical process applications. Not only has the basic composition of membranes evolved over the past few years but also the basic geometry of the systems. Initially, reverse osmosis and ultrafiltration systems were of the tubular or plate-and-frame type design. Currently, hollow fiber and spiral wound configurations are quite common [Orofino (1977), Caraccilo, et al. (1977), Kremen (1977)]. These systems offer the advantage of enclosing large membrane surface areas in a relatively small volume.

Early development of commercial reverse osmosis systems was sparked by an interest of the United States Office of Saline Water (OSW). With the motive of developing an efficient and economic method of seawater and brackish water desalination, the OSW subsidized numerous research efforts during the 1960's and early 1970's. During the same period in Europe, the main objective of reverse osmosis research was to accommodate the sugar industry in finding new methods of juice purification, concentration, and molasses exhaustion [Madsen (1977)].

Additional uses of reverse osmosis in industrial applications are: radioactive laundry water concentration, steam generator blowdown water, separation of oil-water emulsions, acid mine drainage, electroplating waste treatment, hospital waste, municipal waste, ion exchange regenerant, lactose concentration, and fruit juice and food concentration [Stana (1977), Colomb (1977), Besik (1977), and Von Bockelmann, et al. (1977)]. Bansal and Wiley (1977) and Wiley (1972) studied the use of reverse osmosis technology in the pulp and paper industry for the treatment of pulping and various other waste streams.

In general, ultrafiltration applications have been accepted more quickly into industry than have reverse osmosis uses. This is due to the fact that while reverse osmosis has strong competition from evaporation techniques, ultrafiltration often enables the separation of new products from liquid wastes. As a rule, however, ultrafiltration cannot be shown to be economical unless some end use can be derived from both the concentrate and permeate solutions. Currently, ultrafiltration is being successfully used in the dairy industry [Madsen (1977), Delaney & Donnelly (1977), and Lee & Merson (1976)]; electrocoat paint industry [Stana (1977)]; pharmaceutical industry [Walker (1979), Wang, et al. (1968)]; and textile industry [Walker (1979), Hoffman (1979)]. Most recently, the pulp and paper industry has explored the feasibility of using ultrafiltration as a viable method to separate and

fractionate lignosulfonic acids from sulfite pulping liquors. These acids are used for concrete additives, drilling mud dispersants, binders in pelletization processes, dye-stuff dispersants, leather tanning, particle board binders, and the manufacture of vanillin [Lonsky (1980)]. Ultrafiltration represents an excellent replacement for gel separation techniques and is currently being used by Scott Paper Company, Georgia-Pacific Corporation, and Reed Lignin Products for lignosulfonic acid recovery [Walker (1979)]. It is rapidly becoming realized that as unusual separation problems arise, ultrafiltration represents both an economic and efficient alternative to conventional processes.

TRANSMEMBRANE MASS TRANSPORT

The processes of reverse osmosis and ultrafiltration may both be divided into two distinct regions of mass transfer interest. These two regions may be best explained in terms of the unstirred batch cell shown in Fig. 2.

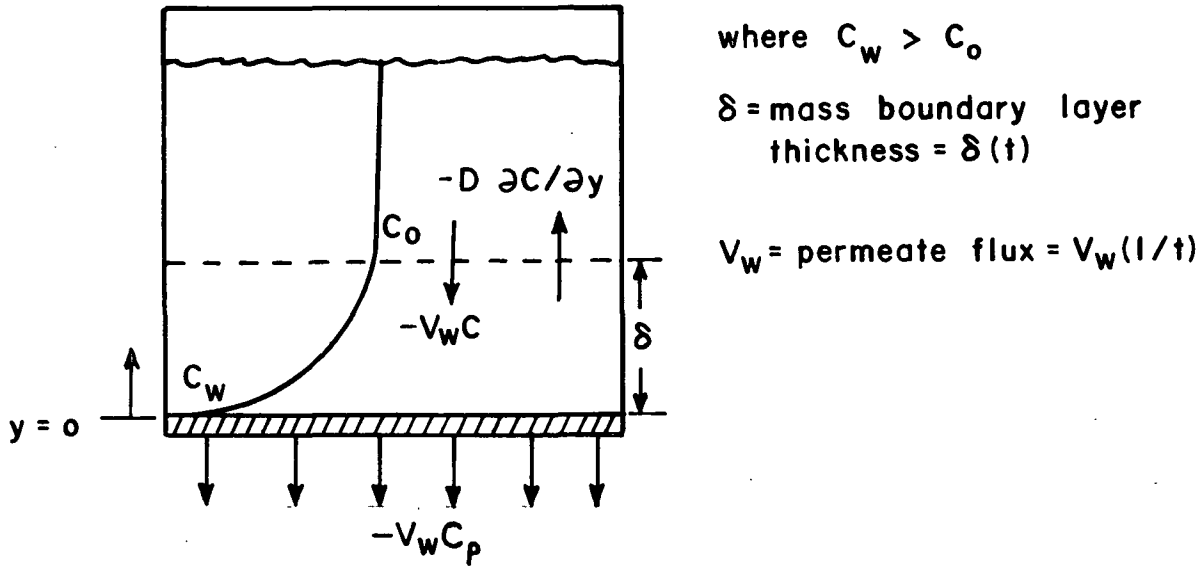

Figure 2. Membrane separations in an unstirred batch cell.

The first region is concerned with the mass transfer aspects of the liquid phase ($y \geq 0$), in particular, the convection of solute to the y = 0 plane and the

corresponding back diffusion of solute from the polarized layer toward the $y = \delta$ plane. Considerable theoretical work has been done concerning this region and shall be discussed in the following section.

The second region of interest involves the mechanism of solute and solvent passage through the membrane itself ($y < 0$). This second region has been the subject of numerous reviews, some of which are Johnson, et al. (1966), Merten (1966), Sourirajan (1977), and Kesting (1977). The study of this area, which is basically physicochemical in nature, is complicated, and agreement of theory is seldom found among researchers. The format of this section will be to present a very simplified analysis of some of the various proposed mechanisms. Clearly, any complete analysis of membrane separations should involve the combined modeling of both regions, coupled through the physical requirement of species continuity, into a composite transport theory. There currently does not exist a suitable model to explain transmembrane flux phenomena completely for reverse osmosis membranes.

One of the first theories dealing with mass transport through reverse osmosis membranes was formulated by Reid and Breton (1959). To explain this phenomenon, they postulated two different mechanisms for the transport of water and ions through cellulose acetate membranes. Those ions and molecules which are not able to hydrogen bond with the membrane are transferred by hole-type diffusion. This hole-type diffusion is inversely related to the amount of bound water within the membrane. These ions and molecules that are able to associate with the membrane (e.g., H_2O) are transported through by alignment-type of diffusion. The alignment-type mechanism is essentially the formation and dissolution of hydrogen bonds between the H_2O molecules and the cellulose acetate molecules. Obviously, the rate of water diffusion through the membrane will be dependent upon the rate of this occurrence. The membrane is treated as essentially nonporous. This permeation mechanism is similar to that proposed by Ticknor (1958).

Sourirajan (1963, 1977), and Sourirajan and Matsuura (1977, 1977*) have proposed a transport theory where the membrane was treated as being heterogeneous, that is, a solid fraction with a dispersed, vertical pore structure. Sourirajan postulated the system shown in Fig. 3 where water is preferentially sorbed by the membrane material and essentially forms a pure water layer of thickness t over the membrane. Permeation occurs from the continuous pore flow of this pure solvent layer through open capillaries in the membrane. The postulated mechanism of separating fresh water from aqueous salt solutions involves a system of four parameters: (1) the nature of the solution, (2) the nature of the film surface in contact with the solution, (3) the critical diameter of the pores in the film, and (4) the optimum pressure necessary to effect the continuous flow of the interfacial liquid through the pores at the optimum rate without incurring unacceptable salt transport. The first two parameters determine the thickness of the pure solvent interface upon which the third parameter depends. The fourth parameter depends on the size, number, and distribution of the pores on the surface as well as the physical internal structure of the pores. This model, however, has various shortcomings, one of which is that it has been shown that salt permeability is independent of salt concentration [Lonsdale, et al. (1965)]. Sourirajan's model predicts a concentration dependent salt permeability.

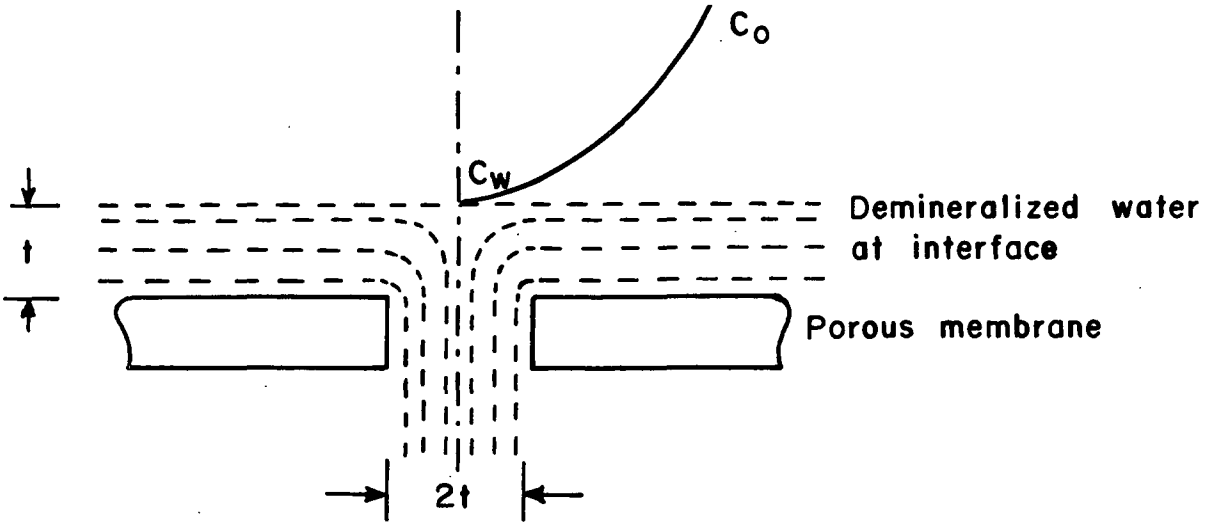

Figure 3. Sourirajan (1963) model for transport through reverse osmosis membranes.

Lonsdale, et al. (1964) calculated the diffusion coefficient for water through a cellulose acetate membrane and found that the value was only slightly smaller than the self-diffusion coefficient of water and other liquids. Based upon this finding, they concluded that the diffusion of water through a cellulose acetate membrane was more closely approximated as liquid-in-liquid diffusion rather than liquid diffusion through a solid as proposed by Reid and Breton. About the same time, Sharples (1963) postulated, based upon his experiments, that the salt flux through the membrane was due entirely to pore flow. Michaels et al. (1965) analyzed the results of the Lonsdale simplification of the actual phenomena of transport. They postulated the following approximate mechanisms to explain solute flow through reverse osmosis membranes:

(1) Water transport occurs predominantly by molecular diffusion through the polymer matrix.

(2) Ion transport appears to take place by three parallel flow mechanisms:
   (a) by sorption and diffusion of ions within the polymer matrix, governed solely by the ion-concentration gradient across the membrane
   (b) by pressure-biased activated diffusion of ions in near-molecular-sized pores in the membrane, governed by both the hydraulic gradient and the ion concentration difference
   (c) by hydrodynamic flow of saline solution through larger pores

(3) The high desalination efficiency of cellulose acetate reverse osmosis membranes is due largely to the high concentration and high diffusivity of water in the polymer and the low concentration and low diffusivity of ionic solutes.

Various simplifications to the Michaels', et al. model have been made by Sherwood, et al. (1967) and Kimura and Sourirajan (1967), as reviewed by Gill, et al.

(1971). Experimental confirmation agrees reasonably well with theory. Based upon their results, it is generally assumed by most current researchers in the field that water transport through a reverse osmosis membrane is primarily due to diffusion, whereas solute flux occurs by some type of convective pore flow.

Some very recent work by Bhattacharyya and his coworkers at the University of Kentucky [Grieves, et al. (1973), Bhattacharyya, et al. (1974), (1979)], has shown that it is possible to obtain excellent separations of ionic solutes of very low molecular weight with charged ultrafiltration membranes of a large pore diameter. This finding gives credibility to the original hypothesis of Sourirajan (1963) involving the interfacial fluid theory. It is suspected that the controversy as to the actual transport mechanism will continue for some time in the future.

Concerning the mechanism of transport through ultrafiltration membranes, which are substantially more porous than reverse osmosis membranes, there is little controversy among researchers that the principal mode is pore flow. Solute rejection is due to the prohibition of the solute molecules from entering the pore due to their relative size (screening mechanism). Solvent and solute molecules which are able to enter the pore pass through in essentially Poiseuille-type flow. It is therefore possible to describe the flow mechanism by the following phenomenological equation:

$$\left| v_w \right| = \frac{\Delta P - \Delta \Pi}{\mu \ (R_m + R_g)} \qquad (1)$$

where

$\left| v_w \right|$ = permeate volumetric flux (cm^3/cm^2-sec)

ΔP = applied pressure gradient (N/m^2)

$\Delta \pi = \pi_w - \pi_p$ = solution osmotic pressure at the membrane surface concentration - solution osmotic pressure at the permeate concentration (N/m^2)

R_m, R_g = hydraulic resistance of membrane, gel layer respectively (1/cm)

μ = solvent viscosity $\frac{(N\text{-sec})}{(m^2)}$

It is reasonable to assume that phenomena such as solute adsorption upon the membrane surface, solute dimerization, and electrokinetic effects between the membrane and solute may influence the transport of solvent. To my knowledge, there has not been any quantitative study performed in order to ascertain the order of magnitude of these effects. However, preliminary studies are planned by A. S. Michaels at Stanford University [Michaels (1979)]. For lack of a more accurate theory incorporating these additional phenomena, it is assumed in this thesis that Eq. (1) is valid in describing transport of solvent through an ultrafiltration membrane.

SOLUTION SIDE MASS TRANSPORT

The study of solution side mass transfer in membrane separations has been significantly more popular than transmembrane mass transfer. Essentially, decoupled from membrane electrokinetic effects, the problem reduces to that of solving the general convective diffusion equation for the appropriate boundary and initial conditions. The majority of membrane mass transfer research has been performed over the past 20 years, with the bulk of brine-side reverse osmosis study done between the years 1960-1970 under the support of the OSW. The amount of research which has been done since 1970 concerning reverse osmosis has been relatively small. Since the primary interest of this thesis is the study of mass transfer mechanisms in ultrafiltration, an in-depth literature review of reverse osmosis work will not be given. An excellent review of mass transfer theory prior to 1970 in reverse osmosis is given by Gill, et al. (1971) for both laminar and turbulent flow regimes.

In contrast to reverse osmosis research, the subject of ultrafiltration began to become active in the literature around 1968 and has continued to remain so. The format of this section will be to review some of the more pertinent research efforts regarding ultrafiltration and analyze the current state of the art.

From the general definition of concentration polarization given previously, it can be seen that, theoretically, concentration polarization in reverse osmosis processes should not differ from the same phenomenon in ultrafiltration. However, when one considers the ultrafiltration of macromolecular solutions, the added complications of concentration-dependent viscosity and diffusivity may become important. Many of the constant property simplifications used in the fundamental theories of concentration polarization in reverse osmosis may not be applicable to macromolecular ultrafiltration. One important practical difference between the two processes is the occurrence of the pressure-independent flux region found in macromolecular ultrafiltration.

Two of the earliest attempts to explain the pressure independent flux behavior in the ultrafiltration of macromolecular solutions were performed by Bixler, et al. (1968) and Michaels (1968). Their initial research was further developed and expanded upon in the subsequent work of Blatt, et al. (1970) and Porter (1972). The collective efforts of these four groups is generally referred to as the "Amicon School." The major concept of their theory is that of the formation of a solute gel layer upon the membrane surface. Predicated upon the assumption of negligible solute osmotic pressure, if the total convective flux of solute toward the membrane exceeds the back diffusional and convective flux away from the membrane, the solute concentration at the membrane surface will increase. Eventually the solubility limit or gel concentration will be reached where further increase of solute concentration at the membrane surface is not possible. Instead, the thickness of the concentrated gel layer will increase. This layer offers an additional hydraulic resistance to solvent flow which is additive to the existing membrane resistance. A subsequent increase in applied pressure does not appreciably increase solvent flux since momentary increases in flux only serve to add to the thickness of the gel layer.

Therefore, the process is self-limiting, and where gel polarization is reached, diffusive back-transport of solute cannot be further increased.

Before discussing the development of the film theory model, it would be advantageous to simplify the general convective diffusion equation in a manner consistent with the basic assumptions made in this thesis. This procedure will clarify the starting equations used in each of the manuscripts presented.

Consider the equation of continuity and general convective diffusion equation for a binary mixture

$$\frac{\partial \rho}{\partial t} + (\nabla \cdot \rho \hat{v}) = 0 \tag{2}$$

$$\frac{\partial c}{\partial t} + (\nabla \cdot c \hat{v}) = \nabla \cdot [\rho D \nabla (c/\rho)] \tag{3}$$

where $\hat{v}$ = velocity vector = $ui + vj + wk$

When constant values of ρ and D are assumed, Eq. (3) may be simplified to:

$$\hat{v} \cdot (\nabla c) = D \nabla^2 c \tag{4}$$

for the steady state case. Writing Eq. (4) in scalar form for the parallel-plate geometry,

$$u \, \partial c/\partial x + v \, \partial c/\partial y = D \left[\partial^2 c/\partial y^2 + \partial^2 c/\partial x^2 \right] \tag{5}$$

noting that a concentration gradient does not exist in the z-direction. It may be additionally shown from an order of magnitude analysis that since

$$\delta << h, \text{ the channel half height,} \tag{6}$$

therefore,

$$\partial^2 c/\partial y^2 >> \partial^2 c/\partial x^2 \tag{7}$$

Finally, Eq. (5) may be written as

$$u\,\partial c/\partial x + v\,\partial c/\partial y = D\,\partial^2 c/\partial y^2 \tag{8}$$

where the boundary conditions of

$$\begin{aligned} y = 0,\ c &= c_w \\ y \geq \delta,\ c &= c_o \end{aligned} \tag{9}$$

$$\begin{bmatrix} -v_w c_w \end{bmatrix} = \begin{bmatrix} -D \left.\frac{\partial c}{\partial y}\right|_{y=o} \end{bmatrix} + \begin{bmatrix} -v_w c_p \end{bmatrix}$$

$$\begin{bmatrix} \text{convective flux} \\ \text{toward membrane} \end{bmatrix} \quad \begin{bmatrix} \text{diffusive flux} \\ \text{from membrane} \end{bmatrix} \quad \begin{bmatrix} \text{convective flux} \\ \text{from membrane} \end{bmatrix}$$

apply.

Equation (8) represents the general convective diffusion equation as applied to ultrafiltration in a parallel plate system where the assumptions of constant solution density and diffusion coefficient are made.

Essentially, the "Amicon School" applied film theory principles to the process of ultrafiltration. That is, with the assumptions of concentration-independent diffusion coefficient and negligible effects of density variations, they employed the unrealistic concept of assuming a thin interfacial fluid layer in which no axial convection exists and across which all transport occurs. As applied to ultrafiltration, film theory postulates the presence of a stagnant film of solution bounded by the membrane on one side, a region of uniform concentration at the opposite side, and in which transverse convection exists. The transport process between the film's boundaries is assumed to be only in the y-direction but the film thickness, δ, is permitted to vary with axial position, x, in such a manner as to account approximately for the actual axial convection [Derzansky (1973)]. The advantage of this approach is that the explicit axial velocity dependence ($u\,\frac{\partial c}{\partial x}$) which appears in the

convective diffusion equation may be accounted for implicitly through the definition of the mass transfer coefficient. A diagram of the film theory approach is shown in Fig. 4 for a cross flow type system. The use of the film theory approach should only be considered as an approximate method.

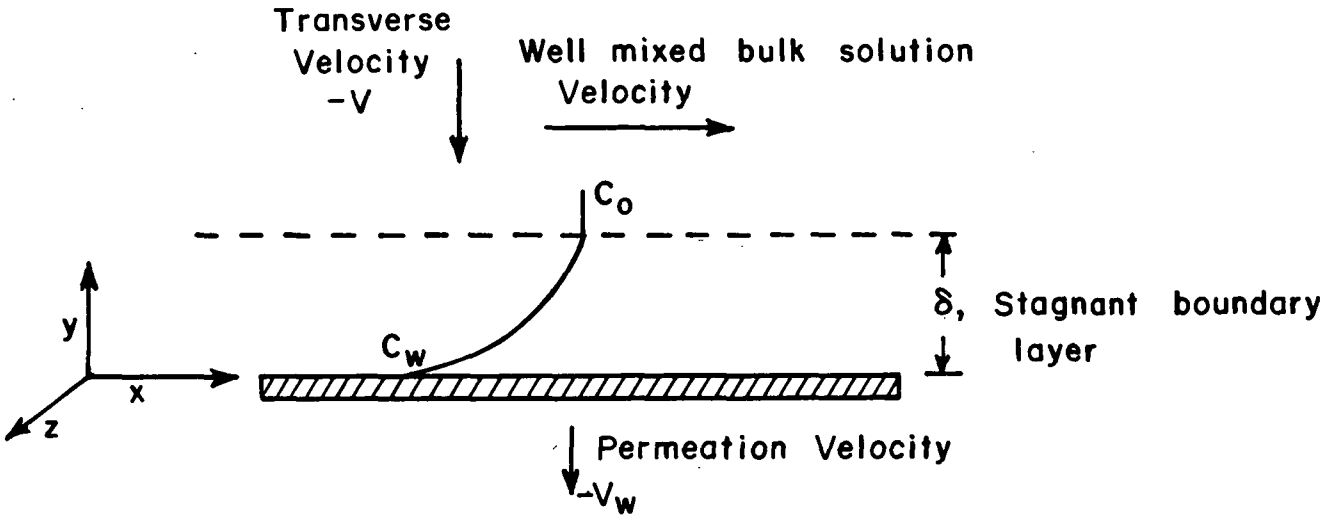

Figure 4. Film theory model [Blatt, et al. (1970)].

The derivation of the film theory model is as follows for the general case: consistent with the film theory model, axial convection is neglected within the film and Eq. (8) becomes

$$v \frac{\partial c}{\partial y} = D \, \partial 2c/\partial y2 \tag{10}$$

Upon integration with respect to y, assuming $v = -|v_w| = v_w$, and substitution of appropriate boundary conditions [Eq. (9)]

$$\frac{c - c_o}{c_w - c_p} = \exp\left[-\frac{|v_w| y}{D}\right] - \exp\left[-\frac{|v_w| \delta}{D}\right] \tag{11}$$

Evaluating Eq. (11) at y = 0 yields

$$|v_w| = \frac{D}{\delta} \ell n \left[\frac{c_w - c_p}{c_o - c_p}\right] \tag{12}$$

To establish a relationship for the quantity D/δ, let us recall the definition of the mass transfer coefficient k:

$$k = \frac{-D \left.\frac{\partial c}{\partial y}\right|_{y=0}}{c_w - c_o} \tag{13}$$

It is generally assumed in the film theory analysis that since the mass boundary layer δ is very small, the term $D \left.\frac{\partial c}{\partial y}\right|_{y=0}$ may be approximated by the relationship $D\left[\frac{c_w - c_o}{\delta}\right]$ and

$$k = \frac{D\left[\frac{c_w - c_o}{\delta}\right]}{c_w - c_o} = \frac{D}{\delta} \tag{14}$$

therefore,

$$\left| v_w \right| = k \, \ell n \left[\frac{c_w - c_p}{c_o - c_p}\right] \tag{15}$$

where $\left| v_w \right|$ and k represent the local permeate volumetric flux and local mass transfer coefficient, respectively. Equation (15) is the general film theory solution which applies to all ultrafiltration systems where δ is much smaller than the hydraulic diameter [i.e., if δ/d_h is very small, the effect of system curvature may be neglected and nonrectangular systems reduce to Eq. (15)]. The value of k is characteristically found by assuming that the interaction of axial convection with transverse diffusion in ultrafiltration systems is not substantially affected by the presence of a small transverse velocity. Equation (8) is therefore solved for the appropriate boundary conditions neglecting the transverse convection term. For example, consider the parallel plate system (rectangular flow channel) in fully developed laminar flow. The method of solution is analogous to the Leveque solution [Bird, et al. (1960)] in heat transfer where constant shear stress in the thin boundary layer and constant fluid properties are assumed.

Considering the axial convective term in Eq. (9) only and assuming the constant wall concentration boundary condition (at $y=0$, $c=c_w$), we may write,

$$u \frac{\partial c}{\partial x} = D \left(\frac{\partial^2 c}{\partial y^2}\right) \tag{16}$$

and let, $u = \frac{3 \langle u \rangle}{h} y = a\, y$ = linearized Poiseuille velocity profile

$$a\, y \frac{\partial c}{\partial x} = D \left(\frac{\partial^2 c}{\partial y^2}\right) \tag{17}$$

Introducing the similarity transformation, η, where

$$\eta = y/\phi \quad \text{and,}$$

$\phi = \phi\ (x)$ = an arbitrary thickness which is a function of x, axial distance

Transforming Eq. (17), $c\ (x,y) \Rightarrow c\ (\eta)$, yields

$$- \eta^2 \left(\frac{a}{D} \phi^2 \frac{\partial \phi}{\partial x}\right) \frac{\partial c}{\partial \eta} = \frac{\partial^2 c}{\partial \eta^2} \tag{18}$$

In order for $c = c\ (\eta)$ only, $\frac{a}{D} \phi^2 \frac{\partial \phi}{\partial x}$ = constant

let

$$\frac{a}{D} \phi^2 \frac{\partial \phi}{\partial \eta} = 1 \tag{19}$$

therefore, integrating, noting that at $x = 0$, $\phi = 0$,

$$\phi = \left(\frac{3Dx}{a} + C_1\right)^{1/3} = \left(\frac{3Dx}{a}\right)^{1/3} \tag{20}$$

and Eq. (18) reduces to

$$-\eta^2 \frac{dc}{d\eta} = \frac{d^2c}{d\eta^2} \tag{21}$$

Integrating Eq. (21) where the appropriate boundary conditions are

$$\eta = 0, \; c = c_w$$

$$\eta = \infty, \; c = c_o$$

yields

$$\frac{dc}{d\eta} = \frac{(c_o - c_w) \exp(-\frac{1}{3}\eta^3)}{\int_0^\infty \exp(-\frac{1}{3}\eta^3) \, d\eta} \tag{22}$$

$$\frac{c - c_w}{c_o - c_w} = \frac{\int_0^\eta \exp(-\frac{1}{3}\eta^3) \, d\eta}{\int_0^\infty \exp(-\frac{1}{3}\eta^3) \, d\eta} \tag{23}$$

Evaluating k,

$$k = \frac{-D \frac{\partial c}{\partial y}\Big|_{y=0}}{c_w - c_o} = \frac{-D \frac{dc}{d\eta}\Big|_{\eta=0}}{\phi (c_w - c_o)} \tag{24}$$

where

$$\frac{dc}{d\eta}\Big|_{\eta=0} = \frac{3^{2/3} (c_o - c_w)}{\Gamma (1/3)} = 0.776 (c_o - c_w) \tag{25}$$

Substituting for $\frac{dc}{d\eta}\Big|_{\eta=0}$ in Eq. (24) yields

$$k = 0.776 \left(\frac{D^2 a}{3x}\right)^{1/3} = 0.776 \left(\frac{D^2}{3x} \cdot \frac{3 \langle u \rangle}{h}\right)^{1/3} \tag{26}$$

It may be immediately recognized that the group of parameters, $\frac{3 \langle u \rangle}{h}$, represents the fluid shear rate at the membrane surface, or

$$\frac{du}{dy}\Big|_{y=0} = \frac{3 \langle u \rangle}{h} = \dot{\gamma}_w \tag{27}$$

When the average mass transfer coefficient over the length of the flow channel is considered, it can be written

$$\overline{k} = \frac{0.776}{L} \int_0^L \left(\frac{D^2}{3x} \dot{\gamma}_w\right)^{1/3} dx = 0.807 \left(\frac{D^2}{L} \dot{\gamma}_w\right)^{1/3} \tag{28}$$

where

$$\left| \overline{v}_w \right| = \overline{k} \ln \left(\frac{c_w - c_p}{c_o - c_p}\right) \tag{29}$$

The value of $\overline{k}$ represented by Eq. (28) may be generalized for various other flow geometries, depending upon the shear rate at the membrane surface.

$$\overline{k} = B \left(\frac{D^2}{L} \dot{\gamma}_w\right)^{1/3} \tag{30}$$

The value of B is determined by the wall boundary condition used in the solution of Eq. (16). Typical values of B and $\dot{\gamma}_w$ for various flow geometries are given in Table I.

Prediction of permeate flux in the turbulent flow regime may be accomplished with the use of various semiempirical relationships found in the literature. In the region of fully developed turbulent flow, the Chilton and Colburn (1934) relationship can be used:

$$\overline{Sh} = \frac{\overline{k} d_h}{D} = 0.023 \, Re^{0.80} \, Sc^{0.33} \tag{31}$$

where $d_h = 4h$

Other relationships include the Calderbank and Young (1961) equation of

$$\overline{Sh} = 0.082\ Re^{0.69}\ Sc^{0.33} \tag{32}$$

For the case of developing velocity and concentration profiles, the Grober, et al. (1961) relationship may be used for Re < 2000.

$$\overline{Sh} = 0.664\ \left(Re\ \frac{dh}{L}\right)^{1/2}\ Sc^{0.33} \tag{33}$$

TABLE I

AVERAGE MASS TRANSFER COEFFICIENT PARAMETERS
(LAMINAR FLOW)

Channel Shape		Numerical Constant B	Wall Boundary Condition[a]	$\dot{\gamma}_w$ Shear Rate
Rectangular slit	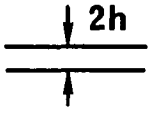	0.807 0.980	CWC CWF	$\frac{3\ \langle u\rangle}{h}$
Circular tube	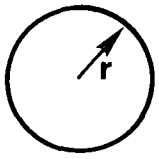	0.807 0.980	CWC CWF	$\frac{4\ \langle u\rangle}{r}$
Triangular channel	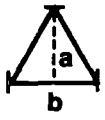	0.807 0.980	CWC CWF	$\frac{30\ \langle u\rangle}{a}\left[\frac{(5\frac{b}{a})^2 + 12}{(27\frac{b}{a})^2 + 20}\right]$

[a] CWC - Constant wall concentration.
CWF - Constant wall flux.

Colton (1969) has studied mass transfer in a stirred batch cell and proposed the following correlations

$$\frac{\overline{kr}}{D} = 0.285\ \left(\frac{\omega r^2}{\upsilon}\right)^{0.55}\ \left(\frac{\upsilon}{D}\right)^{0.33} \tag{34}$$

for laminar flow over the membrane surface

$$8{,}000 < \left(\frac{\omega r^2}{\upsilon}\right) < 32{,}000$$

and,

$$\frac{\overline{kr}}{D} = 0.0443 \left(\frac{\omega r^2}{\upsilon}\right)^{0.75} \left(\frac{\upsilon}{D}\right)^{0.33} \qquad (35)$$

for turbulent flow over the membrane surface

$$32{,}000 < \left(\frac{\omega r^2}{\upsilon}\right) < 82{,}000$$

where

r = cell radius, cm

ω = stirrer speed, radians/sec

υ = kinematic viscosity, cm^2/sec

D = solute diffusivity, cm^2/sec

Although the early work of the "Amicon School" did confirm the existence of gel-polarized behavior in macromolecular ultrafiltration, their interpretation of data in terms of the film theory model was not good. Typical gel-polarized behavior is shown in Fig. 5. Percent difference in predicted flux to experimental flux averaged around 25%. Their work was also plagued by such anomalous behavior as changing values of calculated gel concentration as a function of channel height. In general, the agreement of film theory prediction of flux to experimental value was much better for turbulent rather than laminar flow systems.

The "Amicon School" was the first to point out that in the ultrafiltration of colloidal suspensions, experimental flux rates were found to be 1 to 2 orders of magnitude greater than theoretical prediction based upon film theory. Unable to explain this phenomenon, they postulated the following: (1) either the back diffusion of colloidal particles from the polarized layer is substantially augmented beyond that expected to occur by classical Fickian diffusion mechanisms, or (2) the permeate rate is not limited by the hydraulic resistance of the particle polarized layer.

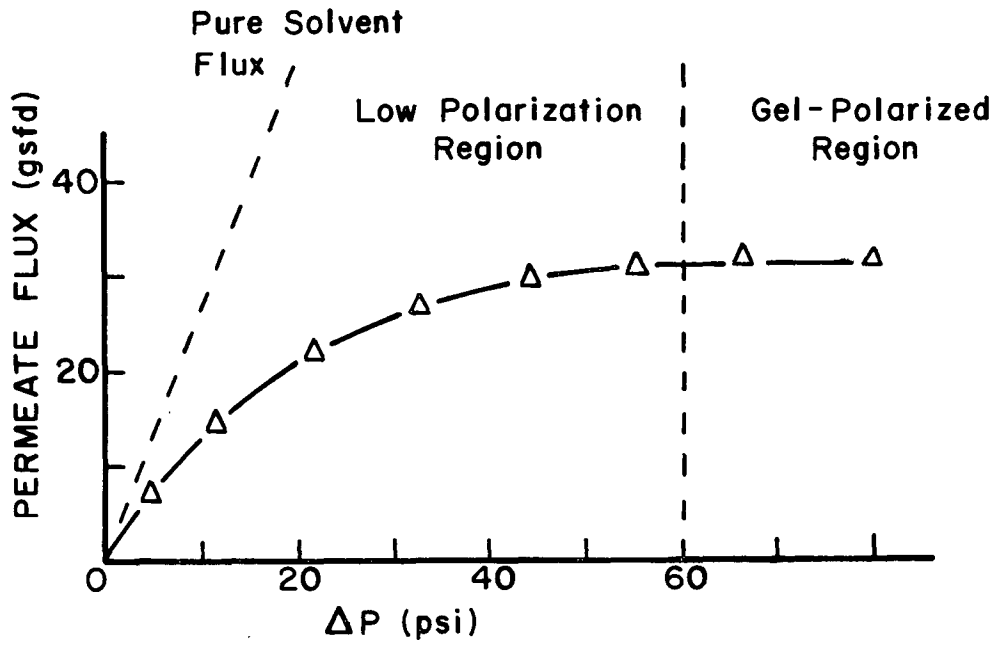

Figure 5. Macromolecular ultrafiltration - gel-polarized behavior.

Goldsmith (1971) and deFilippi and Goldsmith (1970) generally subscribed to the gel polarization model as presented by Michaels (1968). However, they noted that many macromolecular solutions have significant osmotic pressures and that when these solutions were ultrafiltered at moderate pressures, it was unlikely that gel polarization was reached. Consequently, they tried to interpret the pregel or low polarization region in terms of film theory. The ultrafiltration of Dextran and Carbowax (polyethylene oxide) solutions was studied in the three system geometries of stirred batch cell, parallel-plate, and tubular. Both laminar and turbulent flow regimes were studied in each geometry. Data were analyzed by the method of first determining the average value of c_w for the system in question. This was accomplished by measuring $\left| \overline{v_w} \right|$ and determining the average value of $\Delta\pi$ from the equation

$$\left| \overline{v_w} \right| = A \, (\Delta P - \Delta\pi) \tag{36}$$

where

A = membrane permeability = $\frac{1}{\mu R_m}$

$\Delta\pi = \pi_w - \pi_p$

ΔP = applied pressure

By knowing the value of $\Delta\pi$ and c_p, it is possible to calculate c_w from a known relationship of the form

$$\pi = k_1 c (1 + k_2 c)^2 \tag{37}$$

for the solute-solvent system. Thus, with the value of $|\overline{v_w}|$, c_p, c_b, and c_w known, the value of the mass transfer coefficient, $\overline{k}$, was calculated from

$$|\overline{v_w}| = \overline{k} \rho n \left(\frac{c_w - c_p}{c_o - c_p}\right) \tag{29}$$

The experimentally determined values of $\overline{k}$ were compared to the empirical relationships mentioned previously [Chilton-Colburn (1934), Harriott and Hamilton (1965)].

The work of Goldsmith (1971), in particular, contains inconsistencies. Employing the nonconventional technique of varying Reynolds number by changing bulk solution viscosity, turbulent and laminar flow are studied in thin channel ultrafiltration. It is not clear why Goldsmith states that by maintaining the axial volumetric flow rate constant in turbulent flow, the mass transfer coefficient remains unchanged even though the calculated Reynolds number varies over 7-fold based upon bulk solution viscosity change. It is appreciated that variation in the Schmidt (Sc) number tends to offset the variation in the Reynolds (Re) number in the calculation of $\overline{k}$, but the effect is not totally cancelling and a viscosity dependence of $\upsilon^{0.567}$ based upon the Harriott and Hamilton (1965) relationship prevails. The contention is dubiously substantiated by the presentation of turbulent flow data in

which the experimental value of $\overline{k}$ is constant over a Reynolds number change of 7000 to 50,000. The same procedure of Reynolds number variation is used in laminar flow studies where change in mass transfer coefficient is permissible according to Goldsmith. Agreement of the functional dependence of $\overline{k}$ upon Re as predicted by the Grober, et al. (1961) relationship is not good, contrary to what is suggested by Goldsmith. This inadequacy is primarily due to the fact that Sc number variation is not taken into account. Goldsmith's model makes much capital in the ability to predict flux in the pregel region where gel formation has not been reached. All data are interpreted in light of this premise, yet Goldsmith has failed to explain why in a plot of flux versus ln $(c_b - c_p)$ for two different pressures, both lines extrapolate to the same value of ln $(c_w - c_p)$, indicating pressure independence. The interpretation of his data is not obvious, and an explanation of the discrepancies may in part be found in the method of acquisition.

Kozinski (1971) and Kozinski and Lightfoot (1972) modeled ultrafiltration of protein solutions through a rotating disk. Taking into consideration concentration-dependent diffusivity and solution viscosity, the convective diffusion equation, which was coupled to the appropriate Navier-Stokes relationship, was solved by both a method of asymptotic expansion and numerically. The asymptotic solution assumed a linear concentration profile and a linear approximation of solution properties at the membrane. Both asymptotic and numerical solutions described actual experimental data very well. However, the numerical solution was very sensitive to variations in viscosity and diffusivity at high solute concentrations.

Based upon their study of the rotating disk, Kozinski and Lightfoot extended their model to the parallel plate geometry. Equations were solved by similarity transformation using average values of solution properties evaluated between the

bulk solution and wall solute concentrations. Agreement with literature data was not good.

Strathmann (1973) studied the thin channel ultrafiltration of hemoglobin solutions in turbulent flow. The value of the mass transfer coefficient was calculated from the Chilton-Colburn (1934) relationship of

$$\overline{Sh} = 0.023\ Re^{0.80}\ Sc^{0.33} \tag{38}$$

and corresponding values of c_w were then calculated from the film theory relationship

$$\left| \overline{v}_w \right| = \overline{k}\ \ell n \left(\frac{c_w - c_p}{c_o - c_p}\right) \tag{29}$$

The numerical value of the gel concentration was found to be 10 g/100 cc which is definitely low in comparison to the results of others [Dejmek (1975)].

In analyzing Strathmann's data for the laminar flow system, it can be shown that the dependence of flux upon the shear rate $\dot{\gamma}_w$ is closer to 0.50 than the film theory prediction of 0.33 as given by Eq. (30).

$$\overline{k} = B \left(\frac{D^2}{L}\ \dot{\gamma}_w\right)^{1/3} \tag{30}$$

When the mass transfer coefficient is calculated from Eq. (30), different hemoglobin gel concentrations between 5.7 g/100 cc and 51.3 g/100 cc have to be assumed to fit the data to Eq. (29) [Dejmek (1975)].

Grieves, et al. (1973) studied the ultrafiltration of a nonionic surfactant (Triton X-100) and found that the use of Eq. (29) and (30) yielded flux predictions 70% below experimental values in laminar flow. Mitra and Lundbland (1978) studied

the ultrafiltration of immune serum globulin (ISG) and human serum albumin (HSA) in thin channel, laminar flow. Analyzing data in terms of the modified film theory model of

$$\left| \overline{v_w} \right| = A \langle u \rangle^B \ell n \ (c_w/c_o) \tag{39}$$

with multiple regression techniques, they found the best possible agreement had a standard deviation in the value of the constant A of 23%.

The strongest evidence yet presented in support of the film theory model has been published by R. F. Probstein and his students at the Massachusetts Institute of Technology [Shen and Probstein (1977), Probstein, et al. (1978), (1979), Leung and Probstein (1979), Shen and Probstein (1979)].

In Shen and Probstein (1977), the convective diffusion equation is solved by similarity for the thin channel system taking into consideration concentration dependent diffusivity. An approximate correction factor to account for variable diffusivity is derived and semiempirically added to the constant property film theory model. The correction simply amounts to evaluating the value of the diffusion coefficient at the wall concentration rather than the bulk concentration. The thin channel system is also evaluated for the case of variable diffusion and solution viscosity where it is shown by means of a numerical solution that variable viscosity effects are secondary. It is therefore assumed that the corrected film theory model represents a good approximation to a more rigorous solution. Shen and Probstein attempt to interpret the thin channel data of Blatt, et al. (1970) but the experimental axial velocity is misinterpreted and comparative results are not as good as depicted.

In Probstein, et al. (1978), the convective diffusion equation is solved by an integral method for concentration-dependent diffusivity. By deleting higher order

terms, the modified film theory model is obtained analytically. Experimental data are interpreted in terms of film theory and agreement is good.

Leung and Probstein (1979) address the problem of flux prediction in the low polarization or pregel region by solving the convective diffusion equation and Eq. (36) simultaneously. An integral method solution using parabolic velocity and concentration profiles is utilized. As a numerical check, the integral method model was simplified by assuming constant diffusion coefficient and linear osmotic pressure-concentration dependency and compared to Brian's (1966) finite difference solution for reverse osmosis. Thin channel ultrafiltration data were interpreted using the osmotic pressure data of Vilker (1975), and agreement was excellent.

Nakao, et al. (1979) studied the ultrafiltration of polyvinyl alcohol in a tubular system. They essentially found that the concentration of the gel layer was not constant but rather a function of bulk concentration and feed velocity. More importantly, they did not observe the typical logarithmic behavior of permeate flux versus bulk solution concentration plots which are predicted by film theory.

OBJECTIVES OF THESIS

As shown in the preceding literature review, the film theory model currently represents the most widely used theory in the interpretation of ultrafiltration data. Although the film theory model may give somewhat reasonable predictive results in turbulent flow, its value in the laminar region is questionable and has been characteristically overused. At first introduction to the problem, one is often misled by the simplicity of the film theory model. It has been portrayed in the literature that if macromolecular solutions are being ultrafiltered, gel-polarized behavior may be immediately assumed. This is not the case. Although the gel-polarized concept is generally accepted, there has not been any definite study

showing exactly when a process is in the gel-polarized region or not. The proper values of the solute diffusivity and gel concentration are also often shrouded in controversy. Additionally, it still remains to be shown why experimental flux rates in colloidal ultrafiltration are found to be 1 to 2 orders of magnitude greater than macromolecular flux rates. This type of behavior is contrary to that predicted by the film theory model.

In this study it was decided to work initially with the unstirred batch cell. The justification is that by using such a simple system, many of the interfering effects such as variable viscosity and various hydrodynamic mechanisms are absent. The aspect of characterizing these additional effects has often been a major obstacle to previous researchers working with more complicated systems. Once a fundamental knowledge of the batch cell system was acquired, the more complicated cross-flow geometry was considered.

The primary objectives of this study were the following:

(1) To determine the applicability of the film theory model by comparison with a more exact theory and with experimental data.

(2) To develop a theory which would explain the vast differences between the two apparently similar processes of macromolecular and colloidal ultrafiltration.

(3) To contribute to the basic understanding of the low polarization (pregel) and gel-polarized regions in macromolecular ultrafiltration.

This thesis is comprised of four major sections which are represented by manuscripts written during the course of the research work. They appear in the following order and are entitled:

Manuscript No. 1 - "Ultrafiltration in an Unstirred Batch Cell" - I&EC Fundam. 19:189-94(1980).

Manuscript No. 2 - "Ultrafiltration of Colloidal Suspensions and Macromolecular Solutions in an Unstirred Batch Cell" - I&EC Fundam. 20:221-9(1981).

Manuscript No. 3 - "Limiting Flux in Ultrafiltration of Macromolecular Solutions." Chem. Eng. Commun. 4:508-22(1980).

Manuscript No. 4 - "Pressure Independent Ultrafiltration - Is it Gel Limited or Osmotic Pressure Limited?" - ACS Symposium Series, No. 154. Synthetic Membranes: Vol. II Hyper- and Ultrafiltration Uses (1981).

Manuscript No. 1 is concerned with the development of a more exact theory to describe ultrafiltration in the unstirred batch cell. The exact solution is compared with the film theory model, where it is shown that substantial differences exist. Excellent agreement between the exact solution and experimental data is observed, clearly indicating a superior approach.

Manuscript No. 2 addresses the problem of explaining the vast differences between colloidal and macromolecular ultrafiltration flux. It is found that in colloidal ultrafiltration, solute diffusion is negligible, and flux may be described in terms of classical filtration principles, where solute accumulation is important. Directly opposite behavior is found in macromolecular ultrafiltration, where flux is diffusion limited.

Manuscript No. 3 evaluates the applicability of the film theory model to cross-flow ultrafiltration of macromolecules. It is found that the widely used film theory deviates considerably from the exact model, just as in the unstirred batch cell.

Manuscript No. 4 deals with the interpretation of pregel experimental data in terms of the exact model for both batch cell and cross-flow systems. An excellent method of determining whether an ultrafiltration process is gel or osmotically (pregel) limited is presented.

NOMENCLATURE

A = membrane permeability constant = $\frac{1}{\mu R_m}$, $\left(\frac{cm\text{-}m^2}{N\text{-}sec}\right)$

a = linearized Poiseuille velocity constant = $\frac{3\ \langle u \rangle}{h}$, (1/sec)

B = numerical boundary condition constant

c = solute concentration, (g/cm^3)

D = solute diffusion coefficient, (cm^2/sec)

d_h = hydraulic diameter = $\frac{4\ (\text{cross-sectional area})}{\text{wetted perimeter}}$, (cm)

h = channel half height, (cm)

k = local mass transfer coefficient (cm/sec)

$\overline{k}$ = average mass transfer coefficient (cm/sec)

k_1, k_2 = osmotic pressure virial coefficients

L = length of flow conduit (cm)

R = hydraulic resistance (1/cm)

r = radius of tube (cm)

Re = Reynolds number = $\frac{\langle u \rangle\ d_h}{\upsilon}$

Sc = Schmidt number = υ/D

$\overline{Sh}$ = average Sherwood number = $\frac{\overline{k}\ d_h}{D}$

t = time (sec)

u = axial velocity (cm/sec)

$\langle u \rangle$ = average axial velocity (cm/sec)

v = transverse velocity (cm/sec)

$|v_w|$ = local permeate volumetric flux, (cm^3/cm^2-sec)

$|\overline{v_w}|$ = average permeate volumetric flux, (cm^3/cm^2-sec)

$\hat{v}$ = vector velocity = $ui + vj + wk$

w = velocity component in z direction (cm/sec)

x = axial distance coordinate, (cm)

y = transverse distance coordinate, (cm)

z = distance coordinate in z direction, (cm)

GREEK SYMBOLS

∇ = gradient operator

$\nabla\cdot$ = divergence operator

ΔP = total pressure gradient, (N/m^2)

$\Delta\pi$ = osmotic backpressure at membrane surface = $\pi_w - \pi_p$, (N/m^2)

δ = mass boundary layer thickness, (cm)

η = similarity transformation = $y/\left[\frac{3Dx}{a}\right]^{1/3}$

μ = permeate viscosity, $\left[\frac{N\text{-sec}}{m^2}\right]$

υ = kinematic viscosity, (cm^2/sec)

ρ = solution density, (g/cm^3)

$\dot{\gamma}_w$ = hydrodynamic shear rate at membrane surface, (1/sec)

ω = angular velocity, (rad/sec)

π = solution osmotic pressure, (N/m^2)

Γ = Gamma function

SUBSCRIPTS

g = of the gel

m = of the membrane

o = of the bulk solution

p = of the permeate

w = at the wall or membrane surface

LITERATURE CITED

Baker, R. W. Methods of fractionating polymers by ultrafiltration. J. Appl. Polymer Sci. 13:369(1969).

Bansal, I. and Wiley, A. J. Application of reverse osmosis in the pulp and paper industry. In Reverse osmosis and synthetic membranes, S. Sourirajan, editor, NRCC Publications, 1977. p. 459.

Besik, F. Reverse osmosis in treatment of domestic and municipal wastes. In Reverse osmosis and synthetic membranes, S. Sourirajan, editor, NRCC Publications, 1977. p. 495.

Bhattacharyya, D., McCarthy, J. M., and Grieves, R. B. Charged membrane ultrafiltration of inorganic ions in single and multisalt systems. AIChE J. 20(6):1206 (1974).

Bhattacharyya, D., Jumawan, A. B., Jr., and Grieves, R. B. Charged membrane ultrafiltration of heavy metals from nonferrous metal. J. Water Pollution Control Fed. 51(1):176(1979).

Bird, R. B., Stewart, W. E., and Lightfoot, E. N. Transport phenomena. Wiley and Sons, New York, N.Y., 1960.

Bixler, H. J., Nelsen, L. M., and Bluemle, L. W., Jr. The development of a diafiltration system for blood purification. Trans. Am. Soc. Artif. Int. Organs XIV, 1968. p. 99.

Blais, P. Polyamide membranes. In Reverse osmosis and synthetic membranes, S. Sourirajan, editor, NRCC Publications, 1977. p. 167.

Blatt, W. F., Dravid, A., Michaels, A. S., and Nelsen, L. Solute polarization and cake formation in membrane ultrafiltration: causes, consequences, and control techniques. In Reverse osmosis and synthetic membranes, J. E. Flinn, editor, Plenum Press, New York, N.Y., 1970. p. 47.

Brian, P. L. T., In Desalination by reverse osmosis, U. Merten, editor, MIT Press, Cambridge, Mass., 1966. p. 161.

Calderbank, P. H. and Moo-Young, M. B., Chem. Eng. Sci. 16:34(1961).

Caracciolo, V. P., Rosenblatt, N. W., and Tomsic, V. J. Dupont's hollow fiber membranes. In Reverse osmosis and synthetic membranes, S. Sourirajan, editor, NRCC Publications, 1977. p. 343.

Chilton, T. H. and Colburn., A., Ind. Eng. Chem. 26:1183(1934).

Colton, C. K., Ph.D. Thesis, MIT, Dept. of Chemical Eng. (1969).

deFilippi, R. P. and Goldsmith, R. L. Application and theory of membrane processes for biological and other macromolecular solutions. In Membrane science and technology, J. E. Flinn, editor, Plenum Press, New York, N.Y., 1970. p. 33.

Dejmek, P. Concentration polarization. In Ultrafiltration of macromolecules, Ph.D. Thesis, Lund Institute of Technology, Sweden (1975).

Delaney, R. A. M. and Donnelly, J. K. Applications of reverse osmosis in the dairy industry. In Reverse osmosis and synthetic membranes, S. Sourirajan, editor, NRCC Publications, 1977. p. 417.

Derzansky, L. J. An experimental study of reverse osmosis in a horizontal tube: Combined free and forced convection. Ph.D. Thesis, Clarkson College of Technology, Dept. of Chemical Eng., 1973.

Gill, W. N., Derzansky, L. J., and Doshi, M. R. Convective diffusion in laminar and turbulent hyperfiltration (reverse osmosis) systems. In Surface and Colloid Science, Vol. 4, E. Matijevic, editor, Wiley and Sons, New York, N.Y., 1971. p. 261.

Goldsmith, R. L. Macromolecular ultrafiltration with microporous membranes. I&EC Fundam., 10(1):113(1971).

Golomb, A. Application of reverse osmosis to electroplating waste treatment. In reverse osmosis and synthetic membranes, S. Sourirajan, editor, NRCC Publications, 1977. p. 387.

Grieves, R. B., Bhattacharyya, D., Schomp, W. G., and Bewley, J. L. Membrane ultrafiltration of a nonionic surfactent. AIChE J. 19(4):766(1973).

Grober, H., Erk, S., and Grigull, U. Fundamentals of heat transfer. McGraw-Hill, New York, N.Y., 1961.

Harriott, P. and Hamilton, R. M., Chem. Eng. Sci. 20:1973(1965).

Hoffman, C. A. Abcor. Personal communication (1979).

Johnson, J. S., Jr., Dresner, L., and Kraus, K. A. In Principles of desalination, K. S. Spiegler, editor, Academic Press, New York, N.Y., Chapter 8, 1966.

Kesting, R. E. Asymmetric cellulose acetate membranes. In Reverse osmosis and synthetic membranes, S. Sourirajan, editor, NRCC Publications, 1977. p.89.

Kimura, S. and Sourirajan, S., AIChE J. 13:497(1967).

Kozinski, A. A. Ultrafiltration of protein solutions. Ph.D. Thesis, University of Wisconsin, Dept. of Chemical Eng., 1971.

Kozinski, A. A. and Lightfoot, E. N. Protein ultrafiltration: a general example of boundary layer filtration. AIChE J. 18(5):1030(1972).

Kremen, S. Technology and engineering of ROGA spiral-wound reverse osmosis membrane modules. In Reverse osmosis and synthetic membranes, S. Sourirajan, editor, NRCC Publications, 1977. p. 371.

LaConti, A. Advances in development of sulfonated PPO and modified PPO membrane systems for some unique reverse osmosis applications. In Reverse osmosis and synthetic membranes., S. Sourirajan, editor, NRCC Publications, 1977. p. 211.

Lee, D. and Merson, R. L. Prefiltration of cottage cheese whey to reduce fouling of ultrafiltration membranes. J. of Food Science 41:403(1976).

Leung, W. F. and Probstein, R. F. Low polarization in laminar ultrafiltration of macromolecular solutions. I&EC Fundam. 18(3):274(1979).

Loeb, S. and Sourirajan, S. New water desalting process developed at UCLA, University of California, Office of Public Information Press Release, August 23, 1960.

Lonsdale, H. K., Merten, U., and Westmoreland, R. Reverse osmosis for water desalination. GA-5207 report, General Atomics Division of General Dynamics, San Diego, California, May, 1964.

Lonsdale, H. K., Merten, U., and Riley, R. L. Transport properties of cellulose acetate osmotic membranes. J. Appl. Polymer Sci. 9:1341(1965).

Lonsky, W. The Institute of Paper Chemistry, Personal communication, 1980.

Madsen, R. F. Hyperfiltration and ultrafiltration in plate and frame systems. Elsevier Scientific Publishing Company, Amsterdam, 1977.

Merten, U. Editor. Desalination by reverse osmosis. The MIT Press, Cambridge, Massachusetts, 1966.

Michaels, A. S., Bixler, H. J., and Hodges, R. M., Jr. Kinetics of water and salt transport in cellulose acetate reverse osmosis desalination membranes. J. Colloid. Sci. 20:1034(1965).

Mitra, G. and Lundblad, J. L. Ultrafiltration of immune serum globulin and human serum albumin: regression analysis studies. Sepn. Sci. Technol. 13(1):89(1978).

Model, F. S., Davis, H. J., and Poist, J. E. PBI membranes for reverse osmosis. In Reverse osmosis and synthetic membranes, S. Sourirajan, editor, NRCC Publications, 1977. p. 263.

Nakao, S. I., Nomura, T., and Kimura, S. Characteristics of macromolecular gel layer formed on ultrafiltration tubular membrane. AIChE J. 25(4):615(1979).

Orofino, T. A. Technology of hollow fiber reverse osmosis systems. In Reverse osmosis and synthetic membranes, S. Sourirajan, editor, NRCC Publications, 1977. p. 313.

Porter, M. C. Concentration polarization with membrane ultrafiltration. I&EC Prod. Res. 11(3):234(1972).

Probstein, R. F., Shen, J. S., and Leung, W. F. Ultrafiltration of macromolecular solutions at high polarization in laminar channel flow. Desalination 24:1(1978).

Probstein, R. F., Leung, W. F., and Alliance, Y. Determination of diffusivity and gel concentration in macromolecular solutions by ultrafiltration. J. Phys. Chem. 83(9):1228(1979).

Reid, C. E. and Breton, E. J. Water and ion flow across cellulosic membranes. J. Appl. Polymer Sci. 1(2):133(1959).

Rozelle, L. T., Cadotte, J. E., Cobian, K. E., and Kopp, C. V. Non-polysaccharide membranes for reverse osmosis: NS-100 membranes. In Reverse osmosis and synthetic membranes, S. Sourirajan, editor, NRCC Publications, 1977. p. 249.

Sharples, A. Membranes for use in the reverse osmosis process. Arthur D. Little Research Institute, Inverest, Scotland, November, 1963.

Shen, J. J. S. and Probstein, R. F. On the prediction of limiting flux in laminar ultrafiltration of macromolecular solutions. I&EC Fundam. 16(4):459(1977).

Shen, J. S. and Probstein, R. F. Turbulence promotion and hydrodynamic optimization in an ultrafiltration process. I&EC Process Design Devt. 18(3):547(1979).

Sherwood, T. K., Brian, P. L. T., and Fisher, R. E., I&EC Fundam. 6(2):(1967).

Sourirajan, S. The mechanism of demineralization of aqueous sodium chloride solutions by flow, under pressure, through porous membranes. I&EC Fundam. 2(1):51 (1963).

Sourirajan, S. Reverse osmosis. Logos, London, and Academic, New York, 1970.

Sourirajan, S. Reverse osmosis - a general separation technique. In Reverse osmosis and synthetic membranes, S. Sourirajan, editor, NRCC Publications, 1977. p. 1.

Sourirajan, S. and Matsuura, T. Physicochemical criteria for reverse osmosis separations. In Reverse osmosis and synthetic membranes, S. Sourirajan, editor, NRCC Publications, 1977. p. 5.

*Sourirajan, S. and Matsuura, T. Transport through reverse osmosis membranes. In Reverse osmosis and synthetic membranes, S. Sourirajan, editor, NRCC Publications, 1977.

Stana, R. Westinghouse membrane systems. In Reverse osmosis and synthetic membranes, S. Sourirajan, editor, NRCC Publications, 1977. p. 387.

Ticknor, L. B., J. Phys. Chem. 62:1483(1958).

Vilker, V. L., Ph.D. Thesis, MIT, Dept. of Chemical Eng., Cambridge, Massachusetts, 1975.

Von Bockelmann, I., Dejmek, P., Eriksson, G., and Hallstrom, B. Potential applications in food processing. In Reverse osmosis and synthetic membranes, S. Sourirajan, editor, NRCC Publications, 1977. p. 445.

Walker, R. A., UOP-Fluid Systems Division, Personal communication, 1979.

Wang, D. I., Sonoyama, T., and Mateles, R. I. Enzyme and bacteriophage concentration by membrane filtration. Anal. Biochem. 26:277(1968).

Wiley, A. J., Ammerlaan, A. C. F., and Dubey, G. A. Application for reverse osmosis in the pulp and paper industry. In Industrial processing with membranes, R. E. Lacey and S. Loeb, editors, Chapter XI, Wiley and Sons, New York, N.Y., 1972.

Yasuda, H. Composite reverse osmosis membranes prepared by plasma polymerization. In Reverse osmosis and synthetic membranes, S. Sourirajan, editor, NRCC Publications, 1977. p. 263.

SECTION 2 - MANUSCRIPT NUMBER 1

ULTRAFILTRATION IN AN UNSTIRRED BATCH CELL

I&EC Fundam. 19:189-94(1980)

ULTRAFILTRATION IN AN UNSTIRRED BATCH CELL

ABSTRACT

The ultrafiltration of macromolecular solutions in an unstirred batch cell was investigated to isolate the effect of variable diffusion coefficient from that of variable solution viscosity. Solutions of bovine serum albumin (BSA) in 0.15M NaCl (7.40 pH) and 0.10M sodium acetate (4.70 pH) were used. A technique for minimizing the effect of variable membrane properties, as well as pregel (low polarization) region is presented. (BSA) systems are studied over a wide range of concentrations (0.01-0.10 g/cm^3) and at higher pressures than previously reported (10.34 x $10^5 N/m^2$). Results confirm that BSA solutions do reach a pressure-independent flux region at moderate pressures. A constant property integral method solution was developed which agrees well with the exact solution but not with the film theory. Agreement between acquired BSA data and theoretical predictions is excellent, with the average error less than 3%.

INTRODUCTION

Over the past decade, membrane ultrafiltration has become recognized as a viable process for the concentration or separation of moderate to high molecular weight solutes from solutions. Because of the wide application and simplicity of the process, ultrafiltration is currently being used in many commercial and industrial operations from food processing to waste treatment. As a direct result of this increased interest in ultrafiltration, there have been many investigations regarding the nature of the transport phenomena in ultrafiltration [Michaels (1968), Blatt et al. (1970), Goldsmith (1971), Kozinski and Lightfoot (1972), Porter (1972), Shen and Probstein (1977), Mitra and Lundblad (1978), Probstein et al. (1978, 1979)].

Although more rigorous predictive models exist, the mainstay of the ultrafiltration technology continues to center around models based on film theory. Shen and Probstein (1977) and Probstein et al. (1978, 1979) have taken a more exact approach to the problem and have shown that numerical solutions to their exact model for variable viscosity and diffusion coefficient can be closely approximated by a modified film theory model where the value of the diffusion coefficient is evaluated at the solute gelling concentration. Agreement with experimental data for the parallel plate system is excellent if the values of the solute gelling concentration and corresponding diffusion coefficient cited by Probstein et al. (1978, 1979) for bovine serum albumin are employed. Possible limitations of the data of Probstein et al. (1978, 1979) are that flux measurements were taken over a narrow range of solute concentrations. Trettin and Doshi (1980) have theoretically shown with an integral method solution to the solute mass balance equation that permeate flux does not vary logarithmically with solute concentration, which is characteristic of the film theory model. Since there are substantial differences between the two models, there is a definite need for additional data taken over a wider solute concentration range to test the two theories. Besides, existing data have not been corrected for the

pregel region. We appreciate that the pregel region is indeed small. However, permeate rate in the pregel region may not be negligible compared to that in the gel region.

A major obstacle in the comparison of the experimental data with the modified film theory model and more exact solutions is that the proper values of the solute gel concentration and diffusion coefficient are not available. Most previous studies have used forced convection ultrafiltration units where added complications may arise due to variable viscosity. The unstirred batch cell system offers the unique opportunity of studying the ultrafiltration of bovine serum albumin solutions without the interfering effect of variable viscosity. The main objective of this work is to develop the analogous form of the integral method solution derived (for parallel plate system) in the work of Trettin and Doshi (1980), along with the film theory analogy, for the unstirred batch cell. Experimental data taken in the unstirred batch cell ultrafiltration of bovine serum albumin are corrected for the pregel region and compared with both models. Results are further compared to the values of gel concentration and diffusion coefficient determined by Probstein et al. (1978, 1979).

THEORETICAL DEVELOPMENT

Consider the unstirred cell geometry as shown in Fig. 1 where the general solute mass balance equation of

$$\partial c/\partial t + v\, \partial c/\partial y = D\, \partial^2 c/\partial y^2 \qquad (1)$$

applies. It is implicitly assumed in the derivation of Eq. (1) that the density of the solute is approximately that of the solvent.

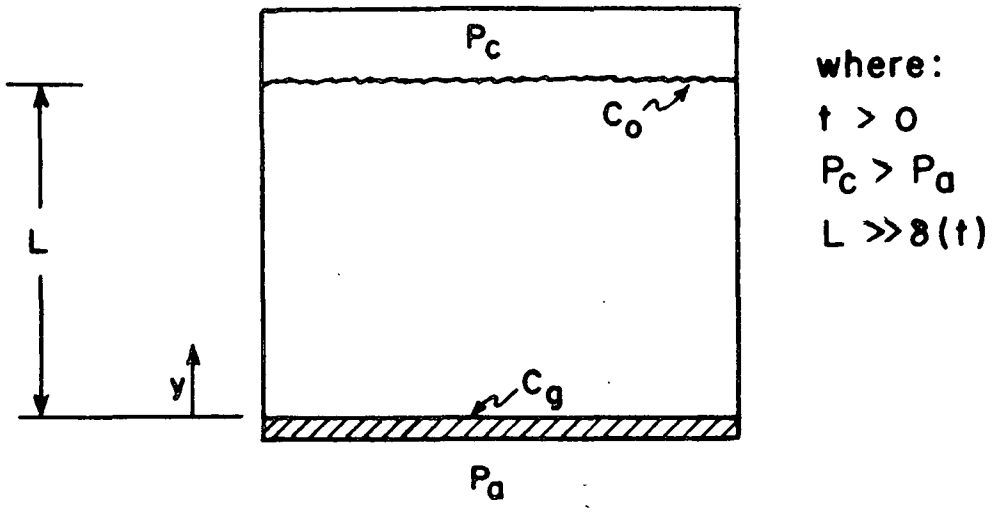

Figure 1. Batch cell geometry.

The appropriate boundary and initial conditions are the following

$$c(0,y) = c_o \qquad \text{for } y > 0 \tag{2}$$

$$c(t,0) = c_g \qquad \text{for all } t \tag{3}$$

$$c(t,\infty) = c_o \qquad \text{for all } t$$

$$v(c_g - c_p) = -\left| v_w \right| (c_g - c_p) = D[\partial c/\partial y]_{y=0} \tag{4}$$

Clearly, the model assumes that a solute gel concentration is reached instantaneously at the membrane surface and that the value of the solute diffusion coefficient is constant. Adopting a similarity transformation of the form

$$\eta = y/(4Dt)^{1/2} \tag{5}$$

Equation (1) may be rewritten as

$$d^2c/d\eta^2 + [2\eta + V_w]dc/d\eta = 0 \tag{6}$$

where

$$V_w = \frac{\left| v_w \right| (4Dt)^{1/2}}{D} = \text{constant} \tag{7}$$

and the boundary conditions of Eq. (2)-(4) reduce to

$$c(0) = c_g \tag{8}$$

$$c(\infty) = c_o \tag{9}$$

$$dc/d\eta \Big|_{\eta=0} = -V_w(c_g-c_p) \tag{10}$$

Integration of Eq. (6) with the substitution of the boundary condition given in Eq. (10) yields

$$\theta = \frac{c_g-c_o}{c_g-c_p} = V_w \int_o^\infty \exp[-(\eta^2 + V_w\eta)]\, d\eta \tag{11}$$

Upon evaluation of the closed integral of Eq. (11), the result is

$$\theta = \frac{\sqrt{\pi}}{2} V_w \exp[V_w^2/4] \operatorname{erfc}[V_w/2] \tag{12}$$

For small values of V_w, Eq. (12) may be simplified to

$$\theta = \frac{\sqrt{\pi}}{2} V_w - \frac{1}{2} V_w^2 + \frac{\sqrt{\pi}}{8} V_w^3 - \frac{1}{12} V_w^4 + \frac{\sqrt{\pi}}{64} V_w^5 - \frac{1}{120} V_w^6 + \ldots \tag{13}$$

Similarly, for large values of V_w, Eq. (12) may be written as

$$\theta = 1 - 2 V_w^{-2} + 12 V_w^{-4} - 120 V_w^{-6} + \ldots \tag{14}$$

It will be interesting to obtain a solution by the integral method in an analagous manner to the previously solved case of the parallel plate (rectangular flow channel) system (Trettin and Doshi, 1980). Assume a concentration profile of the form

$$c = c_o + (c_g-c_o)(1-y/\delta)^n \tag{15}$$

Note that at $y = \delta(t)$, $c = c_o$. The solution involves the integration of Eq. (1) over the boundary layer thickness, $\delta(t)$, with the substitution of the concentration profile equation. The result may be expressed as

$$d\delta/dt = \frac{n(n+1)\ D}{\delta}\left[\frac{c_o-c_p}{c_g-c_p}\right] \tag{16}$$

or, integrating Eq. (16) with respect to t and noting that at $t = 0$, $\delta(t) = 0$

$$\delta = [2n(n+1)]^{1/2}\ D^{1/2}\ \left(\frac{c_o-c_p}{c_g-c_p}\right)^{1/2}\ t^{1/2} \tag{17}$$

Equation (17) may be written in terms of $|\ v_w\ |$ using the boundary condition of Eq. (4)

$$|\ v_w\ | = \left[\frac{c_g-c_o}{c_g-c_p}\right]\left[\frac{c_g-c_p}{c_o-c_p}\right]^{1/2}\left[\frac{nD}{2(n+1)t}\right]^{1/2} \tag{18}$$

Transforming Eq. (18) to dimensionless form using Eq. (7) yields

$$V_w = \left[\frac{F_g-1}{F_g-F_p}\right]\left[K\ \frac{F_g-F_p}{1-F_p}\right]^{1/2} \tag{19}$$

where

$$K = 2n/(n+1);\ F = c/c_o \tag{20}$$

In order to determine the proper value of the coefficient n, a moment technique was applied by multiplying Eq. (1) by y

$$y\ \partial c/\partial t - |\ v_w\ |\ y\ \partial c/\partial y = yD\ \partial^2 c/\partial y^2 \tag{21}$$

Upon substitution of the assumed concentration profile into Eq. (21) and integration over the boundary layer thickness, the result may be expressed as

$$n^2(1-F_p) + n(F_p-F_g) + 2(F_p-F_g) = 0 \tag{22}$$

or, since $n > 0$

$$n = \frac{[F_g-F_p] + [(F_g-F_p)^2 + 8(1-F_p)(F_g-F_p)]^{1/2}}{2(1-F_p)} \tag{23}$$

A comparison of the developed integral method solution was made with the calculated solutions of Eq. (12) within a range of F_g values from 2 to 100. The agreement of the predicted values of V_w between the two solutions is excellent with a difference less than 1%. F_p was assumed to be zero in the comparison. In the calculation of permeate flux, the use of Eq. (19) is more convenient since Eq. (12) must be solved by trial and error.

The unstirred batch cell analogy of the film theory model can be obtained by neglecting the accumulation term from Eq. (1) and integrating

$$1-\theta = \exp\left[-\frac{|v_w|\,\delta}{D}\right] \tag{24}$$

The quantity D/δ is taken to be equal to the unsteady-state mass transfer coefficient (assuming constant wall concentration) in the absence of transverse velocity

$$k = D/\delta = (D/\pi t)^{1/2} \tag{25}$$

Substituting for D/δ in Eq. (24) yields

$$1-\theta = \exp\left[-|v_w|\,(t\pi/D)^{1/2}\right] \tag{26}$$

or, expressed in a more conventional form

$$|v_w| = (D/\pi t)^{1/2}\ \ln\left[\frac{c_g-c_p}{c_o-c_p}\right] \tag{27}$$

Transforming to dimensionless variables with the use of Eq. (7) yields

$$V_w = \frac{2}{\pi^{1/2}} \ln \left(\frac{F_g - F_p}{1 - F_p}\right) \tag{28}$$

A comparison of the film theory solution to the integral method solution for the unstirred batch cell is shown in Table I, where it is noted that the film theory model consistently underpredicts the integral method model with progressively better agreement as the value of F_g approaches unity. Film theory deviates from the more exact theory by more than 25% for all values of F_g greater than 4.0. Similar results were obtained for the case of the parallel plate system [Trettin and Doshi (1980)].

TABLE I

COMPARISON OF FILM THEORY MODEL WITH INTEGRAL METHOD SOLUTION

F_g	V_w, film theory	V_w, integral method	$\frac{V_w(I.M.)}{V_w(F.T.)}$
100	5.20	13.93	2.68
75	4.87	12.01	2.46
50	4.41	9.71	2.20
25	3.63	6.67	1.84
15	5.06	4.97	1.63
10	2.60	3.86	1.49
5	1.82	2.36	1.30
4	1.56	1.95	1.25
2	0.78	0.87	1.12
1.5	0.46	0.49	1.07

EXPERIMENTAL PROCEDURE

Bovine serum albumin (Cohn fraction V), obtained from Sigma Chemicals Co. in granular form, was selected as a macromolecular solute. The justification for this choice of material was twofold. First, BSA is a reasonably well-characterized protein with Newtonian rheological properties [Kozinski and Lightfoot (1972)] and a

narrow molecular weight distribution of approximately 70,000. Second, BSA has been studied extensively by previous investigators [Blatt et al. (1970), Kozinski and Lightfoot (1972), Shen and Probstein (1977), and Probstein et al. (1978, 1979)] so their work provides a comparison with our results. Solutions of BSA prepared in 0.15M NaCl (7.4 pH) and 0.10M sodium acetate (4.7 pH) were used. These buffer solutions are comparable to those studied by Shen and Probstein (1977) and Probstein et al. (1978, 1979). Sodium azide of 200 ppm concentration was added as a preservative and final solutions were filtered through a 0.8-μm millipore filter to remove undissolved solute. Solutions were then refrigerated at 10°C prior to use. BSA solutions which had aged more than two weeks were discarded. Solute concentrations were determined by ultraviolet light absorption with a spectrophotometer at the absorption peak of 280 nm.

The literature contains numerous experimental determinations of the mutual diffusion coefficient of BSA in various buffer solutions [Creeth (1952), Charlwood (1953), Keller et al. (1971), Doherty and Benedek (1974), Phillies et al. (1976)]. The range of reported diffusion coefficient at low concentration is $D = 5.5\text{-}7.0 \times 10^{-7}$ cm^2/sec. However, values at higher concentration show considerable scatter as pointed out by Shen and Probstein (1977). Phillies et al. (1976) have studied BSA solution diffusivity in both 0.025M sodium acetate-0.2M NaCl and 0.15M NaCl buffer systems over the pH range of 4.3-7.6. Their work has shown a negligible concentration dependence of the diffusion coefficient in the acetate buffer system within the 4.6-5.6 pH range. Data taken within the higher pH ranges of the 0.15M NaCl system show considerable scatter and have been interpreted by Probstein et al. (1979) to yield an average value in general agreement with their determination of 6.7×10^{-7} cm^2/sec.

Ultracentrifuge experiments were performed in our laboratory with the acetate and saline buffered BSA solutions (≈ 0.007 g/cm^3) using the optical procedure of

Longsworth (1952) and Creeth (1955) as outlined by Tostevin (1966). Limitations of this method are that only low concentrations of BSA in solution may be studied due to refraction fringe merging at higher concentrations (> 0.01 g/cm^3). Corresponding values of the diffusion coefficient for the 0.10M sodium acetate (4.7 pH) and 0.15M NaCl (7.4 pH) systems are 6.79×10^{-7} and 6.91×10^{-7} cm^2/sec, respectively. Experiments were performed at 23.5°C. Both Creeth (1952) and Charlwood (1953) have reported the diffusivity of dilute BSA solutions to be within the range of 6.6×10^{-7} to 7.1×10^{-7} cm^2/sec at 25°C. Their data also show that the effects of pH value and buffer type upon the diffusion coefficient are negligible. This observation is in agreement with our measurements.

The gelling concentration of BSA in saline solution (7.4 pH, 25°C) has been independently determined by Kozinski and Lightfoot (1972) to be 0.585 g/cm^3. As for BSA in acetate solution (4.7 pH), there are no direct determinations of gelling concentration reported in the literature. Probstein et al. (1978) have indirectly determined the value of gelling concentration to be 0.340 g/cm^3 (4.7 pH, acetate buffer system) through their interpretation of parallel plate data using film theory principles.

Batch cell experiments were performed in stainless steel pressure cells manufactured by the Gelman Filter Co. Average membrane area equalled 15.62 cm^2 and the total cell volume was approximately 230 cm^3. The batch cells were affixed to a support integral with the building structure to prevent extraneous vibration and the room temperature was controlled within the range of 21-24°C. Total permeate volume was gravimetrically measured as a function of time for periods as long as 20 hours. The batch cell geometry was such that a volume correction of 2 mL had to be added to the initial permeate volume measurement to account for permeate trapped in the cell. The value of the correction was confirmed experimentally. Cell pressure was varied from 2.76×10^5 to $10.34 \times 10^5 N/m^2$ (40 to 150 psig). A schematic diagram of the batch cell apparatus is shown in Fig. 2.

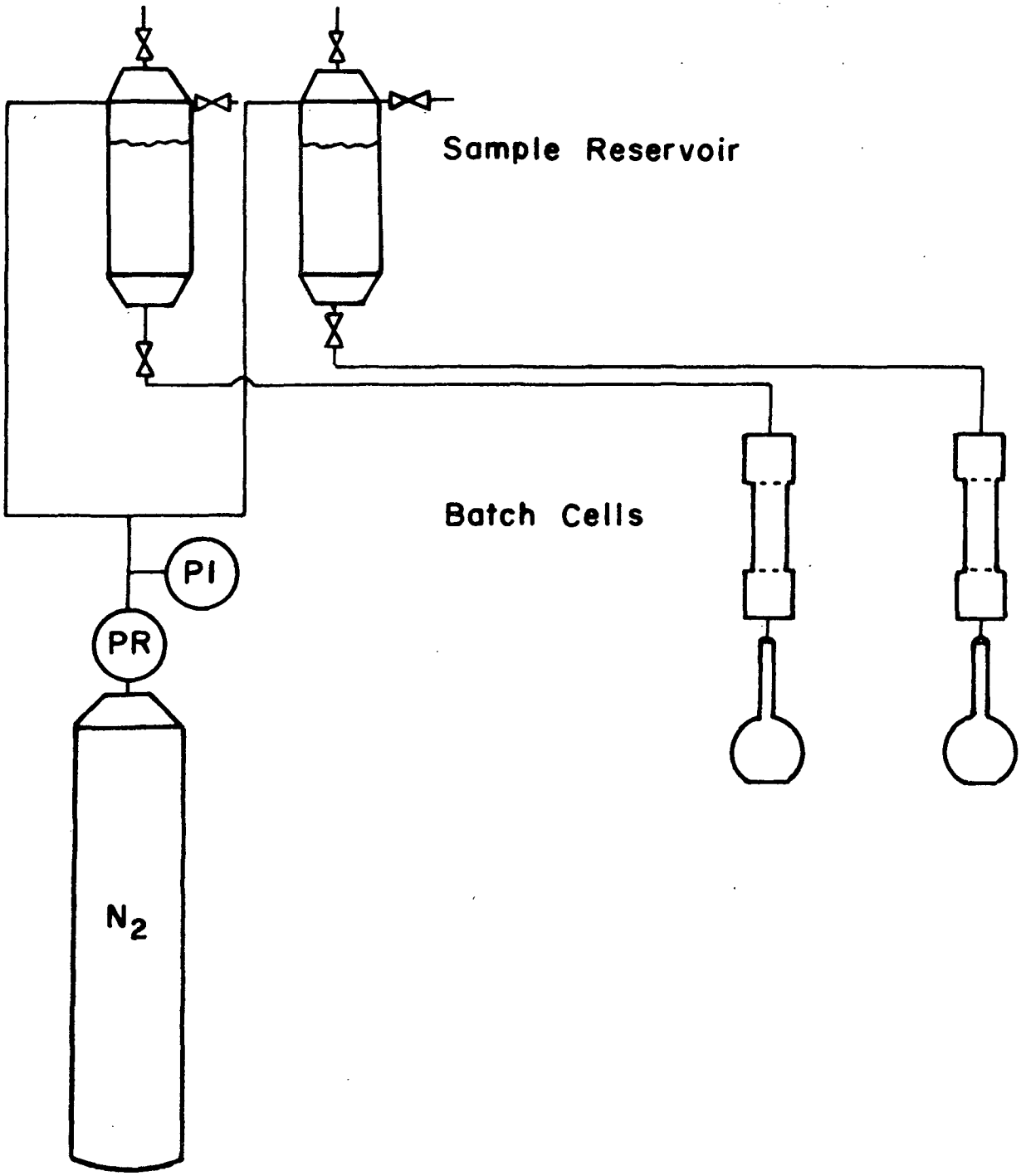

Figure 2. Batch cell arrangement.

The majority of the batch cell experiments were done using cellulose acetate membranes (5,000-10,000 MW cutoff) supplied to us through the courtesy of UOP-Fluid Systems. Several experiments were additionally conducted using a noncellulosic

(X-117) and polysulfone membrane also from UOP-Fluid Systems. Both noncellulosic membranes performed as well as the cellulose acetate membrane, yielding solute rejections greater than 95%.

ANALYSIS OF DATA

From the integral method analysis of the batch cell it was shown that

$$V_w(D/4)^{1/2} = \left| v_w \right| t^{1/2} = \text{constant} \tag{7}$$

Let A = the transport surface area of the membrane, and $B = AV_w(D/4)^{1/2}$; therefore

$$A \left| v_w \right| = Bt^{-1/2} \tag{29}$$

integrating with respect to t from 0 to T yields

$$\int_0^T A \left| v_w \right| dt = \Delta V = 2BT^{1/2} \tag{30}$$

where ΔV equals the total permeate collected from t = 0 to t = T. If ΔV_i represents permeate collected between time t = 0 and $t = T_i$, we have from Eq. (30)

$$\frac{\Delta V_2 - \Delta V_1}{\Delta V_3 - \Delta V_1} = \frac{T_2^{1/2} - T_1^{1/2}}{T_3^{1/2} - T_1^{1/2}} \tag{31}$$

In all experiments, permeate collection measurement times were selected so that $T_2 = 2T_1$ and $T_3 = 4T_1$, giving

$$\frac{T_2^{1/2} - T_1^{1/2}}{T_3^{1/2} - T_1^{1/2}} = 0.4142 \tag{32}$$

Acceptability limits of the data were established as $\pm$ 3% of the 0.4142 value. It may be noted that 83% of the collected data fell within this range, and over 94% of the collected data fell within the $\pm$ 4% range limits. Results of the above analysis show that the average time to reach a limiting condition at the membrane surface is indeed less than the first experimental collection time (T_1).

Even though the duration of the pregel region is short, the permeate collected during this time may represent a sizable percentage of total permeate collected at longer times. This is particularly true for situations where the bulk solute concentrations (c_o) are high and consequent permeate fluxes are small. Also because it was not possible to clean the membranes effectively to restore initial pure solvent flux, new membranes were used in each sample run. This fact introduces the additional complication of variable pure solvent flux and rejection coefficients between experiments which in turn affect the rate of accumulation of solute at the membrane surface in the pregel region. It is, therefore, necessary to utilize a method of data analysis so that the effects of membrane variation in the pregel region may be minimized.

It was observed from experimental data that when values of 2B were calculated from a permeate volume difference relationship, a constant value to within 3% was obtained for the various time intervals used [(T_2, T_1), (T_3, T_1), or (T_3, T_2)]. However, when this same value of 2B was used in Eq. (30) to back calculate the corresponding values of ΔV_1, ΔV_2, and ΔV_3, differences as great as 20% were found between experimental measurements and the calculated values of ΔV. Also, it is known that pregel permeate flux will be greater than the corresponding gel limiting flux, since the secondary hydraulic resistance of the gel layer is not present. Therefore, in a system where both a pregel and gel regions are found, collected permeate will be greater than in the equivalent gel polarized system. In view of the cited observations, a correction factor was subtracted from experimentally measured permeate volumes

$$\Delta V = \Delta V_{exp} - \Delta V_{corr} \tag{33}$$

Clearly, Eq. (33) has no effect upon a permeated volume difference relationship, since the correction volume cancels outs. However, Eq. (30) becomes

$$\Delta V_{exp} - \Delta V_{corr} = 2BT^{1/2} \tag{34}$$

Equation (34) can be rewritten as

$$\frac{\Delta V_{exp}}{T^{1/2}} = 2B + \Delta V_{corr}(1/T^{1/2}) \tag{35}$$

By plotting $\Delta V_{exp}/T^{1/2}$ vs. $1/T^{1/2}$ and extrapolating to infinite time (T), it is possible to minimize the effects of the pregel region (ΔV_{corr}) and determine the appropriate value of 2B. The value of ΔV_{corr} may also be determined from the slope. The true value of $\Delta V/T^{1/2}$ resulting from the pregel region correction is referred to as

$$\lim_{T\to\infty}\left[\frac{\Delta V}{T^{1/2}}\right] = 2B \tag{36}$$

Results of the BSA batch cell experiments are given in Tables II and III. Data are also displayed in Fig. 3 and 4. The noted correlation factors represent the accuracy of the data fit to a straight line. Calculations were performed using a linear regression analysis program, and a factor of 1 represents a perfect correlation. The sample scheme (Table IV) represents the times at which the collected permeate volume was measured.

Average values of bulk concentration and corresponding extrapolated values of $\Delta V_{exp}/T^{1/2}$ (or $\Delta V/T^{1/2}{}_{lim}$) are plotted in Fig. 5 and 6 for the two solvent systems. The dashed line in Fig. 5 represents the theoretically calculated values of $\Delta V/T^{1/2}$ from the integral method solution using Kozinski and Lightfoot's (1972) value of 0.585 g/cm^3 for c_g. The value at the diffusion coefficient was taken as 6.91 x 10^{-7} cm^2/sec from our ultracentrifuge experiments. In comparison, the values of c_g and D used by Probstein et al. (1978, 1979) for BSA in the saline solvent system (7.4 pH) were 0.580 g/cm^3 and 6.7 x 10^{-7} cm^2/sec, respectively. Correspondingly, the dashed line in Fig. 6 represents the integral method solution where the value of diffusion coefficient was taken as 6.79 x 10-7 cm2/sec. Since an independent

TABLE II

BSA, 0.15M NaCl, 7.4 pH

c_o, g/cm^3	$\Delta P \times 10^{-5}$, N/m^3	$(\Delta V/T^{1/2})_{lim}$, mL · sec$^{-1/2}$	Correlation Factor	Sample Scheme	ΔV_{corr}, mL	$\Delta V_{corr}/\Delta V_1$	Curve in Figure 3
0.0051	10.34	0.2014	0.99	B	1.6180	0.07	
0.0098	10.34	0.1434	0.99	A	1.8210	0.13	1
0.0098	10.34	0.1446	1.00	A	1.8623	0.13	2
0.0103	6.89	0.1355	1.00	B	2.4433	0.15	3
0.0103	10.34	0.1362	1.00	B	2.1286	0.13	4
0.0217	4.14	0.0879	1.00	A	1.8621	0.20	5
0.0217	6.89	0.0885	1.00	A	0.9221	0.11	6
0.0219	6.89	0.0879	1.00	A	1.3360	0.15	7
0.0215	10.34	0.0877	1.00	A	0.4945	0.06	8
0.0515	6.89	0.0532	1.00	C	2.1417	0.23	9
0.0510	10.34	0.0529	1.00	C	0.9142	0.11	10
0.0973	6.89	0.0343	1.00	C	0.1065	0.02	11
0.0973	10.34	0.0345	--	C	0.0313	0.01	12

TABLE III

BSA, 0.10M SODIUM ACETATE, 4.7 pH

c_o, g/cm^3	$\Delta P \times 10^{-5}$, N/m^3	$(\Delta V/T^{1/2})_{lim}$, mL · sec$^{-1/2}$	Correlation Factor	Sample Scheme	ΔV_{corr}, mL	$\Delta V_{corr}/\Delta V_1$	Curve in Figure 4
0.0051	6.89	0.1553	--	A	0.1383	0.01	1
0.0050	10.34	0.1564	0.99	B	1.0245	0.06	2
0.0093	6.89	0.1096	1.00	B	2.6298	0.19	3
0.0093	10.34	0.1092	0.99	B	1.4968	0.12	4
0.0213	6.89	0.0680	1.00	A	0.6917	0.11	5
0.0209	10.34	0.0694	0.95	C	0.5202	0.05	6
0.0492	6.89	0.0398	1.00	C	0.9081	0.15	7
0.0493	10.34	0.0404	0.98	C	0.4479	0.08	8
0.0952	6.89	0.0267	1.00	C	0.2411	0.06	9
0.0958	10.34	0.0255	0.99	C	0.2723	0.07	10

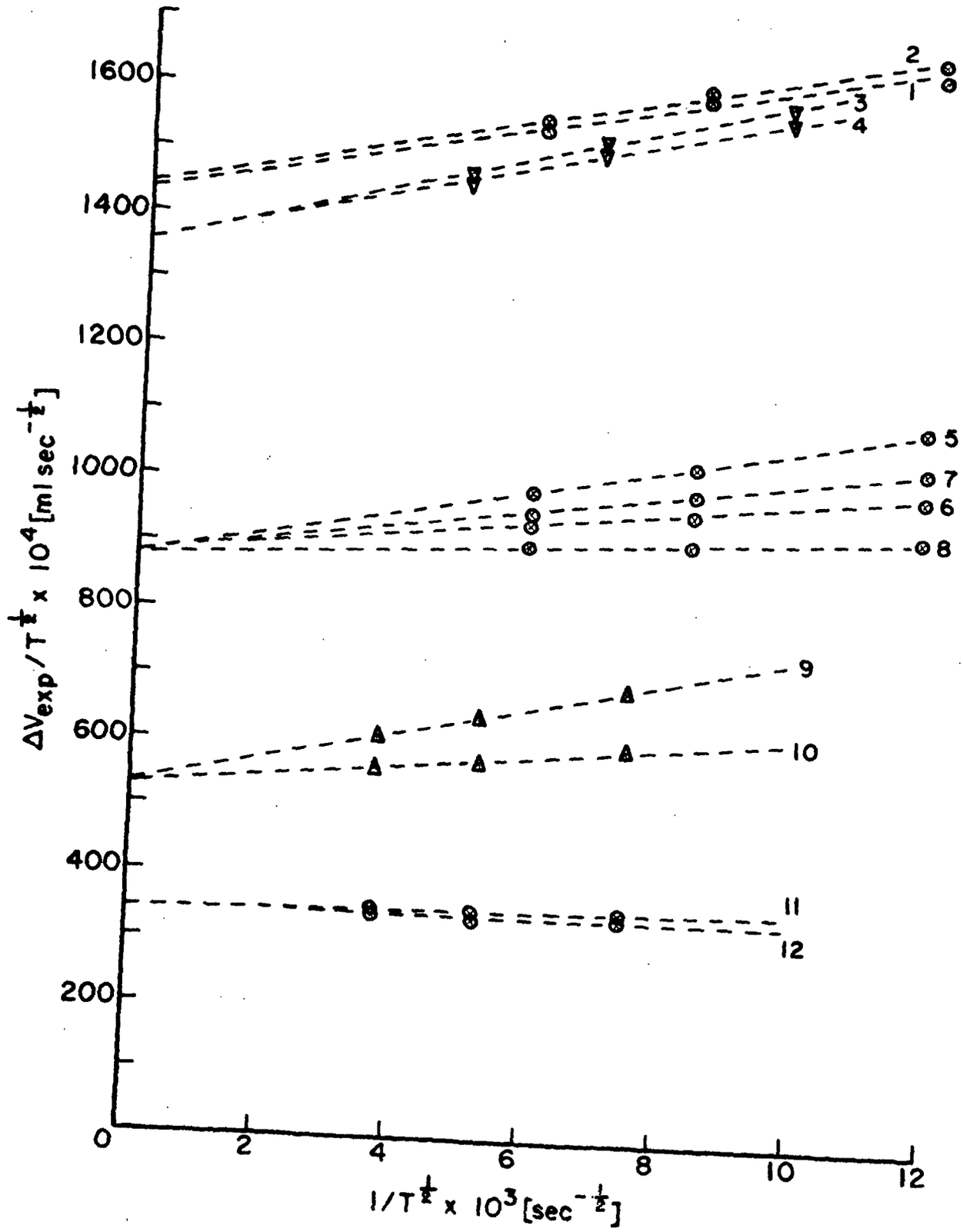

Figure 3. BSA 0.15M NaCl, 7.4 pH.

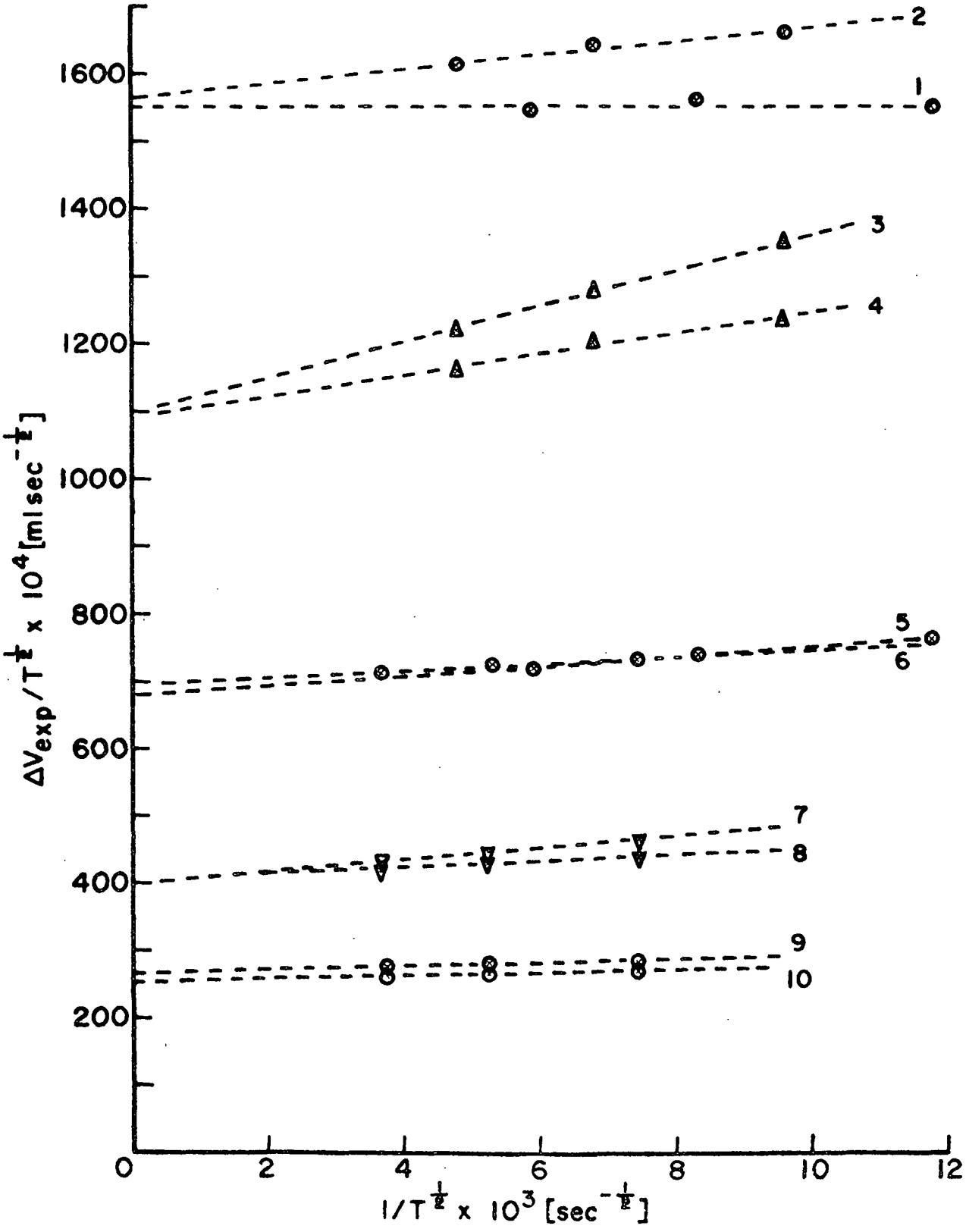

Figure 4. BSA, 0.10M sodium acetate, 4.7 pH.

measurement of c_g for the acetate BSA system is not available, the value of c_g was interpreted to be 0.385 g/cm^3 from fit of data to the integral method solution. The solid lines in Fig. 5 and 6 represent the film theory predictions of $\Delta V/T^{1/2}$ using the respective values of c_g and D cited above for each solvent system. In comparison, the values of c_g and D determined by Probstein et al. (1978, 1979) for BSA in the acetate solvent system (4.7 pH) were 0.340 g/cm^3 and 5.6 x 10^{-7} cm^2/sec, respectively. Since their values for the acetate system vary considerably from ours, plots of the integral method model and the film theory model using their values of c_g and D are also shown in Fig. 6. Both Fig. 5 and 6 indicate that the integral method model fits data well with an average variance of $\pm$ 4%, while the film theory consistently underpredicts experimental flux measurements. If a straight line approximation is fit to the experimental data in an attempt to satisfy the film theory model, the result would necessitate an unrealistically high diffusion coefficient value of 6.1-0.7 x 10^{-6} cm^2/sec. This range of values represents an order of magnitude difference from published values.

TABLE IV

DATA COLLECTION PATTERNS

Sample Scheme	Times of Measurement, hours
A	2, 4, 8
B	3, 6, 12
C	5, 10, 20

Figure 7 is an interesting plot showing that the variable c_g/c_o (or F_g) is the independent variable in the integral method model. This explains the experimental observation of two different permeation rates for the same value of c_o in the saline and acetate systems. This is due to the fact that even though c_o is the same, the values of c_g are different in each solvent system and therefore, c_g/c_o has different values.

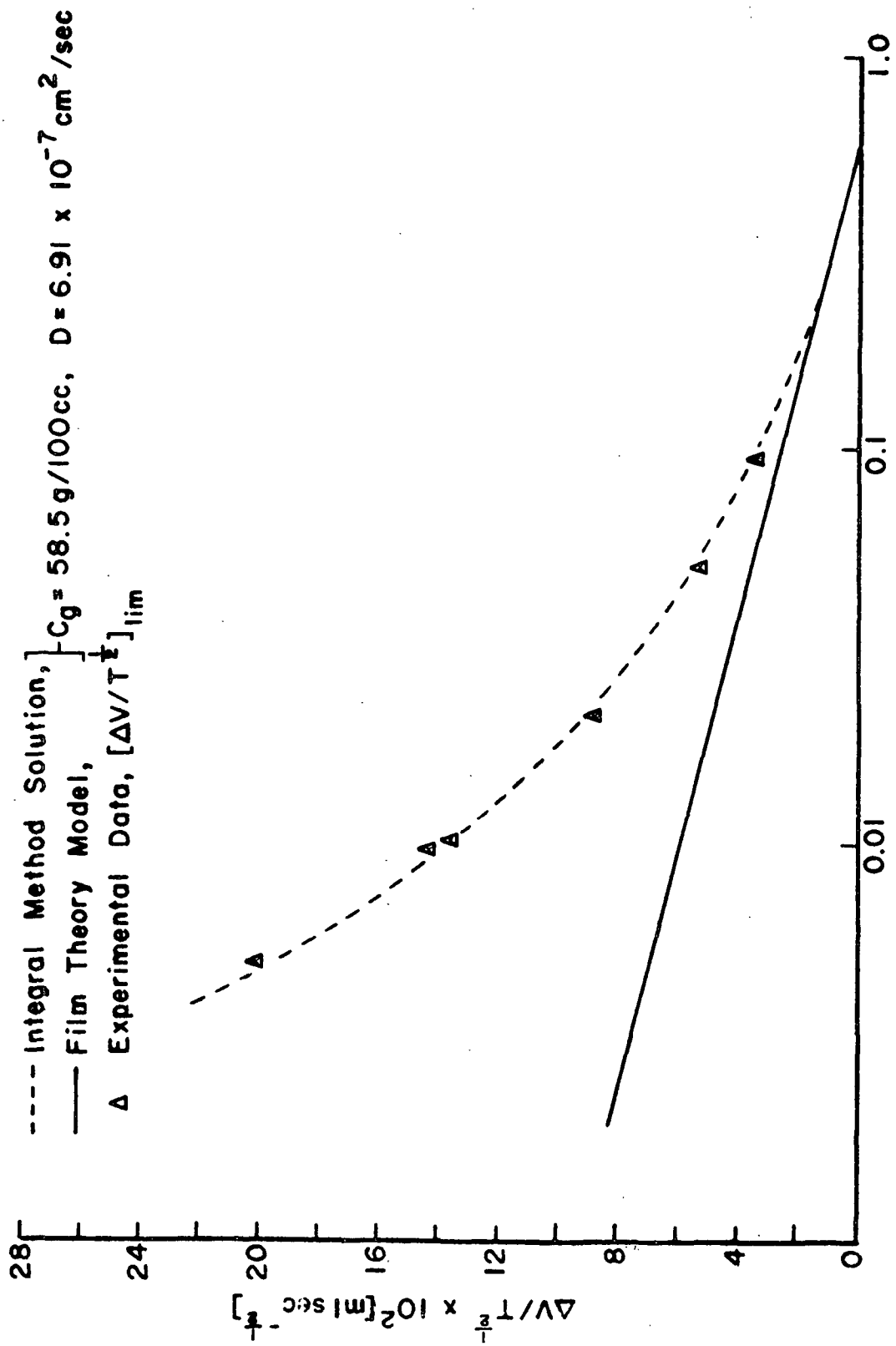

Figure 5. BSA, 0.15M NaCl, 7.4 pH.

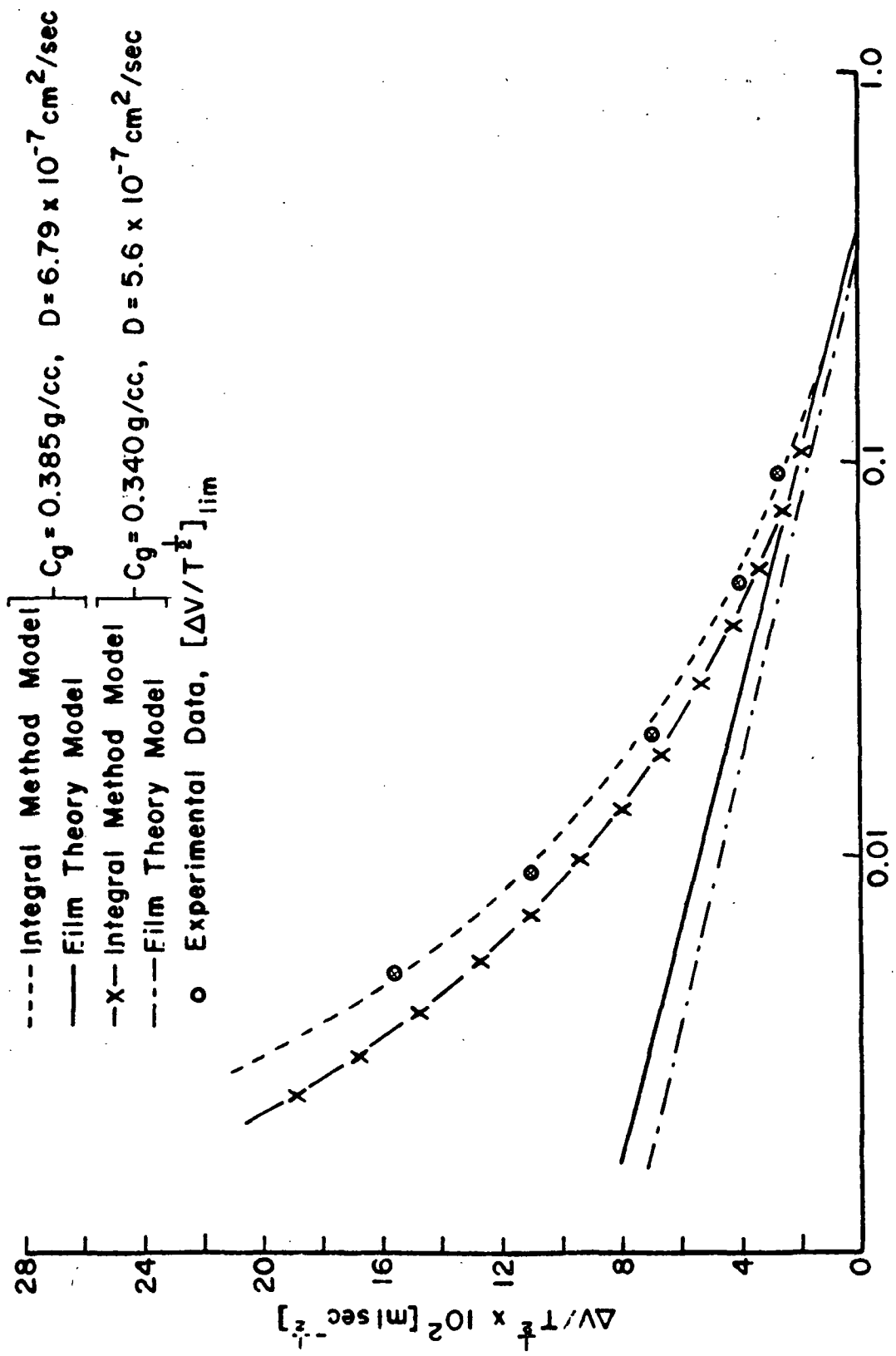

Figure 6. BSA, 0.10M sodium acetate, 4.7 pH.

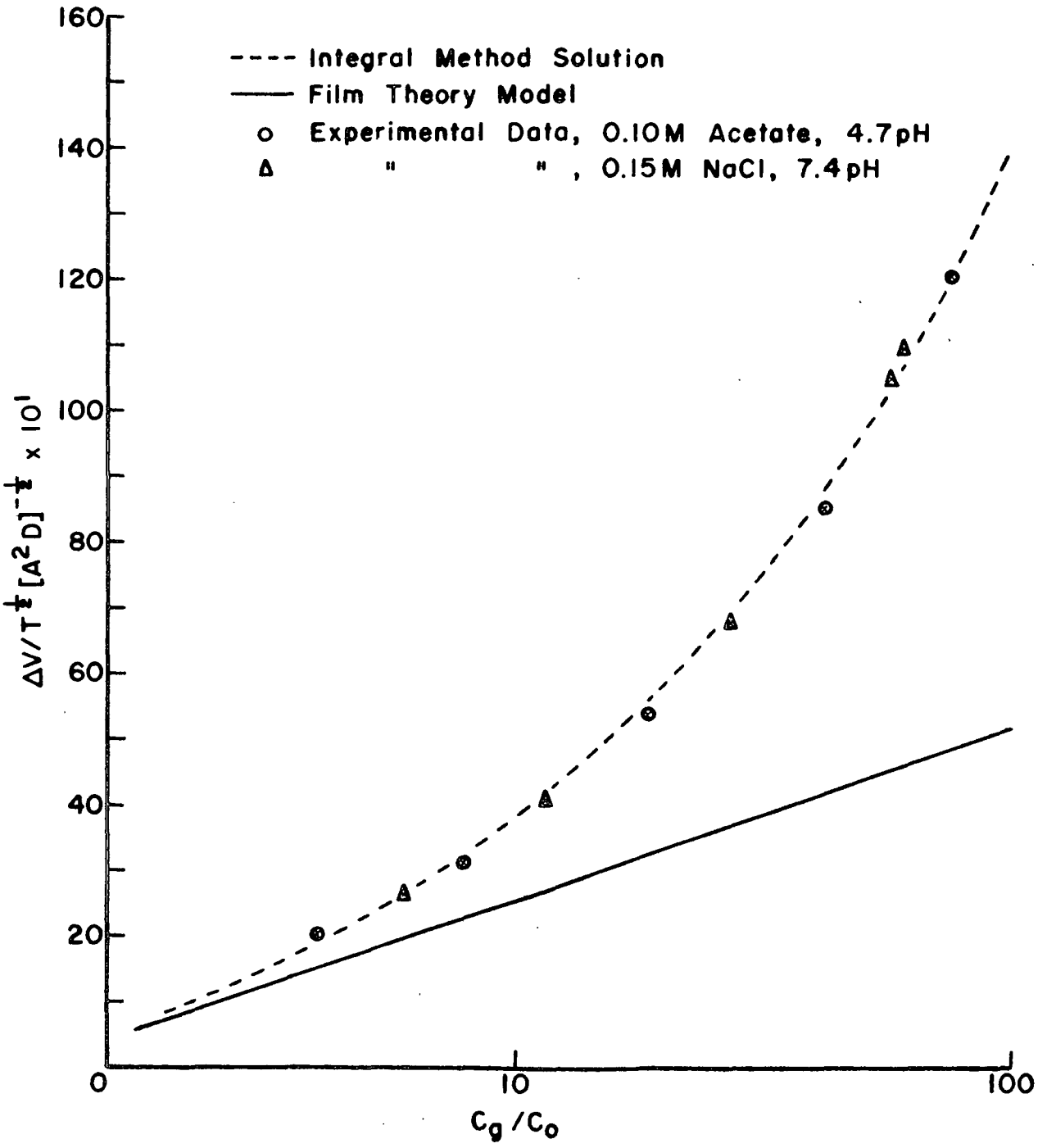

Figure 7. V_w versus c_g/c_o.

Several of the solutions listed in Tables II and III were studied at lower cell pressures, namely, $2.76 \times 10^5 \underline{N}/m^2$ and $4.14 \times 10^5 \underline{N}/m^2$. The analysis of these systems yielded values of $[\Delta V/T^{1/2}]_{lim}$ approximately 10 to 15% less than the values at identical concentration and higher pressure. Also, the extrapolated lines of the $\Delta V_{exp}/T^{1/2}$ *vs.* $1/T^{1/2}$ plots for various low pressures and constant concentration did not intersect at the same point on the y axis as they did in the case of higher pressures. These results may mean that, at the lower pressures, a gel layer was not formed at the wall, but rather, the system was limited by the osmotic pressure of the BSA solution itself.

CONCLUSIONS

The primary conclusion of this work is that the logarithmic permeate flux behavior predicted by the widely accepted film theory model is not encountered in the unstirred batch cell system. Rather, flux rates are accurately predicted by a more exact theory. Values of the gel concentration and diffusion coefficient for the saline solvent system do, however, agree well with those determined by Shen and Probstein (1977) and Probstein et al. (1978, 1979) for their parallel plate system. In the acetate solvent system, there exists a discrepancy between Probstein's (1978) determinations of c_g and D and ours. Accurate analysis of data in terms of the integral method solution, which assumes a constant value of the diffusion coefficient, confirms negligible concentration dependence of the diffusion coefficient for BSA.

The low-pressure observations of linear $\Delta V/T^{1/2}$ vs. $1/T^{1/2}$ plots and nonintersecting values of $[\Delta V/T^{1/2}]_{lim}$ below those for higher system pressures indicate constant solute concentrations at the wall that are less than the corresponding BSA gel concentration.

Ideally, the values of c_g and D should be measured independently. The presented model is intended to be used to predict permeate variation with time. As shown in Fig. 8, a 5% error in the measured value of ΔV can give 8 to 10% error in the calculated value of c_g. We do not recommend the use of batch cell ultrafiltration to determine both c_g and D.

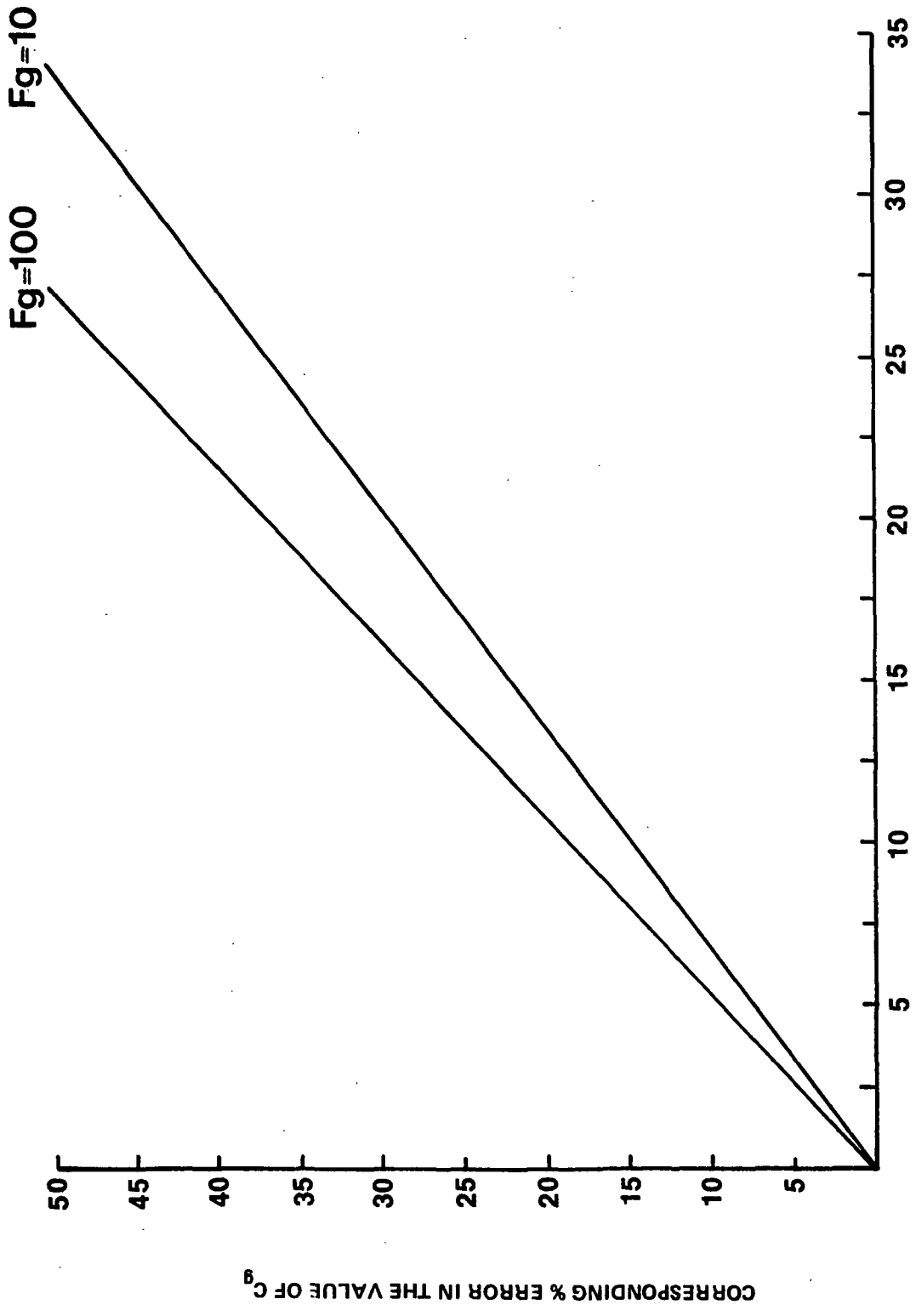

Figure 8. Error analysis - approximate sensitivity of the c_g to change in $\Delta V/T^{1/2}$.

ACKNOWLEDGMENT

The authors wish to express their gratitude to the member companies of The Institute of Paper Chemistry for their support of the graduate program. The authors are thankful to Mr. Richard A. Walker of UOP-Fluid Systems for his valued assistance during the course of the research.

NOMENCLATURE

B = dimensionless constant [Eq. (29)]

c = solute concentration, g/cm^3

D = solute diffusion coefficient, cm^2/sec

$F = c/c_o$

k = mass transfer coefficient, cm/sec

$K = 2n/(n+1)$

L = solution level in batch cell, cm

n = power law coefficient [Eq. (15)]

P = pressure, N/m^2

t = time, sec

T = permeate measurement time interval, sec

v = transverse velocity, cm/sec

V_w = dimensionless permeate constant [Eq. (7)]

y = transverse distance coordinate, cm

Greek Letters

$\delta(t)$ = concentration boundary layer thickness, cm

η = similarity variable [Eq. (15)]

ΔP = total pressure gradient, N/m^2

ΔV = permeate volume collected in time T, cm^3

$\theta = (c_g-c_o)/(c_g-c_p)$

Subscripts

a = at the ambient condition

cell = inside the cell condition

corr = correction

exp = experimental

g = at the gelling condition

i = at measurement i

lim = limiting

o = at the bulk solution condition

p = at the permeate condition

w = at the membrane surface condition

1,2,3 = at measurement 1,2,3

LITERATURE CITED

Blatt, W. F., Dravid, A., Michaels, A. S., and Nelsen, L. In Membrane science and technology, J. E. Flinn, ed., Plenum Press, New York. 1970. p. 47.

Charlwood, P. A., J. Phys. Chem. 57:125(1953).

Creeth, J. M., Biochem. J. 51:10(1952).

Creeth, J. M., J. Am. Chem. Soc. 77:6428(1955).

Doherty, P. and Benedek, G. B., J. Chem. Phys. 61:5426(1974).

Goldsmith, R. L., I&EC Fundam. 10:113(1971).

Keller, K. H., Canales, E. R., and Yum, S. I., J. Phys. Chem. 75:379(1971).

Kozinski, A. A. and Lightfoot, E. N., AIChE J. 18:1031(1972).

Longsworth, L. G., J. Am. Chem. Soc. 74:4155(1952).

Michaels, A. S., Chem. Eng. Prog. 64:31(1968).

Mitra, G. and Lundblad, J. L., Sepn. Sci. Technol. 13:89(1978).

Phillies, G. D. J., Benedek, G. B., and Mazer, N. A., J. Chem. Phys. 65:1883(1976).

Porter, M. C., I&EC Prod. Res. 11:234(1972).

Probstein, R. F., Shen, J. S., and Leung, W. F., Desalination 24:1(1978).

Probstein, R. F., Leung, W. F., and Alliance, Y., J. Phys. Chem. 83:1228(1979).

Shen, J. J. S. and Probstein, R. F., I&EC Fundam. 16:459(1977).

Tostevin, J. E., Ph.D. Dissertation, The Institute of Paper Chemistry, 1966.

Trettin, D. R. and Doshi, M. R. Limiting flux in ultrafiltration of macromolecular solutions. Chem. Eng. Commun. 4:508-22(1980).

SECTION 3 - MANUSCRIPT NUMBER 2

ULTRAFILTRATION OF COLLOIDAL SUSPENSIONS AND MACROMOLECULAR SOLUTIONS IN AN UNSTIRRED BATCH CELL

I&EC Fundam. 20:221-9(1981)

ULTRAFILTRATION OF COLLOIDAL SUSPENSIONS AND MACROMOLECULAR SOLUTIONS IN AN UNSTIRRED BATCH CELL

ABSTRACT

A general asymptotic theory for ultrafiltration in an unstirred batch cell is developed. In the theory, convective transport of solutes or particles to membrane surface is balanced by two components: accumulation of solids at the membrane surface to form a cake or a gel layer and diffusion of solids away from the membrane surface. Macromolecular ultrafiltration where convective flux is balanced by diffusive flux at the membrane surface and colloidal ultrafiltration where convective flux of solids contribute to the increase in cake thickness with negligible diffusive flux are special cases of the general theory. Macromolecular ultrafiltration results were presented in our earlier papers, Trettin and Doshi (1980, 1981). In this paper, we have studied the ultrafiltration of polymer latex suspension over wide concentration (0.001 to 0.150 g/cc) and pressure (2.76 to 9.64 x $10^5 \underline{N}/m^2$) ranges with different membranes. Data seem to follow constant pressure filtration relationships as required by the theory. As expected, the permeability of latex cakes is strongly dependent upon the physicochemical state of the solute. Some cross-flow ultrafiltration data are also presented.

INTRODUCTION

Currently, one of the major potential users of membrane separation equipment is the pulp and paper industry. Ammerlaan, et al. (1969) have studied the application of reverse osmosis to pulp mill effluents. A possible use of ultrafiltration, as noted by Bailey (1973), presently may be found in the treatment of paper machine "white water." Characteristically, white water is recycled back to pulping operations for use as dilution water. Unfortunately, because of the large volumes of white water generated by paper machines, pulping operations often do not provide an adequate outlet for the total flow. Consequently, white water overflow which cannot be reclaimed in some manner must be sent to a waste treatment plant. Besides representing a sizable hydraulic and pollutant load to the waste treatment plant, the purging of the white water system entails the loss of many costly papermaking additives such as TiO_2, clay, and various flocculants and dispersants. In the treatment of white water streams, ultrafiltration represents a viable process for providing clarified water and recovering papermaking chemicals which may be returned to stock preparation operations. Similar applications may be found in the dairy, food, pharmaceutical, metallurgical, paint, and other manufacturing industries. Because many waste effluents are largely colloidal in nature, a great interest has been placed upon the study of mass transfer mechanisms in colloidal ultrafiltration.

It has been known for some time that in continuous colloidal ultrafiltration (cross-flow filtration) the film theory model drastically underpredicts experimental permeate rates. One of the first studies to point out this fact was done by Blatt et al. (1970). In an attempt to explain this observation, Blatt et al. proposed that either (1) the back diffusion of colloidal particles from the polarized layer is substantially augmented beyond that expected to occur by classical Fickian diffusion mechanisms, or that (2) the permeate rate is not limited by the hydraulic resistance of the particle polarized layer. Of these two possibilities, Blatt et

al. favored the second explanation to be the more reasonable. They pointed out that although a gel layer of macromolecules (average particle size of 50-100 A) has a very high specific resistance, cakes formed from micron-sized particles have, in comparison, relatively small specific resistances. They reasoned that, in the ultrafiltration of particulate suspensions, a filter cake would continue to grow until it reached a point where further growth was curtailed by the applied axial fluid shear upon the system. In such a unit, Blatt et al. hypothesized that particle back diffusion from the cake surface may not be an important mass transport mechanism and that the steady-state cake thickness would be determined entirely by fluid dynamics. They concluded by stating that further experiments would be needed to confirm their hypothesis.

Porter (1972) observed essentially the same type of behavior as noted by Blatt et al. in the more than 40 colloidal suspensions he studied. Porter, however, chose the hypothesis of augmented solute back diffusion from the cake surface as an explanation of his observations. He stated that if the particle polarized layer is not the limiting resistance to flow, the following should be true: (1) permeate rate would be independent of concentration, (2) permeate rate would be proportional to the transmembrane pressure drop, and (3) the deposited layer would continue to grow until a significant portion of the channel is filled with cake. Porter clearly found the opposite behavior since he observed (1) decreasing permeation rates with increasing bulk solution concentration, (2) threshold pressures above which permeation rates are independent of pressure, and (3) no decrease in feed concentration and channel pressure drop with time. In an attempt to explain his experimental observations, Porter hypothesized the migration of particles toward the center known as the "tubular pinch effect" [Segre and Silberg (1962), Rubinow and Keller (1961), Karnis et al. (1966), Brenner (1966)]. Obviously, such an additional mechanism will

have a qualitative effect in agreement with experimental observation, but as it turns out, quantitative predictions are not good.

Henry (1972), in a review article on cross-flow filtration, pointed out the long transient flux decline in the ultrafiltration of colloidal suspensions. In the ultrafiltration of bacterial cells, steady-state flux behavior was finally reached after 18 hours of continuous operation. This may be compared to times of 1 hour or less for the attainment of typical macromolecular ultrafiltration steady-state. In the study of the effect of particle concentration upon permeation rate, the characteristic logarithmic behavior predicted by film theory was not observed. Henry found in general that the dependence of the permeation rate on fluid circulation rate (or shear rate) is greater in colloidal ultrafiltration than that predicted by the film theory model. This finding led Henry to the conclusion, like Porter, that an additional transport mechanism was present in such systems. Experiments comparing flocculated to unflocculated particles revealed that increases in flux rates of an order of magnitude could be obtained due to the increase in effective particle size.

Kraus (1974) has treated the observation of transient permeation rate decline in a manner similar to constant pressure filtration theory. Kraus states that a cake formed in cross flow filtration will continue to accumulate until its growth is arrested by the hydrodynamic shear of the system, at which point steady-state is reached. He further adds that, unfortunately, such steady-state operation rarely occurs and permeation often continues to decline in long term operation. It is Kraus' contention that in short term flux decline, the cross-flow filter acts like a conventional filter without cross flow, and the permeate volume varies with the square root of time if the resistance of the filter medium is negligible and the filter cake obeys Darcy's Law:

$$\Delta V = C_1 T^{1/2} \tag{1}$$

$$v_w = \frac{C_1}{2A} t^{-1/2}$$

This model only applies to the formation of an ideal filter cake where the initial cake forming period may be ignored.

Madsen (1977) semiempirically analyzed the problem of particle migration with the use of the particle movement formula of Cox and Brenner (1967, 1968) and the film theory model. He found that experimental permeate rates for cheese whey and hemoglobin were underpredicted by a factor of 50 by the particle migration model. His primary conclusion was that particle migration can only account for a part of the high permeate flux observed in ultrafiltration of colloidal suspensions. In summary, it would be desirable to have a unifying theory to explain the vast differences between the two apparently similar processes of macromolecular and colloidal ultrafiltration. The objective of this paper is to develop a model to explain the observed colloidal ultrafiltration behavior. A step toward this goal is taken here by considering a simple unstirred batch cell system. In the absence of axial convection in such systems, a "tubular pinch" mechanism may be immediately disregarded. A secondary reason for selecting the unstirred batch cell system is that a reliable model for macromolecular ultrafiltration has been previously derived [Trettin and Doshi (1980)] and would serve as a source of comparison to our new results. Experimental data taken in the unstirred batch cell ultrafiltration of styrene-butadiene polymer latex are analyzed in terms of the model. Our cross flow colloidal ultrafiltration data are discussed in light of the batch cell results.

THEORETICAL DEVELOPMENT

Consider the ultrafiltration of macromolecular solutions or colloidal suspensions in an unstirred cell geometry shown in Fig. 1. As the solvent or the suspending

medium permeates through the membrane, rejected solids accumulate at and diffuse away from the membrane surface. The objective is to predict the permeation rate, v_w, by considering both accumulation and diffusion of the rejected solids.

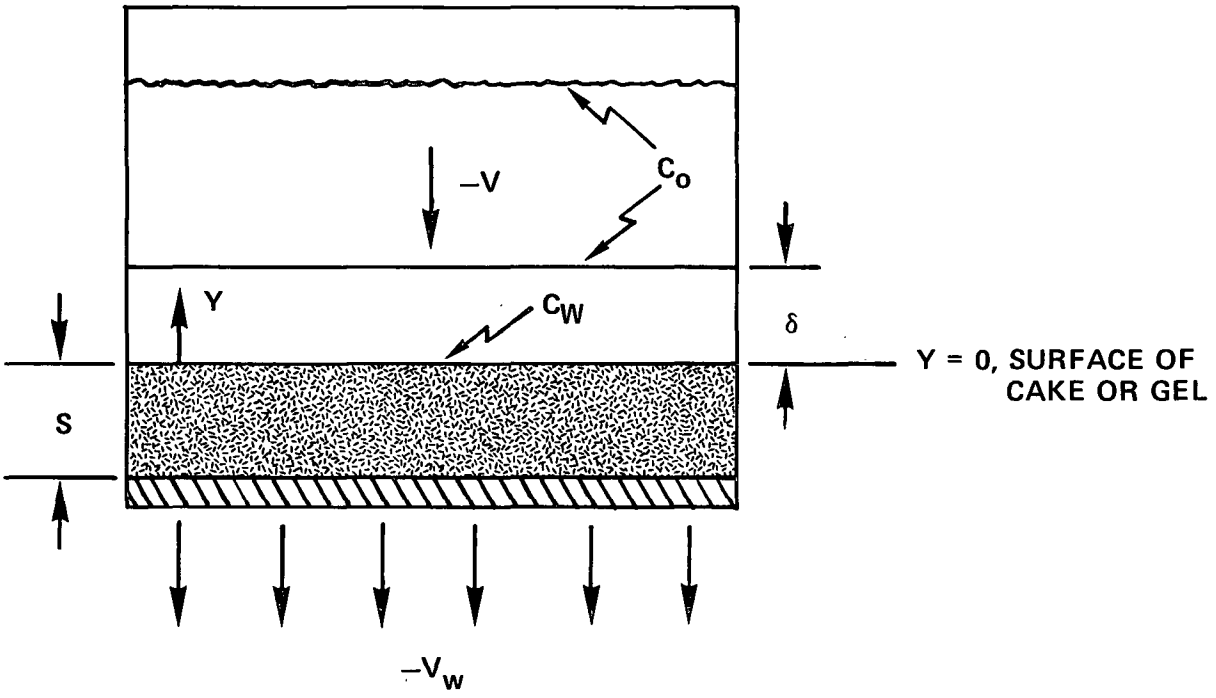

Figure 1. Batch cell geometry.

The solute mass balance equation can be written as:

$$\partial c/\partial t + v\ \partial c/\partial y = D\ \partial^2 c/\partial y^2 \qquad (3)$$

It is implicitly assumed in the derivation of Eq. (3) that the density of the solid is approximately that of the liquid.

The appropriate boundary and initial conditions are

$$c(o,y) = c(t,\ \delta \text{ or } \infty) = c_o \qquad (4)$$

$$c(t,o) = c_w \qquad (5)$$

$$n_s = v\ c_w - D\ [\partial c/\partial y]_{y=o} \qquad (6)$$

Since the velocity, v, in Eq. (3) is relative to the moving cake surface

$$v = v_w - \frac{dS}{dt} = v_w + \frac{n_s}{\rho_s(1-\varepsilon)} \tag{7}$$

From Darcy's Law, the permeation velocity can be written as

$$-v_w = \frac{\Delta P}{\alpha\mu\ \rho_s(1-\varepsilon)S} \tag{8}$$

The boundary condition, Eq. (6) becomes

$$\frac{\Delta P}{\alpha\mu\ \rho_s(1-\varepsilon)}\ v_w - 2\ \frac{dv_w}{dt} = \frac{c_w v_w - D\ \frac{\partial c}{\partial y}\Big|_{y=o}}{c_w - \rho_s(1-\varepsilon)} \tag{9}$$

with the substitution of Eq. (7) and (8).

In order to remain consistent with the large time asymptotic solution used in this model, the hydraulic resistance of the membrane has been neglected in Eq. (8). This is a common assumption used in filtration systems where filtrate flux is much smaller than pure solvent flux under equivalent conditions. Such is found to be the case at large ultrafiltration times.

A notable variation between the model presented in this report and previous ultrafiltration models is that a net solute flux term (n_s) is utilized as shown in Eq. (6), which accounts for solute accumulation at the membrane surface. Also, transverse distance is measured from the cake or gel layer surface instead of the membrane surface, which is characteristic of previous models. While gel thickness in macromolecular ultrafiltration is typically small due to negligible solute accumulation, such is not the case in colloidal ultrafiltration where cake thickness may surpass mass transfer boundary layer thickness (δ). For certain materials both cake buildup and boundary layer could be important.

By defining the following dimensionless variables,

$$\eta = \frac{y}{(4Dt)^{1/2}}, \quad K = \frac{\alpha\mu Dc_o}{\Delta P} \tag{10}$$

$$V_w = -v_w \left(\frac{4t}{D}\right)^{1/2} = \text{constant}, \quad \theta = \frac{c-c_o}{c_o}, \quad \theta_w = \frac{c_w-c_o}{c_o} \tag{11}$$

$$S^+ = \frac{S}{(4Dt)^{1/2}} = \text{constant} \tag{12}$$

$$N_s = -\frac{n_s}{c_o}\left(\frac{4t}{D}\right)^{1/2} = \text{constant}, \quad \phi = 1 - \frac{c_o}{\rho_s(1-\varepsilon)}$$

Equations (3)-(5) may be transformed to

$$\frac{d^2\theta}{d\eta^2} + \left(2\eta + V_w + \frac{2(1-\phi)}{KV_w}\right)\frac{d\theta}{d\eta} = 0 \tag{13}$$

$$\theta\ (\infty) = 0 \tag{14}$$

$$\theta\ (o) = \theta_w \tag{15}$$

Similarly, Eq. (9) transforms to

$$1 = \frac{K}{2}\left(\frac{1}{\phi - \frac{\theta_w}{\theta_w+1}}\right) V_w \left(V_w + \frac{\frac{d\theta}{d\eta}\Big|_{\eta=o}}{\theta_w+1}\right) \tag{16}$$

Equation (13) may be integrated to yield

$$\frac{\theta_w}{\theta_w+1} = \frac{\left(V_w - \frac{2\phi}{KV_w}\right)\frac{\sqrt{\pi}}{2}\left(\exp\left(\frac{V^2}{4}\right)\operatorname{erfc}\left(\frac{V}{2}\right)\right)}{1 - \frac{\sqrt{\pi}}{KV_w}\exp\left(\frac{V^2}{4}\right)\operatorname{erfc}\left(\frac{V}{2}\right)} \tag{17}$$

or simply,

$$\frac{c_o}{c_w} = 1 - \frac{\left(V_w - \frac{2\phi}{KV_w}\right)\frac{\sqrt{\pi}}{2}\left(\exp\left(\frac{V^2}{4}\right)\operatorname{erfc}\left(\frac{V}{2}\right)\right)}{1 - \frac{\sqrt{\pi}}{KV_w}\exp\left(\frac{V^2}{4}\right)\operatorname{erfc}\left(\frac{V}{2}\right)} \tag{18}$$

where

$$V = V_w + \frac{2(1-\phi)}{KV_w} \tag{19}$$

It can be shown from Eq. (8) and (9)-(12) that

$$K = \frac{2(1-\phi)}{V_w}\left[\frac{(Dt)^{1/2}}{S}\right] \tag{20}$$

or, since δ is proportional to $(Dt)^{1/2}$,

$$K \propto \frac{\delta}{S} \tag{21}$$

Thus in physical terms, the parameter K is proportional to the ratio of the mass transfer boundary layer thickness to the accumulated cake thickness.

When we consider the limiting case where solute accumulation is negligible ($n_s \to o$) Eq. (19) and (20) reduce to

$$K \to \infty,\ V \to V_w \tag{22}$$

Equation (18) for the case of no solute accumulation becomes

$$\frac{c_o}{c_w} = 1 - \frac{\sqrt{\pi}}{2} V_w \exp\left[\frac{V_w^2}{4}\right] \operatorname{erfc}\left[\frac{V_w}{2}\right] \tag{23}$$

Equation (23) is identical to the limiting flux relationship derived by Trettin and Doshi (1980, 1981). In the unstirred batch cell ultrafiltration of macromolecular solutions, c_w approaches an asymptotic value in a relatively short period (generally less than a minute) when the permeate rate is independent of pressure. The

asymptotic value of c_w may correspond to the solute solubility limit when gel formation occurs (gel limited case) or c_w may be equal to the concentration at which osmotic pressure is the same as the applied pressure (osmotic pressure limited case). Trettin and Doshi (1980, 1981) have shown that Eq. (23) yields excellent predictive results for permeation rates in the unstirred batch cell ultrafiltration of bovine serum albumin. Also we have shown (Trettin and Doshi, 1981) that an unstirred batch cell can be used to determine whether macromolecular ultrafiltration is gel limited or osmotic pressure limited.

When the limiting condition of negligible solute back diffusion is considered, mass transfer boundary layer thickness, θ_w and K will approach zero. From Eq. (17), then

$$\frac{2\phi}{K} \rightarrow V_w^2 \tag{24}$$

The equation, $V_w = -v_w \left(\frac{4t}{D}\right)^{1/2}$, is applicable to both the macromolecular and colloidal ultrafiltration. Since V_w is constant, one can conclude that the limiting flux in unstirred batch ultrafiltration is inversely proportional to the square root of time irrespective of the nature of the dissolved or suspended material.

For ultrafiltration of colloidal suspensions where solute back diffusion from the cake surface may be neglected, Eq. (11) and (24) can be combined to give

$$\left| v_w \right| = \left(\frac{2\phi}{K}\right)^{1/2} \left(\frac{D}{4t}\right)^{1/2} = \left(\frac{D\phi}{2K}\right)^{1/2} t^{-1/2} \tag{25}$$

Integrating Eq. (25) between the arbitrary time, T^*, which represents the initial time where Eq. (25) applies, and the variable time, T, yields

$$\int_{T^*}^{T} A \left| v_w \right| dt = \left(\frac{A^2 D\phi}{2K}\right)^{1/2} \int_{T^*}^{T} t^{-1/2}\, dt \tag{26}$$

$$\Delta V = \Delta V^* = \left(\frac{2A^2 D\phi}{K}\right)^{1/2} \left[T^{1/2} - T^{*1/2}\right] \tag{27}$$

Let $\Delta V_{corr} = \left(\frac{2A^2 D\phi}{K}\right)^{1/2} T^{*1/2} - \Delta V^*$ = constant, so that Eq. (27) becomes

$$\Delta V = \left(\frac{2A^2 D\phi}{K}\right)^{1/2} T^{1/2} - \Delta V_{corr} \tag{28}$$

where,

$$\frac{2A^2 D\phi}{K} = \frac{2A^2 \Delta P}{\alpha \mu k}, \quad k = \frac{c_o \rho_s}{\rho_s - \left(\frac{1}{1-\varepsilon}\right) c_o}, \quad \alpha = \frac{150(1-\varepsilon)}{D_p{}^2 \varepsilon^3 \rho_s} \tag{29}$$

The value of α (the specific cake resistance) is determined from the Kozeny-Carman relationship for flow through porous media. Equations (25) and (28) are similar to those developed by Kraus (1974) for cross-flow filtration.

Let us compare flux predictions using Eq. (25) and the film theory model for the unstirred batch cell, which is presented in Eq. (30)

$$\left| v_w \right| = \left[\frac{D}{\pi t}\right]^{1/2} \ln\left[\frac{c_w}{c_o}\right] \tag{30}$$

Adopting Porter's (1972) values of

$$c_w = 0.75 \text{ g/cc}, \quad c_o = 0.10 \text{ g/cc}$$

$$D_p = 1.9 \times 10^{-5} \text{ cm}, \quad \varepsilon = 0.25$$

$$\Delta P = 4.14 \times 10^5 \underline{N}/m^2, \quad D = 2.3 \times 10^{-8} \text{ cm}^2/\text{sec}$$

for styrene-butadiene latex particles, from Eq. (25)

$$\left| v_w \right| = 9.91 \times 10^{-3} \left[t^{-1/2}\right] \text{ (cm/sec)}$$

and, from Eq. (30)

$$\left| v_w \right| = 1.72 \times 10^{-4} \left[t^{-1/2}\right] \text{ (cm/sec)}$$

Equation (25) predicts a flux rate which is 58 times greater than the corresponding film theory model. This order of magnitude difference for the unstirred batch cell system certainly agrees well with the experimental differences cited by both Blatt et al. (1970) and Porter (1972) for the cross-flow ultrafiltration system. Thus, a detailed investigation may validate Kraus' (1976) contention that a cross-flow filtration system behaves like a batch system.

In summary, a general theory has been developed which unifies the two separate theories of macromolecular ultrafiltration and constant pressure filtration. It has been shown that the value of the parameter, K, is critical in the determination of the principal transport mechanism. When $K \to \infty$, back diffusion of solute from the gel surface is limiting and is typical of macromolecular ultrafiltration. In such cases, the net solute transport to the gel, n_s, is negligible. When $K \to 0$, the principal transport mechanism is transverse convection with accumulation of solute at the membrane surface. This condition will be shown in the data analysis section to apply to the ultrafiltration of latex particles in the size range of 0.2-0.5 micron. It is interesting to note that in the ultrafiltration of very small particles (< 0.0 micron), or, a mixture of macromolecules and colloidal particles, a condition may be reached where Eq. (23) or (24) will not apply. Bixler and Rappe (1970) have observed that macromolecular ultrafiltration rates can be increased by the addition of a small amount of spherical glass beads to the cross-flow system. This flux augmentation was attributed to the presence of a "tubular pinch mechanism" which aided the back diffusion of retained solute from the membrane surface. Doshi (1979) has shown, however, that such augmentation of flux is also achieved in the unstirred batch cell by the addition of TiO_2 particles to starch solution. In this case, it is possible that the value of the constant K is somewhere between the two extreme limits of zero (colloidal filtration) and infinity (macromolecular ultrafiltration).

It is hypothesized that large particles interfere with the formation of a coherent gel structure and thereby increase permeability.

The variations of dimensionless V_w with c_w/c_o for various values of ϕ and K, as predicted from Eq. (18) are depicted in Fig. 2 and 3. It may be noted the Eq. (18) is relatively insensitive to change in ϕ and large values of K (K > 1). Filtration in the intermediate regions should, however, follow the general form of Eq. (18).

ANALYSIS OF DATA

The unstirred batch cell ultrafiltration of polymer latex was studied over a wide concentration (0.001-0.150 g/cc) and pressure (2.76-9.65 x 10^5N/m^2) range. The latex used was obtained through the courtesy of Dow Chemical Company (Dow DPP-722) and the particle size distribution was fairly narrow (average particle size = 4.0 x 10^{-5} cm). Solutions were prepared in distilled-deionized water and adjusted to 8.50 pH by the addition of sodium hydroxide. In experiments where flocculated solutions were studied, alum [Na $Al(SO_4)_2$ • 18 H_2O] of concentration 18 g latex/1 g alum was added as the flocculant and the pH was adjusted to 5.50. Total permeate volume was gravimetrically measured as a function of time for periods up to approximately 22 hours. Batch cell experiments were performed in stainless steel pressure cells manufactured by the Gelman Filter Company. Average membrane area equalled 15.62 cm^2 and the total cell volume was approximately 230 cm^3. The batch cells were affixed to a support integral with the building structure to prevent extraneous vibration, and average room temperatures were recorded during the experimental period for each solution tested. The batch cell geometry was such that a volume correction of 2 mL had to be added to the initial permeate volume measurement to account for permeate trapped in the cell. This volume correction was confirmed experimentally. A schematic diagram of the batch cell apparatus is shown in Fig. 4.

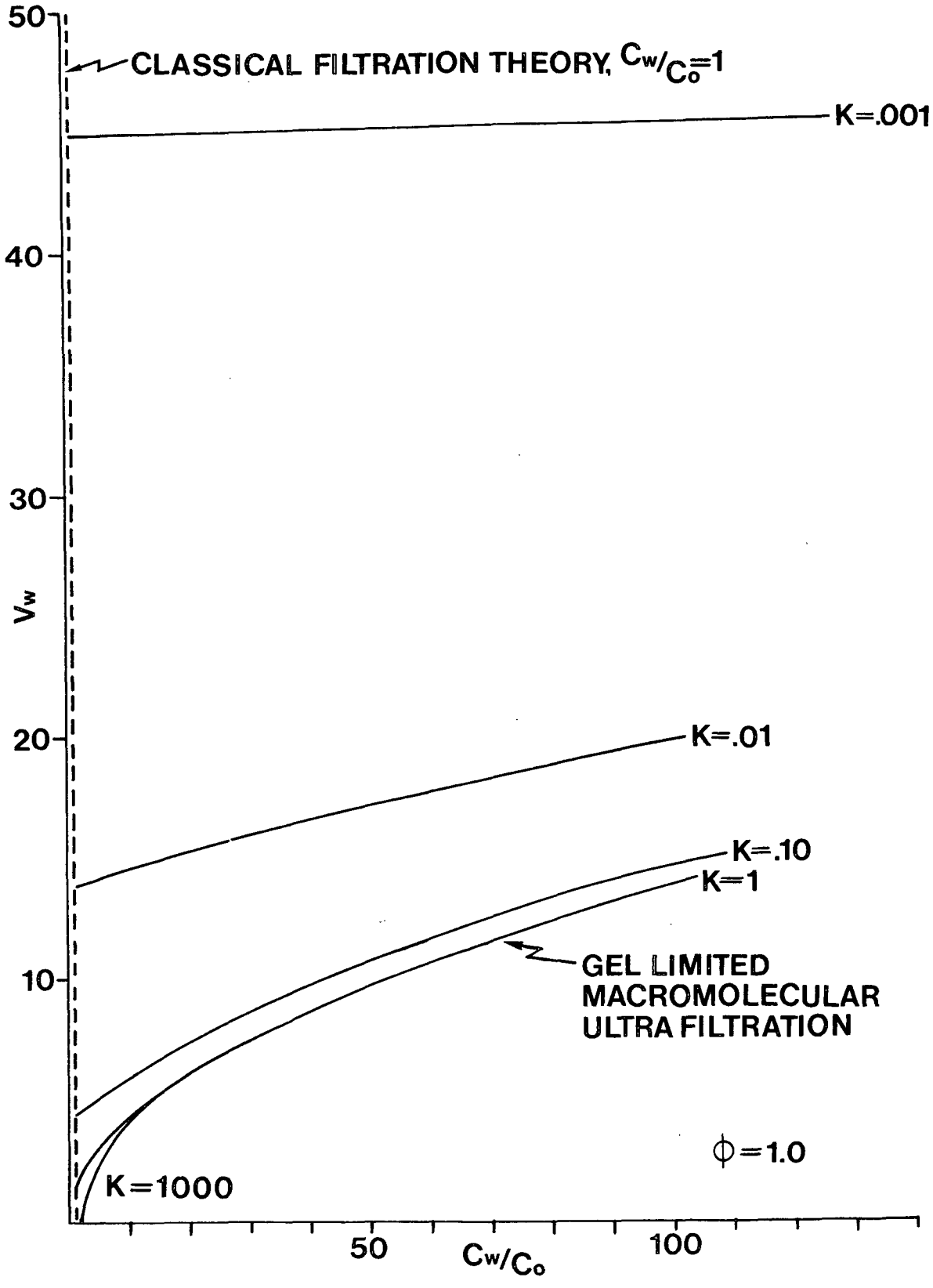

Figure 2. General theory of filtration for unstirred batch cell, ϕ = 1.

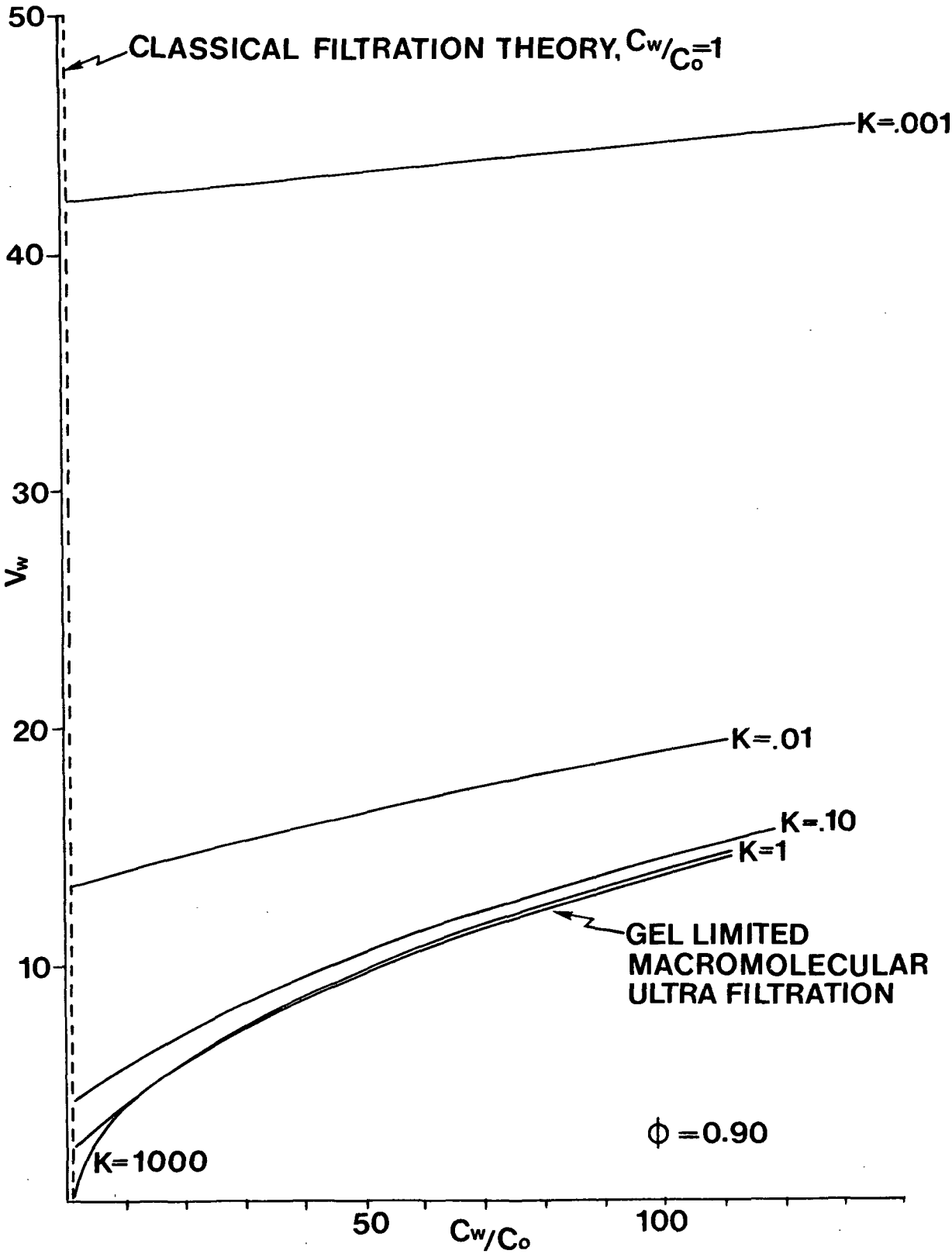

Figure 3. General theory of filtration for unstirred batch cell, ϕ = 0.90.

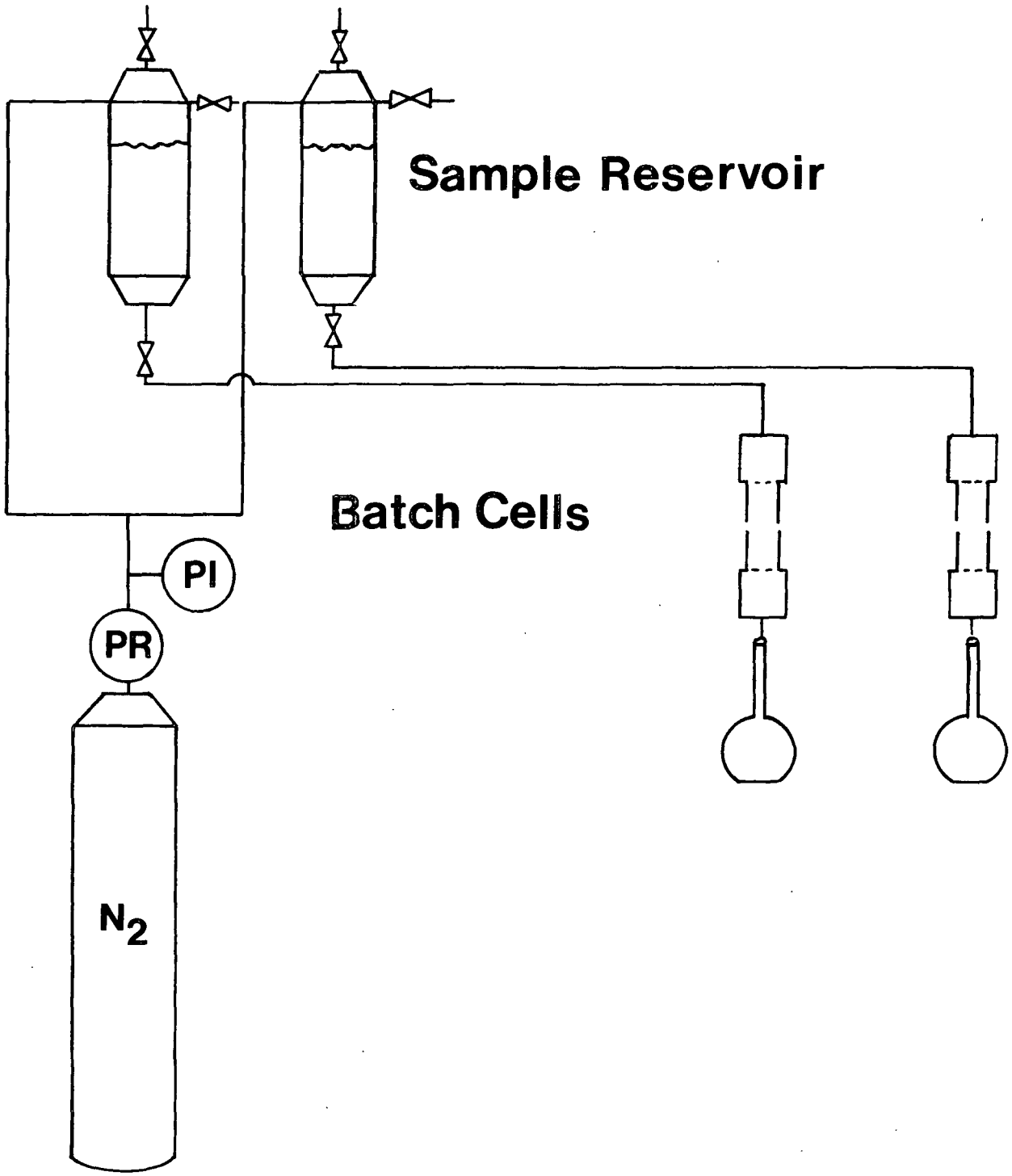

Figure 4. Batch cell schematic.

The majority of batch cell experiments were done using cellulose acetate membranes (5,000-10,000 MW cutoff) supplied to us through the courtesy of UOP-Fluid Systems. Solute rejection was complete. r_m Values given in Tables I-VIII were calculated from pure solvent flux measurements at the designated pressure.

Figure 5 represents data taken at constant concentration (c_o = 0.0324 g/cc latex) and variable pressure. Data are analyzed in terms of Eq. (28). Table I contains the calculated values of α, the specific cake resistance, for the data shown in Fig. 5. Data reveal a change in α with pressure, indicating latex compressibility. This variation of α with pressure may be approximately analyzed in terms of the relationship

$$\alpha = 6.22 \times 10^{11} (\Delta P)^{0.247} \tag{31}$$

Figure 6 represents data taken at constant pressure ($5.52 \times 10^5 \underline{N}/m^2$) and variable concentration for unflocculated latex suspensions. Table II contains calculated values for α for the data shown in Fig. 6, which indicate that as bulk concentration (c_o) increases, α also increases. This seemingly contradictory behavior will be discussed later. Results may be roughly correlated to the empirical relationship of

$$\alpha = 8.43 \times 10^{13} c_o^{0.422} \tag{32}$$

If an approximate calculation of cake porosity is made using the average value of 2.0×10^{13} cm/g for α, we find

$$\alpha = \frac{150\ (1-\varepsilon)}{D_p^2\ \varepsilon^3\ \rho_s}\ ,\ \varepsilon = 0.155 \tag{33}$$

where

$$D_p = 4.0 \times 10^{-5} \text{ cm.}$$

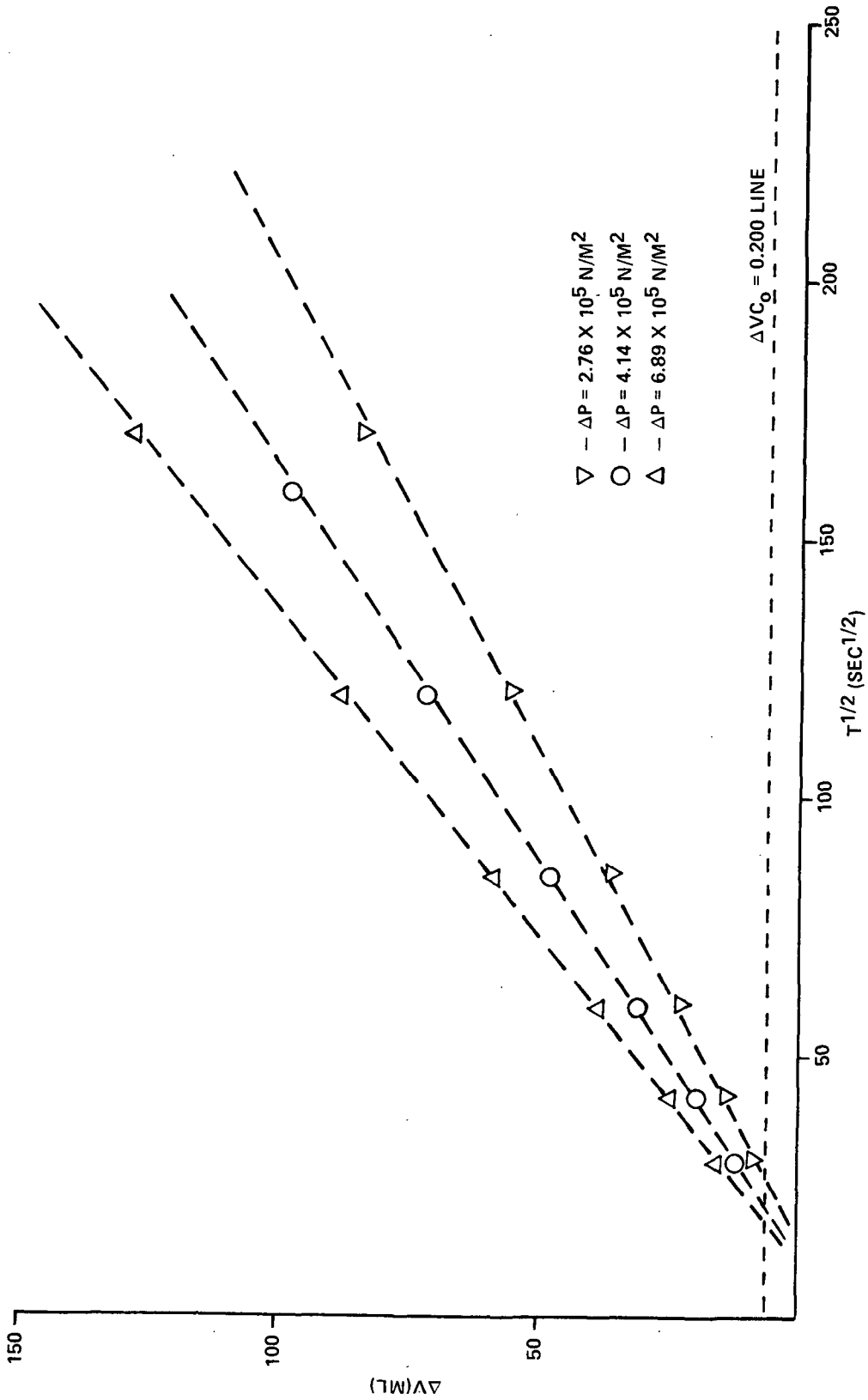

Figure 5. Ultrafiltration of latex with constant c_o and variable pressure, c_o = 0.032 g/cc latex, cellulose acetate membrane.

This value of ε is low compared with the reported porosities of many other similar materials. The observation that latex is compressible along with the fact that there is a slight nonuniformity with regard to particle size of latex used may account for the low porosity. Geometrically, the minimum porosity (or void fraction) which is possible with rigid spheres of uniform size is 0.26. In order to check the validity of our results the following experiments were performed.

TABLE I

ULTRAFILTRATION OF LATEX USING CELLULOSE ACETATE MEMBRANE (SEE FIG. 5)

$c_o = 3.24 \times 10^{-2}$ g/cc

$P \times 10^{-5}$ [N/m^2]	Slope [cm^3/sec]	V_{corr} [cm^3]	$k \times 10^2$ [g/cc]	$\times 10^4$ N-sec/m^2	$\times 10^{-13}$ [cm/g]	$r_m \times 10^{-11}$ [1/cm]
2.76	0.555	9.94	3.35	9.14	1.43	1.92
4.14	0.673	8.92	3.35	9.14	1.46	1.68
6.89	0.795	8.43	3.35	9.14	1.74	1.96

Instead of measuring transient permeate volume, 200 mL of a latex suspension of known concentration was added to the batch cell. The cell was then attached to the pure water reservoir and pressurized. Cells were allowed to run until steady state was reached (about 16 hours). Permeation rates were then measured at several pressures. Experiments were carried out with both unflocculated and flocculated latex. Since the mass of the latex in the cell was known, values could be calculated from the equation

$$\mu \left| v_w \right| = \frac{\Delta P}{r_m + \frac{\alpha m}{A}} \tag{34}$$

where m = gram mass of filter cake and A = area of cake base.

Tables III, IV and V list the results for unflocculated latex (cellulose acetate membrane), flocculated latex (cellulose acetate membrane), and flocculated latex (0.22 micron Millipore filter).

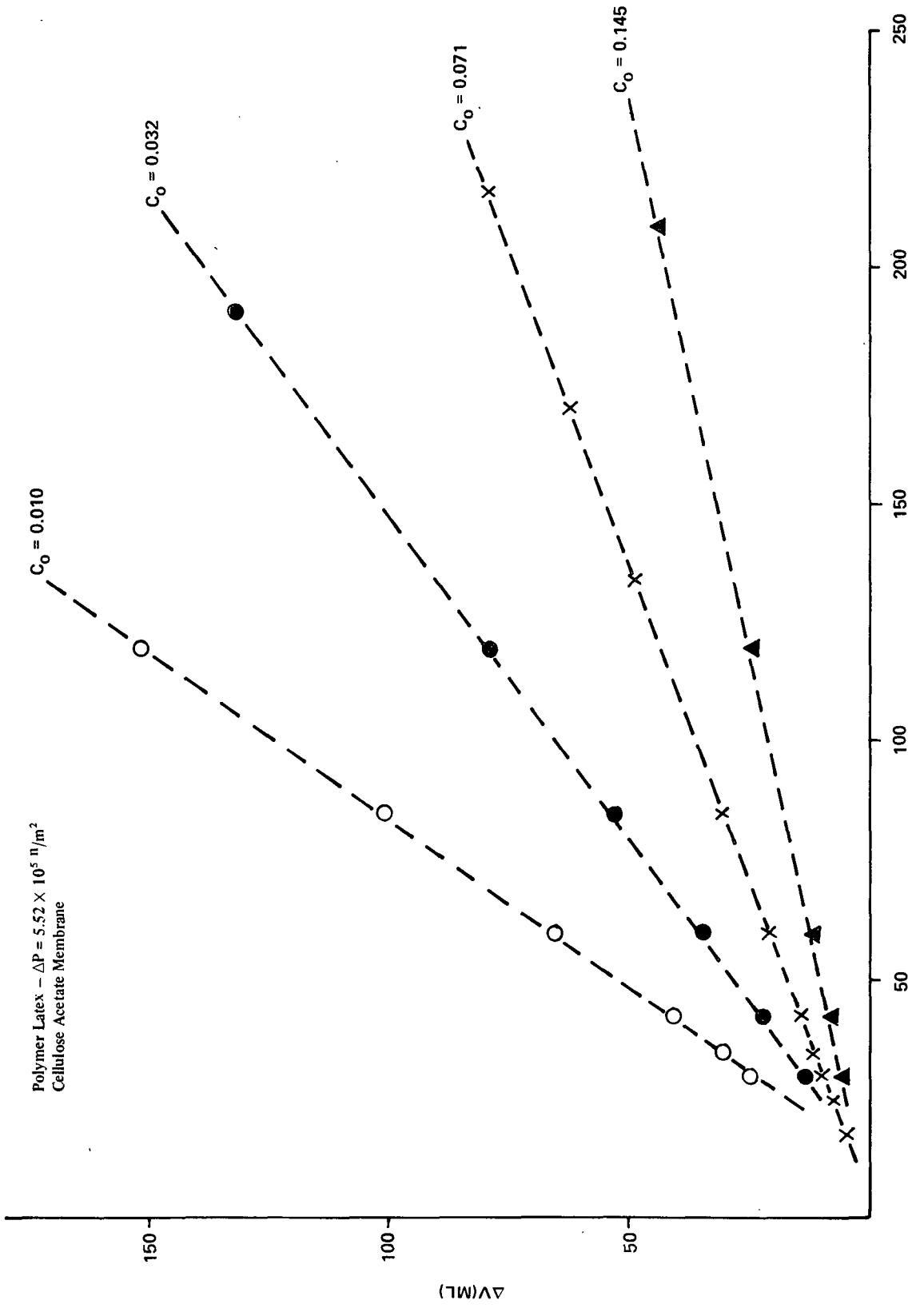

Figure 6. Ultrafiltration of latex with constant pressure and variable c_o. $\Delta P = 5.52 \times 10^5 \times 10^5 N/m^2$ cellulose acetate membrane.

TABLE II

ULTRAFILTRATION OF LATEX USING CELLULOSE ACETATE MEMBRANE (SEE FIG. 6)

$P = 5.52 \times 10^5 N/m^2$

$c_o \times 10^2$ [g/cc]	Slope [cm^3/sec]	V_{corr} [cm^3]	$k \times 10^2$ [g/cc]	$\times 10^4$ N-sec/m^2	$\times 10^{-13}$ [cm/g]	$r_m \times 10^{-11}$ [1/cm]
1.03	1.44	20.3	1.04	9.14	1.37	1.57
3.18	0.741	9.50	3.30	9.14	1.63	1.76
7.10	0.373	1.55	7.69	8.74	2.88	1.71
14.5	0.219	1.50	17.13	8.36	3.92	1.90

TABLE III

UNFLOCCULATED LATEX (2.98 g CAKE) CELLULOSE ACETATE MEMBRANE - CAKE FORMED AT $5.52 \times 10^5 N/m^2$

$\Delta P \times 10^{-5}$ [N/m^2]	$\lvert v_w \rvert \times 10^4$ [cm/sec]	$\mu \times 10^4$ [N-sec/m^2]	$r_m \times 10^{-11}$ [1/cm]	$\alpha \times 10^{-13}$ [cm/g]
5.52	2.32	8.01	4.79	1.31
6.89	2.89	8.01	4.79	1.31
8.27	3.27	8.01	4.79	1.40
9.65	3.67	8.01	4.79	1.47

TABLE IV

FLOCCULATED LATEX (3.32 g CAKE) CELLULOSE ACETATE MEMBRANE - CAKE FORMED AT $5.52 \times 10^5 N/m^2$

$\Delta P \times 10^{-5}$ [N/m^2]	$\lvert v_w \rvert \times 10^4$ [cm/sec]	$\mu \times 10^4$ [N-sec/m^2]	$r_m \times 10^{-11}$ [1/cm]	$\alpha \times 10^{-13}$ [cm/g]
5.52	7.76	8.74	4.79	0.158
6.89	10.6	8.74	4.79	0.125
8.27	11.1	8.64	4.79	0.180
9.65	14.8	8.64	4.79	0.130

TABLE V

FLOCCULATED LATEX (3.27 g CAKE) 0.22 MICRON MILLIPORE FILTER - CAKE FORMED AT $5.52 \times 10^5 N/m^2$

$\Delta P \times 10^{-5}$ [N/m^2]	$\lvert v_w \rvert \times 10^4$ [cm/sec]	$\mu \times 10^4$ [$\frac{N\text{-sec}}{m^2}$]	$r_m \times 10^{-8}$ [1/cm]	$\alpha \times 10^{-13}$ [cm/g]	Grace (1953) $\alpha \times 10^{-13}$ [cm/g]
2.76	20.2	9.14	9.10	0.0710	0.050
4.14	31.1	9.14	9.10	0.0691	0.060
5.52	40.8	9.14	9.10	0.0703	0.067
6.98	50.6	9.14	9.10	0.0717	0.074
8.27	59.1	9.14	9.10	0.0727	0.075
9.65	71.8	9.14	9.10	0.0698	0.075

The fact that the values α given in Table III do not differ appreciably from those given in Table I confirms the validity of the steady-state technique.

Data in Tables III and IV show that a decrease of 90% in the specific cake resistance can be obtained when the latex suspension is flocculated. Decreases of 95% occur in the specific cake resistance when flocculated latex is filtered with a 0.22 micron Millipore filter (Table V). Grace (1953) performed a fairly comprehensive study of water permeation through latex beds with a compression-permeability apparatus. His experiments were done with highly flocculated suspensions, and the latex used was of the same particle diameter as ours but of a more uniform size distribution. Our values of flocculated latex cake resistance agree very well with the results reported by Grace (1953), as shown in Table V.

Results reported in Table VI show the effect of forming latex cakes from flocculated suspensions of different concentration upon the value of α. Results may be roughly correlated with the empirical relationship

$$\alpha = 7.12 \times 10^{10} \, c_o^{-0.515} \tag{35}$$

TABLE VI

FLOCCULATED LATEX - ABCOR HFA-180 MEMBRANE - CAKES FORMED AT $5.52 \times 10^5 \underline{N}/m^2$

$c_o \times 10^2$ [g/cc]	$\Delta P \times 10^{-5}$ [N/m^2]	$\lvert v_w \rvert \times 10^4$ [cm/sec]	$\mu \times 10^4$ [$\frac{N\text{-sec}}{m^2}$]	$r_m \times 10^{-10}$ [1/cm]	m [g]	Grace (1953) $\alpha \times 10^{-13}$ [cm/g]
1.03	5.52	36.6	8.18	8.85	2.06	0.0727
7.10	5.52	17.4	8.55	8.20	14.2	0.0318
14.5	5.52	15.8	8.55	8.34	29.0	0.0175

Before the analysis of data is concluded, mention must first be given to the seemingly contradictory observations given in Table II and Eq. (32) for unflocculated latex and Table VI and Eq. (35) for flocculated latex. Decreasing values of α with increasing bulk concentration is an effect which is well accepted in the filtration of particulate suspensions which are flocculated or have low particle surface charge [Heertjes (1975)]. The primary explanation of this effect is that as suspension concentration is increased, the particle flux to the septum surface is increased. Since there are only a limited number of available pores for liquid to pass, more particles converge upon the same pore. This gives rise to appreciable particle bridging around each pore, and consequently, a cake of higher porosity is formed. This less dense cake structure is propagated throughout the entire cake formation process because of the relatively lower resistance of the deposited layer.

It is hypothesized that in the ultrafiltration of unflocculated or highly charged particles, the interparticle repulsion has a sizable effect upon the permeability of the subsequent cake that is formed. This point may be best explained with the use of Fig. 7 and 8.

When a highly charged particle suspended in a medium of low particle concentration approaches the cake surface, it has several possible locations to make contact with the cake. Position 1 is the optimum from the electrostatic repulsion point of

view, since less of the particle surface area will be exposed to identically charged particles. Therefore a less resistive cake is formed. This process is depicted in Fig. 8.

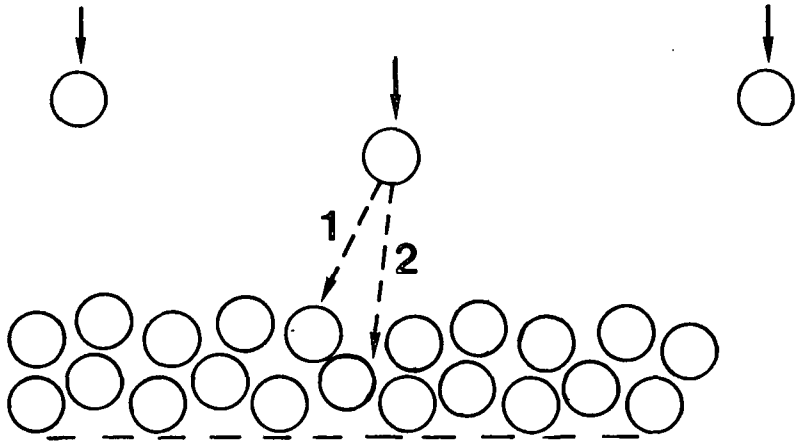

Figure 7. Unflocculated particles at low concentration.

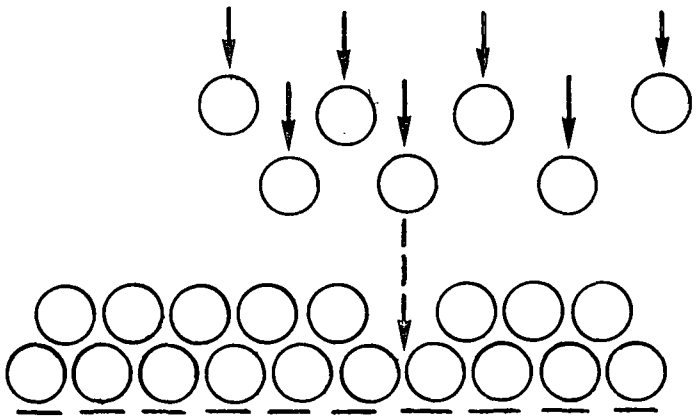

Figure 8. Unflocculated particles at high concentration.

As particle concentration is increased in the suspending medium, more particles compete for these optimum positions. Also, each particle experiences increased repulsion from neighboring particles in suspension. Therefore, a greater number of particles are forced into more closely packed positions, although they are less attractive from an electrostatic standpoint. The net result is the formation of a more resistive cake. This process is depicted in Fig. 8.

This effect may be a possible explanation of why Porter (1972) observed decreasing permeate rates with increasing concentration of unflocculated solute. The reason was that, even though the final cake thickness may have been the same at steady state due to constant shear for the various concentrations studied, the specific resistance of the filter cake increased with increasing feed concentration. Consequently, decreasing flux rates with increasing feed concentration were observed.

The ultrafiltration of latex suspensions was studied in a cross-flow, parallel plate (thin channel) system having the dimensions h = 0.318 cm, w = 14.92 cm, and L = 198.12 cm. The channel had a calming length of 91.44 cm before the active membrane section (total unit length = 289.56 cm) to insure a fully developed velocity profile. The permeate collection chamber was partitioned so that flux could be measured incrementally along the length of the channel. Triton X-100 was added as a surfactant to the concentration of 400 ppm. There was no difference between pure water and water + Triton X-100 solution flux using an Abcor HFM-180 membrane. The ultrafiltration of latex solutions was studied under two conditions: permeate returned to feed tank and permeate not returned. Feed solutions were recycled through the unit, and the bulk concentration in the feed tank was measured each time permeate flux was recorded. The membrane was rinsed clean after each velocity run. A schematic diagram of the flow system is given in Fig. 9. Results are given in Tables VII and VIII where average values of $|v_w|$ calculated from incremental measurements are reported. No significant trend in incremental flux variation from end-to-end was noted. Incremental flux measurements deviated from the average by less than 15%.

The analysis of Tables VII and VIII yields very interesting results. In Table VII, where permeate is being returned to the feed tank, we see a continuous decrease in bulk solution latex concentration with time. This behavior is indicative of particles being removed from suspension or the formation of a cake upon the membrane surface. It is also clear that steady-state behavior is not achieved even after

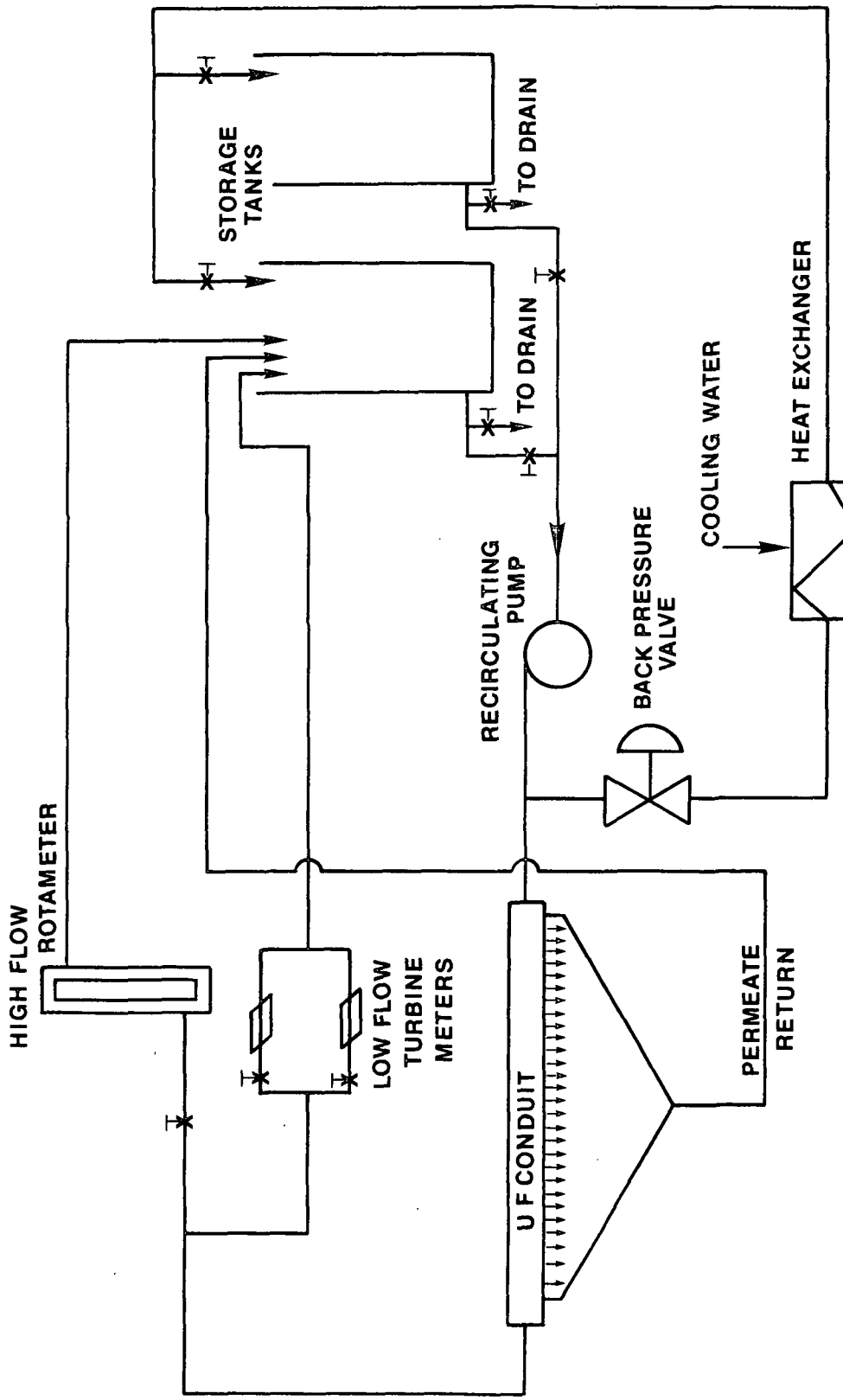

Figure 9. Schematic diagram of parallel-plate system.

TABLE VII

PARALLEL PLATE EXPERIMENTS - LATEX W/PERMEATE RETURN

$\dot{Q}$ (L/sec)	$t \times 10^{-3}$ (sec)	$\lvert \bar{v}_w \rvert \times 10^4$ (cm/sec)	c_o (g/100 cc)	$\Delta P \times 10^{-5}$ (N/m^2)
0.0871	0	15.2	1.09	3.59
	21.6	3.90	0.984	$r_m = 2.38 \times 10^{11}$ (1/cm)
	32.4	2.38	0.910	T = 20.6°C
	61.2	1.59	0.825	
	82.8	1.28	0.766	
	90.0	1.20	0.741	
0.1994[a]	120.6	1.80	0.836	
	165.6	1.38	0.823	
	198.0	1.24	0.808	
	212.4	1.18	0.790	
0.5047	0	61.3	0.432	2.76
	4.20	13.0	--	
	9.70	9.7	--	$r_m = 4.94 \times 10^{10}$ (1/cm)
	22.5	7.2	0.252	T = 23.9°C
	35.7	6.7	--	
	42.0	6.5	0.253	

[a]Axial flow rate ($\dot{Q}$) changed at $t = 97.2 \times 10^3$ sec from 0.0871 to 0.1994 liter/sec.

long periods (up to 59 hours) of operation. The first set of data in Table VIII show that when permeate is not returned to the feed tank, the latex concentration of the feed solution remains essentially constant. This observation may be interpreted as indicating that all particles which are transversely convected to the membrane contribute to the increase in the cake mass. In other words, the hydrodynamic effect of the cross-flow stream in sweeping particles back into suspension from the cake surface is negligible. This observation is consistent with the findings of Kraus (1974). At the higher axial velocity (volumetric flow rate) shown in the second data set of Table VIII, we begin to see the effect of the cross-flow stream where the feed solution is concentrating with time indicating that particles are being swept back into solution. It is indeed interesting to note that during the primary stages of cross-flow filtration the system behaves like the unstirred batch cell. That is, there is no effect of the cross-flow velocity upon improving permeation

rates. Once the latex particles become consolidated into a cake, they apparently are very difficult to remove by shear forces. If the preceding analysis is accurate, it should be possible to interpret the first data set of Table VIII using the constant pressure batch cell filtration equation with simultaneous buildup of cake. From Eq. (25)

$$\left| v_w \right| = \left[\frac{\Delta P}{2\mu \ \alpha \ k} \right]^{1/2} t^{-1/2} \tag{36}$$

when the data of Table VIII are plotted in terms of $\left| v_w \right|$ versus $t^{-1/2}$, it is found that

$$\frac{\Delta P}{2\alpha \ \mu \ k} = 1.388 \times 10^{-3} \ cm^2/sec \tag{37}$$

or, solving for α assuming $\varepsilon = 0.20$,

$$\alpha = 8.13 \times 10^{12} \ (cm/g) \tag{38}$$

TABLE VIII

PARALLEL PLATE EXPERIMENTS - LATEX W/O PERMEATE RETURN

$T = 20°C$, $r_m = 2.38 \times 10^{11}$ (1/cm)

$\dot{Q}$ (L/sec)	$t \times 10^{-3}$ (sec)	$\left\| \overline{v_w} \right\| \times 10^4$ (cm/sec)	c_o (g/100 cc)	$\Delta P \times 10^{-5}$ (N/m^2)
0.1981	0	--	1.49	3.45
	7.20	4.42	1.50	
	18.0	2.76	1.57	
	28.8	2.21	1.52	
	39.6	1.94	1.53	
0.7129	0	--	1.46	3.45
	7.20	5.29	1.47	
	18.0	4.32	1.54	
	28.8	4.10	1.65	
	39.6	3.99	1.76	
	79.2	3.77	1.76	

In order to check the valid range of this value, a sample of the feed tank solution was ultrafiltered in the unstirred batch cell where the same type of membrane was used. The results of the analysis yielded the corresponding value of

$$\alpha = 8.29 \times 10^{12} \text{ (cm/g)} \tag{39}$$

This agreement confirms the fact that the convective ultrafiltration of latex suspensions follows constant pressure batch cell filtration theory. The reason for the apparent drop in α from an average of 15.0×10^{12} to 8.13×10^{12} (cm/g) may be explained by the fact that in systems of high shear (from pump, valves, etc.) a certain amount of surfactant is removed from the latex surface and consequently, flocculation occurs. This change in α is consistent with the batch cell experiments using alum-flocculated latex.

CONCLUSIONS

The interpretation of unstirred batch cell permeation rates with regard to macromolecular and colloidal ultrafiltration has been unified by a common mathematical model. An important dimensionless parameter, K, emerging from the model is proportional to the ratio of mass transfer boundary layer thickness to cake thickness. For macromolecular ultrafiltration, cake thickness is negligible and K approaches infinity, whereas for colloidal ultrafiltration, diffusion transport is negligible so that K tends to zero. The general model is applicable to these two extreme cases ($K \to \infty$ and $K \to 0$). The model is probably valid for all values of K, but we do not have experimental data for intermediate values of K to support this.

Results from batch cell ultrafiltration of latex suspensions could be interpreted in terms of constant pressure filtration relationship as suggested by the model. Also, our unsteady state cross-flow ultrafiltration results could be correlated by constant pressure filtration Eq. (36). Certainly, more work is needed to identify parameters governing the existence of steady state and unsteady state in cross-flow ultrafiltration of suspensions.

NOMENCLATURE

A	Surface area of membrane (cm^2)
C_1	Constant in Eq. (1) and (2) ($cm^3/sec^{1/2}$)
c	Solute concentration (g/cm^3)
D	Solute diffusion coefficient (cm^2/sec)
D_p	Solute particle diameter (cm)
h	Channel half height (cm)
K	$\frac{\alpha\mu D c_o}{\Delta P}$ = constant
k	Constant = $\frac{c_o \rho_s}{\rho_s - \left(\frac{1}{1-\varepsilon}\right) c_o}$ (g/cm^3)
L	Channel membrane length (cm)
m	Mass of cake (grams)
n_s	Net solute flux away from membrane surface (g/cm^2-sec)
N_s	$-\frac{n_s}{c_o}\left(\frac{4t}{D}\right)^{1/2}$
r	Hydraulic resistance (1/cm)
S	Cake thickness (cm)
S^+	$\frac{S}{(4Dt)^{1/2}}$
T	Permeate measurement time (sec)
T^*	Arbitrary time (sec)
t	Time (sec)
v	Transverse velocity in the cell (cm/sec)
V	$V_w + \frac{2(1-\phi)}{KV_w}$
V_w	Permeate flux constant defined by Eq. (12)
v_w	Permeate volumetric flux (cm/sec)
w	Channel width (cm)
y	Transverse distance coordinate (cm)

Greek Letters

α	Specific cake or gel resistance = $\frac{150(1-\varepsilon)}{D_p^2 \varepsilon^3 \rho_s}$ (cm/g)
ΔP	Total pressure gradient (N/m^2)
ΔV	Permeate volume collected in time T (cm^3)
ΔV_{corr}	Correction volume defined in Eq. (32)
δ	Mass boundary layer thickness (cm)
ε	Cake or gel porosity
η	Similarity variable = $\frac{y}{(4Dt)^{1/2}}$
θ	$\frac{c-c_o}{c_o}$
μ	Solvent viscosity
ϕ	$1 - \frac{c_o}{\rho_s (1-\varepsilon)}$
ρ	Density (g/cm^3)

Subscripts

c	of the cake
m	of the membrane
o	of the bulk solution
s	of the solute
w	at the cake or gel surface

LITERATURE CITED

Ammerlaan, A. C. F., Lueck, B. F., and Wiley, A. J. Membrane processing of dilute pulping wastes by reverse osmosis. Tappi 52(1):118(1969).

Bailey, M. W. Solute interactions in ultrafiltration treatment of paper mill wastes. Ph.D. Dissertation, North Carolina State University, Raleigh, 1973.

Bixler, H. J. and Rappe, G. C. Ultrafiltration process, U.S. pat. 3,541,006 (Nov. 17, 1970).

Blatt, W. F., Dravid, A., Michaels, A. S., and Nelson, L. Solute polarization and cake formation in membrane ultrafiltration: causes, consequences, and control techniques, in Membrane science and technology, J. E. Flinn, ed., Plenum Press, New York, NY, 1970. p. 47.

Brenner, H. Hydrodynamic resistance of particles at small Reynolds numbers. In Advances in chemical engineering, T. B. Drew, J. W. Hoopes, and T. Vermeulen, eds., Academic Press, New York, NY 6:287(1966).

Cox, R. G. and Brenner, H. Effect of finite boundaries on the Stokes resistance of an arbitrary particle. J. Fluid Mech. 28:391(1967).

Cox, R. G. and Brenner, H. The lateral migration of solid particles in Poiseuille flow. Chem. Eng. Sci. 23:147(1968).

Doshi, M. R. Unpublished work, The Institute of Paper Chemistry, 1979.

Grace, H. P. Resistance and compressibility of filter cakes. Chem. Eng. Progress 49(6):303(1953).

Heertjes, P. M. Formation of filter cakes and precoates. In The scientific basis of filtration, K. J. Ives, ed., Noordhoff International Publishing, The Netherlands, 1975. p. 297.

Henry, J. D., Jr. Cross flow filtration. In Recent development in separation science, CRC Press, Cleveland, OH 2:205(1972).

Karnis, A., Goldsmith, H. L., and Mason, S. G. The flow of suspensions through tubes. V. Inertial effects. Can. J. Chem. Eng. August, 1966. 181.

Kraus, K. A. Cross-flow filtration and axial filtration. Paper presented at the 29th Annual Purdue Industrial Waste Conference, Lafayette, Indiana, May, 1974.

Madsen, R. E. Hyperfiltration and ultrafiltration in plate-and-frame systems. Elsevier Scientific Publishing Company, New York, NY, 1977.

Porter, M. C. Concentration polarization with membrane ultrafiltration. I&EC Prod. Res. 11(3):234(1972).

Rubinow, S. I. and Keller, J. B. The transverse force on a spinning sphere moving in a viscous fluid. J. Fluid Mech. 11:447(1967).

Segre, G. and Silberberg, A. Behavior of macroscopic rigid spheres in Poiseuille flow. J. Fluid Mech. 14:136(1962).

Trettin, D. R. and Doshi, M. R. Ultrafiltration in an unstirred batch cell. I&EC Fundam. 19:189(1980).

Trettin, D. R. and Doshi, M. R. Pressure independent ultrafiltration - is it gel limited or osmotic pressure limited? ACS Symposium Series, No. 154. Synthetic Membranes: Vol. II Hyper- and Ultrafiltration Uses, 1981.

SECTION 4 - MANUSCRIPT NUMBER 3

LIMITING FLUX IN ULTRAFILTRATION OF MACROMOLECULAR SOLUTIONS

Chem. Eng. Commun. 4:507-22(1980)

LIMITING FLUX IN ULTRAFILTRATION OF MACROMOLECULAR SOLUTIONS

ABSTRACT

The mass transfer equation describing the process of gel polarized ultrafiltration is solved using an integral method. A concentration profile is assumed to be an nth degree polynomial. In conventional integral method, "n" is arbitrarily assigned an integer value. In this paper we have taken the first moment of the convective diffusion equation to determine "n" as a function of the system parameters. The agreement between the closed form integral method solution and the exact numerical solution is excellent, whereas the widely used film theory deviates considerably.

INTRODUCTION

Macromolecular ultrafiltration has attracted recognition over the past decade as a simple and convenient technique for concentration, purification, and separation of medium to high molecular weight solutes from solutions. The main advantage is that ultrafiltration does not involve a phase change or interphase mass transfer. Basically, ultrafiltration involves the pressure-activated separation of chemical constituents which have different permeability through a membrane. As a pressurized solution flows past a selective membrane, solvent permeates through the membrane while rejected solute accumulates in the vicinity of the membrane. In order for the criterion of steady state mass transfer to be satisfied, the net rate of convective transport toward and parallel to the membrane surface must equal the rate of transport by diffusion away from the membrane surface. The net result is a layer of solution adjacent to the membrane surface of substantially greater solute concentration than that of the bulk solution within the channel.

The phenomenon of concentration polarization always operates to reduce the permeate rate of the ultrafiltration process. In the ultrafiltration of solutions containing low molecular weight solutes, concentration polarization decreases the effective pressure gradient by increasing osmotic backpressure at the membrane surface. In the case of solutions composed of high molecular weight solutes where osmotic pressures are typically negligible, solute concentration at the membrane surface continues to increase until solubility limits are reached at which point a gelatinous precipitate matrix is formed upon the membrane. This "gel" layer offers an additional hydraulic resistance to solvent flow. When a laminar flow ultrafiltration system is operated in the "gel polarized" region, permeate flux rates are governed primarily by the transport mechanisms of convection and molecular diffusion. Pressure dependence is secondary - increase in pressure merely increases gel thickness with little effect on permeate flux. Although osmotic backpressure

and gel polarization have the same deleterious effect upon permeate flux, there are substantial differences between the two phenomena. In the operation of an ultrafiltration system which is gel polarized, wall concentration (c_w) is constant and equal to c_g, the gelling concentration of the solute material. In the case of limiting osmotic pressure, c_w continues to be a function of axial position along the conduit. The form of this function will be determined by the relationship of osmotic pressure to solute concentration. Also, permeate flux is a function of system pressure. It is the region of developing wall concentration (c_w) with axial position that we term "pregel" in this paper. A drawing depicting the two regions is shown in Fig. 1

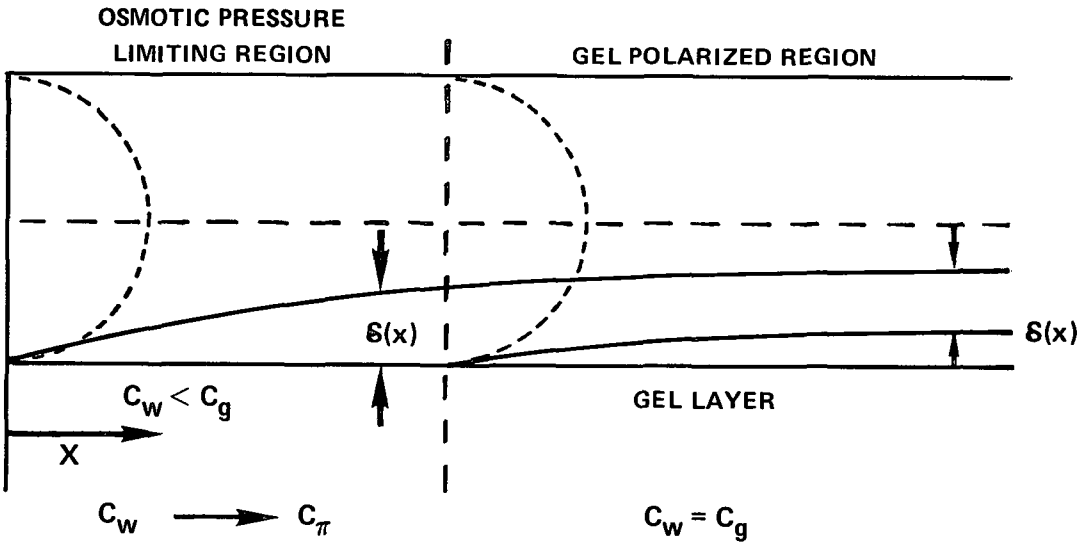

Figure 1. Comparative drawing of osmotic pressure limiting region and gel-polarized region.

PREVIOUS DEVELOPMENTS

A quantitative prediction of solvent flux requires an analysis of the basic transport mechanisms which take place within the ultrafiltration system. Currently, the most widely accepted model is based on film theory principles. The film theory model is formulated on the assumption that axial convection in the mass balance

equation may be accounted for in an indirect way. Constant fluid properties are assumed, and the model when applied to the gel-polarized region assumes wall concentration to be constant and equal to gel concentration of the solute material. Therefore, the mass balance equation reduces to

$$v \frac{\partial c}{\partial y} = D \frac{\partial^2 c}{\partial y^2} \tag{1}$$

The boundary conditions are

$$\text{at } y = 0 \text{ (membrane surface)}, \; c = c_g \tag{2a}$$

$$- \left| v_w \right| c_g = D_g \left. \frac{\partial c}{\partial y} \right|_{y=0} \tag{2b}$$

$$\text{at } y \geq \delta(x), \; c = c_B, \tag{2c}$$

where $\delta(x)$ equals the mass transfer boundary layer thickness. In Eq. (2b) we have assumed that the membrane rejects solute completely.

Upon integration and substitution of the boundary conditions one gets

$$\left| v_w \right| = \frac{D}{\delta(x)} \ln \left[\frac{c_g}{c_B} \right] \tag{3}$$

The quantity, $D/\delta(xc)$, may be approximated as the mass transfer coefficient, k, calculated by solving the solute balance equation where transverse convection has been neglected

$$u \frac{\partial c}{\partial x} = D \frac{\partial^2 c}{\partial y^2} \tag{4}$$

for either constant wall concentration or constant wall flux boundary condition. Assuming a linear axial velocity profile, the entrance region Leveque solution for a parallel plate system may be given in terms of the mass transfer coefficient as

$$k = A \left(\frac{D^2 a}{3x} \right)^{1/3} \tag{5}$$

where A = 0.776 (for constant wall concentration), A = 0.942 (for constant wall flux), and a = 3 $\langle u \rangle / h$.

In summary, it can be seen that the film theory analysis is a patching method by which axial dependence, which appears explicitly through the term, $u\, \partial c/\partial x$, is replaced by one which arises implicitly through the boundary layer thickness $\delta(x)$.

One of the first extensive studies on ultrafiltration using the film theory was published by Blatt, et al. (1970). These investigators used natural macromolecular solutions such as casein, albumin and plasma, and their studies confirmed the existence of the pressure-independent gel-polarized region. Their data displayed trends in system performance as predicted by film theory. However, quantitative agreement was not good. Thus, for example, the diffusion coefficient calculated from their albumin data will be about 10.0×10^{-7} cm^2/sec which is much higher than the value of 6.0 to 7.0×10^{-7} cm^2/sec reported in the literature [Shen (1977), Phillies, et al. (1976), Keller, et al. (1971), Doherty and Benedek (1974)].

Goldsmith (1971) performed experiments using Dextran and Carbowax solutions. His work pointed out the importance of considering the osmotic pressure effect at the membrane surface. Data were analyzed by solving two simultaneous equations, one derived from the film theory,

$$| v_w | = k \ln \left[\frac{c_w - c_p}{c_B - c_p} \right] \tag{6a}$$

and the other was a phenomenological law, relating permeate flux to the effective driving force,

$$| v_w | = \overline{A} (\Delta P - \Delta \pi) \tag{6b}$$

Both parallel plate and stirred cell systems were studied in laminar and turbulent flow. Since only partially developed flow was attained in the test unit, the mass transfer coefficient expression of

$$\frac{kd}{D} = 0.664 \left(Re \cdot \frac{d}{\ell}\right)^{1/2} Sc^{1/3} \qquad (6c)$$

was used. Because of the fact that reported data were mainly in the pregel region, where c_w is not constant, and the membranes used were very permeable to solute molecules, Goldsmith's data are not relevant to the present work.

Kozinski and Lightfoot (1972) developed a theoretical model for predicting permeate flux through a rotating disk taking into consideration concentration dependent diffusivity and viscosity. Experimental data agreed reasonably well with theory, although some hysteresis in permeate flux measurements was found. This phenomenon was attributed to solute polymerization in the concentration layer adjacent to the membrane surface. They extended their model to parallel plate systems and considered Blatt's thin channel ultrafiltration data for serum albumin. The limitations of Blatt, et al. data were pointed out by Kozinski and Lightfoot.

Mitra and Lundblad (1978) published data taken in a parallel plate system with immune serum globulin and human serum albumin. They attempted to correlate data using a film theory model in the following form

$$\left| v_w \right| = A_1 \langle u \rangle^{B_1} \ln \left(\frac{c_w}{c_B}\right) \qquad (7)$$

where A_1 and B_1 are constants. Consistent agreement was found for the value of B_1, but the value of A_1 was variable with a 21% standard deviation.

Shen and Probstein (1977) reported a theoretical treatment of the parallel plate system. Their model, like Kozinski and Lightfoot's, considered both concentration-dependent viscosity and diffusivity. Considering the general mass equation, Shen

and Probstein utilized a Leveque combination of variables technique. Resulting ordinary differential equations were solved numerically to calculate flux rates. Through comparison of calculated values, they state that the variable fluid property numerical solution can be approximated by a modified film theory. The modification simply amounts to replacing the value of the diffusion coefficient evaluated at c_B by one evaluated at c_g.

Shen and Probstein applied their modified film theory model to Blatt's serum albumin data. Data values were extrapolated into the gel-polarized region (extrapolated to limiting values) and were checked by us to be correct. Similar extrapolated values were obtained by Kozinski and Lighfoot. According to Blatt (1978), their thin-channel cell consisted of a parallel array of four 1/4-inch wide, 10-mil deep, 16-inch long channels. Unfortunately, this system design has been misinterpreted by Shen and Probstein as well as by Kozinski and Lightfoot (1972). These investigators appear to use the value of the recirculation rate for the bulk channel velocity ($\langle u \rangle$). Realistic values of $\langle u \rangle$ should be 1/4 of the recirculation rate, since the initial flow is divided equally between four separate channels.

Although the widely used film theory model yields qualitative results in general agreement with experimental observation, quantitative permeate flux predictions leave room for improvement. The objective of this paper is to develop a reliable closed form relationship for the limiting flux due to gel polarization from a more exact analysis than film theory.

THEORETICAL DEVELOPMENT

The general mass balance equation of

$$u \frac{\partial c}{\partial x} + v \frac{\partial c}{\partial y} = \frac{\partial}{\partial y} \left[D \frac{\partial c}{\partial y} \right] \tag{8}$$

may be transformed to an ordinary differential equation by a method described by Shen and Probstein (1977). This method is analogous to the Leveque solution for laminar flow. Assuming constant fluid viscosity, the following mathematical development pertains to a parallel plate system where x is measured longitudinally along the membrane surface and y is measured transverse to the membrane surface. Consistent with a thin mass transfer boundary layer as compared with the channel half width, characteristic of a high Schmidt number systems, a linear axial velocity may also be assumed. The respective velocity components are written as

$$u = \text{axial velocity} = \frac{3\langle u\rangle}{h}\, y \tag{9a}$$

$$v = \text{transverse velocity} = -\left| v_w \right| \tag{9b}$$

where $\left| v_w \right|$ is the limiting (or pressure-independent) permeate flux at the membrane surface. Boundary conditions are identical to those previously mentioned for the film theory model applied to the gel-polarized region with the exception that y is taken to infinity as the upper limit, namely

$$y \to \infty,\ c = c_B \tag{10}$$

Transforming the mass balance equation into dimensionless variables using the following relationships

$$\eta = y \left(\frac{3xD_B}{a}\right)^{-1/3} \tag{11a}$$

$$F(\eta) = \frac{c}{c_B} \tag{11b}$$

$$u = \left(\frac{3xD_B}{a^2}\right)^{1/3} \eta \tag{12a}$$

$$\left| v_w \right| = \left(\frac{D_B{}^2 a}{3x}\right)^{1/3} V_w \tag{12b}$$

$$\overline{D} = \frac{D(c)}{D_B} \tag{12c}$$

where $a = 3\langle u\rangle/h$, and V_w = positive permeate constant. The resulting equation may be expressed

$$\frac{d}{d\eta}\left[\overline{D}\,\frac{dF}{d\eta}\right] + (\eta^2 + V_w)\,\frac{dF}{d\eta} = 0 \tag{13}$$

where the transformed boundary conditions are

$$\text{at } \eta = 0,\ F = F_g,\ -V_w F_g = \left.\frac{dF}{d\eta}\right|_{\eta=0} \tag{14a}$$

and,

$$\text{at } \eta = \infty,\ F = 1 \tag{14b}$$

Upon integration the following equation results

$$\frac{1}{F_g} = 1 - V_w \int_o^\infty \frac{1}{\overline{D}} \cdot \exp\left(-\int_o^\eta \left[\frac{\eta^2 + V_w}{\overline{D}}\right] d\eta\right) d\eta \tag{15}$$

If one makes the simplification of constant diffusion coefficient, Eq. (15) becomes

$$\frac{1}{F_g} = 1 - V_w \int_o^\infty \exp\left(-\frac{1}{3}\eta^3\right) \cdot \exp\left(-V_w\eta\right) d\eta \tag{16}$$

Equation (15) is identical to the relationship derived by Shen and Probstein (1977). Equation (16) may be approximated by an infinite series solution for small values of V_w. The series solution may be expressed in terms of the gamma function

$$\frac{1}{F_g} = 1 - \sum_{n=1}^{\infty} (-1)^{n+1} \left(\frac{b^{n/3}}{n!}\right) \Gamma\left(\frac{n+3}{3}\right) \tag{17}$$

where $b = 3V_w^3$

The first 6 terms of Eq. (17) are:

$$1/F_g = 1 - 1.288\ V_w + 0.939\ V_w^2 - 0.499\ V_w^3 + 0.215\ V_w^4 - 0.078\ V_w^5 + 0.025\ V_w^6 - \ldots \quad (18)$$

For large values of V_w, Eq. (16) may be approximated by carrying out appropriate integration by parts:

$$1/F_g = 2/V_w^3 - 40/V_w^6 + 2.24 \times 10^3/V_w^9 - 2.46 \times 10^5/V_w^{12} + 3.85 \times 10^7/V_w 15 - \ldots \quad (19)$$

For Eq. (15) through (19), values of V_w are typically within the range of 0 to 10 with V_w varying directly with F_g. A graphical comparison of the approximate equations with regard to the numerical solution of Eq. (16) are shown in Fig. 2 and 3. Equations (18) and (19) are plotted under the titles approximation (1) and integration by parts, respectively. As shown in Fig. 2 and 3, Eq. (18) is reasonable for F_g less than 4 while Eq. (19) is accurate for F_g greater than about 70.

In lieu of the limited applicability of the approximate solutions, an integral method was applied to the mass balance equation

$$\frac{3\langle u\rangle}{h}\, y\, \frac{\partial c}{\partial x} - \left| v_w \right| \frac{\partial c}{\partial y} = \frac{\partial}{\partial y}\left[D\, \frac{\partial c}{\partial y} \right] \quad (20)$$

where the boundary conditions are

$$\text{at } y = \delta(x),\ c = c_B \quad (21a)$$

and

$$\text{at } y = 0,\ c = c_g,\ -\left| v_w \right| c_g = D_g \left.\frac{\partial c}{\partial y}\right|_{y=0} \quad (21b)$$

Integrating Eq. (20) with respect to y from y = 0 to y = δ yields

$$\frac{3\langle u\rangle}{h}\left[\frac{d}{dx}\int_0^{\delta} ycdy - c_B\delta\, \frac{d\delta}{dx} \right] = \left| v_w \right| c_B \quad (22)$$

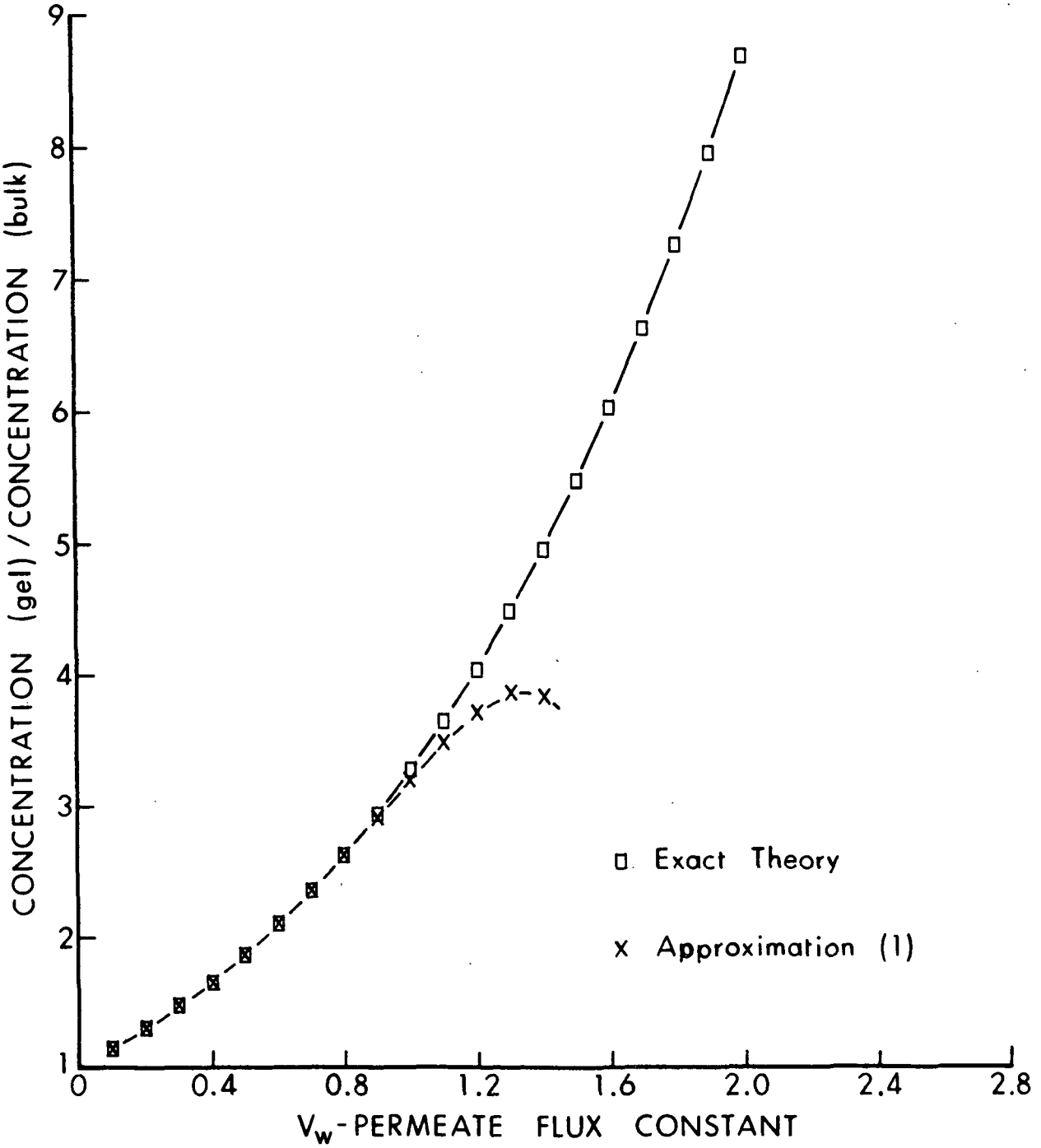

Figure 2. Comparison of exact UF equation to approximate solution [Eq. (18)].

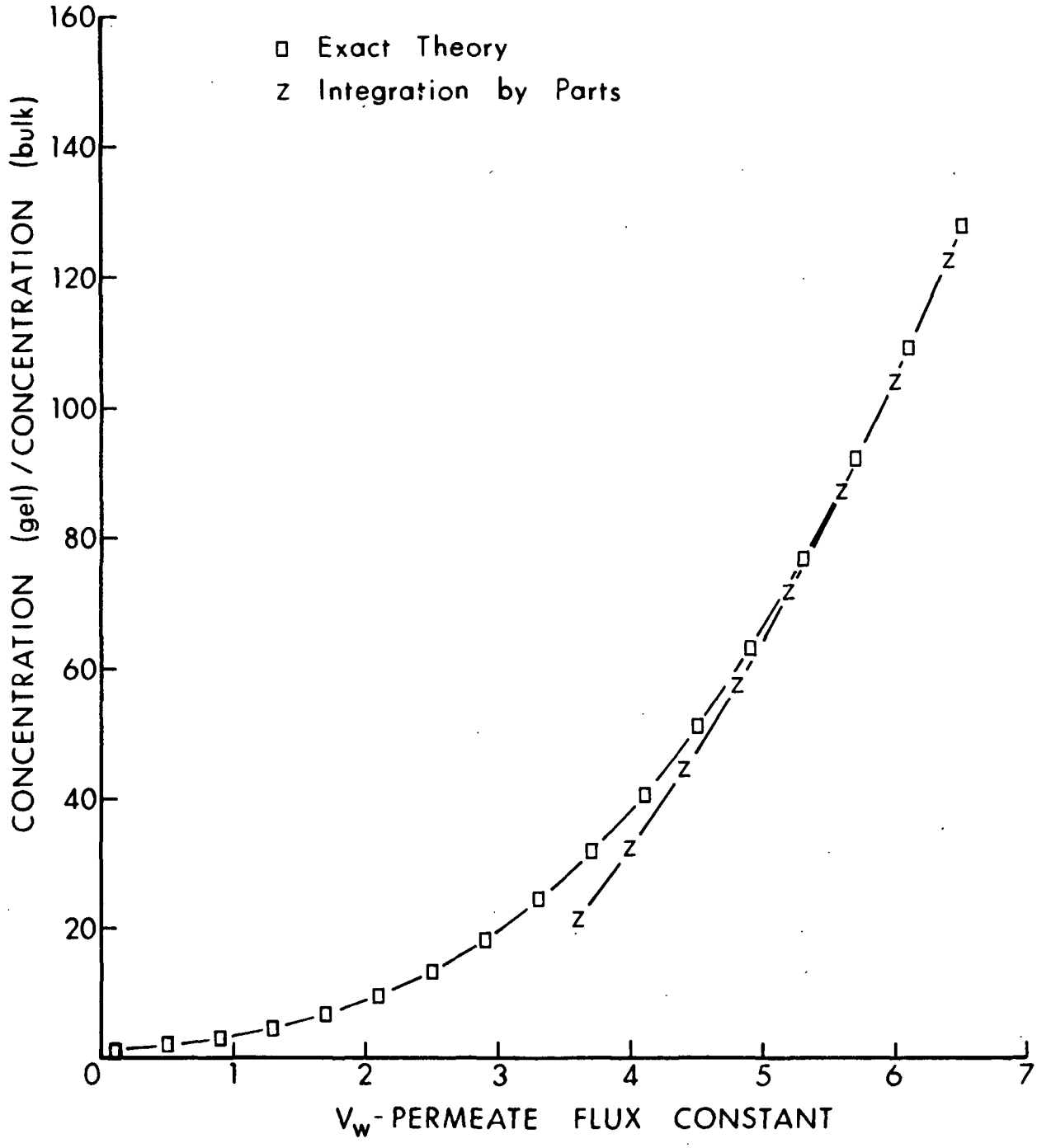

Figure 3. Comparison of exact UF equation to approximate solution [Eq. (19)].

Following Doshi, et al. (1971), a concentration profile of the form

$$c = c_B + (c_g - c_B)\left(1 - \frac{y}{\delta}\right)^n \tag{23}$$

was assumed. In order for the boundary condition of Eq. (21b) to be satisfied,

$$\frac{n}{\delta}(c_g - c_B) D_g = |v_w| c_g \tag{24a}$$

therefore,

$$\delta = \frac{nD_g}{|v_w|}\left(\frac{c_g - c_B}{c_g}\right), \text{ or,}$$

$$|v_w| = \frac{nD_g}{\delta}\left(\frac{c_g - c_B}{c_g}\right) \tag{24b}$$

Substituting the assumed concentration profile into Eq. (22) and completing the integration yields

$$\frac{3\langle u\rangle}{h(n+1)(n+2)} \frac{d}{dx}(\delta^2(c_g - c_B)) = |v_w| c_B \tag{25}$$

Using Eq. (24b) to eliminate $|v_w|$ and rearranging gives

$$\frac{d}{dx}(\delta^3) = \frac{n(n+1)(n+2) D_g h c_B}{2\langle u\rangle c_g} \tag{26}$$

Integrating Eq. (26), noting that at $x = 0$, $\delta = 0$, gives

$$\delta^3 = \frac{n(n+1)(n+2) D_g h c_B x}{2\langle u\rangle c_g} \tag{27}$$

or, from Eq. (24b),

$$|v_w| = nD_g\left(\frac{c_g - c_B}{c_g}\right)\left[\frac{2\langle u\rangle c_g}{n(n+1)(n+2) D_g h c_B x}\right]^{1/3} \tag{27b}$$

Transforming to dimensionless variables, using Eq. (11b, 12b, and 12c) one obtains

$$V_w = \frac{F_g - 1}{F_g}\left[\frac{2n^2F_g}{(n+1)(n+2)}\right]^{1/3}(\overline{D}_g)^{2/3} \tag{28a}$$

or

$$V_w = \frac{F_g - 1}{F_g}[KF_g]^{1/3}(\overline{D}_g)^{2/3} \tag{28b}$$

where $K = 2n^2/(n+1)(n+2)$.

It bears mentioning at this point that Probstein, Shen, and Leung (1978) apply an integral method to the general mass balance equation. Their resulting equation for limiting wall flux is expressed as

$$|v_w| = \left[\frac{2}{3}\frac{\langle u\rangle D_g^2}{hx}\right]^{1/3}\frac{F_g - 1}{F_g^{2/3}} \tag{29a}$$

or, expressed in terms of V_w

$$V_w = \left(\frac{2}{3}\right)^{1/3}\left[\frac{F_g - 1}{F_g^{2/3}}\right]\overline{D}_g^{2/3} = \left[\frac{2}{3}F_g\right]^{1/3}\left[\frac{F_g - 1}{F_g}\right]\overline{D}_g^{2/3} \tag{29b}$$

It is apparent that their limiting flux equation is identical to Eq. (28b) for the case $n = 2$, $K = 2/3$.

In this analysis it was assumed that constant n was some function of F_g. The integral method was applied again to ascertain the form of this function.

Multiplying Eq. (20) throughout by y

$$\frac{3\langle u\rangle}{h}y^2\frac{\partial c}{\partial x} - |v_w|\,y\frac{\partial c}{\partial y} = y\frac{\partial}{\partial y}\left(D\frac{\partial c}{\partial y}\right) \tag{30}$$

and integrating with respect to y from y = 0 to y = δ yields

$$\frac{3\langle u\rangle}{h}\left[\frac{d}{dx}\left(\int_0^{\delta} y^2\, c\,dy\right) - \delta^2 c_B \frac{d\delta}{dx}\right] + |v_w| \int_0^{\delta} c\,dy = |v_w|\,\delta c_B - \int D\frac{\partial c}{\partial y}\,dy \qquad (31)$$

Substituting the concentration profile of Eq. (23) and assuming linear concentration dependency of diffusion coefficient, gives

$$\frac{3\langle u\rangle}{h}\left[\frac{2(c_g - c_B)}{(n+1)(n+2)(n+3)}\right]\frac{d}{dx}(\delta^3) + \frac{|v_w|\,\delta(c_g - c_B)}{n+1} = D_g c_g - D_B c_B + \frac{1}{2}\left(-\frac{dD}{dc}\right)(c_g^2 - c_B^2) \qquad (32)$$

Combining Eq. (32) with Eq. (24b) and (26), one gets

$$\frac{3nc_B}{(n+3)c_g} + \frac{n}{n+1}\left[1 - \frac{c_B}{c_g}\right] = B \qquad (33)$$

where

$$B = \frac{\overline{D}_g F_g - 1}{\overline{D}_g (F_g - 1)} + \frac{A}{2}\frac{F_g + 1}{F_g} \quad \text{and} \quad A = \frac{c_g}{D_g}\left(-\frac{dD}{dc}\right) \qquad (33a)$$

Converting to dimensionless variables and rearranging Eq. (33)

$$F_g = \frac{2n^2}{(n+3)}\,[B(n+1) - n]^{-1} \qquad (34)$$

For values of $B < 1 + 2/F_g$, Eq. (34) may be converted to a more usable form:

$$n = \frac{(4B - 3)\,F_g + [(3 - 2B)^2 F_g^2 + 24\,BF_g]^{1/2}}{2[2 + (1 - B)\,F_g]} \qquad (35a)$$

For values of $B \geq 1 + 2/F_g$, it is assumed that $n = \infty$, $K = 2$.

For the case of constant diffusion coefficient, $D_g = 1$, $A = 0$, and $B = 1$, Eq. (35a) simplifies to:

$$n = (1/4)\ [F_g + (F_g^2 + 24\ F_g)^{1/2}] \qquad (35b)$$

Comparison of the integral method with variable n and constant diffusion coefficient is made with the numerical solution of Eq. (16) in Table I. Agreement between calculated values is excellent with less than 1% error.

TABLE I

COMPARISON OF INTEGRAL METHOD WITH VARIABLE n WITH NUMERICAL SOLUTION OF EQ. (16)

F_g	n	K	Integral Method, V_w	Numerical Integration, V_w
116.0	60.86	1.91	6.00	5.99
58.0	31.74	1.824	4.65	4.64
29.0	17.05	1.691	3.53	3.53
19.3	12.05	1.584	2.96	3.00
14.5	9.53	1.496	2.60	2.60
11.6	7.98	1.421	2.33	2.32
9.7	6.95	1.358	2.12	2.11
8.3	6.17	1.300	1.94	1.94
2.32	2.53	0.803	0.700	0.694

Use of the variable n integral solution in calculating flux rates is favored over the more tedious approximate solutions to Eq. (16) from the standpoint of accuracy and wide-range of application.

The film theory model [Eq. (3) for constant wall concentration and constant wall flux] along with the exact solution model are plotted in Fig. 4. All solutions are

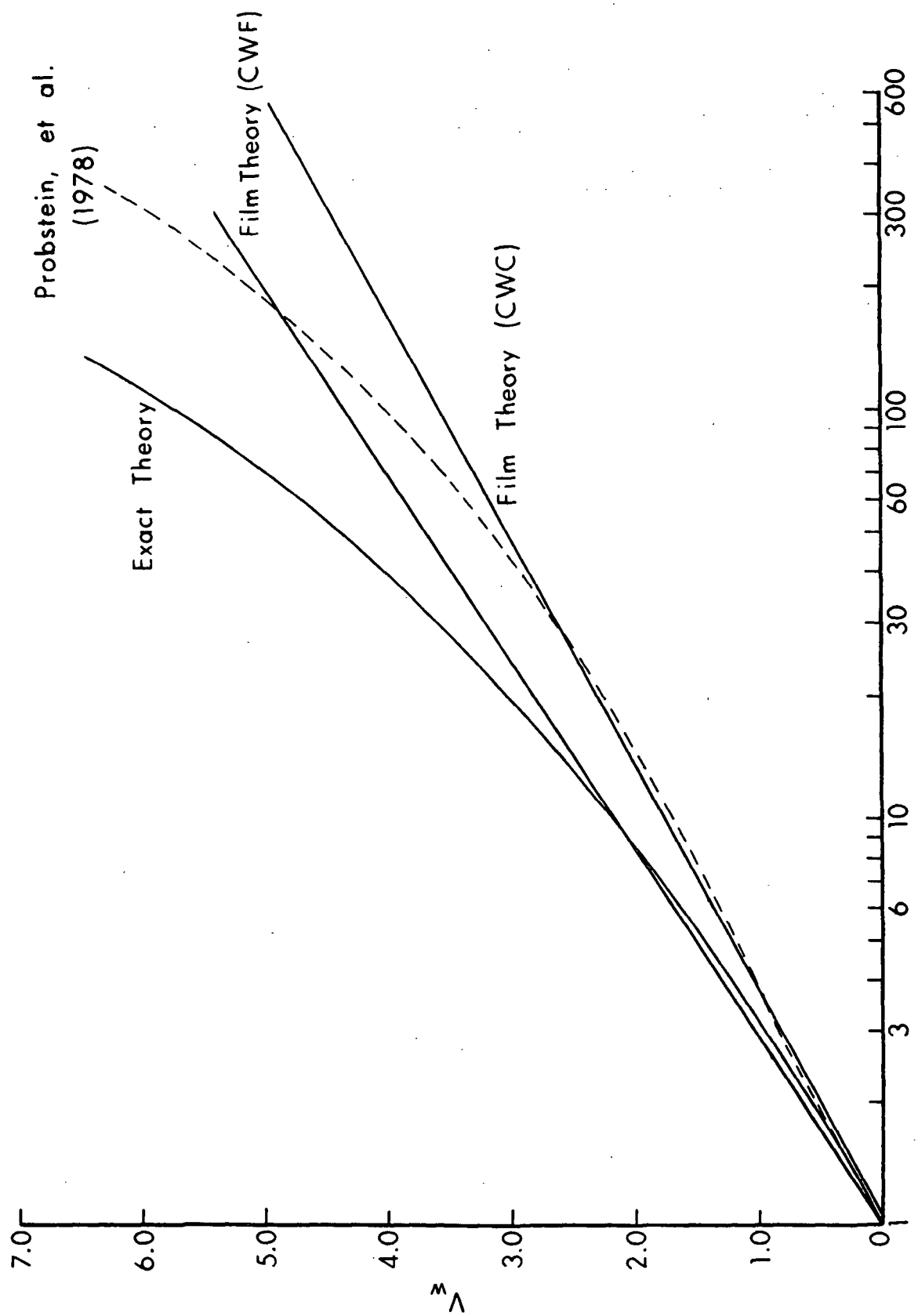

Figure 4. Comparison of integral method solutions with film theory models.

for constant fluid properties. The range of V_w values is from 0 to 7. This range is believed to encompass most probable operating conditions. Results indicate that the film theory model agrees with the exact solution for $F_g < 4$ when the constant wall concentration boundary condition is used. It is also shown that for the higher values of F_g, that is, for lower feed concentration, the exact solution model consistently predicts higher permeate flux rates than do either of the film theory models. The Probstein, et al. (1978) integral method relationship expressed by Eq. (29b) is also plotted as a dashed line in Fig. 4. Although predictive differences exist between our exact model and the Probstein, et al. model, the same upsloping flux behavior is observed.

Even though in the gel-polarized region where the CWC boundary condition seems reasonable, the CWF boundary condition gives better agreement, up to $F_g \approx 12$. It is not clear why the CWF boundary condition gives better agreement than the CWC boundary condition, which has been widely used. One may note that in the case of a reverse osmosis system, which is somewhat analogous to the corresponding pregel region in ultrafiltration, Gill, et al. (1965, 1971) have shown that the CWF boundary condition is more realistic.

The effect of concentration dependent diffusion coefficient is shown in Fig. 5. For the case of bovine serum albumin at pH 7.4, the parameter A can be estimated to be:

$$A = \frac{c_g}{D_g}\left(-\frac{dD}{dc}\right) = 0.187$$

where

$$D(c) = (5.9 - 0.016c) \times 10^{-7} \text{ [from Phillies, et al. (1976),}$$

$$c = \text{g/100 cc]}$$

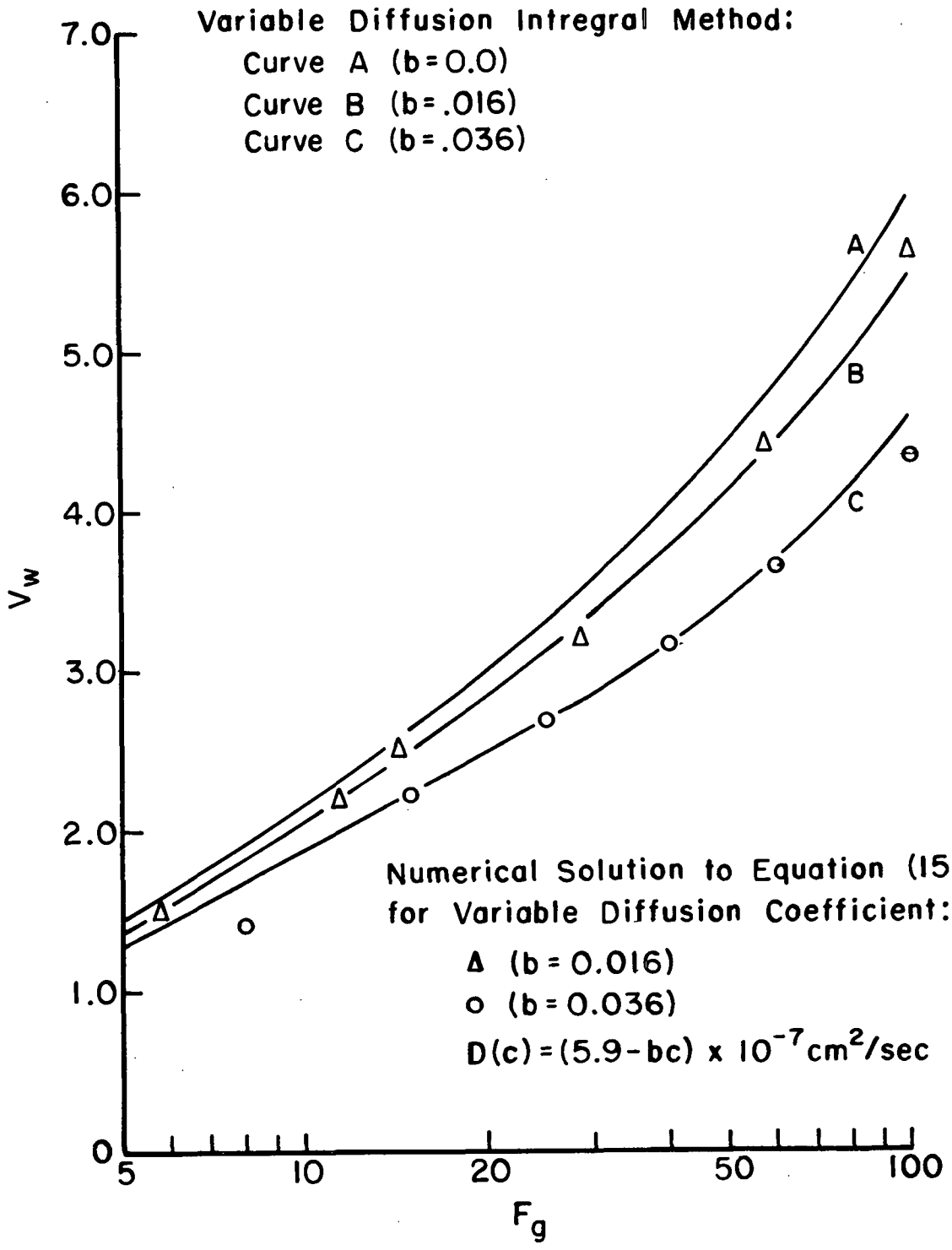

Figure 5. Comparison of Eq. (15) to integral method solution for concentration dependent diffusivity.

APPLICATION OF THEORY TO EXPERIMENTAL DATA

The availability of reliable data in the area of macromolecular ultrafiltration is rather limited. A characteristic problem encountered when comparing experimental flux rates with theory is the lack of a reliable value of the solute "gel" concentration and the concentration dependent diffusion coefficient. The measurement of the diffusion coefficient of bovine serum albumin has been reported by Keller, et al. (1971), Phillies, et al. (1976), Doherty and Benedek (1974). Unfortunately, results are often contradictory.

If one accepts the functional form of the film theory model, it is possible to extrapolate the value of c_g from ultrafiltration experiments. By measuring limiting flux rates at several values of c_B, the results are plotted semilogarithmically, and a straight line is drawn through the data points. This line is extended to the point of zero flux where the corresponding value of c_B is taken to equal c_g. In light of the developed integral solution, the potential error is apparent. By using experimental flux rates at low values of c_B, which is common in the literature, it is possible that an erroneous prediction of c_g may result. Probstein, et al. (1979) hint at this possibility in the form of a note [Ref. (19) of their paper] added at the end. Since the integral method solution may be approximated by the film theory model at values of $F_g < 4$, it is feasible to use the semilogrithmic, straight line extrapolation of experimental flux rates at high values of c_B in cases where c_g is approximately known. Whenever possible, it is recommended that an independent method be used in the determination of c_g as done by Kozinski and Lightfoot (1972). Although accurate ultrafiltration data for bovine serum albumin have been obtained by Probstein, et al. (1979) in a parallel plate system, their data cover only a narrow range of low concentration. More data over a wider range of concentration are needed to test theoretical models.

CONCLUSIONS

The agreement between the closed form integral method solution and the more exact numerical solution, for the case of constant diffusion coefficient, is excellent, deviations being less than 1 percent. However, the widely used film theory underpredicts flux by 20 and 30 percent for F_g = 15 and 50, respectively, where F_g is the ratio of the gel concentration to the feed concentration.

In the case of a concentration dependent diffusion coefficient, the integral method is satisfactory. Film theory results still deviate from the exact solution though not as much as in the case of a constant diffusion coefficient.

On the basis of film theory, the plot of permeate flux against feed concentration on a semilog graph should yield a straight line. This line, when extrapolated to zero flux, gives the gel concentration. In view of the significant deviations between film theory results and exact solution, such an extrapolation may not be valid and may underpredict gel concentration. We recommend that either experimental data should be taken over a wider range of feed concentration so that extrapolation could be reliable, or more exact theory should be used to determine gel concentration.

NOTATION

$\overline{A}$	Membrane pure water permeability constant [cm^3/dyne-s)], cm^2/dyne-sec
a	$3\langle u\rangle/h$[(1/sec)], 1/sec
c	Solute concentration, g solute/100 cc solutions
c_π	Solute concentration which corresponds to a developed osmotic pressure equivalent to ΔP, g solute/100 cc solution
D	Diffusion coefficient, cm^2/sec
d	Hydraulic diameter of membrane channel, cm
$\overline{D}$	$D(c)/D_B$
F	c/c_B
h	Channel half-height, cm
k	Mass transfer coefficient, cm/sec
l	Total length of membrane section, cm
P	Total pressure at a point, dynes/cm^2
Re	Reynolds number = $\langle u\rangle d/v$
Sc	Schmidt number = v/D
u	= Axial velocity, cm/sec
$\langle u\rangle$	Average axial velocity, cm/sec
v	Transverse velocity, cm/sec
$\lvert v_w \rvert$	Limiting permeate velocity at membrane surface, cm/sec
V_w	Positive permeate constant
w	Width of flow channel, cm
x	Axial distance coordinate, cm
y	Transverse distance coordinate, cm

GREEK LETTERS

$\delta(x)$	Concentration (mass) boundary layer thickness, cm
π	Osmotic pressure, dynes/cm^2

η Similarity variable

Γ Gamma function

$\Delta\pi$ Osmotic pressure difference across membrane, dynes/cm^2

ΔP Total applied pressure difference across membrane, dynes/cm^2

υ Kinematic viscosity, cm^2/sec

SUBSCRIPTS

g At the gelling condition

w At the membrane surface

B At the bulk condition

P At the permeate condition

ACKNOLWEDGMENTS

We wish to express our gratitude to Professor Ronald F. Probstein of the Massachusetts Institute of Technology for furnishing unpublished manuscripts. We are also grateful to member companies of The Institute of Paper Chemistry for their support of the graduate program.

We are thankful to Dr. William F. Blatt of the Amicon Corporation for supplying information about his experiments.

LITERATURE CITED

Blatt, W. F. Personal communication, 1978.

Blatt, W. F., Dravid, A., Michaels, A. S., and Nelsen, L. Solute polarization and cake formation in membrane ultrafiltration: causes, consequences, and control techniques. In Membrane science and technology, J. E. Flinn, ed., Plenum Press, New York, 1970. p. 47.

Doherty, P. and Benedek, G. B. The effect of electric charge on the diffusion of macromolecules. J. Chem. Phys. 61:5426(1974).

Doshi, M. R., Dewan, A. K., and Gill, W. N. The effect of concentration dependent viscosity and diffusivity on concentration polarization in reverse osmosis flow systems. AIChE Symp. Series 68:323(1971).

Gill, W. N., Tien, C., and Zeh, D. W. Concentration polarization effects in a reverse osmosis system. I&EC Fundam. 4:433(1965).

Gill, W. N., Derzansky, L. J., and Doshi, M. R. Convection diffusion in laminar and turbulent hyperfiltration (reverse osmosis) systems. In Surface and colloid science, E. Matijevic, ed., Wiley-Interscience, New York, N.Y. 4:261(1971).

Goldsmith, R. L. Macromolecular ultrafiltration with microporous membranes. I&EC Fundam. 10:113(1971).

Keller, K. H., Canales, E. R., and Yum, S. I. Tracer and mutual diffusion coefficients of proteins. J. Phys. Chem. 75:379(1971).

Kozinski, A. A. and Lightfoot, E. N. Protein ultrafiltration: a general example of boundary layer filtration. AIChE J. 18:1031(1972).

Mitra, G. and Lundblad, J. L. Ultrafiltration of immune serum globulin and human serum albumin: regression analysis studies. Sep. Sci. Tech. 13:89(1978).

Phillies, G. D. J., Benedek, G. B., and Mazer, N. A. Diffusion in protein solutions at high concentrations: a study by quasielastic light scattering spectroscopy. J. Chem. Phys. 65:1883(1976).

Probstein, R. F., Shen, J. S., and Leung, W. F. Ultrafiltration of macromolecular solutions at high polarization in laminar channel flow. Desalination 24:1(1978).

Probstein, R. F., Leung, W. F., and Alliance, Y. Determination of diffusivity and gel concentration in macromolecular solutions by ultrafiltration. J. Phys. Chem. 83(9):1228(1979).

Shen, J. J. S. and Probstein, R. F. On the prediction of limiting flux in laminar ultrafiltration of macromolecular solutions. I&EC Fundam. 16:459(1977).

SECTION 5 - MANUSCRIPT NUMBER 4

PRESSURE INDEPENDENT ULTRAFILTRATION - IS IT GEL LIMITED OR OSMOTIC PRESSURE LIMITED?

ACS Symposium Series, No. 154. Synthetic membranes: Vol. II Hyper- and Ultrafiltration Uses (1981)

PRESSURE-INDEPENDENT ULTRAFILTRATION - IS IT GEL LIMITED OR OSMOTIC PRESSURE LIMITED?

ABSTRACT

In macromolecular ultrafiltration, as pressure is increased, permeate flux first increases and then in a large number of cases levels out and remains more or less pressure independent. This could be due to the increase in solute concentration at the membrane surface such that either gel formation occurs or the corresponding osmotic pressure approaches the applied pressure. Limiting flux for the gel-polarized case was recently analyzed for cross-flow and unstirred batch cell systems by Trettin and Doshi (1980a,b). In this paper we have analyzed the osmotic pressure limited ultrafiltration for the two systems. Our unstirred batch cell data and the literature cross-flow data agree quite well with the theory. We have further shown that an unstirred batch cell system can be used to determine whether pressure-independent ultrafiltration of macromolecular solution is gel or osmotic pressure limited. Other causes for the observed pressure independence may be present but are not considered in this paper.

INTRODUCTION

Ultrafiltration involves the pressure-activated separation of chemical species which have different permeability through a membrane. Solute retention is achieved on the basis of steric exclusion, that is, a sieving-type of mechanism; solvent passes through by pore flow. As an initially homogeneous solution is pressurized over a selective membrane, solvent permeates through while rejected solute accumulates in the vicinity of the membrane. The net result is a layer of solution adjacent to the membrane surface of substantially greater solute concentration than that of the bulk solution. This phenomenon of concentration polarization always operates to reduce the solvent permeation rate, which may become pressure independent in some cases.

In the ultrafiltration of macromolecular solutions, a large number of investigators have observed that as pressure is increased, permeate flux first increases and then remains more or less pressure independent. Blatt, et al. (1970), among others, argued that one of the reasons for the observed pressure independence could be the formation of a gel layer on the membrane surface. The permeate rate in this case may be expressed as:

$$| v_w | = \frac{\Delta P - \Delta \pi}{\mu (R_m + R_g)} \qquad (1)$$

where R_m and R_g are the hydraulic resistances of the membrane and gel layer, respectively, ΔP and $\Delta \pi$ represent the applied pressure and osmotic back pressure, and μ is the permeate viscosity. In the case of pressure independent ultrafiltration of macromolecular solutions, if the applied pressure is much greater than the osmotic pressure difference across the membrane, and since the gel resistance is generally substantially greater than that of a membrane, Eq. (1) can be simplified to:

$$v_w \simeq \frac{\Delta P}{\mu R_g}, \quad \Delta P >> \Delta\pi, \quad R_g >> R_m$$

Any increase in pressure after the occurrence of gel formation merely increases gel thickness and, hence, R_g so that the permeate flux remains essentially independent of pressure.

There could be other possibilities for the observed pressure independence. We know that, in the absence of gel formation, increase in the applied pressure results in the increase in solute concentration at the membrane surface. If osmotic pressure is quite sensitive to the changes in solute concentration, it is possible that an increase in ΔP gives rise to proportional increase in $\Delta\pi$ so that the net driving force, $(\Delta P - \Delta\pi)$ remains virtually constant. From Eq. (1), then, the permeate rate in the absence of gel formation ($R_g = 0$) can be pressure independent due to osmotic pressure limitation. Other phenomena, for example, solute-membrane interactions may give rise to pressure-independent permeate rate.

Gel-polarized ultrafiltration was recently analyzed for cross-flow and unstirred batch cell systems by Trettin and Doshi (1980 a,b). We have shown in these papers that the widely used film theory does not predict the limiting flux accurately. The objective of this paper is to derive an expression for the permeate flux when the pressure independent ultrafiltration of macromolecular solutions is osmotic pressure limited. We will also attempt to distinguish between gel and osmotic pressure limited ultrafiltration of macromolecular solutions.

The effect of osmotic pressure in macromolecular ultrafiltration has not been analyzed in detail, although many similarities between this process and reverse osmosis may be drawn. An excellent review of reverse osmosis research has been given by Gill et al. (1971). It is generally found, however, that the simple linear osmotic pressure-concentration relationship used in reverse osmosis studies cannot be

applied to ultrafiltration, where the concentration dependency of macromolecular solutions is more complex. It is also reasonable to assume that variable viscosity effects may be more pronounced in macromolecular ultrafiltration as opposed to reverse osmosis. Similarly, because of the relatively low diffusivity of macromolecules compared with typical reverse osmosis solutes (by a factor of 100), concentration polarization effects are more severe in ultrafiltration.

An early work considering osmotic pressure in the ultrafiltration of macromolecular solutions was done by Blatt, et al., (1970), who employed a theory which had been developed for cross-flow reverse osmosis systems. They essentially suggested that the film theory relationship given by Eq. (2) could be solved simultaneously with Eq. (1) to predict permeate rates, where the value of k was determined from a Leveque-type solution of the convective diffusion equation neglecting transverse velocity.

$$\left| v_w \right| = k \ln \left[\frac{c_w - c_p}{c_o - c_p} \right] \tag{2}$$

Presented data were not analyzed in terms of this model, however, because it was felt that macromolecular solutions generally had very low osmotic pressures.

Goldsmith (1971) pointed out that developed osmotic pressures for macromolecular solutions were not necessarily negligible. The ultrafiltration of Carbowax 20M (polyethylene oxide) and various Dextrans was studied in thin channel and tube flow as well as stirred batch cell. Both turbulent and laminar flow regimes were considered. Data were analyzed with the use of Eq. (2) and the phenomenological relationship of Eq. (1) with $R_g = 0$. From Eq. (1) it was possible to calculate an average value of $\Delta\pi$ where R_m, the membrane resistance, ΔP, and experimental flux $\left| \overline{v_w} \right|$ were known. The average value of c_w could be extracted from a known osmotic

pressure relationship, and an experimental value of $\overline{k}$ could finally be found from Eq. (2). Experimental values of $\overline{k}$ were compared to theoretical values to estimate the molecular diffusion coefficient. The difference between the experimental and the literature values of the diffusion coefficient was attributed to the concentration dependency of viscosity and diffusion coefficient.

Kozinski and Lightfoot (1972) modeled the ultrafiltration of bovine serum albumin (BSA) through a rotating disk. Concentration dependent viscosity and diffusivity were assumed, and the one-dimensional convective diffusion equation, which was coupled to the appropriate Navier-Stokes equation, was solved numerically. Osmotic pressure data of Scatchard et al. (1944) were used. Numerical prediction of flux agreed very well with experimental results for the rotating disk. Their model was extended to other flow geometries, such as tubular and thin channel, where average values of viscosity and diffusivity were used. The convective diffusion equation in this case was solved through similarity transformation. The published data of Blatt, et al., (1970) were analyzed in terms of the developed model, but agreement was not good.

Mitra and Lundblad (1978) studied the thin channel ultrafiltration of immune serum globulin (ISG) and human serum albumin (HSA). Data were interpreted using the film theory relationship of:

$$\left| \overline{v}_w \right| = A \langle u \rangle^B \ln (c_w/c_o) \qquad (3)$$

where multiple regression techniques were employed to solve for the value of the constants A, B, and c_w. The value of c_w was assumed to equal the corresponding concentration at which the developed osmotic pressure approximately equalled the applied system pressure. Agreement of data with the general model was not good, the

calculated value of A exhibiting a 21% standard deviation. Large axial pressure drops along the thin channel at the higher velocities studied may be a partial explanation of the discrepancy.

Leung and Probstein (1979) studied the ultrafiltration of macromolecular solutions in steady state, laminar channel flow. The convective diffusion equation was solved by an integral method. A parabolic concentration profile was assumed. The osmotic pressure relationship of Vilker (1975) for 0.15M saline BSA solutions at pH 4.5, and a diffusivity relationship obtained by linearly interpolating the diffusion coefficient value between the gel and dilute solution concentration limits were used. The determination of this diffusivity relationship has been outlined in a previous paper [Probstein, et al. (1979)]. The integral solution was checked in the limiting case of a linear osmotic pressure-concentration relationship and constant diffusivity with Brian's (1966) finite difference solution for reverse osmosis systems. Thin channel ultrafiltration data were acquired by Leung and Probstein using BSA in 0.10M acetate solution at pH 4.7.

A discrepancy emerges in the use of Vilker's osmotic pressure relationship, however. In an earlier paper, Probstein, et al., (1979) determined the gelling (solubility limit) concentration of BSA in 0.10M acetate solution (pH 4.7) to be 34 g/100 cc. We have determined the value to be approximately 38.5 g/100 cc [Trettin and Doshi (1980b)]. It is clear from Fig. 5 that Vilker has determined osmotic pressures for BSA in 0.15M saline solutions (pH 4.5) up to concentrations of 48 g/100 cc. This finding suggests the effect of buffer type is substantial in influencing solute solubility limits and most probably solution osmotic pressure. Therefore, it is hardly admissible to use Vilker's saline buffer osmotic pressure data to interpret the thin channel ultrafiltration data of BSA in acetate buffer without further confirmation of the effect of buffer type.

The preceding review has shown that although many advances have been made in the understanding of macromolecular ultrafiltration, some very fundamental questions still remain unanswered. For instance, the establishment of when an ultrafiltration process is osmotic pressure limited or gel limited needs to be more clearly defined. In macromolecular ultrafiltration solution, osmotic pressure is often a strong function of moderate-to-high solute concentration (c_w) due to the increased importance of the second and third order virial terms in the Flory equation [Brandup and Immergut (1967), Billmeyer (1971)]. In this event, the ultrafiltration flux may be limited by the osmotic pressure and/or by the formation of a gel layer depending on the nature of the solute and operating conditions. The determination of a flux-limiting cause is the primary concern of this paper.

THEORETICAL DEVELOPMENT

Consider the unstirred batch cell geometry shown in Fig. 1 where the general solute mass balance equation of

$$\frac{\partial c}{\partial t} - \left| v_w \right| \frac{\partial c}{\partial y} = D \, \partial^2 c / \partial y^2 \qquad (4)$$

applies. It is implicitly assumed in the derivation of Eq. (4) that the solution density and diffusion coefficient are independent of solute concentration.

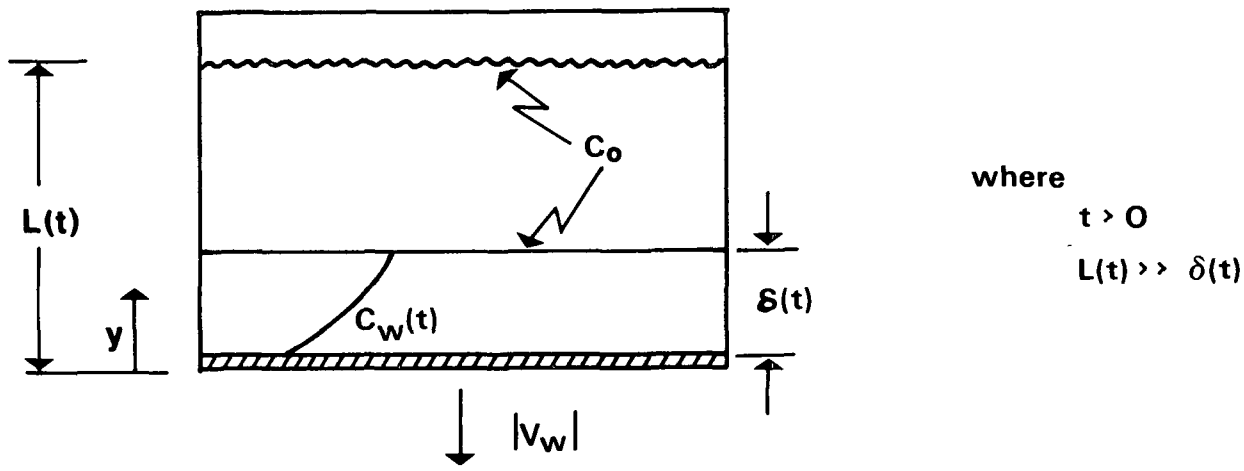

Figure 1. Batch cell geometry.

The appropriate boundary and initial conditions are:

$$\text{at } y = 0 \; ; \; c = c_w(t) \tag{5}$$

$$-\left| v_w \right| \; c_w \; R = D \left. \frac{\partial c}{\partial y} \right|_{y=0} \tag{6}$$

$$y \to \infty, \; c = c_o \text{ for all } t \tag{7}$$

where

$$R = 1 - c_p/c_w \tag{8}$$

The phenomenological equation of permeate velocity is

$$\left| v_w \right| = A\Delta P \; (1 - \frac{\Delta\pi}{\Delta P}); \; A = \frac{1}{\mu R_m} \tag{9}$$

where

$$\Delta\pi = \pi_w - \pi_p \tag{10}$$

If osmotic pressure is related to solute concentration by a cubic equation:

$$\pi = b_0 c + b_1 c^2 + b_2 c^3$$

then

$$\Delta\pi = B \; c_w \; \Delta P \; [1 + \alpha_1 \; c_w + \alpha_2 \; c_w^2] \tag{11}$$

where

$$B = \frac{R b_0}{\Delta P}, \; \alpha_1 = \frac{b_1 \; (2-R)}{b_0} \text{ and } \alpha_2 = \frac{b_2 \; (3-3R+R^2)}{b_0} \tag{12}$$

Our objective is to derive an expression for the permeate velocity when ultrafiltration is osmotic pressure limited. We, therefore, introduce equivalent wall concentration, c_{wa}, for which the osmotic pressure is equal to the applied pressure. In the asymptotic case, as $\Delta\pi$ approaches ΔP, the permeate velocity will approach zero, Eq. (9), and from Eq. (11) we have:

$$1 = B \; c_{wa} \; (1 + \alpha_1 \; c_{wa} + \alpha_2 \; c_{wa}^2) \tag{13}$$

Equation (13) is then the defining equation for c_{wa}. We will use c_{wa} as a characteristic concentration in making local concentration dimensionless. Time, distance, and velocity are expressed in dimensionless forms by a proper combination of a characteristic velocity $A\Delta P$ and diffusion coefficient, D:

$$\tau = \frac{(A\ \Delta P)^2 t}{D},\quad z = \frac{A\ \Delta P}{D}\ y,\quad w = \frac{|\ v_w\ |}{A\ \Delta P},\quad \theta = c/c_{wa} \tag{14}$$

Eq. (4) may be transformed to

$$\frac{\partial \theta}{\partial \tau} - w\frac{\partial \theta}{\partial z} = \frac{\partial^2 \theta}{\partial z^2} \tag{15}$$

where the boundary conditions of Eq. (5)-(8) become

$$-\ R\ w\ \theta_w = \frac{\partial \theta}{\partial z}\Big|_{z=0} \tag{16}$$

$$\theta(\tau,0) = \frac{c_w(t)}{c_{wa}} = \theta_w \tag{17}$$

$$\theta\ (0,z) = \theta\ (\tau,\infty) = \frac{c_o}{c_{wa}} = \theta_o \tag{18}$$

and Eq. (9) may be rewritten as

$$w = 1 - Bc_{wa}\ \theta_w\ (1 + \alpha_1 c_{wa}\ \theta_w + \alpha_2 {c_{wa}}^2\ {\theta_w}^2) \tag{19}$$

Introducing the similarity coordinate

$$x = z/(4\tau)^{1/2} \tag{20}$$

Equations (15)-(18) become [$\theta(\tau,x) \Rightarrow \theta(\tau,x)$]

$$4\tau\ \frac{\partial \theta}{\partial \tau} - 2\ (x + w\sqrt{\tau})\ \frac{\partial \theta}{\partial x} = \frac{\partial^2 \theta}{\partial x^2} \tag{21}$$

$$- 2\sqrt{\tau}\ R\ w\ \theta_w = \frac{\partial \theta}{\partial x}\Big|_{x=0} \tag{22}$$

$$\theta\ (\tau,0) = \theta_w,\ \theta\ (\tau,\infty) = \theta_o \tag{23}$$

The similarity transformation, Eq. (20), used here is generally applied to obtain small time solution. However, in the case of gel polarized ultrafiltration, Trettin and Doshi (1980b) have used such similarity transformation to obtain an expression for the limiting permeate velocity. We have, therefore, used similarity transformation to evaluate osmotic pressure limited permeate velocity. In the case of gel polarized ultrafiltration, $c_w = c_g$ = constant and consequently, Eq. (21) to (23) can be solved by considering θ as a function of x only and by setting $w\ \tau^{0.5}$ as a constant. However, in the osmotic pressure limiting case considered here, c_w is a function of time. We can solve Eq. (21) to (23) in the form of a power series in $\tau^{-0.5}$:

$$\theta = f_0(x) + \frac{f_1(x)}{\tau^{1/2}} + \frac{f_2(x)}{\tau} + \ldots \tag{24}$$

then

$$\theta_w = 1 + \frac{f_1(0)}{\tau^{1/2}} + \frac{f_2(0)}{\tau} + \ldots \tag{25}$$

where

$$\lim_{\tau\to\infty} \theta_w = f_0(0) = 1 \tag{26}$$

Substituting for θ_w in Eq. (19) and rearranging yields:

$$w\sqrt{\tau} = \beta_1 f_1(0) + \frac{\beta_2}{\tau^{1/2}} + \ldots \tag{27}$$

where

$$\beta_1 = -\ (1 + B\ \alpha_1\ c_{wa}^2 + 2B\ \alpha_2\ c_{wa}^3) \tag{28}$$

The value of β_2 remains to be determined.

Substituting for θ and $w\sqrt{\tau}$ in Eq. (21) and considering terms of coefficient τ^0 only gives

$$-2xf_0' - 2\beta_1 f_1(0)f_0' = f_0'' \tag{29}$$

where the boundary conditions of Eq. (22)-(23) become

$$-2R\,[\beta_1 f_1(0)]\, f_0(0) = f_0'(0) \tag{30}$$

$$f_0(\infty) = \theta_o \tag{31}$$

$$f_0(0) = 1 \tag{32}$$

Equation (29) may be integrated to yield

$$\theta_o = 1 + I_1 \exp\,[\beta_1^2 f_1^2(0)] \int_{\beta_1 f_1(0)}^{\infty} \exp\,(-\xi^2)\, d\,\xi \tag{33}$$

where

$$\xi = x + \beta_1 f_1(0) \tag{34}$$

or, more simply,

$$I_1 = \frac{2(\theta_o - 1)}{\sqrt{\pi}\,\exp\left(\frac{V_w^2}{4}\right)\,\operatorname{erfc}\left(\frac{V_w}{2}\right)} \tag{35}$$

where $\frac{V_w}{2} = \beta_1 f_1(0)$

Considering the wall boundary condition of Eq. (30), Eq. (35) becomes

$$\frac{V_w}{2} = \frac{1-\theta_o}{R\sqrt{\pi}\,\exp\left(\frac{V_w^2}{4}\right)\,\operatorname{erfc}\left(\frac{V_w}{2}\right)} \tag{36}$$

In a similar manner as previously, consider coefficients of $\tau^{-1/2}$ only in Eq. (21)

$$f_1'' + 2f_1' (x + \beta_1 f_1(0)] + 2f_1 = - 2\beta_2 I_1 \exp [- (x^2 + 2\beta_1 f_1(0)x)] \tag{37}$$

Considering the coefficients of $\tau^{-1/2}$ for the wall boundary condition of Eq. (22) yields

$$-2R (\beta_1 f_1^2(0) + \beta_2) = f_1'(0) \tag{38}$$

where

$$\beta_1 f_1(0) = I_1/2R; \; f_1(\infty) = 0 \tag{39}$$

The solution for f_1 is:

$$f_1 = [f_1(0) + \beta_2 I_1 \sqrt{\pi} \int_{\frac{V_w}{2}}^{r} \exp(r^2)\operatorname{erfc}(r)dr]$$

$$\exp\left[\frac{V_w^2}{4}\right] \exp(-r^2)$$

where $r = x + \frac{V_w}{2}$, and

$$\lim_{\substack{x \to \infty \\ r \to \infty}} f_1 = 0, \qquad \lim_{x \to 0} f_1 = f_1(0) = - \frac{I_1}{2R\beta_1} \tag{41}$$

Evaluating the first derivative of Eq. (40) at x = 0 gives

$$f'(0) = -2\beta_1 f_1^2(0) + \beta_2 I_1 \sqrt{\pi} \exp\left(\frac{V_w^2}{4}\right) \operatorname{erfc}\left(\frac{V_w}{2}\right) \tag{42}$$

The wall boundary condition of Eq. (38) may be equated to Eq. (42) to yield a relationship for the value of β_2, namely

$$\beta_2 = \frac{\beta_1 f_1^2(0)(1-R)}{(R-1) + \theta_o} \tag{43}$$

Substituting for β_2 in Eq. (27), neglecting terms smaller than $\tau^{-1/2}$ yields

$$w\sqrt{\tau} = \beta_1 f_1(0)\left[1 - \frac{f_1(0)(R-1)}{\sqrt{\tau}(R-1)+\theta_o]}\right] \tag{44}$$

The dimensionless permeate velocity will be proportional to $\tau^{-1/2}$ when

$$\sqrt{\tau} >> \frac{f_1(0)(R-1)}{[(R+1)+\theta_o]} = \frac{I_1(1-R)}{2R\ \beta_1\ [(R-1)+\theta_o]} \tag{45}$$

Equation (45) is written in dimensional form as

$$t >> \frac{D}{(A\ \Delta P)^2}\left[\frac{V_w\ (1-R)}{|\beta_1|\ [(R-1)\ +\ \theta_o]}\right] \tag{46}$$

If the criterion suggested in Eq. (46) is met, solute concentration at the membrane surface will be approximately equal to the asymptotic value, c_{wa}. The solute concentration distribution can be described by a single independent variable, x. The problem then becomes analogous to the gel polarized ultrafiltration case solved in Trettin and Doshi (1980b). In this same paper, an integral method solution is also derived. A plot of calculated values of V_w vs. θ_o which satisfy Eq. (36) is given in Fig. 2 for various values of R. An unpublished work of Vilker (1975) has recently come to our attention where a similar concept is presented.

An analogous treatment to the unstirred batch cell may be performed for the thin channel system where

$$u\frac{\partial c}{\partial \tilde{x}} - |v_w|\frac{\partial c}{\partial y} = D\frac{\partial^2 c}{\partial y^2} \tag{47}$$

and the boundary conditions are

$$\text{at } y = 0 \qquad c = c_w\ (\tilde{x}) \tag{48}$$

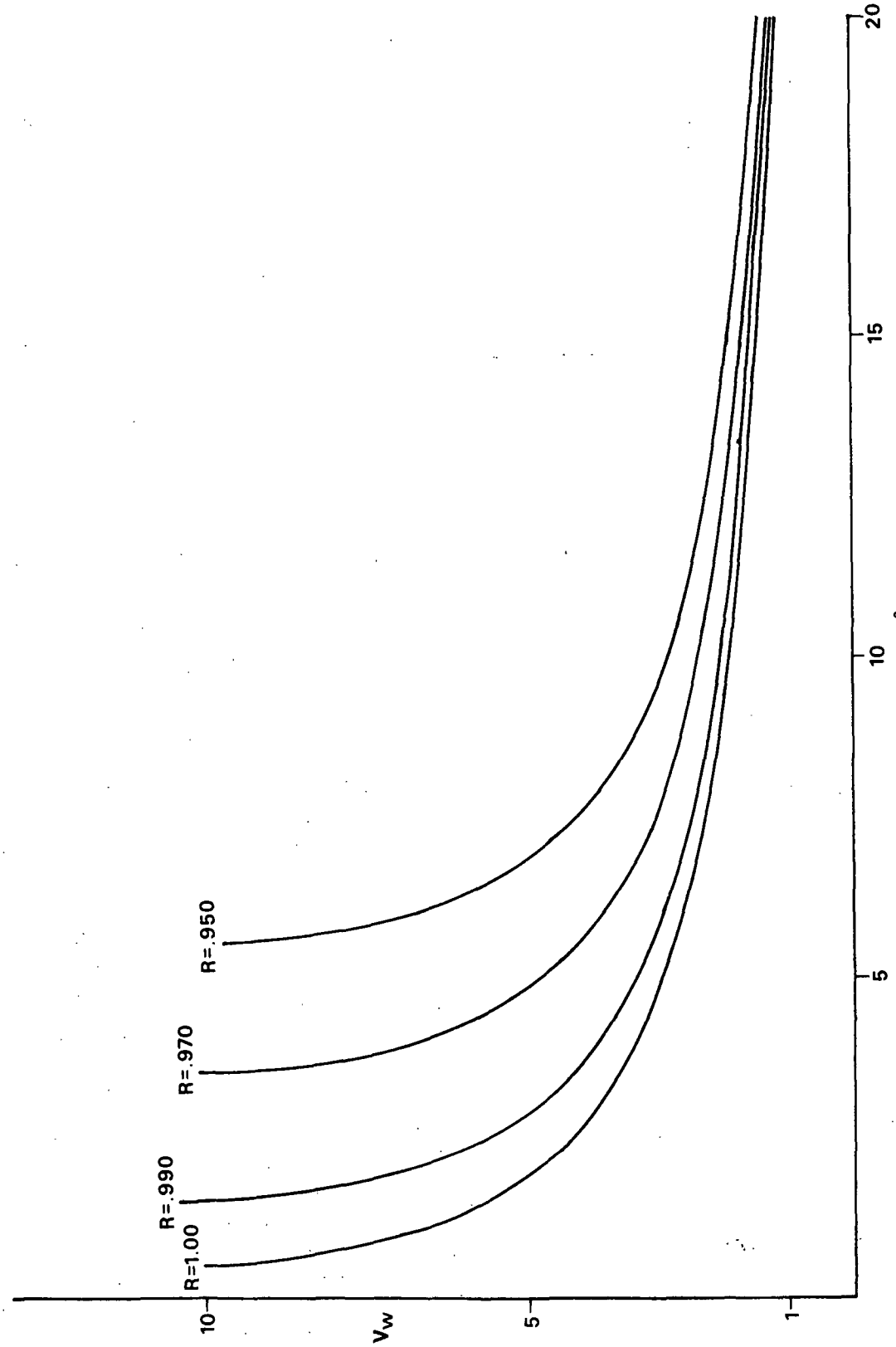

Figure 2. V_w vs. θ_o calculated from Eq. (41) for various values of R.

$$-\left|v_w\right| \; c_w \; R = D \left.\frac{\partial c}{\partial y}\right|_{y=0} \tag{49}$$

$$y \to \infty, \; c = c_o \text{ for all } \tilde{x} \tag{50}$$

$$\tilde{x} \to 0, \; c = c_o \text{ for all } y \tag{51}$$

A diagram of the thin-channel system is shown in Fig. 3.

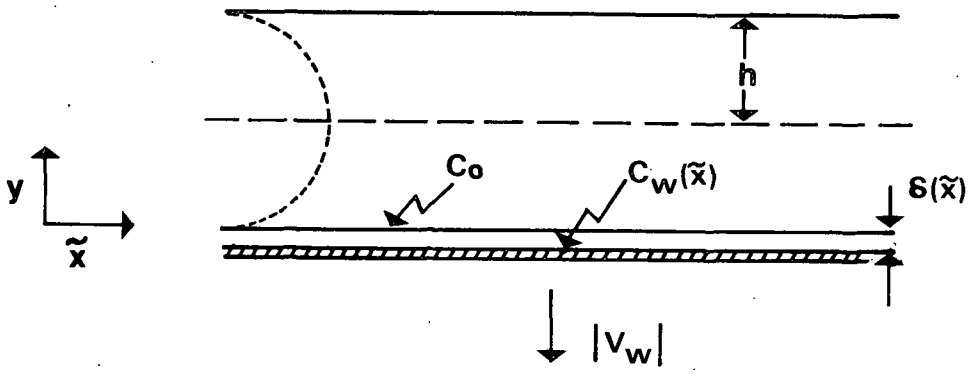

Figure 3. Thin-channel cross flow system.

Transforming Eq. (47) to dimensionless form, we find

$$\phi \; z \frac{\partial \theta}{\partial \lambda} - w \frac{\partial \theta}{\partial z} = \frac{\partial^2 \theta}{\partial z^2} \tag{52}$$

where

$$z = \frac{A \; \Delta P}{D} \; y, \; w = \frac{\left|v_w\right|}{A \; \Delta P}, \; \theta$$

$$= c/c_{wa}, \; \lambda = \frac{(A \; \Delta P)^2 \; \tilde{x}}{\langle u \rangle \; D}, \; \phi = \frac{3D}{h \; A \; \Delta P} \tag{53}$$

and assuming a linearized axial velocity profile, namely,

$$u = \frac{3\langle u \rangle}{h} \; y \tag{54}$$

The boundary conditions of Eq. (48)-(51) become

$$- R\ w\ \theta_w = \frac{\partial \theta}{\partial z}\Big|_{z=0} \tag{55}$$

$$\theta\ (\lambda,0) = \frac{c_w(\tilde{x})}{c_{wa}} = \theta_w \tag{56}$$

$$\theta\ (0,z) = \theta(\lambda,\infty) = c_o/c_{wa} = \theta_o \tag{57}$$

Equation (19) remains unchanged except that θ_w is now a function of λ instead of τ.

$$w = 1 - Bc_{wa}\ \theta_w\ (1 + \alpha_1 c_{wa}\ \theta_w + \alpha_2 c_{wa}^2\ \theta_w^2) \tag{19}$$

Introducing the similarity coordinate, analogous to the unstirred batch cell problem, Eq. (20),

$$\eta = z/\left(\frac{3\lambda}{\phi}\right)^{1/3} \tag{58}$$

Equation (52), (55)-(57) become [$\theta\ (\lambda,z) \Rightarrow \theta\ (\lambda,\eta)$]

$$3\ \lambda\ \eta\ \frac{\partial \theta}{\partial \lambda} - \left(\eta^2 + w\ \left(\frac{3\lambda}{\phi}\right)^{1/3}\right)\ \frac{\partial \theta}{\partial \eta} = \frac{\partial^2 \theta}{\partial \eta^2} \tag{59}$$

$$- \left(\frac{3\lambda}{\theta}\right)^{1/3} R\ w\ \theta_w = \frac{\partial \theta}{\partial \eta}\Big|_{\eta=0} \tag{60}$$

$$\theta(\lambda,0) = \theta_w \tag{61}$$

$$\theta(\lambda,\infty) = \theta_o \tag{62}$$

The corresponding gel polarized ultrafiltration problem, where $c_w = c_g$ = constant, is solved by Trettin and Doshi (1980a) by considering θ as a function of η only. In the osmotic pressure limited case, as we have done for the unstirred batch cell, we expand θ in the following form:

$$\theta = g_o(\eta) + \frac{g_1(\eta)}{\lambda^{1/3}} + \frac{g_2(\eta)}{\lambda^{2/3}} + \ldots \tag{63}$$

$$\theta_w = 1 + \frac{g_1(0)}{\lambda^{1/3}} + \frac{g_2(0)}{\lambda^{2/3}} + \ldots \tag{64}$$

where

$$\lim_{\lambda \to \infty} \theta_w = g_o(0) = 1 \tag{65}$$

Substituting for θ_w in Eq. (19) and rearranging yields

$$w\,\lambda^{1/3} = \beta_1\, g_1(0) + \frac{\beta_2}{\lambda^{1/3}} + \ldots \tag{66}$$

Substituting for θ and $w\,\lambda^{1/3}$ in Eq. (59) and considering terms of coefficient λ^0 only gives

$$-\eta^2\, g_0' - \left(\frac{3}{\phi}\right)^{1/3} \beta_1\, g_1(0)\, g_0' = g_0'' \tag{67}$$

where the boundary conditions of Eq. (60)-(62) become

$$-\left(\frac{3}{\phi}\right)^{1/3} \beta_1\, g_1(0)\, g_0(0)\, R = g_0'(0) \tag{68}$$

$$g_0(\infty) = \theta_o \tag{69}$$

$$g_0(0) = 1 \tag{70}$$

Equation (67) may be integrated using the boundary conditions of Eq. (69)-(70) to yield

$$I_1 = \frac{\theta_o - 1}{\int_0^\infty \exp\left[-\left(\frac{1}{3}\eta^3 + W_w\,\eta\right)\right] d\eta} \tag{71}$$

where

$$-W_w\, R = g_0'(0) = I_1 \tag{72}$$

Considering the wall boundary condition of Eq. (68), Eq. (71) becomes

$$W_w = \frac{1 - \theta_o}{R \int_0^\infty \exp\left[-\left(\frac{1}{3}\eta^3 + W_w \eta\right)\right] d\eta} \tag{73}$$

Without considering coefficients of $\lambda^{-1/3}$, we may develop an approximate relationship defining the parameters which influence the rate at which an asymptotic wall concentration is reached. From Eq. (64)

$$\theta_w = 1 + \frac{g_1(0)}{\lambda^{1/3}} + \ldots \tag{74}$$

Therefore, for $c_w \approx c_{wa}$,

$$\lambda^{1/3} >> g_1(0) \tag{75}$$

or simply,

$$\tilde{x} >> \frac{D^2 \langle u \rangle}{h(A\ \Delta P)^3} \left(\frac{W_w}{|\beta_1|}\right)^3 \tag{76}$$

From Eq. (76) it can be seen that the membrane pure solvent flux (A ΔP) has a large effect in determining the required channel length to reach an asymptotic wall concentration ($c_w \approx c_{wa}$). Since $\dot{\gamma}_w = \frac{3\langle u \rangle}{h}$, it may be seen that hydrodynamic shear at the membrane surface is also an important factor and Eq. (76) becomes:

$$\tilde{x} >> \frac{D^2\ \dot{\gamma}_w}{3(A\ \Delta P)^3} \left[\frac{W_w}{|\beta_1|}\right]^3 \tag{77}$$

When the criterion of Eq. (46) for the unstirred batch cell, or Eq. (77) for the cross-flow parallel plate system, is satisfied, it is possible to make the

simplifying assumption of constant wall concentration ($c_w \approx c_{wa}$). Consequently, Eq. (36) becomes

$$\frac{c_{wa} - c_o}{c_{wa} - c_p} = \frac{\sqrt{\pi}}{2} V_w \exp\left(\frac{V_w^2}{4}\right) \operatorname{erfc}\left(\frac{V_w}{2}\right) \tag{78}$$

where

$$V_w = w\sqrt{4\tau} = |v_w| (4t/D)^{1/2} \tag{79}$$

for the unstirred batch cell and Eq. (73) becomes

$$\frac{c_{wa} - c_o}{c_{wa} - c_p} = W_w \int_0^\infty \exp\left[-\left(\frac{1}{3}\eta^3 + W_w \eta\right)\right] d\eta \tag{80}$$

where

$$W_w = |v_w| \left[\frac{h \tilde{x}}{\langle u \rangle D^2}\right]^{1/3} \tag{81}$$

for the cross-flow parallel plate systems.

An integral method solution of Eq. (78) has been derived by Trettin and Doshi (1980b) and may be represented as

$$V_w = \left[\frac{c_{wa} - c_o}{c_{wa} - c_p}\right] \left[K_1 \frac{c_{wa} - c_p}{c_o - c_p}\right]^{1/2} \tag{82}$$

where

$$K_1 = 2n_1/(n_1 + 1) \tag{83}$$

and

$$n_1 = \frac{1}{2}\left[\left(\frac{c_{wa} - c_p}{c_o - c_p}\right) + \left(\left(\frac{c_{wa} - c_p}{c_o - c_p}\right)^2 + 8\left(\frac{c_{wa} - c_p}{c_o - c_p}\right)\right)^{1/2}\right] \tag{84}$$

Similarly, the solution of Eq. (80) for the parallel plate system has been derived by Trettin and Doshi (1980a) and is represented as

$$W_w = \left[\frac{c_{wa} - c_p}{c_{wa} - c_p}\right] \left[K_2 \frac{c_{wa} - c_p}{c_o - c_p}\right]^{1/3} \tag{85}$$

where

$$K_2 = 2n_2^2/(n_2 + 1)\ (n_2 + 2) \tag{86}$$

and

$$n_2 = \frac{1}{4}\left[\left(\frac{c_{wa} - c_p}{c_o - c_p}\right) + \left(\left(\frac{c_{wa} - c_p}{c_o - c_p}\right)^2 + 24\left(\frac{c_{wa} - c_p}{c_o - c_p}\right)\right)^{1/2}\right] \tag{87}$$

In both integral method solutions the value of D and solution density are assumed constant. Additionally, as shown in Trettin and Doshi (1980a,b), both integral method solutions agree very well with their corresponding exact solutions. Note that if one wants to calculate V_w or W_w, integral method results, Eq. (82)-(87) are convenient, whereas for the calculation of the asymptotic wall concentration, c_{wa}, exact solution, Eq. (78)-(81) are convenient.

In unstirred batch cell ultrafiltration, the value of $|v_w|$ is typically very small and therefore difficult to measure instantaneously. It is possible, however, to accurately measure eluted permeate volume (ΔV) as a function of time. Therefore, upon integration, Eq. (79) becomes

$$\Delta V = 2A_t\ V_w\ (D/4)^{1/2}\ T^{1/2} \tag{88}$$

where

A_t = the transport surface area of membrane

T = time of permeate collection

$\Delta V = \int_o^T A_t\ |v_w|\ dt$ = eluted permeate volume in time T

When accumulated permeate volume is measured at three consecutive times (T_1, T_2, T_3), it is possible to write

$$\frac{\Delta V_2 - \Delta V_1}{\Delta V_3 - \Delta V_1} = \frac{T_2^{1/2} - T_1^{1/2}}{T_3^{1/2} - T_1^{1/2}} \tag{89}$$

If sample times are selected such that $T_2 = 2T_1$, $T_3 = 4T_1$, an accuracy of data may be checked:

$$\frac{\Delta V_2 - \Delta V_1}{\Delta V_3 - \Delta V_1} = 0.4142 \tag{90}$$

In all batch cell experiments, data acceptability limits were established as $\pm$ 3% of the 0.4142 value. Acquired data which were not within these limits were deleted.

As outlined in Trettin and Doshi (1980b), a correction must be made to the experimentally measured value of ΔV to adjust for the permeate collected during the initial period of filtration when $c_w < c_{wa}$ or c_g. Although the duration of this region is small, it occurs at a time when permeate flux is greatest and is therefore necessary to correct for. Experimentally collected permeate may be adjusted as follows

$$\Delta V = \Delta V_{exp} - \Delta V_{corr} \tag{91}$$

Subtituting for ΔV in Eq. (88) and rearranging yields

$$\frac{\Delta V_{exp}}{T^{1/2}} = 2A_t V_w (D/4)^{1/2} + \Delta V_{corr} (1/T^{1/2}) \tag{92}$$

or

$$\frac{\Delta V_{exp}}{T^{1/2}} = \left[\frac{\Delta V}{T^{1/2}}\right]_{lim} + \Delta V_{corr} (1/T^{1/2}) \tag{93}$$

By plotting $\frac{\Delta V_{exp}}{T^{1/2}}$ vs. $1/T^{1/2}$ and extrapolating to infinite time (T), we can minimize the effects of the initial region where c_w is not constant and determine the true value of $\Delta V/T^{1/2}$ [or $(\Delta V/T^{1/2})_{lim}$] as predicted by Eq. (88).

It is important to digress momentarily to discuss in further detail the interpretation of the $\frac{\Delta V_{exp}}{T^{1/2}}$ vs. $1/T^{1/2}$ plot. Since both models presented in Trettin and Doshi (1980a,b) were derived explicitly for the constant wall concentration boundary condition, and in particular for gel polarization, the question arises as to the difference between gel polarized behavior and constant wall concentration (osmotic pressure equivalent) behavior. The major similarity between the two processes of gel polarized and osmotic pressure equivalent ultrafiltration is that the solute concentration at the membrane surface is constant with respect to time, as in the unstirred batch cell case, or axial position, as in the cross-flow case. Therefore, a plot a $\frac{\Delta V_{exp}}{T^{1/2}}$ vs. $1/T^{1/2}$ will be linear in the unstirred batch cell case. The major difference between the two processes is that in gel polarized ultrafiltration, not only is the wall concentration constant, but it is also independent of applied pressure. This is not true of osmotic pressure equivalent ultrafiltration, where wall concentration is pressure dependent. Therefore, in a $\frac{\Delta V_{exp}}{T^{1/2}}$ vs. $1/T^{1/2}$ plot, gel polarization is indicated by an intersection of variable ΔP lines (at constant c_o) at the same value of $\left[\frac{\Delta V_{exp}}{T^{1/2}}\right]_{lim}$. A process which is osmotic pressure limited will intersect at a different value of $\frac{\Delta V_{exp}}{T^{1/2}}$ for each applied pressure tested. As can be seen, the unstirred batch cell technique represents a unique method for characterizing macromolecular solutions as to the pressure range in which gel polarization occurs. One must be cautious in using the batch cell technique, however, to select ΔP increments which are large enough to cause a discernible change in the value of c_{wa}. This is particularly true in cases where solution osmotic pressure is a strong function of concentration.

With the ultrafiltration of macromolecular solutions in cross-flow systems such as thin channel or tubular systems, it is usually the procedure to measure average flux rates at steady state. Therefore, Eq. (81) may be integrated to give

$$\left| \overline{v_w} \right| = 1.5 \left[\frac{D^2 \langle u \rangle}{h\ L} \right]^{1/3} W_w \tag{94}$$

$$\dot{Q}_p = 1.5 \left[\frac{D^2 \langle u \rangle}{h} L^2 \right]^{1/3} s\ W_w \tag{95}$$

where

$\left| \overline{v_w} \right|$ = average permeate flux

and $\dot{Q}_p = s\ L \left| v_w \right|$ = average volumetric permeate rate

An analogous relationship to Eq. (93) can be written to account for initial effects where $c_w < c_{wa}$:

$$\frac{\left| \dot{Q}_p \right|_{exp}}{L^{2/3}} = \left[\frac{\left| \dot{Q}_p \right|}{L^{2/3}} \right]_{lim} + \left| \dot{Q}_p \right|_{corr} (1/L^{2/3}) \tag{96}$$

In all ultrafiltration systems reported in the literature, average volumetric flux rates at consecutively increasing lengths along the conduit are not measured. As a result it is not possible to plot $\frac{\left| \dot{Q}_p \right|_{exp}}{L^{2/3}}$ vs. $1/L^{2/3}$ and extrapolate to infinite length to find the true value of $\left[\frac{\left| \dot{Q}_p \right|}{L^{2/3}} \right]_{lim}$. Therefore, in the interpretation of the available cross flow ultrafiltration data, the correction term, to a first order approximation, is neglected. This is a reasonable assumption for the cross-flow system in which the length of the initial region may be small in comparison to the total conduit length. The reason is that, unlike the batch cell system where average flux is 2 orders of magnitude less than pure solvent flux, average flux in cross-flow systems is only 10 times less than pure solvent flux.

EXPERIMENTAL PROCEDURE

Bovine serum albumin (BSA) (Sigma Chemicals - Cohn fraction V) was selected as a solute material to be studied in batch cell ultrafiltration. The justification of this choice was based on the fact that BSA has been used by previous investigators; their work would offer a source of comparison to our results [Blatt, et al. (1970), Kozinski and Lightfoot (1972), Shen and Probstein (1977, 1979), Probstein et al. (1978, 1979), Goldsmith (1971), and Mitra and Lundblad (1978)]. Solutions of BSA discussed in this paper were prepared in aqueous 0.15M NaCl and adjusted to pH 7.4. Sodium azide of 200 ppm concentration was added as a preservative, and final solutions were filtered through a 0.8 μm Millipore filter to remove undissolved solute. All solutions were refrigerated at 10°C prior to use, and solutions which had aged more than 2 weeks, or showed appreciable sedimentation, were discarded. Solute concentration was determined by ultraviolet light absorption with a spectrophotometer at the absorption peak of 280 nm.

Ultracentrifuge experiments were performed in our laboratory with BSA solutions, using the optical procedure of Longsworth (1952) and Creeth (1955) as outlined by Tostevin (1966). A limitation of this method is that only low solute concentrations may be studied due to refraction fringe merging at higher concentrations (> 0.01 g/cc).

The literature contains numerous experimental determinations of the mutual diffusion coefficient of BSA in various buffer solutions [Creeth (1952), Phillies, et al. (1976)]. The range of the reported diffusion coefficient at low concentration is $D = 5.5 - 7.0 \times 10^{-7}$ cm^2/sec. However, values at higher concentrations show considerable scatter as pointed out by Shen and Probstein (1977). Phillies, et al. (1976) have studied BSA solution diffusivity in 0.15M NaCl aqueous systems over the pH range of 4.3-7.6. Their data taken within the higher pH and concentration

ranges have been interpreted by Probstein, et al. (1979) to yield an average value of 6.7×10^{-7} cm^2/sec. Both Creeth (1952) and Charlwood (1953) have reported the diffusivity of dilute BSA solutions to be within the range of 6.6×10^{-7} cm^2/sec to 7.1×10^{-7} cm^2/sec at 25°C. Their data also show that the effects of pH and buffer type upon the diffusion coefficient are negligible. The value of the diffusion coefficient for 0.15M NaCl BSA solution (pH 7.4) was determined to be 6.91×10^{-7} cm^2/sec from our ultracentrifuge experiments at 23.5°C. It has been shown by Trettin and Doshi (1980b) that this value is reasonably constant over a wide range of concentration in the ultrafiltration of saline BSA solutions.

Batch cell experiments were performed in stainless steel pressure cells manufactured by the Gelman Filter Company. The average membrane area equalled 15.62 cm^2, and the total cell volume was approximately 230 cm^3. The batch cells were affixed to a support integral with the building structure to prevent extraneous vibration. The room temperature was controlled within the range of 21-24°C. Total permeate volume was gravimetrically measured as a function of time for periods as long as 24 hours. Cell pressure was varied from 2.76×10^5 - $17.24 \times 10^5 N/m^2$ (40 to 250 psi).

The majority of experiments were done using cellulose acetate membranes (5,000 - 10,000 MW cutoff) supplied by UOP- Fluid Systems. Several experiments were additionally conducted using noncellulosic (X-117) and polysulfone membranes also from UOP. Both noncellulosic membranes performed as well as the cellulose acetate membrane, yielding solute rejections greater than 95%.

RESULTS AND DISCUSSION

In Trettin and Doshi (1980b), a plot of 0.15M saline BSA solution data (pH 7.4) was presented showing that above 6.89 x 10^5N/m^2 applied pressure, a gel layer may have formed upon the membrane surface. This graph has been reproduced in Fig. 4 of this paper with additional data taken at 2.76 x 10^5N/m^2 and 4.14 x 10^5N/m^2. At cell pressures of 6.89 x 10^5N/m^2 or greater, the presence of gel polarization (pressure independence) is indicated by the intersection of $\frac{\Delta V_{exp}}{T^{1/2}}$ vs. $1/T^{1/2}$ plots as $T \to \infty$ for two different pressures at constant bulk solution concentration. When the data at lower pressures are examined, they do not intersect at the same value of $\left[\frac{\Delta V}{T^{1/2}}\right]_{lim}$ as the higher pressure data. It is interesting to note, however, that the lower pressure data plots are linear, indicating constant wall concentration. The wall concentration in this case corresponds approximately to the osmotic pressure equivalent (c_{wa}) of the applied pressure.

Osmotic pressure limited ultrafiltration data were analyzed by using Eq. (92) and the osmotic pressure data of Vilker (1975) for 0.15M Saline BSA solutions at pH 7.4. Vilker's data are reproduced in Fig. 5 for BSA in both 7.4 and 4.5 pH 0.15M saline solution. The comparison between theory and experiment is quite good as shown in Table I where the value of D was taken as 6.91 x 10^{-7} cm^2/sec.

In order to add insight into the time required to reach an asymptotic wall concentration in the batch cell, we can calculate the value of t from Eq. (46).

$$t >> \frac{D}{(A\,\Delta P)^2}\left[\frac{V_w(1-R)}{\beta_1[(R-1)+\theta_o]}\right]^2 \qquad (46)$$

where we have assumed the value of R to equal 0.990. The approximate relationship of

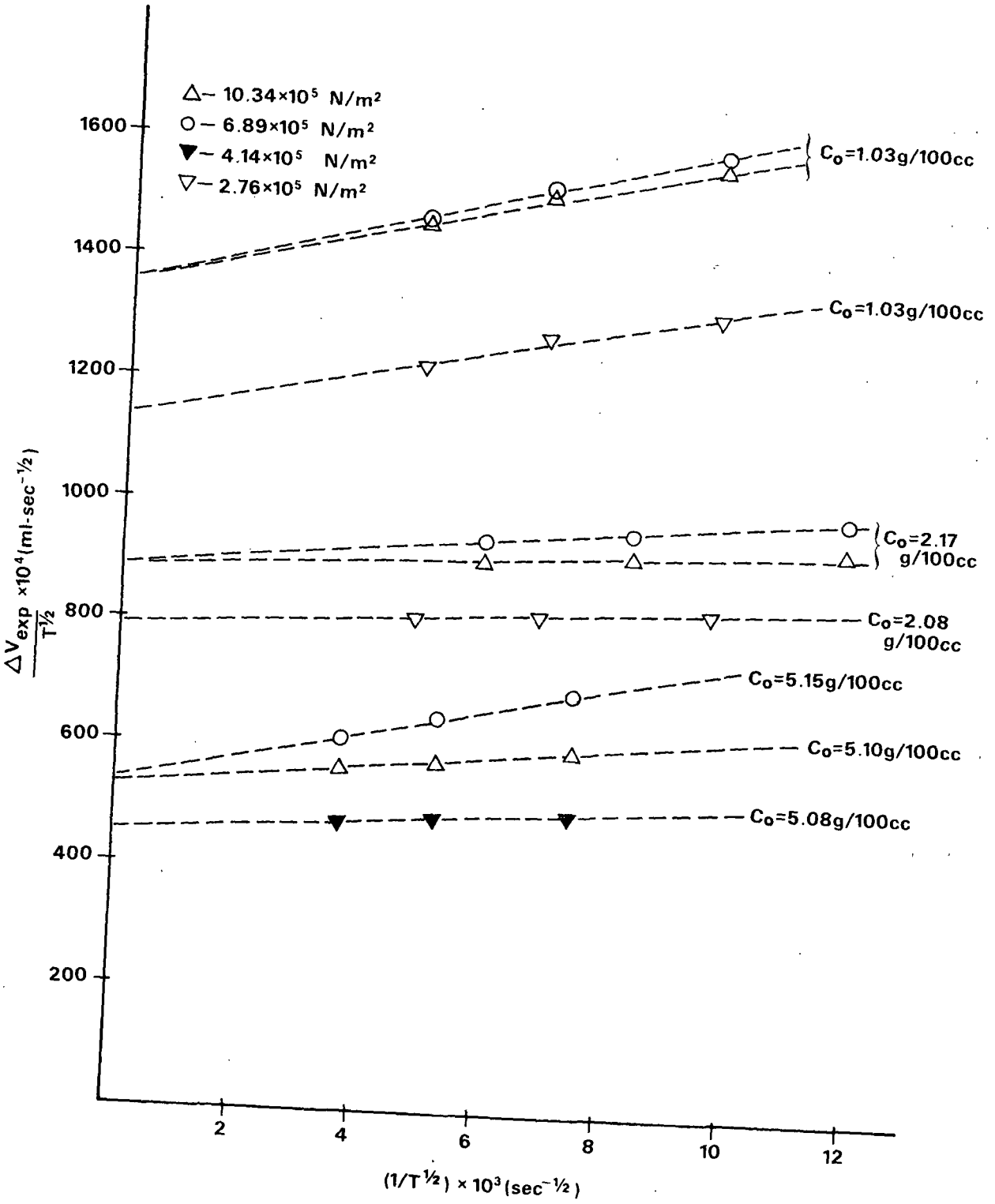

Figure 4. Unstirred batch cell UF of 0.15M NaCl BSA solution (T = 21-24°C, pH 7.4) at various solute concentrations and applied pressures.

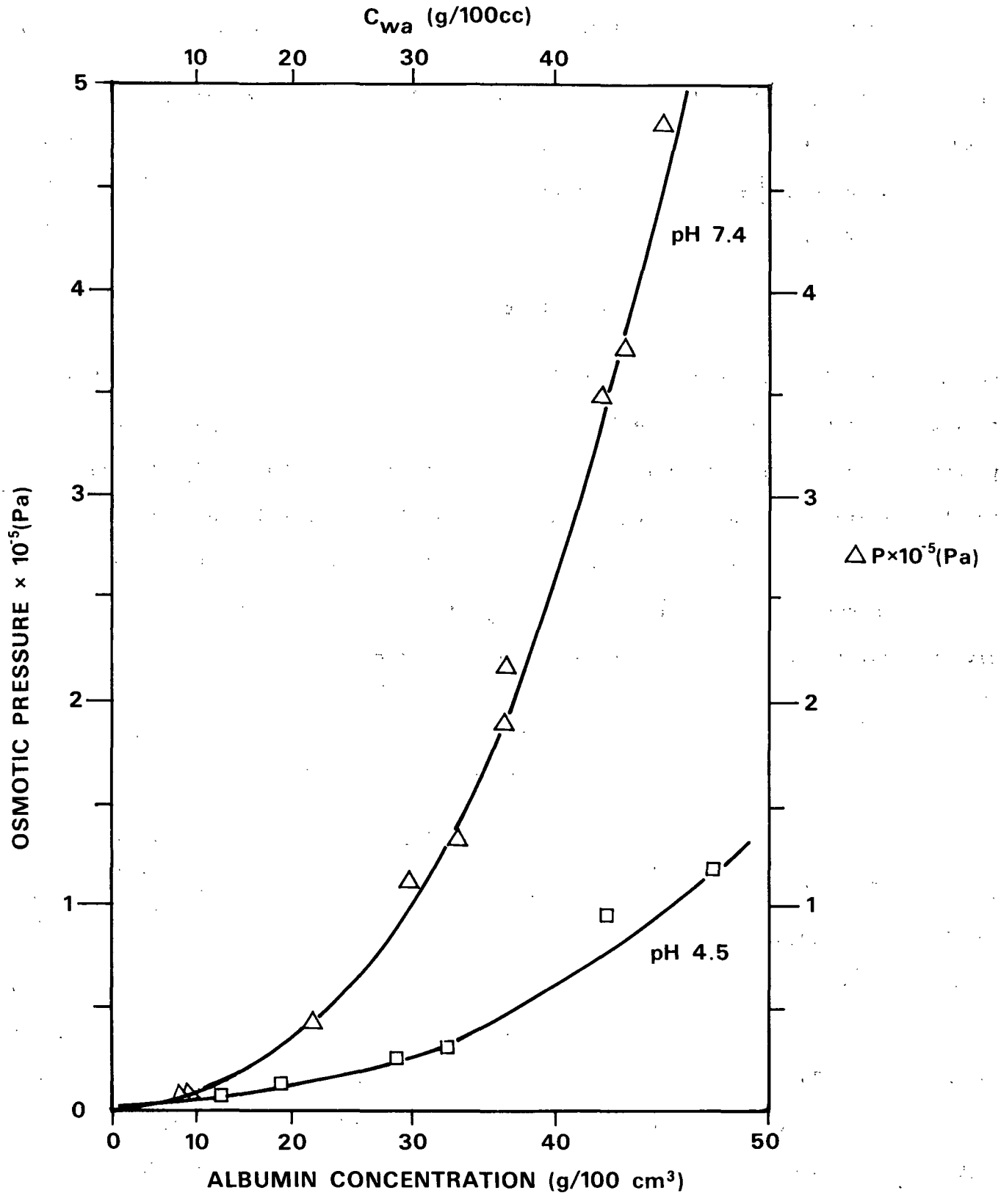

Figure 5. Solution osmotic pressure vs. solute concentration: 0.15M NaCl BSA solution (27).

$$\pi = 1.42 \times 10^4 c - 8.96 \times 10^2 c^2 + 17.74 c^3, \quad 25 \leq c \leq 40 \text{ g/100 cc} \tag{97}$$

where $\pi = [\underline{N}/m^2]$, $c = [g/100\ cc]$ is used to calculate $|\beta_1|$. Selecting the first data point in Table I, we find $\theta_o = 2.55 \times 10^{-2}$, and from Fig. 2, $V_w = 5.55$. The calculated value of $|\beta_1|$ is found to equal 4.20, and $A = 5.0 \times 10^{-9} \frac{m^2\text{-cm}}{\underline{N}\text{-sec}}$ is specified. Therefore,

$$t \gg 0.264 \text{ second} \tag{98}$$

which is indeed a very short time period to reach the asymptotic wall concentration at the membrane surface. Vilker's pH 7.4 data were linearly extrapolated to higher pressures where we have experienced gel polarization. At $6.89 \times 10^5 \underline{N}/m^2$, the extrapolation indicates a value of c_{wa} equal to 54 g/100 cc. This is in reasonable agreement with our, and Kozinski and Lightfoot's (1972), determination of 58.5 g/100 cc (gel concentration) considering the accuracy of the extrapolated value and the relative insensitivity of the model to small changes in c_{wa}.

TABLE I

0.15M SALINE BSA SOLUTION (pH 7.4) DATA-BATCH CELL

c_o, g/100 cc	c_p, g/100 cc	$\Delta P \times 10^{-5}$, $\underline{N}/m^2$	c_{wa}, g/100 cc	Experimental $[\Delta V/T^{1/2}]_{lim}$, mL-sec$^{-1/2}$	Theoretical $[\Delta V/T^{1/2}]_{lim}$, mL-sec$^{-1/2}$	R_a[a]
1.030	0.0033	2.76	40.45	0.1137	0.1127	0.989
1.030	0.0042	4.14	44.20	0.1248	0.1164	0.931
2.080	0.0058	2.76	40.45	0.0792	0.0752	0.949
2.140	0.7090	2.76	40.45	0.0897	0.0917	1.02
2.170	0.3472	4.14	44.20	0.0880	0.0847	0.964
5.080	0.0603	4.14	44.20	0.0455	0.0461	1.01

[a] R_a = ratio of $\frac{\text{theoretical } [\Delta V/T^{1/2}]_{lim}}{\text{experimental } [\Delta T^{1/2}]_{lim}}$.

The cross-flow, thin channel data of Probstein, et al., (1978) and Mitra and Lundblad (1978) were analyzed in terms of the osmotic pressure equivalent model using Vilker's osmotic pressure data for 0.15M Saline BSA solutions (pH 7.4). Although Mitra and Lundblad did not study BSA directly but rather human serum albumin (HSA), it was felt that sufficient similarity existed between the two solutes that an approximate comparison using BSA parameters could be made [Scatchard, et al. (1944)]. Data were interpreted theoretically using the relationship of Eq. (94). In the analysis of Probstein, et al. data, the cited values of h = 0.19 cm (channel half width) and L = 43 cm (channel length) were used. Similarly, in the analysis of Mitra and Lundblad's 0.15M Saline HSA solution (pH 6.9) data, the cited values of h = 0.019 cm and L = 76 cm were used. The value of D was taken to be 6.91×10^{-7} cm^2/sec in all calculations, and solute rejection at the membrane surface was assumed to be complete. The interpretation of Probstein, et al. and Mitra and Lundblad's data are shown in Tables II and III, respectively. The data of Mitra and Lundblad which were acquired at axial velocities above 65.56 cm/sec were not considered, due to high pressure drops along the thin channel length.

It is interesting to note in Table II that, although theoretical prediction of flux agrees well with experimental values at applied pressures above $1.0 \times 10^5 N/m^2$, at lower pressures experimental flux is substantially overpredicted by theory. This observation may be explained in terms of the approximate relationship of

$$\tilde{x} >> \frac{D^2 \dot{\gamma}_w}{3(A\ \Delta P)^3}\left[\frac{W_w}{|\beta_1|}\right]^3 = L^* \qquad (77)$$

At low pressures and high axial velocities, the ratio of $\frac{\dot{\gamma}_w}{(A\ \Delta P)^3}$ is large, and therefore longer axial distances are required to reach an asymptotic wall concentration.

TABLE II

THIN CHANNEL UF OF 0.15M SALINE BSA SOLUTIONS
(pH 7.4) - PROBSTEIN, et al. (1978)

c_o, g/100 cc	100 L,* cm	$\Delta P \times 10^{-5}$, N/m^2	c_{wa}, g/100 cc	$\langle u \rangle$ cm/sec	Experimental $\lvert v_w \rvert \times 10^4$, cm/sec	Theoretical $\lvert v_w \rvert \times 10^4$, cm/sec	R_a
1.74	0.490	2.76	40.34	34.5	6.38	5.87	0.920
1.76				23.0	4.71	5.10	1.08
1.78				17.3	4.19	4.62	1.10
1.80				11.5	3.67	4.01	1.09
1.87	0.075			5.8	3.04	3.14	1.03
1.74	2.13	2.07	37.33	34.5	6.10	5.68	0.931
1.76				23.0	4.71	4.93	1.05
1.80				11.5	3.67	3.88	1.06
1.87	0.325			5.8	3.04	3.04	1.00
1.74	6.53	1.38	32.83	34.5	5.58	5.36	0.961
1.76				23.0	4.56	4.66	1.02
1.78				17.3	4.06	4.22	1.04
1.80				11.5	3.60	3.66	1.02
1.87	1.00			5.8	2.96	2.86	0.966
1.78	6.82	1.03	30.50	17.3	3.79	4.08	1.08
1.80				11.5	3.33	3.53	1.06
1.87	2.15			5.8	3.04	2.77	0.911
1.74	60.0	0.689	26.00	34.5	3.60	4.81	1.34
1.76				23.0	3.25	4.18	1.29
1.78				17.3	3.15	3.78	1.20
1.80				11.5	2.90	3.28	1.13
1.87	9.10			5.8	2.40	2.57	1.07

When these initial distances, where $c_w < c_{wa}$ are appreciable, the osmotic pressure equivalent model does not apply and the integral method or numerical technique employed by Leung and Probstein (1979) may have to be used. It is shown by the $0.689 \times 10^5 \underline{N}/m^2$ data in Table II that progressively better agreement with theory is obtained as shear rate is decreased. This observation is consistent with Eq. (77).

TABLE III

THIN CHANNEL UF OF 0.15M SALINE HSA SOLUTIONS (pH 6.9)-MITRA AND LUNDBLAD (1978), $\Delta P = 1.72 \times 10^5 \underline{N}/m^2$, $c_{wa} = 35.33$ g/100 cc

c_o, g/100 cc	$\langle u \rangle$ cm/sec	Experimental $\lvert \overline{v_w} \rvert \times 10^4$, cm/sec	Theoretical $\lvert \overline{v_w} \rvert \times 10^4$, cm/sec	R_a
3.83	33.70	6.25	6.95	1.11
4.5	33.70	5.63	6.23	1.11
6.05	33.70	5.00	5.30	1.06
7.83	33.70	4.17	4.43	1.06
9.43	33.70	3.54	3.83	1.08
3.25	49.86	8.25	8.63	1.05
4.66	49.86	7.29	7.09	0.973
6.75	49.86	5.00	5.61	1.12
8.66	49.86	4.58	4.68	1.02
10.63	49.86	3.92	3.94	1.01
13.41	49.86	2.92	3.13	1.07
3.44	65.56	9.38	9.18	0.979
4.09	65.56	8.33	8.36	1.00
7.12	65.56	6.46	5.92	1.01

In Table III, experimental flux is consistently overpredicted theoretically by approximately 5%. This discrepancy may be due to the use of BSA solution parameters (D, π) to interpret HSA solution data.

Previous workers [Shen and Probstein (1977, 1979), Probstein, et al. (1978, 1979)] have interpreted gel polarization of BSA solutions to occur between 2.76 x 10^5 and 4.14 x 10^5N/m^2 applied system pressure based upon flux vs. pressure plots. Our batch cell work has shown that gel polarization of saline BSA solutions does not occur at pressures below 6.89 x 10^5N/m^2. This apparent discrepancy may be resolved in the following manner. In Fig. 6, we plot the value of W_w, which is directly proportional to flux, vs. ΔP, the applied pressure. The value of W_w is calculated from Eq. (94) for the thin-channel system using the appropriate value of c_{wa} at each specific applied pressure. The value of c_{wa} is determined from Vilker's saline BSA solution data (pH 7.4). In Fig. 6 it can be seen that at low ΔP, the value of $\frac{d\ W_w}{d\ \Delta P}$ is large and sharply decreases to a small value at values of ΔP above 3.0 x 10^5N/m^2. This behavior is characteristic of actual experimental plots. In fact, the difference in predicted W_w between ΔP values of 2.76 x 10^5 and 4.14 x 10^5N/m^2 is only 5%. It is our contention that a plot of flux vs. ΔP does not necessarily indicate the presence of gel polarization at the point where flux appears to become independent of applied pressure. The small flux change behavior as a function of pressure may be due solely to the solution osmotic pressure. The pressure range of 2.76-4.14 x 10^5N/m^2 is too narrow to yield an accurate interpretation of gel polarization with an average error less than 5%. Table IV gives the calculated value of $\frac{d\ W_w}{d\ \Delta P}$ as a function of ΔP for various values of c_o. The experimentally observed behavior of higher concentration solutions reaching a plateau region at smaller values of ΔP as compared to low concentration solutions is explained by the fact that the value of $\frac{d\ W_w}{d\ \Delta P}$ decreases (at constant ΔP) as the solution concentration increases.

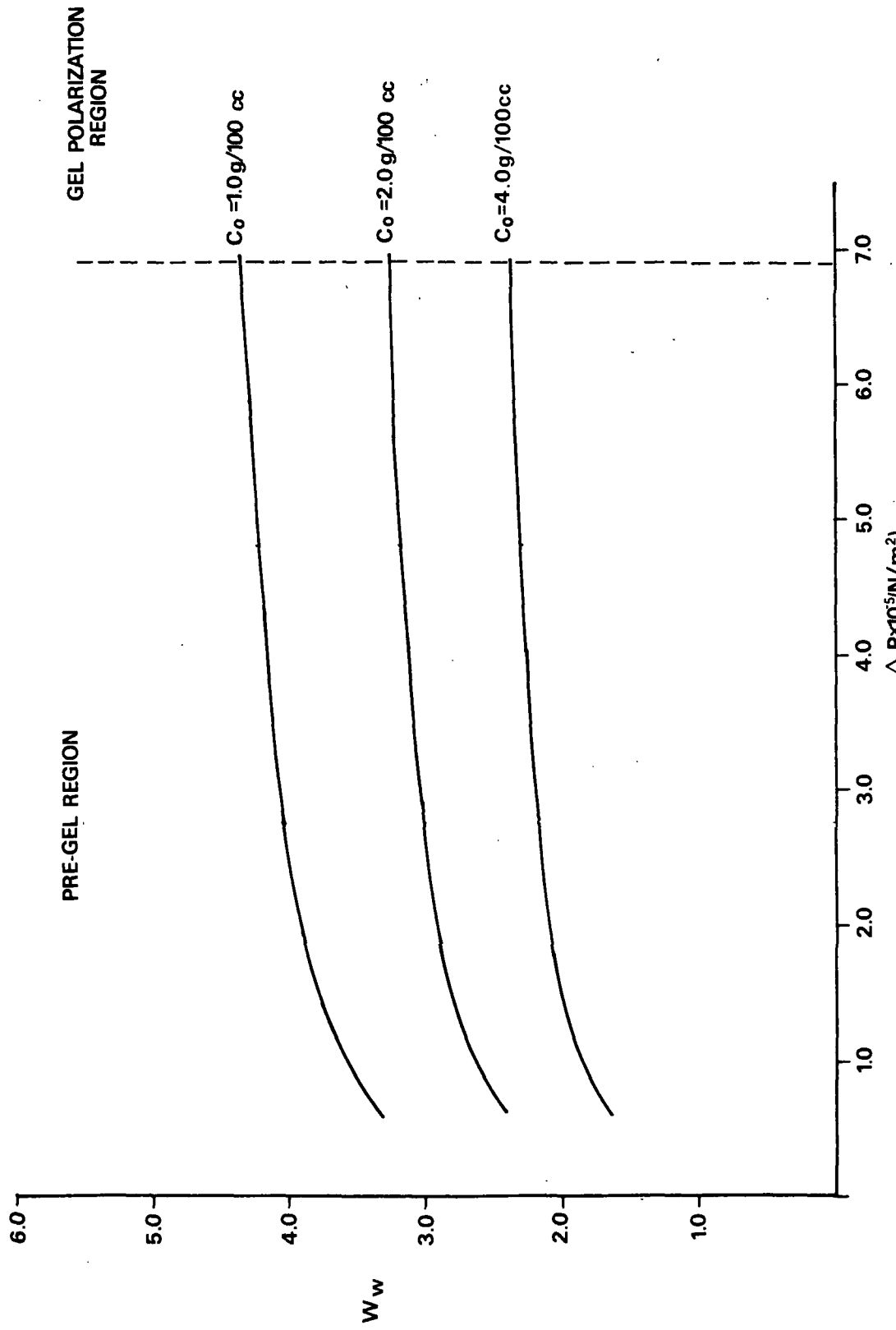

Figure 6. W_w vs. ΔP thin-channel cross-flow system. Values of c_{wa} calculated from Fig. 5 for various applied pressures.

TABLE IV

$\frac{d\ W_w}{d\ \Delta P}$ VERSUS ΔP - THIN-CHANNEL SYSTEM

(From Fig. 6)

$\Delta P \times 10^{-5}$, N/m^2	$\frac{d\ W_w}{d\ \Delta P}$ (c_o = 1.0 g/100 cc)	$\frac{d\ W_w}{d\ \Delta P}$ (c_o = 2.0 g/100 cc)	$\frac{d\ W_w}{d\ \Delta P}$ (c_o = 4.0 g/100 cc)
0.58	1.15	1.00	0.90
1.00	0.62	0.55	0.45
1.65	0.37	0.31	0.26
2.60	0.22	0.18	0.16
4.45	0.10	0.09	0.08
6.89	0.07	0.06	0.05

CONCLUSIONS

It is theoretically shown for the unstirred batch cell that, in limiting cases, the assumption of constant wall (membrane) concentration with respect to time may be made even in the absence of gel formation. Although the assumption of constant wall concentration is similar in both gel and osmotic pressure limited ultrafiltration, it is important to recognize that in gel polarized ultrafiltration, wall concentration is also pressure independent since it corresponds to the solute solubility limit. This is not the case in osmotic pressure limited ultrafiltration, where c_w is approximately equal to the concentration at which the developed osmotic pressure at the membrane surface equals the applied system pressure. Criteria are presented - Eq. (46) for the unstirred batch cell and Eq. (77) for the parallel-plate system - to establish the validity of the constant wall concentration (osmotic pressure equivalent) assumption in osmotic pressure limited ultrafiltration.

When the assumption of constant wall concentration is justified, data for the unstirred batch cell and thin-channel systems may be interpreted using models presented in Trettin and Doshi (1980a,b). Such an analysis is performed where agreement is shown to be very good between theory and osmotic pressure limited ultrafiltration experiments.

It is further shown that the current practice of plotting permeate flux vs. ΔP in macromolecular cross-flow ultrafiltration may lead to serious misinterpretation of gel polarization. It is therefore recommended that solutions be studied in the unstirred batch cell prior to study in cross-flow systems in order to determine the pressure at which gel polarization actually occurs. In previous work, pressure-independent flux is assumed to be due to the presence of gel polarization even at low pressures. Probably, the gel polarization is the exception rather than the rule

in most industrial-type applications. Obviously, more care must be taken in solute and solution characterization with regard to the interpretation of ultrafiltraton data.

ACKNOWLEDGMENTS

We express our gratitude to the member companies of The Institute of Paper Chemistry for their support of the graduate program.

Portions of this work were used by one of the authors (DRT) as partial fulfillment of the requirements for the Ph.D. degree at The Institute of Paper Chemistry.

NOMENCLATURE

A = membrane coefficient = $\frac{1}{\mu R_m}$ $\left(\frac{m^2\text{-sec}}{N\text{-sec}}\right)$

A_T = membrane transport surface area, cm^2

B = constant as defined by Eq. (13), cm^3/g

b_o = osmotic pressure constant as defined by Eq. (12), $\left(\frac{N\text{-}cm^3}{m^2\text{-}g}\right)$

b_1 = osmotic pressure constant as defined by Eq. (12), $\left(\frac{N}{m^2} \cdot \left(\frac{cm^3}{g}\right)^2\right)$

b_2 = osmotic pressure constant as defined by Eq. (12), $\left(\frac{N}{m^2} \cdot \left(\frac{cm^3}{g}\right)^3\right)$

c = solute concentration, g/cm^3 unless otherwise noted

D = solute diffusion coefficient, cm^2/sec

d_h = hydraulic diameter, cm

h = channel half height, cm

I_1, I_2 = constants of integration

K_1 = dimensionless constant defined by Eq. (83)

K_2 = dimensionless constant defined by Eq. (86)

K = mass transfer coefficient, cm/sec

$\overline{k}$ = average mass transfer coefficient, cm/sec

L = channel length, cm

n_1 = dimensionless constant defined by Eq. (84)

n_2 = dimensionless constant defined by Eq. (87)

$\dot{Q}_p$ = $S\ L \left| \overline{V}_w \right|$ = average volumetric permeate rate, cm^3/sec

r = $x + \frac{W_w}{2}$

R_a = ratio of $\frac{\text{theoretical flux}}{\text{experimental flux}}$

R_e = Reynolds number = $\frac{\langle u \rangle d_h \rho}{\mu}$

R = Solute rejection coefficient = $1 - c_p/c_w$

Sc = Schmidt number = $\mu/D\rho$

S = width of membrane, cm

$\overline{Sh}$ = average Sherwood number = $\frac{\overline{k}d_n}{D}$

t = time, sec

T = time period, sec

u = axial velocity, cm/sec

$\langle u \rangle$ = average axial velocity, cm/sec

$|\overline{v_w}|$ = average permeate volumetric flux, cm/sec

$|v_w|$ = permeate volumetric flux, cm/sec

V_w = dimensionless positive flux constant for batch cell [Eq. (79)]

W_w = dimensionless positive permeate flux constant for thin channel [Eq. (81)]

w = dimensionless permeate flux defined by Eq. (14)

$\tilde{x}$ = axial distance coordinate, cm

x = similarity coordinate defined by Eq. (20)

y = transverse distance coordinate, cm

z = dimensionless transverse distance defined by Eq. (14)

Greek Letters

α_1, α_2 = osmotic pressure constants defined by Eq. (12) $\left(\frac{cc}{g}, \frac{cc^2}{g}\right)$

β_1 = constant defined by Eq. (28)

Γ_1, Γ_2 = osmotic pressure virial coefficients

γ_w = wall shear rate, 1/sec

δ = mass boundary layer thickness, cm

ξ = defined by Eq. (34)

η = similarity coordinate for thin-channel system defined by Eq. (58)

θ = dimensionless solute concentration defined by Eq. (14)

λ = dimensionless axial distance coordinate defined by Eq. (53)

μ = solution viscosity $\frac{\text{N-sec}}{m^2}$

π = solution osmotic pressue, $\underline{N}/m^2$

ρ = solution density, g/cm^3

τ = dimensionless time as defined by Eq. (14)

θ = dimensionless constant defined by Eq. (53)

ΔP = applied hydrostatic pressue, $\underline{N}/m^2$

ΔV = total permeate volume, cm^3

$\Delta\pi$ = $\pi_w - \pi_p$ = solution osmotic pressure difference between wall concentration solution and permeate, $\underline{N}/m^2$

Subscripts

g = of gel

m = of membrane

o = of bulk solution

p = of permeate solution

w = at wall position

wa = of asymptotic solution

1, 2, 3, = at measurement times

exp = experimentally measured

corr = correction

LITERATURE CITED

Blatt, W. F., Dravid, A., Michaels, A. S., and Nelsen, L. Solute polarization and cake formation in membrane ultrafiltration: causes, consequences, and control techniques. In Membrane science and technology, J. E. Flinn, ed., Plenum Press, New York, N.Y., 1970. p. 47.

Billmeyer, F. W., Jr. Textbook of polymer science. Second ed., Interscience, New York, 1967.

Brandrup, J. and Immergut, E. H., Polymer handbook, Interscience, New York, 1967.

Brian, P. L. T., In Desalination by reverse osmosis, U. Merten, ed., MIT Press, Cambridge, Mass., 1966. p. 161.

Charlwood, P. A. Estimation of heterogeneity from diffusion measurements. J. Phys. Chem. 57:125(1953).

Creeth, J. M. The use of the Gouy diffusiometer with dilute protein solutions. An assessment of the accuracy of the method. Biochem. J. 51:10(1952).

Creeth, J. M. Studies of free diffusion in liquids with the Rayleigh method. J. Am. Chem. Soc. 77:6428(1955).

Deissler, R. G. Analysis of turbulent heat transfer, mass transfer, and friction in smooth tubes at high Prandtl and Schmidt numbers. NACA Report No. 1210, 1955.

Doherty, P. and Benedek, G. B. The effect of electric charge on the diffusion of macromolecules. J. Chem. Phys. 61:5426(1974).

Gill, W. N., Derzansky, L. J., and Doshi, M. R. Convective diffusion in laminar and turbulent hyperfiltration (reverse osmosis) systems. In Surface and colloid science, E. Matijevic, ed., Wiley and Sons, New York, N.Y. 4:261(1971).

Goldsmith, R. L. Macromolecular ultrafiltration with micoporous membranes. I&EC Fundam. 10(1):113(1971).

Keller, K. H., Canales, E. R., and Yum, S. I. Tracer and mutual diffusion coefficients of proteins. J. Phys. Chem. 75:379(1971).

Kozinski, A. A. and Lightfoot, E. N. Protein ultrafiltration: a general example of boundary layer filtration. AIChE J. 18(5):1030(1972).

Leung, W. F. and Probstein, R. F. Low polarization in laminar ultrafiltration of macromolecular solutions. I&EC Fundam. 18(3):274(1979).

Longsworth, L. G. Diffusion measurement, at 1°, of aqueous solutions of amino acids, peptides, and sugars. J. Am. Chem. Soc. 74:4155(1952).

Michaels, A. S. New separation technique for the CPI. Chem. Eng. Progress 64(12): 31(1968).

Mitra, F. and Lundblad, J. L. Ultrafiltration of immune serum globulin and human serum albumin: regression analysis studies. Sepn. Sci. Technol. 13(1):89(1978).

Phillies, G. D. J., Benedek, G. B., and Mazer, N. A. Diffusion in protein solutions at high concentrations: a study of quasielastic light scattering spectroscopy. J. Chem. Phys. 65:1883(1976).

Porter, M. C. Concentration polarization with membrane ultrafiltration. I&EC Prod. Res. 11(3):234(1972).

Probstein, R. F., Shen, J. S., and Leung, W. F. Ultrafiltration of macromolecular solutions at high polarization in laminar channel flow. Desalination 24:1(1978).

Scatchard, G., Batchelder, A. C., and Brown, A. Chemical, clinical and immunological studies on the products of human plasma fractionation. VI. The osmotic pressure of plasma and of serum albumin. J. Clinical Investigation 23:458(1944).

Shen, J. S. and Probstein, R. F. On the prediction of limiting flux in laminar ultrafiltration of macromolecular solutions. I&EC Fundam. 16(4):459(1977).

Shen, J. S. and Probstein, R. F. Turbulence promotion and hydrodynamic optimization in an ultrafiltration process. I&EC Process Design Devt. 18(3):547(1979).

Tostevin, J. E. The hydrodynamic properties of the alditol oligosaccharides. Ph.D. Dissertation, The Institute of Paper Chemistry, 1966.

Trettin, D. R. and Doshi, M. R. Limiting flux in ultrafiltration of macromolecular solutions. Chem. Eng. Commun. 4:508-22(1980).

Trettin, D. R. and Doshi, M. R. Ultrafiltration in an unstirred batch cell. I&EC Fundam. 19:189-94(1980).

Vilker, V. L., Ph.D. Thesis, MIT, Dept. of Chemical Engineering, Cambridge, Mass., 1975.

SECTION 6 - GENERAL SUMMARY

GENERAL SUMMARY

DISCUSSION OF RESULTS

The current state-of-the-art regarding the study of mass transfer in ultrafiltration centers primarily around models derived from film theory principles. Although the film theory model is simple to use, its predictive value is questionable and has been characteristically overused in the interpretation of macromolecular ultrafiltration data. Consequently, it would be desirable to compare the film theory model with a more exact theory. Furthermore, it has been previously unexplained why in the ultrafiltration of colloidal suspensions flux rates are so severely underpredicted by the film theory. Although the concept of gel polarization is reasonably well accepted, little work has been done in defining when an ultrafiltration process is gel limited or osmotic pressure limited. It is toward the resolution of these questions that this thesis has been directed.

It has been shown with the ultrafiltration of macromolecular solutions in an unstirred batch cell that permeate flux may be accurately predicted by a more exact theory and that comparison of the exact model and film theory indicates substantial differences. When the two models are extended to the more practical cross-flow system (parallel-plate), the same magnitude of difference is encountered.

Regarding the ultrafiltration of colloidal suspensions, a theoretical model has been developed which, in limiting cases, explains the large difference between colloidal and macromolecular flux behavior. It is found that in colloidal ultrafiltration, solute diffusion is negligible and flux may be described in terms of classical filtration principles where solute accumulation is important. Directly opposite behavior is found in macromolecular ultrafiltration where flux is diffusion limited. With the ultrafiltration of colloidal suspensions in cross-flow systems,

it has been found that the initial stages of filtration are not influenced by the cross-flow axial velocity. That is, the cross flow system behaves in a manner similar to the unstirred batch cell where permeate flux is proportioned to $t^{1/2}$. Only at high shear rates is axial velocity effective in improving flux or limiting transient cake growth.

In the study of pregel (low polarization) ultrafiltration, it has been shown both theoretically and experimentally that it is possible to reach constant wall concentration asymptotically under certain limiting conditions in the absence of gel formation. Previously, this assumption was only made in the case of gel polarized ultrafiltration. When the assumption of constant wall concentration is justified, data may be accurately interpreted using the integral method solutions developed herein for both the pregel and gel-polarized regions. Previous investigations have assumed that the osmotic pressure of macromolecular solutions may be generally neglected and that the formation of a gel layer upon the membrane surface occurs in the majority of cases. Based upon the results presented in this thesis, this assumption may not be valid. Furthermore, the conventional use of flux versus applied pressure plots to determine the presence of gel polarization in cross-flow systems may be misinterpreted depending upon the solution osmotic pressure-concentration relationship for the particular solute in question.

SUGGESTIONS FOR FUTURE RESEARCH

This research work in general assumed a negligible effect of such phenomena as solute-membrane and solute-solute interactions. Judging by experimental agreement with theory, this assumption appears reasonable although it has not been confirmed independently. Future work of interest should be directed toward the study of electrokinetic effects and solute adsorption upon the membrane surface, and in particular, around pores.

Another area of interest emerges from the fact that we were not able to successfully study the ultrafiltration of macromolecular solutions in the test parallel-plate unit. It is believed this was due primarily to the inability to effectively eliminate rust and scale from the test loop. Although the residue did not give any problem in the ultrafiltration of latex suspensions, the combination of rust and polymer severely fouled the membrane to the point of completely blinding it over in portions. It is believed that some type of metal ion complexing had occurred. Obviously, a study of this type of fouling mechanism would be of great value in improving permeate flux, particularly in industrial systems. Clearly, in future work, more attention should be placed on studying the chemical solution properties and better methods of characterizing solutions as to their potential for gelling at typical ultrafiltration pressures.

Although many industries such as pharmaceutical, dairy, food, and paint have been conducting pioneering work to implement ultrafiltration technology into their particular processes, the pulp and paper industry has performed minimal study concerning ultrafiltration. This is due in large part to the lack of immediate applications. However, in years to come when pollution regulations become more stringent and as energy costs continue to escalate, the use of ultrafiltration as a viable separation process will continue to become more attractive in the treatment of waste streams. Also, it is important that as new markets become uncovered for the use of pulping by-products, such as lignosulfonic acids, economic and efficient methods be available to recover them. Ultrafiltration has the potential of playing a key role in such development. Therefore, more effort should be given to the study of such applications in the pulp and paper industry so that the technology is available when the imminent need arises.

SECTION 7 APPENDIX

APPENDIX I

EXPERIMENTAL TECHNIQUE

SOLUTION PREPARATION

The following solute materials were studied during the course of the research:

1. Bovine serum albumin - Cohn fraction V - obtained in granular form from Sigma Chemicals.
2. Carbowax 20M (polyethylene oxide) - obtained in dry form from Union Carbide.
3. CMC - 12M8 (carboxymethylcellulose) - obtained in granular form from Hercules Corporation.
4. PVA (polyvinyl alcohol) - obtained in granular form from Aldrich Chemical. Approximate molecular weight = 80,000.
5. Dow DPP-722 (styrene butadiene latex) - obtained in 48% slurry from Dow Chemical.

Solutions of bovine serum albumin (BSA) were prepared in 0.15M NaCl (7.4 pH) and 0.10M sodium acetate (4.7 pH) solution. Sodium azide of 200 ppm concentration was added as a preservative, and final solutions were filtered through a 0.8 micron Millipore filter to remove undissolved solute material. Solution concentrations were determined by UV spectrophotometric techniques at 279 nm wavelength. Standard BSA solutions were prepared in the appropriate solvent systems by first drying the granular BSA in a vacuum oven at 70°C (35 inches H_2O vacuum) for 48 hours. The moisture content of the bulk BSA was found to be approximately 3% by weight. Solutions were then prepared, and a calibration curve was derived which is given in Fig. A-1. It should be noted that it is very important to reference the particular solute concentration measurement against the appropriate solvent since both sodium azide and sodium acetate absorb slightly at 279 nm. The calculated extinction

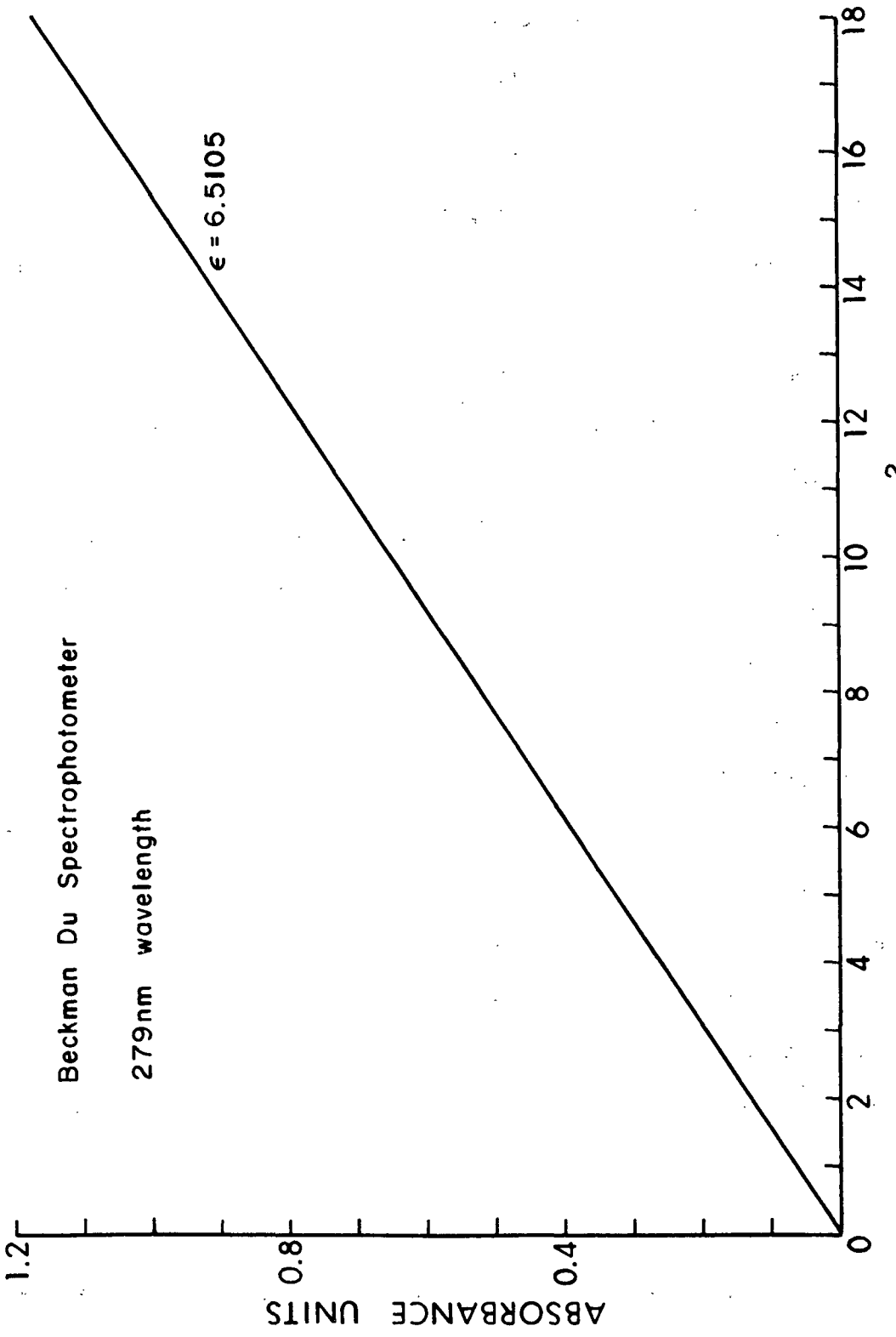

Figure A-1. BSA solution - spectrophotometer calibration.

coefficient, ε, from Fig. A-1 equals 6.5105. This compares very favorably with the value of $\varepsilon = 6.5$ determined by Kozinski and Lightfoot (1972).

The determination of solute concentration in Carbowax 20M solutions was performed in a similar manner at the adsorption peak of 279 nm. It was not possible to effectively dry the solid Carbowax because of the low melting point (66°C). Therefore, the standard solution solute concentration was determined by total carbon analysis. All unknown solution concentration measurements were referenced against the standard. In the calibration curve shown in Fig. A-2, it can be seen that absorbance becomes nonlinear with concentration above 0.30 g/100 cc. In order to avoid this nonlinearity, standard solutions were prepared around the approximate concentration of 0.10 g/100 cc, and care was taken that the unknowns were sufficiently diluted below the 0.30 g/100 cc maximum.

The determination of solution concentration involving CMC, PVA, and latex was done gravimetrically by weighing out samples, evaporating to dryness, and reweighing. The density of the solutions was assumed to equal 1.0 g/cc in all cases. This is reasonable since the solutions studied were fairly dilute (< 10 g/100 cc normally), and the corresponding polymer and latex solutions at high concentration exhibit small variance from a density of 1.0 g/cc (Carbowax 20M - ρ = 1.05 g/cc at c_o = 30 g/100 cc, latex - ρ = 1.04 g/cc at c_o - 48 g/100 cc, and CMC - ρ = 1.11 at c_o = 30 g/100 cc) [Lepori and Mollica (1978), Hercules (1976), and Heiser (1979)].

The pH of Carbowax 20M, CMC, and PVA solutions was adjusted to 7.5. Latex suspensions were adjusted to 8.5 pH. All adjustments were made by the addition of NaOH or HCl. Polymer solutions were stored at 10°C prior to use.

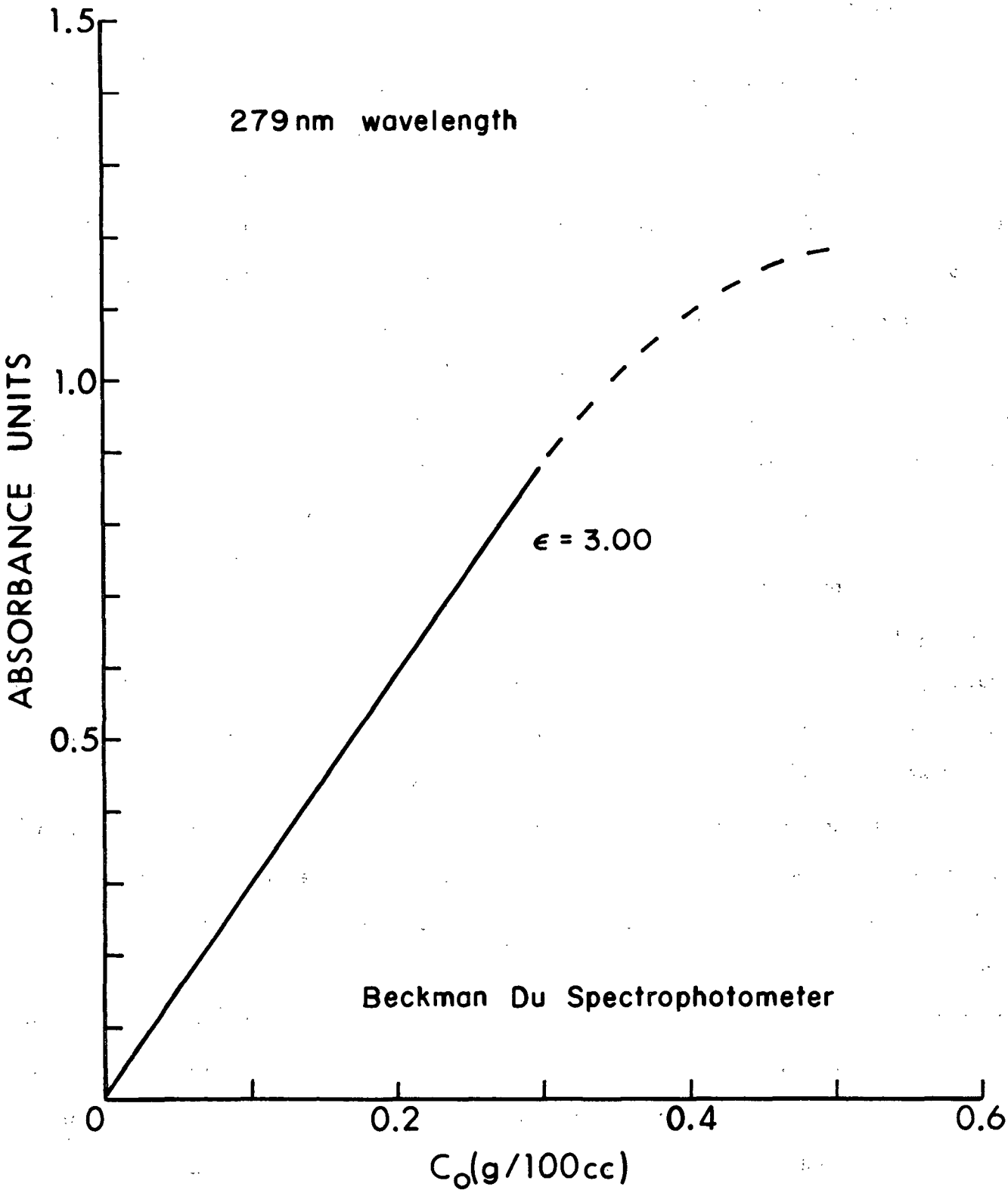

Figure A-2. Carbowax 20M solution - spectrophotometer calibration.

OSMOTIC PRESSURE DETERMINATION

It was initially intended to use vapor pressure osmometry techniques to determine solution osmotic pressure for the solute materials of CMC, Carbowax 20M, and PVA. Preliminary experiments with CMC in a Hewlett-Packard Model 302B osmometer encountered numerous problems which could not be resolved. Difficulty was incurred in attempting to calibrate the system with a NaCl solution standard where results deviated from previous calibrations by a considerable amount. It was further found that a signal response could only be achieved above 60°C for the CMC solutions. This type of signal dependence ($\alpha\ \Delta\pi$) upon temperature is far greater than what is predicted by classical osmotic pressure relationships. In lieu of these problems, the use of vapor pressure osmometry was dropped from further consideration.

A modified membrane osmometry technique was developed which consisted of completely filling a batch cell with polymer solution of known concentration at a temperature slightly above ($\approx$ 1°C), the temperature of the immersion bath. The cell was completely sealed with a pressure gage mounted at the top and then placed in the bath of distilled water (at 18°C). The cell was periodically shaken to disrupt any diffusional boundary layer and was allowed to remain in the bath until equilibrium was reached ($\approx$ 24 hours). At equilibrium, the gage pressure was recorded and the batch cell solution concentration was measured. In all cases, the concentration had changed negligibly ($<$ 0.5%). Results using this technique were excellent for Carbowax solutions. It was not possible to effectively study CMC and PVA solutions in this manner because of high solution viscosity at the concentrations of interest and the inability to disrupt the diffusional boundary layer within the cell. As a consequence, exceedingly long times were required to reach equilibrium (weeks) which deemed the method impractical.

DIFFUSION COEFFICIENT DETERMINATION

The determination of solute diffusion coefficient by ultracentrifuge methods has been discussed by numerous workers in the literature [Creeth (1955), Longsworth (1955), Tostevin (1966), and Kindler (1971)], and therefore a comprehensive review will not be given here. The format of this section will be to outline some of the key points and limitations of the method, and to present data from experiments conducted with BSA, CMC, PVA, and Carbowax 20M solutions.

Consider Fick's second law of diffusion for a rectangular cell where a perfect concentration interface exists at t = 0 and where no transverse convection occurs. The system is shown in Fig. A-3. The value of D is assumed concentration independent.

$$\partial c/\partial t = D\, \partial^2 c/\partial y^2 \qquad (1)$$

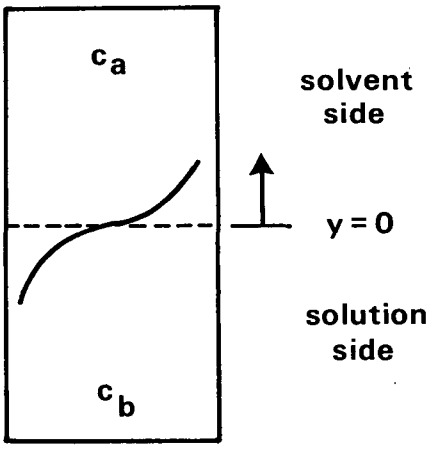

Figure A-3. Rectangular diffusion cell.

where the boundary and initial conditions are:

$$\text{at } t = 0,\ c = c_a \text{ at } y > 0$$

$$c = c_b \text{ at } y < 0$$

$$c = \frac{c_a + c_b}{2} \text{ at } y = 0$$

and for $t > 0$

$$c = c_a \text{ as } y \longrightarrow \infty$$

$$c = c_b \text{ as } y \longrightarrow -\infty$$

$$c = \frac{c_a + c_b}{2} \text{ at } y = 0$$

Since symmetry exists for $y < 0$ and $y > 0$, that is, at $t = t_1$, $c = c_1$ at $y = y_1$ and $-y_1$, let us consider only the mass transfer for $y \geq 0$ side of the cell.

Introducing the similarity transformation for small time,

$$\eta = y/(4\pi D t)^{1/2} \tag{2}$$

Eq. (1) may be written as

$$-2\pi\eta \frac{dc}{d\eta} = \frac{d^2c}{d\eta^2} \tag{3}$$

where the boundary conditions become

$$\text{at } \eta = \infty, \; c = c_a \tag{4}$$

$$\text{at } \eta = 0, \; c = \frac{c_a + c_b}{2} \tag{5}$$

Eq. (3) may be integrated to yield

$$c = \frac{c_a}{2} (1 + \text{erf } (y/(4Dt)^{1/2})) + \frac{c_b}{2} \text{ erfc } (y/(4Dt)^{1/2}) \tag{6}$$

Since in most ultracentrifuge experiments, c_a corresponds to the solute concentration of the solvent ($c_a = 0$), Eq. (6) may be further simplified to

$$c = \frac{c_b}{2} \text{ erfc } (y/(4Dt)^{1/2})) \tag{7}$$

and

$$\frac{\partial c}{\partial y} = - \frac{c_b}{2\sqrt{\pi Dt}} \exp\left(- \frac{y^2}{4\pi Dt}\right) \tag{8}$$

In order to use standard optical methods for diffusion measurements, an expression is required relating the refractive index or the refractive index gradient to the diffusion coefficient. If the refractive index, n, is a linear function of the solute concentration over the range encountered in the experiment, then

$$n = Rc \tag{9}$$

and Eq. (7) and (8) becomes

$$n = \frac{Rc_b}{2} \operatorname{erfc}(y/(4Dt)^{1/2}) \tag{10}$$

$$\frac{\partial n}{\partial y} = - \frac{Rc_b}{2\sqrt{\pi Dt}} \exp\ (-y^2/4\pi Dt) \tag{11}$$

The development so far has been in reference to a rectangular diffusion cell and a homogeneous gravitational field. In order to extend the treatment to experiments conducted in an ultracentrifuge, it is necessary to consider the sectorial shape of the cell and the inhomogeneity of the gravitational field. This analysis has been performed by Schumaker (1963), as outlined by Tostevin (1966), and shall not be repeated here. Let it suffice to say that the ultracentrifuge system may be accurately modeled by the simple rectangular cell if the following criteria are satisified.

1. The solute material is homogeneous.
2. The concentration dependence of the sedimentation coefficient is small.
3. The sedimentation coefficient itself is small.
4. The diffusion coefficient is not strongly concentration dependent.
5. The lowest rotor velocity necessary to maintain gravitational stability is used.

In order to interpret Rayleigh interferometer data, which identifies lines of constant concentration (fringes), we make use of the property of similarity. That is, any two concentration fringes located at different similarity coordinates (Z) differ by only a scale factor. We define this scale factor as

$$\frac{2j}{J} = \frac{2c}{c_b} \tag{12}$$

where j = the number of the fringe corresponding to the concentration c

J = the total number of fringes in the boundary

Substituting into Eq. (7) yields

$$\frac{2j}{J} = \text{erfc}\ (z) \tag{13}$$

where $z = y/(4Dt)^{1/2}$

In the interpretation of photographic fringe patterns, J is constant with respect to time. Only the separation between fringes changes. This is shown in Fig. A-4.

For each fringe on the right of the y = 0 line in Fig. A-4 a value of z may be calculated from Eq. (13). Each value of z may then be divided into X_i, the actual measured fringe distance from y = 0 to j_i.

$$\frac{X_i}{z} = \frac{X_i}{y_i}\, 2(Dt_i)^{1/2} = 2G(Dt_i)^{1/2} \tag{14}$$

where G is the magnification factor for the instrument. This process may be repeated for each fringe at measurement time $t = t_i$, therefore

$$D_i = \frac{\left[\frac{X_i}{x}\right]^2_{\text{average}}}{4G^2 t_i} \tag{15}$$

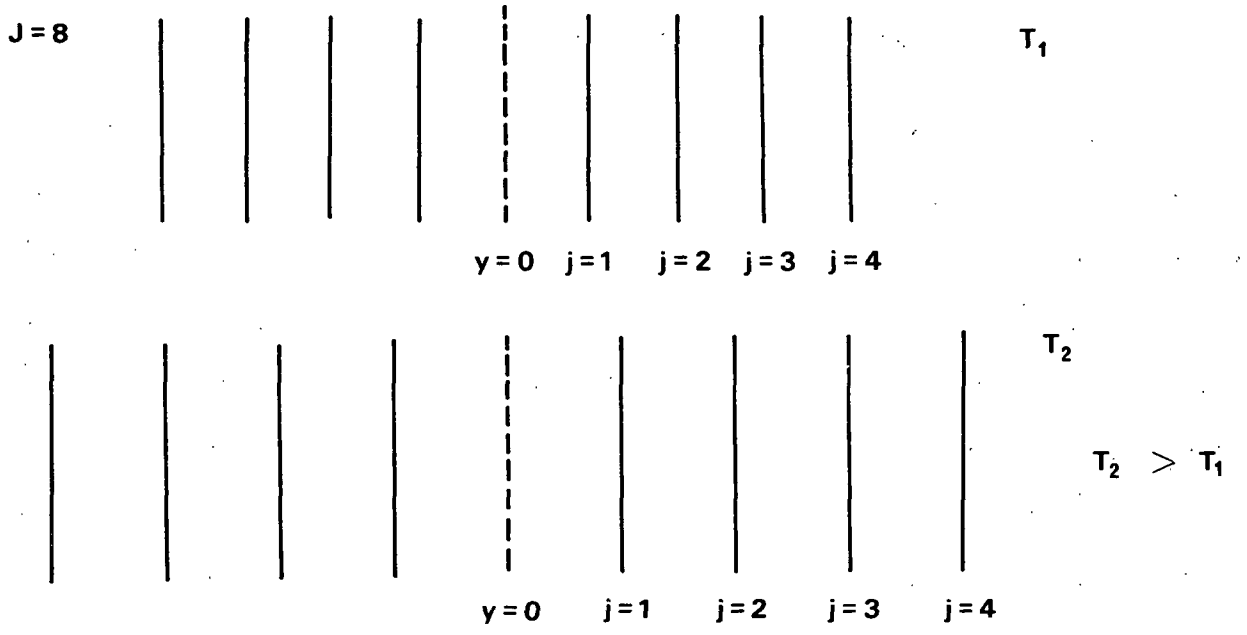

Figure A-4. Typical fringe pattern.

Because of uncertainties in the determination of the t = 0 point, a method of correction is used to minimize this effect from Eq. (14)

$$D_i t_i = D(t_i + \Delta t) \tag{16}$$

where D_i = the calculated value of diffusion coefficient at t_i

t_i = the measured value of time

Δt = the time correction

D = the true value of the diffusion coefficient

Eq. (16) may be rewritten,

$$D_i = D\,\Delta t(1/t_i) + D \tag{17}$$

By plotting D_i versus $1/t_i$ and extrapolating to infinite t_i ($1/t_i \longrightarrow 0$), the true value of the diffusion coefficient may be determined.

In order to eliminate the problem of determining the y = 0 plane in photographs, various schemes have been devised to pair fringes across the boundary layer. These methods may be found in Longsworth (1955) and Creeth (1955).

In the interpretation of data collected in this work, a computer program (DIFCO) was used which numerically evaluates the error function and analyzes the fringe patterns to calculate the value of D_i for each time increment. A copy of the program is listed in Kindler (1971). Photographic plates of the fringe patterns for the various solutes studied are stored in the Biochemical Laboratory under the title A-400 Trettin. The remainder of this section contains tabulated data of the diffusion coefficient measurements of dilute solutions of BSA, PVA, CMC, and Carbowax 20M. The diffusion data for BSA solutions were the only determinations used in the analysis of ultrafiltration data due to the wide polydispersity of the other solutes and the consequent unapplicability of the ultracentrifuge technique.

TABLE A-1

0.15M SALINE BSA SOLUTION (7.40 pH, c_o < 1 g/cc). T = 23.5°C

$1/t_i \times 10^3$ (sec^{-1})	$D_i \times 10^7$ (cm^2/sec)	J
8.33	18.32	19
4.17	12.65	
2.78	10.77	
2.08	9.66	
1.67	9.26	
1.39	8.81	
1.19	8.50	$D = 6.91 \times 10^{-7}$ cm^2/sec
1.04	8.39	Δt = 298 seconds
0.926	8.17	

TABLE A-2

0.10M SODIUM ACETATE BSA SOLUTION (4.70 pH, c_o < 1 g/cc). T = 23.5°C

$1/t_i \times 10^3$ (sec^{-1})	$D_i \times 10^7$ (cm^2/sec)	J
9.09	18.81	19
4.35	12.58	
2.86	10.68	
2.13	9.62	
1.69	9.06	
1.41	8.63	
1.20	8.37	$D = 6.79 \times 10^{-7}$ cm^2/sec
1.05	8.12	Δt = 195 seconds
0.935	8.00	

TABLE A-3

CMC-12M8 SOLUTION (7.5 pH, c_o < 1 g/cc). T = 23.5°C

$1/t_i \times 10^3$ (sec^{-1})	$D_i \times 10^6$ (cm^2/sec)	J
5.56	7.08	36
3.33	6.37	
2.38	6.05	
1.85	5.90	$D = 5.33 \times 10^{-6}$ cm^2/sec
1.52	5.83	Δt = 59 seconds

TABLE A-4

CARBOWAX 20M SOLUTION (7.5 pH, c_o < 1 g/cc). T = 19°C

$1/t_i \times 10^3$ (sec^{-1})	$D_i \times 10^7$ (cm^2/sec)	J
5.56	7.26	14
3.33	6.04	
2.38	5.37	
1.85	4.99	
1.52	4.87	
1.28	4.88	
1.11	4.87	
0.980	4.88	
0.877	4.73	
0.794	4.76	
0.725	4.66	$D = 4.26 \times 10^{-7}$ cm^2/sec
0.667	4.66	Δt = 122 seconds
0.617	4.68	
0.575	4.57	

MEMBRANES

Table A-7 lists the various membranes used in this study. The polysulfone, SAN, and cellulose acetate membranes were supplied by the Fluid Systems Division of UOP. The HFM membrane was purchased from Abcor, Incorporated. All membranes exhibited compressibility to some extent and it was therefore necessary to precondition them in some fashion to obtain maximum solute rejection. This was accomplished by passing solvent through the membrane at high pressure (10.3 - 13.8 x $10^5 N/m^2$) for 15 to 30 minutes. During this time period, appreciable flux decline was observed

indicating compression. New membranes were used for each batch cell run because of the fact that it was not always possible to restore initial solvent flux upon cleaning of the membrane between runs. The majority of BSA and CMC experiments were done using the cellulose acetate membranes. Other experiments used the HFM-180 membranes. Solute rejections were typically above 96%.

TABLE A-5

PVA SOLUTION (7.5 pH, c_o < 1 g/cc). T = 19°C

$1/t_i \times 10^3$ (sec^{-1})	$D_i \times 10^7$ (cm^2/sec)	J
1.04	2.74	21
0.833	2.66	
0.694	2.61	
0.595	2.60	
0.521	2.56	
0.463	2.56	$D = 2.41 \times 10^{-7}$ cm^2/sec
0.417	2.54	Δt = 128 seconds
0.379	2.53	

TABLE A-6

PVA SOLUTION (7.5 pH, c_o < 1 g/cc). T = 28°C

$1/t_i \times 10^3$ (sec^{-1})	$D_i \times 10^7$ (cm^2/sec)	J
1.282	3.53	21
0.980	3.45	
0.794	3.38	
0.667	3.36	
0.575	3.34	$D = 3.13 \times 10^{-7}$ cm^2/sec
0.505	3.28	
0.450	3.25	

TABLE A-7

MEMBRANES USED IN ULTRAFILTRATION EXPERIMENTS

Membrane Type	Average MW Cutoff	$\overline{R}_m \times 10^{-11}$ (1/cm)
Polysulfone	10,000 - 50,000	1.00
SAN (No. X-117)	5,000 - 10,000	2.60
Cellulose Acetate	5,000 - 10,000	5.00
HFM - 180	18,000	1.75
WRP	10,000	2.50

Figures A-5 through A-10 show photomicrographs of the various membranes used at different degrees of magnification.

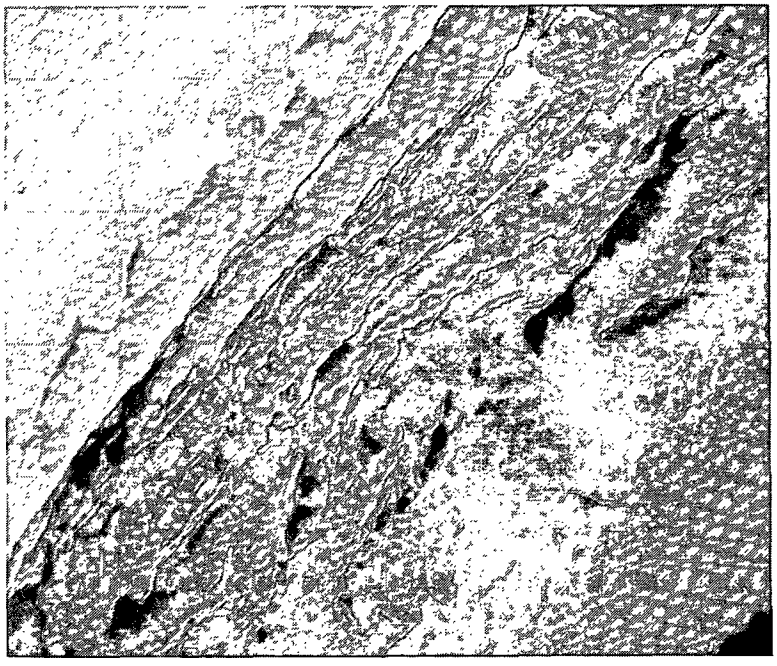

Figure A-5. Cellulose Acetate Membrane - Cross Section - 5000X.

BATCH CELL SYSTEM

Because the batch cell system has been discussed in detail previously, an in depth treatment will not be given here. The unstirred batch cell system is

inherently very simple, containing only three parts. They are: a cylinder section, and top and bottom screw caps. The stainless steel cell is manufactured by the Gelman Company, and its assembled volume is approximately 230 mL. A support screen is located in the bottom screw cap over which a membrane of area 15.62 cm^2 is placed. The membrane is secured by a Teflon washer over which the cylinder section is screwed into place. The cell is pressurized through a port in the top screw cap, and the assembled unit is mounted vertically in a conventional pipe holder. An additional reservoir (3000 mL) is used in cases where it is wished to extend the effective volume of the cell beyond the 230 mL limit.

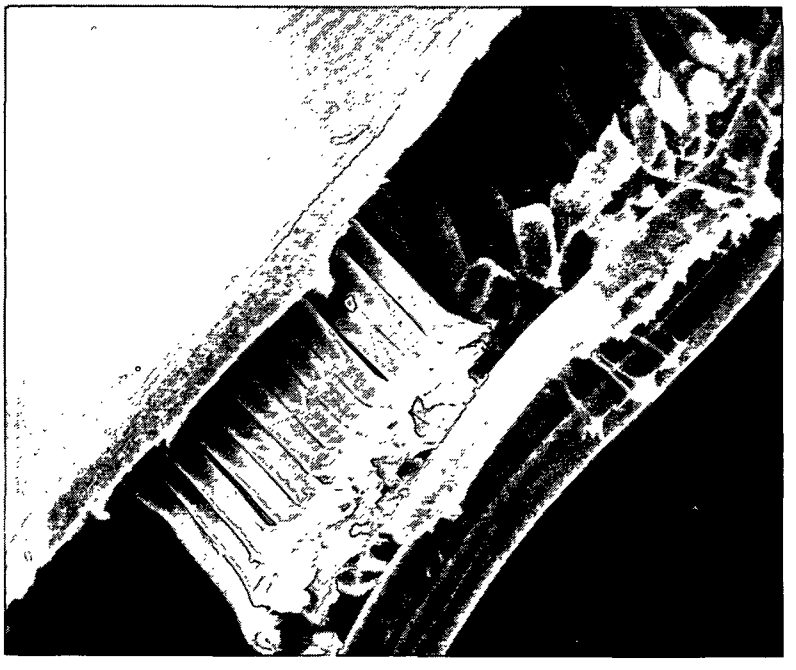

Figure A-6. Cellulose acetate membrane + woven substrate - cross section - 300X.

Experimental runs are made by first conditioning the membrane with pure solvent at high pressure. The cell is then filled with solution and pressurized with nitrogen to the desired level. Permeate flux (eluted volume) is measured as a function of time. The solute concentration of the permeate was either measured at each time

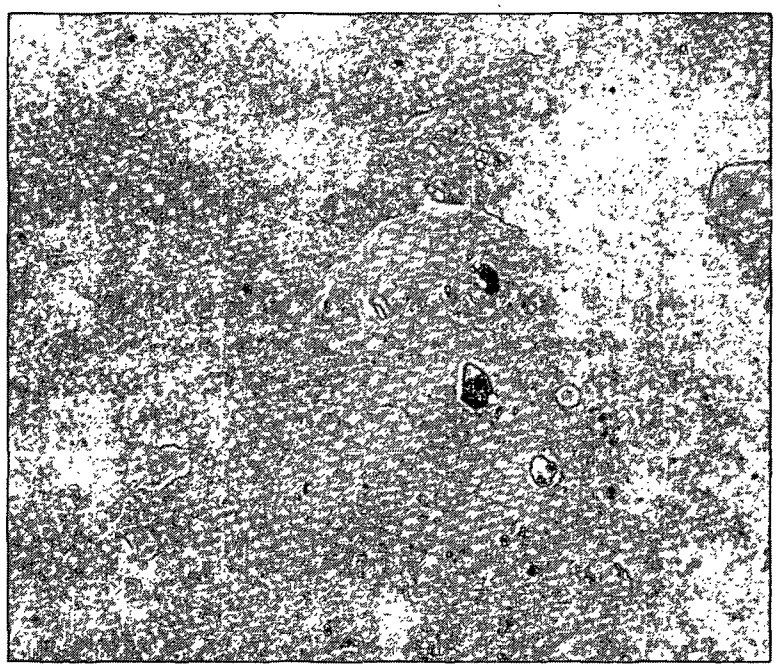

Figure A-7. SAN (No. X-117) membrane - top view - 10,000X.

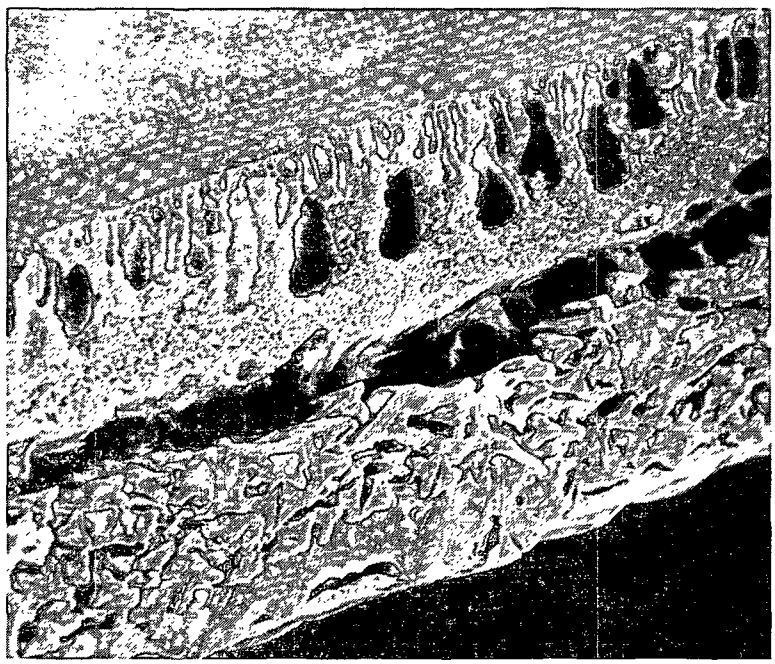

Figure A-8. SAN (No. X-117) membrane + nonwoven substrate - cross section - 200X.

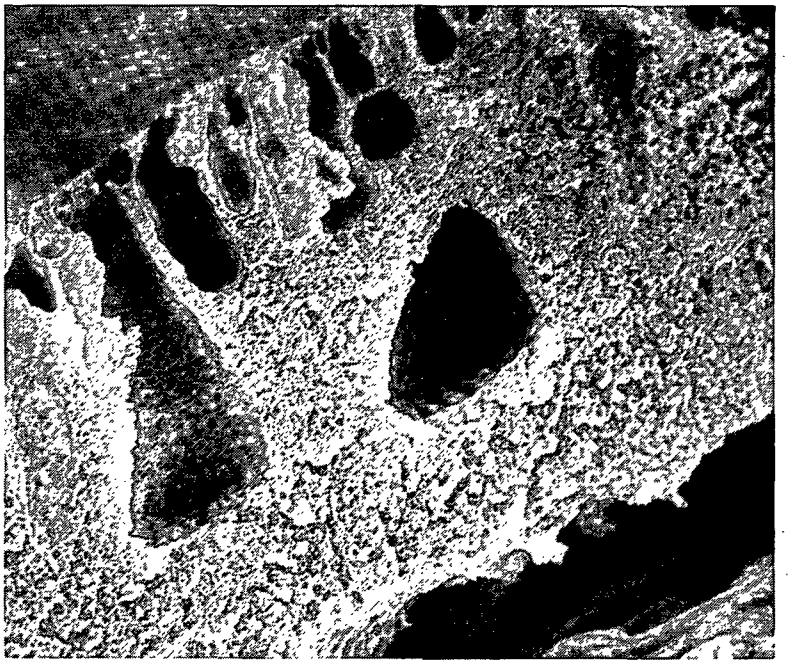

Figure A-9. SAN (No. X-117) membrane - cross section - 500X.

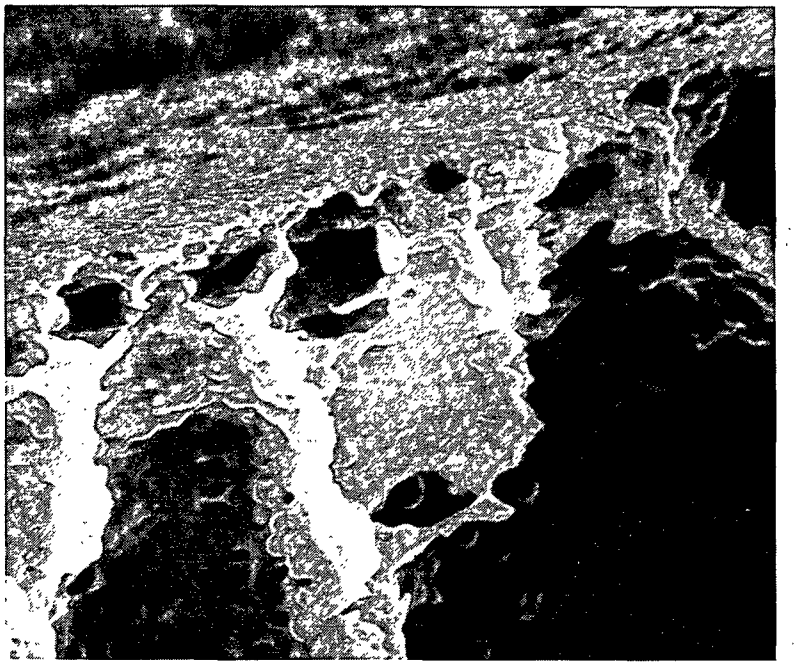

Figure A-10. SAN (No. X-117) membrane - cross section - 10,000X.

interval, or the average concentration of the total permeate volume was measured at the end of the run. In the majority of cases, there were not substantial differences between the two methods. Average permeate concentrations are reported in Appendix II.

In the experiments where the steady state flux through latex cakes (constant thickness) was measured, the cell was charged with a known volume of latex suspension of known concentration. The cell was then attached to a reservoir of pure solvent which was pressurized. The cell was allowed to reach steady state permeate flux, which was then recorded. A photograph of the batch cell equipment is given in Fig. A-11.

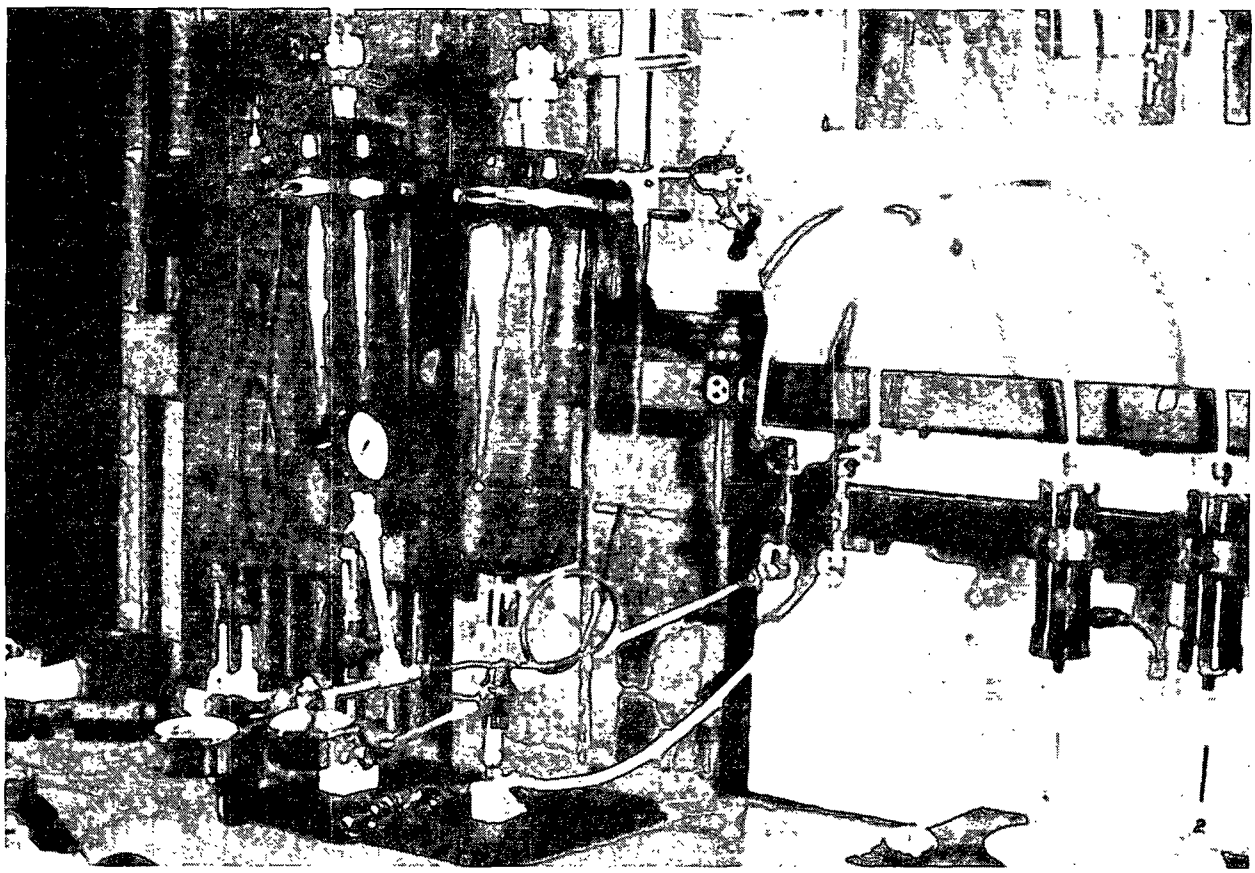

Figure A-11. Batch cell apparatus.

A technique was attempted to measure the solute concentration close to the membrane surface after the mass boundary layer was significantly developed. A small stainless steel capillary (1.5 mm) was welded into the cell and located approximately 2 mm from the membrane surface. At the end of the run, a sample of the solution was bled off through the capillary and the concentration was measured. The technique was not successful due to the fact that at least 10-15 mL of solution needed to be drained off in order to measure the concentration. The removal of such large volumes disrupt the cell (boundary layer) and the concentrations which are measured are only slightly greater than the bulk solution concentration ($\approx$ 2 times). This method may prove more successful if the need for large samples (10-15 mL) could be reduced.

As mentioned in Manuscript Number 1, a correction volume of 2 mL was added to the first experimentally measured permeate volume (ΔV_1) in all cases to account for permeate trapped in the bottom of the cell and not recoverable. The value of 2 mL was approximated experimentally. It should be noted, however, that the value of 2B (intercept) is not dependent upon the value of the correction used.

PARALLEL-PLATE SYSTEM

A parallel-plate ultrafiltration conduit was constructed which incorporated incremental permeate sampling ports along its length. The purpose of this design was to enable the measurement of permeate flux as a function of axial distance (developing boundary layer thickness). The flow channel was of the dimensions: h (channel half height) = 0.32 cm, w (channel width) = 14.92 cm, and L (active membrane length) = 198.12 cm. The conduit had a 91.44 cm calming section prior to the active membrane section in order to insure fully developed velocity profiles for Re less than 2500 based upon the Grober, et al. (1961) relationship of

$$\frac{L^*}{4h} = 0.029\ Re \qquad (18)$$

where L^* = required calming length for fully developed flow.

As mentioned, the conduit consisted of incremental permeate sampling ports along the active membrane length. This was accomplished by dividing the unit into collection chambers of the following number and dimension: eight 1-inch long chambers (membrane area = 37.90 cm^2 each), ten 2-inch long chambers (membrane area = 75.80 cm^2 each), ten 3-inch long chambers (membrane area = 113.70 cm^2 each), and five 4-inch long chambers (membrane area = 151.60 cm^2 each), or in total, 33 sampling ports. The sampling port scheme is given in Fig. A-12.

Mechanically, the conduit was constructed primarily of PVC plastic and Plexiglas. The unit was supported upon a 1/2 inch steel bed plate and held together by 3/8 inch stainless steel thru-bolts located at 3-inch increments around the periphery of the conduit. Additional reinforcement was achieved by lateral tie rods (3/8-inch) located every 10 inches along the length, and supplementary internal ribbing. The channel cover was made of 1-inch thick Plexiglas plate which was further supported from buckling by 1/2-inch steel bars (2 inches wide) over each thru-bolt. The HFM-180 membrane was installed over a porous (R_m = 5.0 x 10^7 1/cm), incompressible sheet of Kynar (3/16 inch thick) and held in place by an L-shaped brass O-ring frame which served also as the water seal. Figure A-13 shows cross section A-A of the conduit which details the sealing arrangement. Figure A-14 shows cross section B-B of the conduit, in which the sampling compartment arrangement is detailed. All given dimensions are in inches.

Feed solution was recirculated through the ultrafiltration conduit by means of a Sundstrand (Sun-Flo) centrifugal pump which was capable of flow rates as high as 15

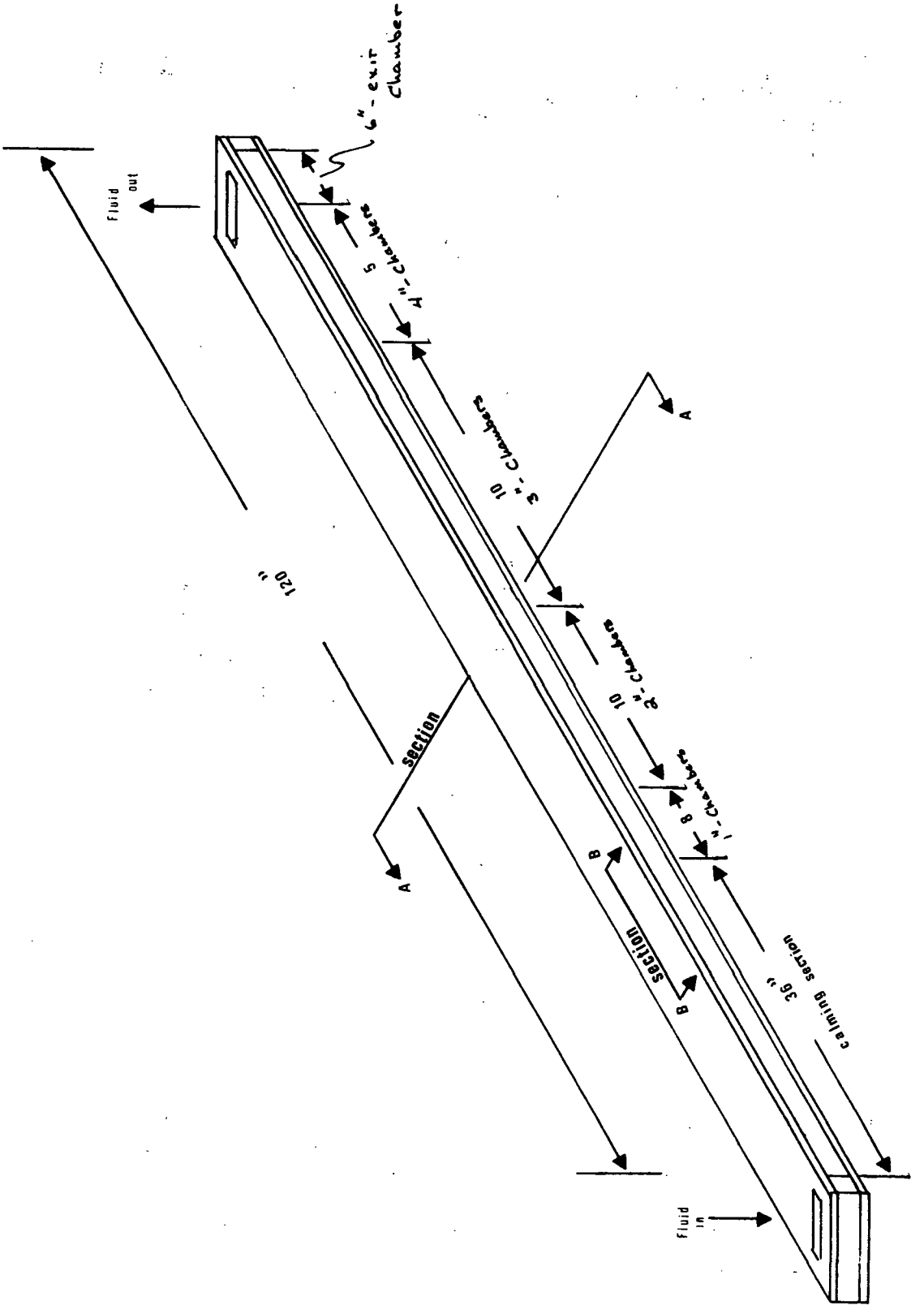

Figure A-12. Experimental UF conduit - sampling chamber scheme.

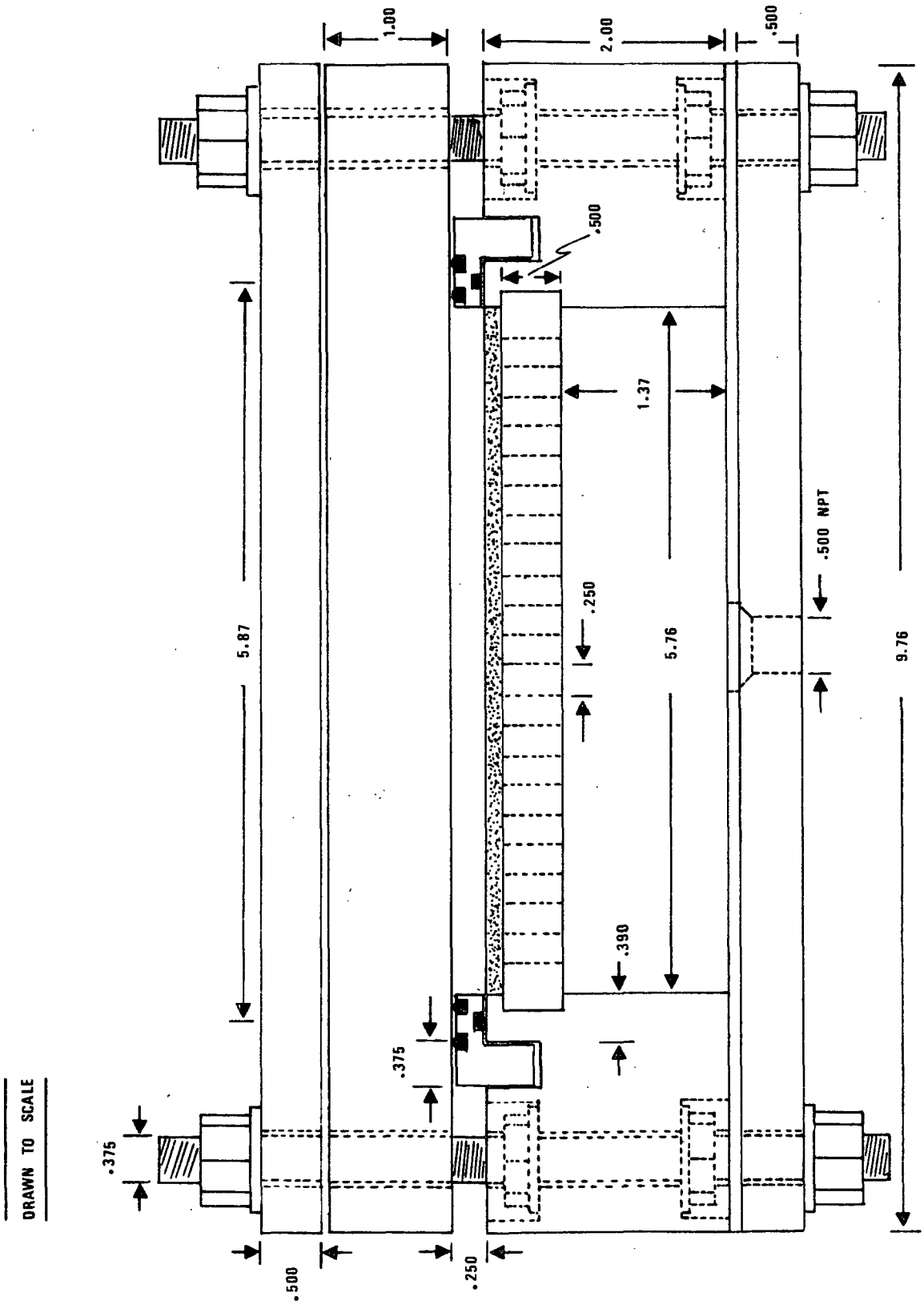

Figure A-13. Ultrafiltration conduit - Section A-A.

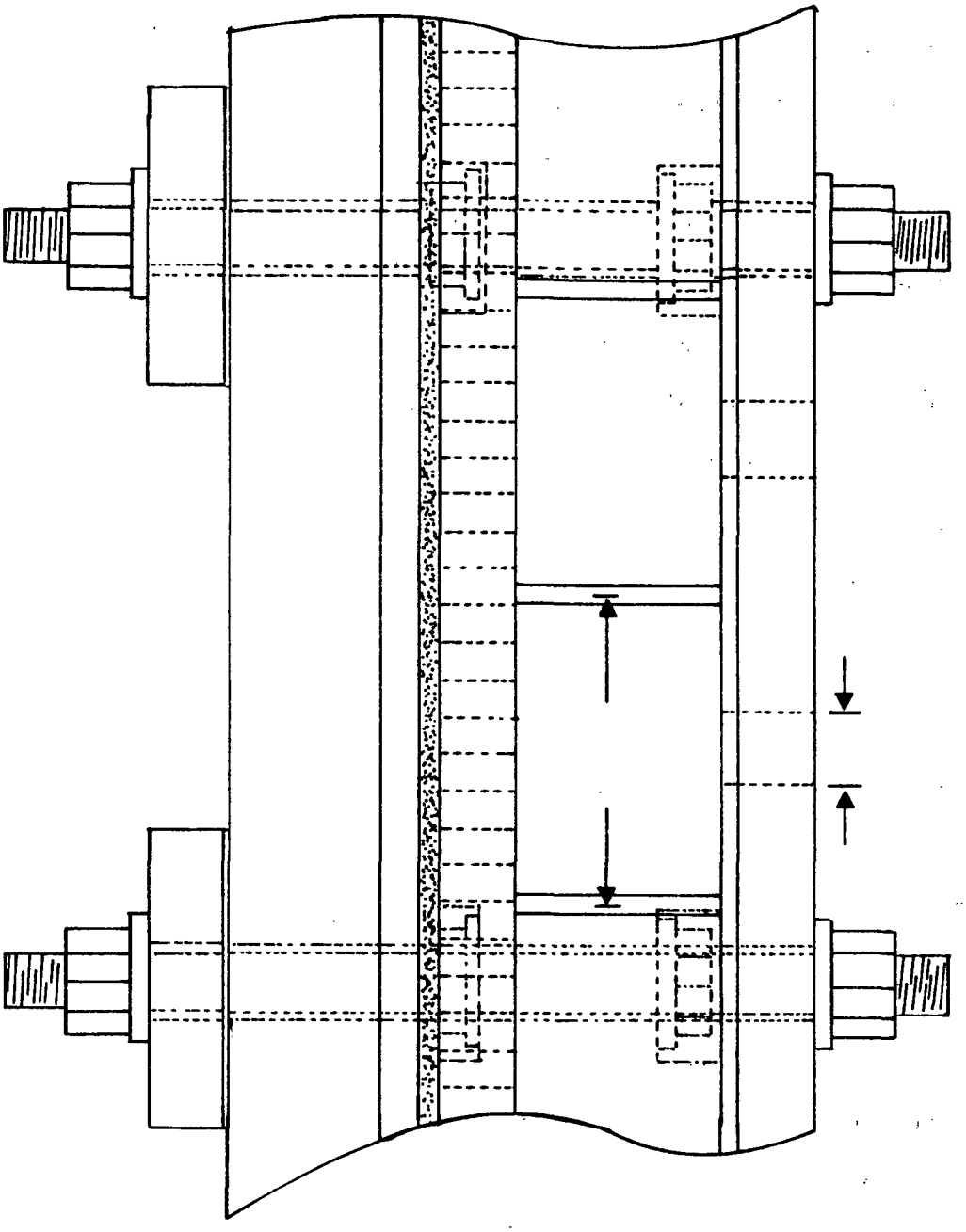

DRAWN TO SCALE

Figure A-14. UF conduit - Section B-B.

gpm at 100 psig. A portion of the total pump flow was directly returned to the feed tank via a backpressure regulator and heat exchanger. This method was successful in controlling system temperature and pressure in the ultrafiltration conduit. Axial pressure drop through the conduit was measured by a manometer and found to be negligible (< 1 psig) for all flow rates studied. The process flow diagram is given in Fig. 11 of Manuscript Number 2. All high-pressure piping was 304 S.S., whereas low-pressure piping was PVC. The pump, valves, heat exchanger, backpressure regulator, and feed tanks were of stainless steel construction or trim. Permeate was collected from each port through 1/2-inch I.D. Tygon tubes which led to a general header arrangement. Permeate which drained from the header was either measured gravimetrically for each port or collected into a tray from which it was pumped back into the feed tank.

Membranes were preconditioned by recirculating the solvent through the unit at the desired operating pressure (40 - 80 psig) until steady state flux behavior was observed. Axial flow rates were measured by Fischer and Porter rotameters (high flow) or Fischer and Porter turbine flowmeters (low flow). Materials used in the construction of the unit are listed in Appendix IV (Bill of Materials).

The start-up procedure was to close the flow valve to the ultrafiltration unit, start the recirculation pump, and circulate solution through the heat exchanger back into the feed tank. When the desired solution temperature was reached, the flow valve to the ultrafiltration unit was opened and the desired axial flow rate and pressure was adjusted. The system was checked periodically for drift in the set-point flow rate. Shutdown was simply to cut off the recirculation pump and shut off the heat exchanger cooling water. The membrane was normally rinsed by switching over the pump and return line to the water tank and restarting the recirculation pump. Permeate from this step was sewered. A more complete cleaning of the

membrane necessitated disassembling the conduit and sponging the membrane with soap and water.

Although experiments with latex suspensions were successful, experiments with various macromolecular solutions were not. This was due to the fact that it was not possible to totally eliminate rust or scale from the system. It is believed that some type of metal-ion complexing had occurred between the rust (or scale) and the polymer in solution. This complex formation caused severe fouling of the membrane to the point of completely blinding over in parts. It is suggested that if this system is to be used again to study macromolecular ultrafiltration, all piping be replaced by a higher grade of stainless steel (Type 316 or 317). Photographs of the system are shown in Fig. A-15 and A-16.

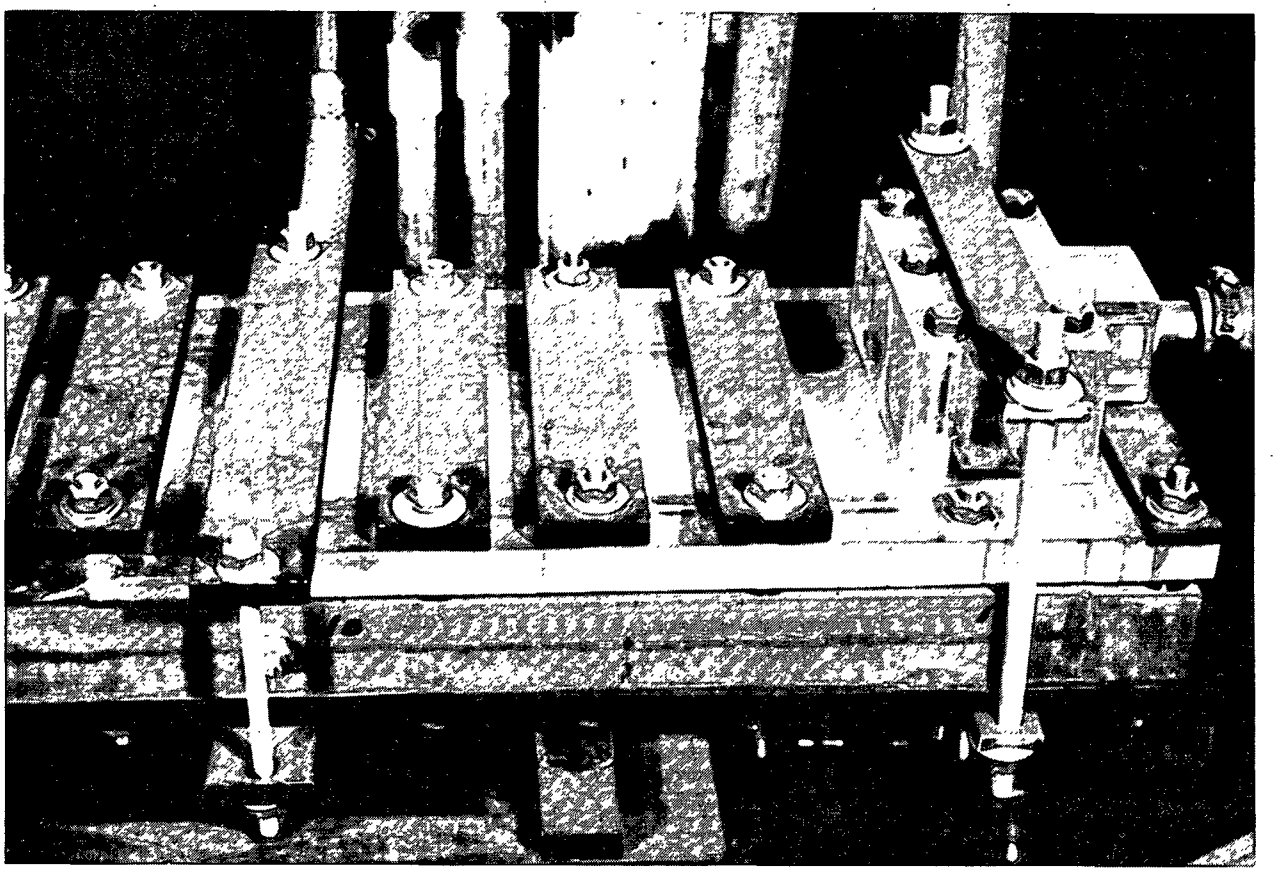

Figure A-15. Parallel plate ultrafiltration system - top view.

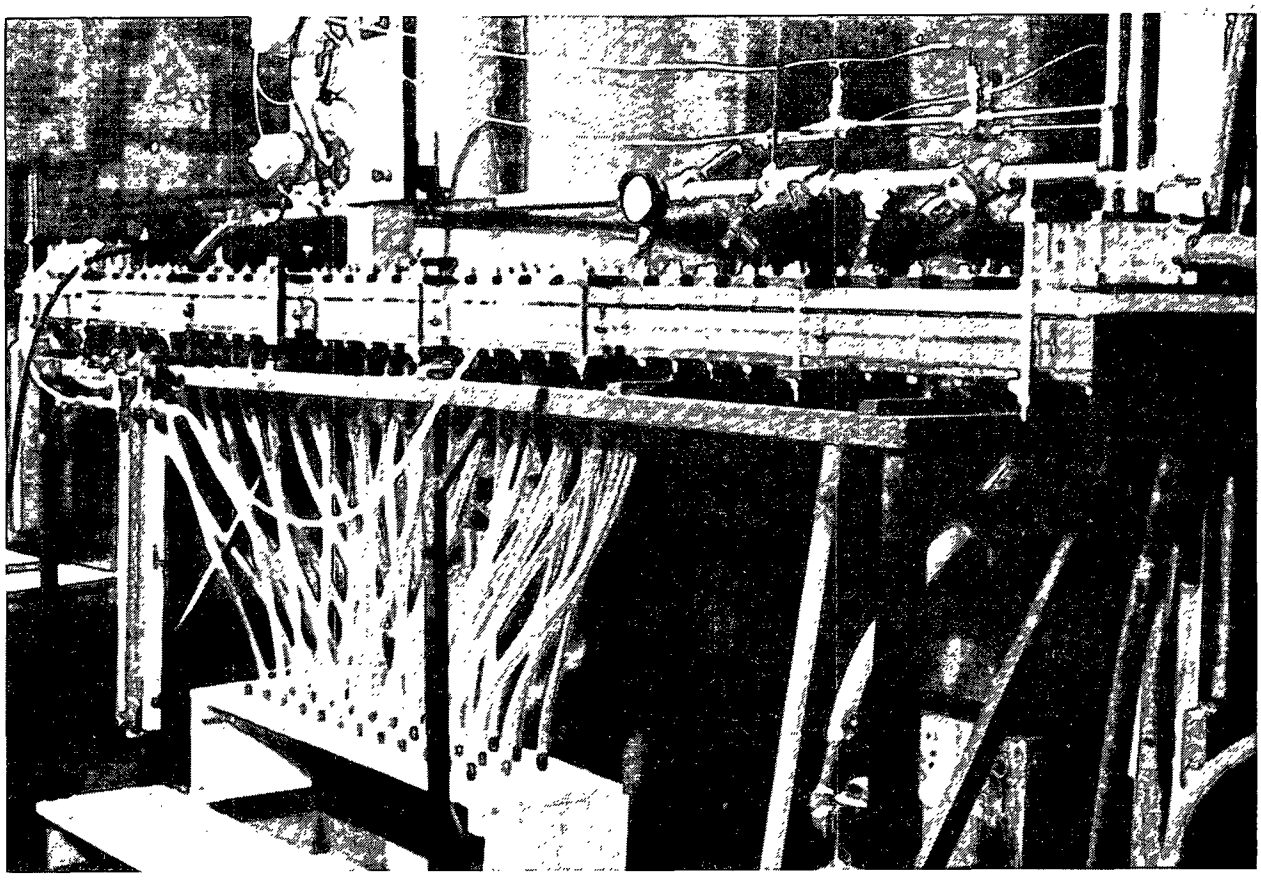

Figure A-16. Parallel plate ultrafiltration system - overall view.

LITERATURE CITED

Creeth, J. M. Studies of free diffusion in liquids with the Rayleigh method. J. Am. Chem. Soc. 77:6428(1955).

Grober, H., Erk, S., and Grigull, U. Fundamentals of heat transfer. McGraw-Hill, New York, NY, 1961.

Heiser, E. J., Dow Chemical Company, Personal communication, 1979.

Hercules, Cellulose Gum - Chemical and Physical Properties, Technical Booklet, Hercules, Incorporated, Wilmington, Delaware, 1976.

Kindler, W. A., Jr. Adsorption kinetics in the polyethylenimine - cellulose fiber system. Ph.D. Thesis, The Institute of Paper Chemistry, January, 1971.

Kozinski, A. A. and Lightfoot, E. N. Protein ultrafiltration: a general example of boundary layer filtration. AIChE J. 18(5):1030(1972).

Lepori, L. and Mollica, V. Volumetric properties of dilute aqueous solutions of poly(ethylene) glycols. J. Polymer Sci.: Polymer Phys. Edition 16:1123(1978).

Longsworth, L. G., In Electrochemistry in biology and medicine, T. Shedlovsky, editor, Chapter 12, Wiley, New York, 1955.

Schumaker, V., Arch. Biochem. Biophys. 103:139(1963).

Tostevin, J. E. The hydrodynamic properties of the alditol oligosaccharides. Ph.D. Thesis, The Institute of Paper Chemistry, June, 1966.

APPENDIX II

COMPUTER PROGRAMS

This section contains two computer programs which were used to numerically integrate the convective diffusion equation for both the unstirred batch cell and parallel-plate systems [Eq. (11) of Manuscript Number 1, and Eq. (15) of Manuscript Number 3]. Also listed is a trial and error program used to analyze the unstirred batch cell data cited in Manuscript Number 4.

All values of concentration, diffusion coefficient, and VLIM are entered, or calculated, as g/100 cc, cm^2/sec, and $mL\text{-}sec^{-1/2}$, respectively.

```
/JOB GO,TIME=20
/FTC LIST
C......THIS PROGRAM IS CALLED VARDB(DRT)IN THE IPC COMPUTER LIBRARY AND
C......IS USED TO NUMERICALLY INTEGRATE THE EXACT SOLUTION (EQUATION(11)
C......MANUSCRIPT NUMBER 1) TO THE CONVECTIVE DIFFUSION EQUATION FOR THE
C......UNSTIRRED BATCH CELL SYSTEM. THE VALUE OF CGEL(OR CWALL) IS SPECI-
C......FIED AND THE CORRESPONDING VALUE OF DIMENSIONLESS VW (PERMEATE
C......FLUX  CONSTANT ) IS CALCULATED FOR VARIOUS VALUES OF CB (BULK
C......SOLUTION CONCENTRATION ). INTEGRATION IS ACHIEVED USING SIMPSON'S
C......RULE. THE DEPENDENCE OF THE DIFFUSION COEFFICIENT UPON SOLUTE
C......CONCENTRATION MUST BE KNOWN AND SPECIFIED IN TERMS OF THE PARA-
C......METERS DGEL,DBUL,AND DE(I) IN THE  PROGRAM.
      DIMENSION DE(1001), ETA(1001), AO(1001),F(1001),
     1 G(1001), SUB(1001),AT(1001),CB(50),VN(3),FN(3)
C......INITIALIZE SYSTEM
      VW= 1.0
      CB(1)= 0.0
      CGEL= 58.0
C......CP EQUALS  THE  PERMEATE CONCENTRATION
      CP= C.CO
C......NA EQUALS THE RANGE OF CB COVERED. MAXIMUM VALUE CAN BE INTEGER
C......VALUE OF CGEL
      NA = 30
      AINC= .01
      MA=1001
C......WRITE THE DIFFUSION COEFFICIENT-CONCENTRATION RELATIONSHIP
C......FOR THE SPECIFIC SOLUTE IN QUESTION AT CGELL CONCENTRATION
      DGEL=((7.1E-07)/(.159*CGEL))*(EXP(.159*CGEL)-EXP(-.159*CGEL))/
     1 (EXP(.159*CGEL)+EXP(-.159*CGEL))
C......MA = ETA(MAX)/AINC + 1
      ETA(1)= 0.0
C......CALCULATE VALUES OF DELTA
      DO 1 I=2,MA
    1 ETA(I)=ETA(I-1) + AINC
      DO 21  J=2,NA,1
      KONT=1
      CB(J)= CB(J-1) + 1.0
C......WRITE THE DIFFUSION COEFFICIENT-CONCENTRATION RELATIONSHIP FOR
C......THE SPECIFIC SOLUTE IN QUESTION AT CBUL CONCENTRATION
      DBUL=(7.1E-07/(.159*CB(J)))*(EXP(.159*CB(J))
     1 -EXP(-.159*CB(J)))/(EXP(.159*CB(J))+EXP(-.159*CB(J)))
      C = CGEL/DBUL
      DE(1)=DGEL/DBUL
      SUB(1)= DBUL/DGEL
      F(1)= CGEL/CB(J)
C......CALCULATION OF F(2)
    2 G(1)= (ETA(1)*2.0 + VW)/D
      G(2)= (ETA(2)*2.0 + VW)/D
      AO(1)=(AINC/2.)*(G(1) + G(2))
      SUB(2)= (1./D)* EXP(-AO(1))
      AT(1)= (AINC/2.)*(SUB(1)+SUB(2))
      C = CGEL-(VW*(CGEL-CP)*AT(1))
C......SUBSTITUTE THE PROPER DIFFUSION COEFFICIENT-CONCENTRATION
C......RELATIONSHIP FOR DE(2)
      U= .159*C
      DE(2)=(1./U)*((EXP(U)-EXP(-U))/(EXP(U)+EXP(-U)))
     1 *(7.1E-07/DBUL)
      VAR= ABS(DE(2)-D) - (1.0E-04)
```

```
      IF(VAR) 4,4,3
    3 C = DE(2)
      GO TO 2
    4 F(2) = C/CB(J)
C.....CALCULATION OF F(3)
    5 G(3) = (ETA(3)*2.0 + VW)/D
      AO(2)=(AINC/3.)*(G(1)+ 4.*G(2) + G(3))
      SUB(3) = (1./D)*EXP(-AO(2))
      AT(2)=(AINC/3.)*(SUB(1)+4.*SUB(2)+SUB(3))
      C = CGEL-(VW*(CGEL-CP)*AT(2))
C.....SUBSTITUTE THE PROPER DIFFUSION COEFFICIENT-CONCENTRATION
C.....RELATIONSHIP FOR DE(3)
      U=.159*C
      DE(3)=(1./U)*((EXP(U)-EXP(-U))/(EXP(U)+EXP(-U)))
     1*(7.1E-07/DBUL)
      VAR = ABS(DE(3)-D) - (1.0E-04)
      IF(VAR) 7,7,6
    6 C = DE(3)
      GO TO 5
    7 F(3)= C/CB(J)
C.....CALCULATION OF F(ETA)
      DO 11 I=4,MA
    8 G(I)=(ETA(I)*2.0 + VW)/D
      AO(I-1)=(AINC/3.)*(G(I-2)+4.*G(I-1)+G(I))+AO(I-3)
      SUB(I)=(1./D)*EXP(-AO(I-1))
      AT(I-1)=(AINC/3.)*(SUB(I-2)+4.*SUB(I-1)+SUB(I))+AT(I-3)
      C=CGEL-(VW*(CGEL-CP)*AT(I-1))
C.....SUBSTITUTE THE PROPER DIFFUSION COEFFICIENT-CONCENTRATION
C.....RELATIONSHIP FOR DE(I)
      U=.159*C
      DE(I)=(1./U)*((EXP(U)-EXP(-U))/(EXP(U)+EXP(-U)))
     1*(7.1E-07/DBUL)
      VAR=ABS(DE(I)-D) -  (1.0E-04)
      IF (VAR) 10,10,9
    9 C=DE(I)
      GO TO 8
   10 F(I) = C/CB(J)
   11 CONTINUE
C.....TEST FOR CONVERGENCE
      TEST= F(MA-20)-F(MA-10)
      IF(TEST-1.0E-06) 13,13,12
   12 WRITE(6,9022)
      GO TO 21
   13 VARA=ABS(F(MA-2)-1.0) - 1.0E-04
      IF(VARA) 20,20,14
   14 IF(F(MA-2)-1.0) 15,20,17
   15 IF(KONT-2) 16,16,19
   16 VN(KONT)=VW
      FN(KONT)=F(MA-2)
      VW=VW-.10
      D=DGEL/DBUL
      KONT=KONT+1
      IF(KONT-2) 2,2,19
   17 IF(KONT-2) 18,18,19
   18 VN(KONT)=VW
      FN(KONT)=F(MA-2)
      VW=VW+.10
      D=DGEL/DBUL
      KONT=KONT+1
      IF(KONT-2) 2,2,19
```

```
   19   FN(2)=F(MA-2)
        VN(3)=(VN(1)*(FN(2)-1.0)+VN(2)*(1.-FN(1)))/(FN(2)-FN(1))
        WRITE(6,9023) FN(1),FN(2),VN(3)
        VW=VN(3)
        VN(1)=VN(2)
        FN(1)=FN(2)
        VN(2)=VN(3)
        GO TO 2
   20   CONTINUE
        WRITE(6,9024) VW,CB(J)
        WRITE(6,9025)
        WRITE(6,9026)(ETA(I),F(I),AT(I),DE(I),I=1,MA,100)
   21   CONTINUE
        CALL EXIT
 9022   FORMAT(' SYSTEM NOT CONVERGED ')
 9023   FORMAT('FN(1) EQUALS',F8.4,4X,'FN(2) EQUALS',F8.4,4X,
     1  'VN(3) EQUALS',F8.4)
 9024   FORMAT('VW EQUALS',F9.3,10X,'CB EQUALS',F5.1)
 9025   FORMAT('       ETA',9X,'F(ETA)',7X,'TOTAL INTEGRAL',
     1  7X,'DIFFUSION COEFFICIENT')
 9026   FORMAT(F11.4,F13.4,F17.4,E27.4)
        END

/END CARD READ, JOB TERMINATED
```

```
/JOB GO,TIME=20
/FTC LIST
C.....THIS PROGRAM IS CALLED VARD(DRT) IN THE IPC COMPUTER LIBRARY AND
C.....IS USED TO NUMERICALLY INTEGRATE THE EXACT SOLUTION (EQUATION(15)
C.....MANUSCRIPT NUMBER 3) TO THE CONVECTIVE DIFFUSION EQUATION FOR THE
C.....PARALLEL PLATE (THIN-CHANNEL) SYSYEM. THE VALUE OF CGEL(OR CWALL)
C.....IS SPECIFIED AND THE CORRESPONDING VALUE OF DIMENSIONLESS VW
C.....(PERMEATE FLUX CONSTANT) IS CALCULATED FOR VARIOUS VALUES OF
C.....CB(BULK SOLUTION CONCENTRATION). INTEGRATION IS ACHIEVED USING
C.....SIMPSON'S RULE.  THE DEPENDENCE OF THE DIFFUSION COEFFICIENT
C.....UPON SOLUTE CONCENTRATION MUST BE KNOWN AND SPECIFIED IN TERMS
C.....OF THE PARAMETERS DGEL, DBUL, AND DE(I) IN THE PROGRAM
      DIMENSION DE(1001), ETA(1001), AO(1001),F(1001),
     1 G(1001), SUB(1001),AT(1001),CB(50),VN(3),FN(3)
C.....INITIALIZE SYSTEM
      VW= 1.0
      CB(1)= 0.0
      CGEL= 58.0
C.....CP EQUALS THE SOLUTE CONCENTRATION OF THE PERMEATE
      CP = 0.00
C.....NA EQUALS THE RANGE OF CB COVERED. MAXIMUM VALUE CAN BE INTEGER
C.....VALUE OF CGEL
      NA = 30
      AINC= .01
      MA=1001
C.....WRITE THE DIFFUSION COEFFICIENT-CONCENTRATION RELATIONSHIP
C.....FOR THE SPECIFIC SOLUTE IN QUESTION AT CGELL CONCENTRATION
      DGEL=((7.1E-07)/(.159*CGEL))*(EXP(.159*CGEL)-EXP(-.159*CGEL))/
     1 (EXP(.159*CGEL)+EXP(-.159*CGEL))
C.....MA = ETA(MAX)/AINC + 1
      ETA(1)= 0.0
C.....CALCULATE VALUES OF DELTA
      DO 1 I=2,MA
    1 ETA(I)=ETA(I-1) + AINC
      DO 26  J=2,NA,1
      KONT=1
      CB(J)= CB(J-1) + 1.0
C.....WRITE THE DIFFUSION COEFFICIENT-CONCENTRATION RELATIONSHIP FOR
C.....THE SPECIFIC SOLUTE IN QUESTION AT CBUL CONCENTRATION
      DBUL=(7.1E-07/(.159*CB(J)))*(EXP(.159*CB(J))
     1 -EXP(-.159*CB(J)))/(EXP(.159*CB(J))+EXP(-.159*CB(J)))
      D = DGEL/DBUL
      DE(1)=DGEL/DBUL
      SUB(1)= DBUL/DGEL
      F(1)= CGEL/CB(J)
C.....CALCULATION OF F(2)
    2 G(1)= (ETA(1)**2  + VW)/D
      G(2)= (ETA(2)**2  + VW)/D
      AO(1)=(AINC/2.)*(G(1) + G(2))
      SUB(2)= (1./D)* EXP(-AO(1))
      AT(1)= (AINC/2.)*(SUB(1)+SUB(2))
      C = CGEL-(VW*(CGEL-CP)*AT(1))
C.....SUBSTITUTE THE PROPER DIFFUSION COEFFICIENT-CONCENTRATION
C.....RELATIONSHIP FOR DE(2)
      U= .159*C
      DE(2)=(1./U)*((EXP(U)-EXP(-U))/(EXP(U)+EXP(-U)))
     1 *(7.1E-07/DBUL)
      VAR= ABS(DE(2)-D) - (1.0E-04)
```

```
      IF(VAR) 4,4,3
    3 D = DE(2)
      GO TO 2
    4 F(2) = C/CB(J)
C.....CALCULATION OF F(3)
    5 G(3) = (ETA(3)**2  + VW)/D
      AO(2)=(AINC/3.)*(G(1)+ 4.*G(2) + G(3))
      SUB(3) = (1./D)*EXP(-AO(2))
      AT(2)=(AINC/3.)*(SUB(1)+4.*SUB(2)+SUB(3))
      C = CGEL-(VW*(CGEL-CP)*AT(2))
C.....SUBSTITUTE THE PROPER DIFFUSION COEFFICIENT-CONCENTRATION
C.....RELATIONSHIP FOR DE(3)
      U=.159*C
      DE(3)=(1./U)*((EXP(U)-EXP(-U))/(EXP(U)+EXP(-U)))
     1*(7.1E-07/DBUL)
      VAR = ABS(DE(3)-D) - (1.0E-04)
      IF(VAR) 7,7,6
    6 D = DE(3)
      GO TO 5
    7 F(3)= C/CB(J)
C.....CALCULATION OF F(ETA)
      DO 11 I=4,MA
    8 G(I)=(ETA(I)**2  + VW)/D
      AO(I-1)=(AINC/3.)*(G(I-2)+4.*G(I-1)+G(I))+AO(I-3)
      SUB(I)=(1./D)*EXP(-AO(I-1))
      AT(I-1)=(AINC/3.)*(SUB(I-2)+4.*SUB(I-1)+SUB(I))+AT(I-3)
      C=CGEL-(VW*(CGEL-CP)*AT(I-1))
C.....SUBSTITUTE THE PROPER DIFFUSION COEFFICIENT-CONCENTRATION
C.....RELATIONSHIP FOR DE(I)
      U=.159*C
      DE(I)=(1./U)*((EXP(U)-EXP(-U))/(EXP(U)+EXP(-U)))
     1*(7.1E-07/DBUL)
      VAR=ABS(DE(I)-D) -  (1.0E-04)
      IF (VAR) 10,10,9
    9 D=DE(I)
      GO TO 8
   10 F(I) = C/CB(J)
   11 CONTINUE
C.....TEST FOR CONVERGENCE
      TEST= F(MA-20)-F(MA-10)
      IF(TEST-1.0E-06) 14,14,12
   12 WRITE(6,9013)
      GO TO 26
   14 VARA=ABS(F(MA-2)-1.0) - 1.0E-04
      IF(VARA) 22,22,15
   15 IF(F(MA-2)-1.0) 16,22,18
   16 IF(KONT-2) 17,17,20
   17 VN(KONT)=VW
      FN(KONT)=F(MA-2)
      VW=VW-.10
      D=DGEL/DBUL
      KONT=KONT+1
      IF(KONT-2) 2,2,20
   18 IF(KONT-2) 19,19,20
   19 VN(KONT)=VW
      FN(KONT)=F(MA-2)
      VW=VW+.10
      D=DGEL/DBUL
      KONT=KONT+1
      IF(KONT-2) 2,2,20
```

```
   20  FN(2)=F(MA-2)
       VN(3)=(VN(1)*(FN(2)-1.0)+VN(2)*(1.-FN(1)))/(FN(2)-FN(1))
       WRITE(6,9021) FN(1),FN(2),VN(3)
       VW=VN(3)
       VN(1)=VN(2)
       FN(1)=FN(2)
       VN(2)=VN(3)
       GO TO 2
   22  CONTINUE
       WRITE(6,9023) VW,CB(J)
       WRITE(6,9024)
       WRITE(6,9025)(ETA(I),F(I),AT(I),DE(I),I=1,MA,100)
   26  CONTINUE
       CALL EXIT
 9013  FORMAT(' SYSTEM NOT CONVERGED ')
 9021  FORMAT('FN(1) EQUALS',F8.4,4X,'FN(2) EQUALS',F8.4,4X,
     1 'VN(3) EQUALS',F8.4)
 9023  FORMAT('VW EQUALS',F6.3,10X,'CB EQUALS',F5.1)
 9024  FORMAT('      ETA',9X,'F(ETA)',7X,'TOTAL INTEGRAL',
     1 7X,'DIFFUSION COEFFICIENT')
 9025  FORMAT(F11.4,F13.4,F17.4,E27.4)
       END

/END CARD READ, JOB TERMINATED
```

```
/JOB GO,TIME=20
C......THIS PROGRAM IS CALLED BATFT(DRT) AND IS USED TO FIT BATCH
C......CELL ULTRAFILTRATION DATA USING AN INTEGRAL METHOD MODEL.
C......THE VALUES OF CO(BULK SOLUTION CONCENTRATION),VLIM,AND CP ARE
C......ENTERED ALONG WITH A STARTING VALUE OF THE DIFFUSION COEFFICIENT.
C......THE MODEL CONVERGES UPON THE APPROPRIATE VALUE OF CWALL(OR CGEL)
C......BY UTILIZING A REGULA FALSI METHOD. CP EQUALS THE SOLUTE CONCEN-
C......TRATION OF THE PERMEATE. VLIM EQUALS THE LIMITING VALUE OF THE
C......PERMEATE VOLUME DIVIDED BY THE VALUE OF TIME TO THE ONE-
C......HALF POWER. THE VALUE OF DIFF(DIFFUSION COEFFICIENT) IS FOUND
C......BY SETTING LIMITS UPON THE ALLOWABLE STANDARD DEVIATION BETWEEN
C......THE  CALCULATED VALUES OF CWALL FOR EACH DATA POINT. IT IS NEC-
C......ESSARY IN  ORDER TO INSURE THE VALIDITY OF THE RESULT TO CONVERGE
C......FROM BOTH A HIGHER AND LOWER ARBITRARY VALUE OF THE DIFFUSION
C......COEFFICIENT. IF THE VALUE IS UNIQUE, THE SAME VALUE WILL RESULT
C......TO WITHIN REASONABLE LIMITS. THE DETERMINATION OF THE VALUE OF
C......THE DIFFUSION COEFFICIENT BY THIS METHOD IS A TRIAL AND ERROR
C......PROCESS.
      DIMENSION CO(15),VLIM(15),CP(15),FW(15),FP(15),X(15),Y(15),
     1 CWALL(15),VW(15),TEST(2),STD(15)
C......N EQUALS THE NUMBER OF DATA POINTS ENTERED
C......F EQUALS THE NUMBER OF DATA POINTS ENTERED
      N=9
      F=9.0
      TEST(1)=0.0
      TEST(2)=0.0
      READ(5,9001)(CO(J),VLIM(J),CP(J),J=1,N,1)
C......A EQUALS THE TRANSPORT AREA OF THE MEMBRANE(SQ.CM)
      A= 15.62
C......DIFF EQUALS THE STARTING VALUE OF DIFFUSION COEFFICIENT
      DIFF= 10.00E-09
    2 CON= 1.0/(((A**2)*DIFF)**.5)
      DO 10 I=1,N,1
      FW(1)=  2.0
      FW(2)= FW(1) + 1.0
      FP(I)= CP(I)/CO(I)
      X(1)=(( FW(1)-FP(I)) + ((( FW(1)-FP(I))**2) + 8.0*(1.0-FP(I))*
     1 (FW(1)-FP(I)))**.5)/(2.0*(1.0-FP(I)))
      Y(1)= (2.0*X(1))/(X(1) + 1.0)
      VW(1)= ((FW(1) - 1.0)/(FW(1) - FP(I)))*(( Y(1)*((FW(1)-FP(I))/
     1 (1.0 - FP(I))))**.5) - VLIM(I)*CON
    3 X(2)=(( FW(2)-FP(I)) + ((( FW(2)-FP(I))**2) + 8.0*(1.0-FP(I))*
     1 (FW(2)-FP(I)))**.5)/(2.0*(1.0-FP(I)))
      Y(2)= (2.0*X(2))/(X(2) + 1.0)
      VW(2)= ((FW(2)-1.0)/(FW(2)-FP(I)))* (( Y(2)*((FW(2)-FP(I))/
     1 (1.0 - FP(I))))**.5) - VLIM(I)*CON
      VAR= ABS(VW(2))
      IF(VAR - .001) 10,10,4
    4 IF(VW(1)) 5,5,6
    5 IF(VW(2)) 7,7,8
    6 IF(VW(2)) 8,8,7
    7 FW(3)= (VW(2)/(VW(2)-VW(1)))*(FW(1)-((VW(1)/VW(2))*FW(2)))
      GO TO 9
    8 FW(3)= (VW(2)/(VW(2)+VW(1)))*(FW(1) + ((VW(1)/VW(2))*FW(2)))
    9 FW(1)= FW(2)
      VW(1)= VW(2)
      FW(2)= FW(3)
      GO  TO 1000
   10 CWALL(I)=CO(I)*FW(2)
```

```
      AVEC= 0.0
      CO 11 M=1,N,1
   11 AVEC= AVEC + CWALL(M)
      AVEC = AVEC/F
      SMAX=0.0
      DC 13 K=1,N,1
      STD(K)=ABS(AVEC- CWALL(K))
      IF(STD(K)-SMAX) 13,12,12
   12 SMAX=STD(K)
   13 CONTINUE
C.....ENTER THE DEGREE OF ACCURACY OF STD DEVIATION IN 'IF' STATEMENT
      SMAX=SMAX/AVEC
      IF(SMAX- .10) 23,23,14
   14 IF(CWALL(1)-CWALL(N)) 19,23,15
   15 TEST(1)=TEST(1) + 1.0
      IF(TEST(2)) 18,18,16
   16 WRITE(6,9017)
      GO TO 27
   18 DIFF=DIFF +1.00E-08
      GC TO 2
   19 TEST(2)= TEST(2) + 1.0
      IF(TEST(1)) 22,22,20
   20 WRITE(6,9021)
      GO TO 27
   22 DIFF=DIFF -1.00E-08
      GC TO 2
   23 WRITE(6,9024)(CWALL(I),I=1,N,1)
      WRITE(6,9025) DIFF
      WRITE(6,9026) AVEC,SMAX
   27 CONTINUE
      CALL EXIT
C..... LIST DATA IN INCREASING VALUE OF CO(CO,VLIM.CP)
 9001 FORMAT(3(F8.4,10X))
 9017 FORMAT(15X,'SYSTEM NOT CONVERGING')
 9021 FORMAT(15X,'SYSTEM NOT CONVERGING')
 9024 FORMAT('CWALL EQUALS',3X,F9.4,///)
 9025 FORMAT('DIFFUSION COEFFICIENT EQUALS',3X,E10.3)
 9026 FORMAT(5X,'AVE CW   ',F6.2,'   STAN DEV   ',F6.2)
      END

/END CARD READ, JOB TERMINATED
```

APPENDIX III

TABULATED EXPERIMENTAL DATA

The following pages contain tabulations of the experimental data from which the results given in Manuscripts 1 through 4 have been obtained. In unstirred batch cell experiments, individual values of $\Delta V_{exp}/T^{1/2}$ are given for each measurement time, T. The extrapolated values of $(\Delta V/T^{1/2})_{lim}$ as $T \longrightarrow \infty$ are also calculated. Unstirred batch cell data are listed in Tables A-8 through A-14 of this section for the various solutes studied in order of increasing bulk solution concentration (c_o).

Tables A-15 through A-26 list parallel plate data for the various solutes studied. Values of permeate volumetric flux at specific port locations along the conduit length are given at various measurement times (T). Data are listed in order of increasing bulk solution concentration for each solute material studied.

TABLE A-8

BATCH CELL DATA - BSA (0.15M NaCL, 7.40 pH)

c_o (g/100 cc)	c_p (g/100 cc)	$T \times 10^{-4}$ (sec)	$\frac{\Delta V_{exp}}{T^{1/2}}$ (mL-sec$^{-1/2}$)	$R_m \times 10^{-11}$ (1/cm)	$\Delta P \times 10^{-5}$ (N/m^2)	Temp. (°C)	$\frac{\Delta V_2 - \Delta V_1}{\Delta V_3 - \Delta V_1}$	Membrane Type	$\left[\frac{\Delta V}{T^{1/2}}\right]_{Lim}$ (mL-sec$^{-1/2}$)
0.50	0.011	0.72	0.2177	1.61	6.89	21	0.4406	C.A.	0.2147
		1.44	0.2202						
		2.88	0.2152						
0.51	0.010	1.08	0.2167	1.76	10.34	23	0.4223	C.A.	0.2015
		2.16	0.2133						
		4.32	0.2088						
0.98	0.015	0.72	0.1645	1.74	10.34	22	0.4262	SAN	0.1437
		1.44	0.1595						
		2.88	0.1538						
0.98	0.026	0.72	0.1662	1.23	10.34	22	0.4233	SAN	0.1451
		1.44	0.1608						
		2.88	0.1554						
1.03	0.004	1.08	0.1325	2.09	2.76	22	0.4296	C.A.	0.1137
		2.16	0.1281						
		4.32	0.1228						
1.03	0.004	1.08	0.1592	1.67	4.14	23	0.4288	C.A.	0.1248
		2.16	0.1502						
		4.32	0.1417						
1.03	0.004	1.08	0.1589	1.96	6.89	23	0.4187	C.A.	0.1355
		2.16	0.1524						
		4.32	0.1471						

TABLE A-8 (Continued)

BATCH CELL DATA - BSA (0.15M NaCL, 7.40 pH)

c_o (g/100 cc)	c_p (g/100 cc)	$T \times 10^{-4}$ (sec)	$\frac{\Delta V_{exp}}{T^{1/2}}$ (mL-sec$^{-1/2}$)	$R_m \times 10^{-11}$ (1/cm)	$\Delta P \times 10^{-5}$ (N/m^2)	Temp. (°C)	$\frac{\Delta V_2 - \Delta V_1}{\Delta V_3 - \Delta V_1}$	Membrane Type	$\left[\frac{\Delta V}{T^{1/2}}\right]_{Lim.}$ (mL-sec$^{-1/2}$)
1.03	0.006	1.08	0.1565	2.74	10.34	23	0.4199	C.A.	0.1362
		2.16	0.1511						
		4.32	0.1462						
1.01	0.016	1.08	0.1714	2.07	10.34	21	0.4210	C.A.	0.1386
		2.16	0.1624						
		4.32	0.1548						
1.01	0.007	1.08	0.1775	1.87	10.34	21	0.4342	C.A.	0.1532
		2.16	0.1722						
		4.32	0.1648						
2.08	0.006	1.08	0.0828	2.24	2.76	23	0.4142	C.A.	0.0792
		2.16	0.0817						
		4.32	0.0810						
2.14	0.709	0.72	0.1014	1.51	2.76	23	0.4177	SAN	0.0897
		1.44	0.0982						
		2.88	0.0955						
2.15	0.040	0.72	0.0935	1.60	10.34	20	0.4122	C.A.	0.0884
		1.44	0.0918						
		2.88	0.0908						
		8.10	0.0900						
2.17	0.347	0.72	0.1098	1.52	4.14	23	0.4145	SAN	0.0880
		1.44	0.1034						
		2.88	0.0989						

TABLE A-8 (Continued)

BATCH CELL DATA - BSA (0.15M NaCL, 7.40 pH)

c_o (g/100 cc)	c_p (g/100 cc)	$T \times 10^{-4}$ (sec)	$\frac{\Delta V_{exp}}{T^{1/2}}$ (mL-sec$^{-1/2}$)	$R_m \times 10^{-11}$ (1/cm)	$\Delta P \times 10^{-5}$ (N/m^2)	Temp. (°C)	$\frac{\Delta V_2 - \Delta V_1}{\Delta V_3 - \Delta V_1}$	Membrane Type	$\left[\frac{\Delta V}{T^{1/2}}\right]_{Lim}$ (mL-sec$^{-1/2}$)
2.17	0.066	0.72	0.0993	3.01	6.89	23	0.4092	SAN	0.0888
		1.44	0.0960						
		2.88	0.0941						
2.18	0.045	0.72	0.1068	2.31	10.34	22	0.4336	SAN	0.0914
		1.44	0.1034						
		2.88	0.0988						
2.19	0.227	0.72	0.1036	2.13	6.89	22	0.4159	SAN	0.0883
		1.44	0.0992						
		2.88	0.0959						
5.08	0.060	1.8	0.0496	1.45	4.14	19	0.4115	C.A.	0.0455
		3.6	0.0483						
		7.2	0.0476						
5.10	0.209	1.8	0.0597	1.47	10.34	21	0.4125	SAN	0.0528
		3.6	0.0576						
		7.2	0.0563						
5.15	0.768	1.8	0.0691	1.95	6.89	23	0.4228	Polysulfone	0.0532
		3.6	0.0646						
		7.2	0.0611						
9.66	0.041	1.8	0.0347	1.67	10.34	23	0.4007	C.A.	0.0343
		3.6	0.0343						
		7.2	0.0346						
9.73	0.112	1.8	0.0351	1.54	6.89	22	0.4183	C.A.	0.0345
		3.6	0.0349						
		7.2	0.0348						

TABLE A-9

BATCH CELL DATA - BSA (0.10M SODIUM ACETATE, 4.70 pH)

c_o (g/100 cc)	c_p (g/100 cc)	$T \times 10^{-4}$ (sec)	$\frac{\Delta V_{exp}}{T^{1/2}}$ (mL-sec$^{-1/2}$)	$R_m \times 10^{-11}$ (1/cm)	$\Delta P \times 10^{-5}$ (N/m^2)	Temp. (°C)	$\frac{\Delta V_2 - \Delta V_1}{\Delta V_3 - \Delta V_1}$	Membrane Type	$\left[\frac{\Delta V}{T^{1/2}}\right]_{Lim}$ (mL-sec$^{-1/2}$)
0.51	0.011	0.72	0.1551	1.72	6.89	21	0.4296	C.A.	0.1543
		1.44	0.1563						
		2.88	0.1543						
0.50	0.010	1.08	0.1662	1.65	10.34	23	0.4205	C.A.	0.1563
		2.16	0.1639						
		4.32	0.1611						
0.93	0.003	1.08	0.1094	2.21	2.76	22	0.4167	C.A.	0.0943
		2.16	0.1052						
		4.32	0.1018						
0.93	0.002	1.08	0.1168	2.15	4.14	23	0.4330	C.A.	0.1019
		2.16	0.1136						
		4.32	0.1090						
0.93	0.007	1.08	0.1348	2.83	6.89	23	0.4207	C.A.	0.1097
		2.16	0.1279						
		4.32	0.1221						
0.93	0.007	1.08	0.1234	2.90	10.34	23	0.4258	C.A.	0.1092
		2.16	0.1200						
		4.32	0.1161						
2.07	0.004	1.08	0.0645	2.29	2.76	23	0.4343	C.A.	0.0615
		2.16	0.0644						
		4.32	0.0628						

TABLE A-9 (Continued)

BATCH CELL DATA - BSA (0.10M SODIUM ACETATE, 4.70 pH)

c_o (g/100 cc)	c_p (g/100 cc)	$T \times 10^{-4}$ (sec)	$\frac{\Delta V_{exp}}{T^{1/2}}$ (mL-sec$^{-1/2}$)	$R_m \times 10^{-11}$ (1/cm)	$\Delta P \times 10^{-5}$ (N/m^2)	Temp. (°C)	$\frac{\Delta V_2 - \Delta V_1}{\Delta V_3 - \Delta V_1}$	Membrane Type	$\left[\frac{\Delta V}{T^{1/2}}\right]_{Lim}$ (mL-sec$^{-1/2}$)
2.09	0.093	0.72	0.0834	1.72	10.34	20	0.4285	C.A.	0.0695
		1.44	0.0806						
		2.88	0.0774						
		8.10	0.0731						
2.12	0.083	0.72	0.0776	2.26	4.14	23	0.4139	SAN	0.0642
		1.44	0.0737						
		2.88	0.0709						
2.13	0.014	0.72	0.0760	3.33	6.89	23	0.4176	SAN	0.0683
		1.44	0.0739						
		2.88	0.0721						
2.14	0.237	0.72	0.0748	3.05	2.76	23	0.4159	SAN	0.0644
		1.44	0.0718						
		2.88	0.0696						
2.14	0.019	0.72	0.0808	4.08	10.34	22	0.4308	SAN	0.0718
		1.44	0.0789						
		2.88	0.0761						
2.17	0.123	0.72	0.0822	1.74	6.89	22	0.4298	SAN	0.0752
		1.44	0.0808						
		2.88	0.0785						
4.88	0.105	1.8	0.0383	1.52	4.14	19	0.4174	C.A.	0.0335
		3.6	0.0369						
		7.2	0.0359						

TABLE A-9 (Continued)

BATCH CELL DATA - BSA (0.10M SODIUM ACETATE, 4.70 pH)

c_o (g/100 cc)	c_p (g/100 cc)	T x 10^{-4} (sec)	$\frac{\Delta V_{exp}}{T^{1/2}}$ (mL-$sec^{-1/2}$)	R_m x 10^{-11} (1/cm)	ΔP x 10^{-5} (N/m^2)	Temp. (°C)	$\frac{\Delta V_2 - \Delta V_1}{\Delta V_3 - \Delta V_1}$	Membrane Type	$\left[\frac{\Delta V}{T^{1/2}}\right]_{Lim}$ (mL-$sec^{-1/2}$)
4.90	0.058	1.8	0.0510	2.96	10.34	21	0.4288	SAN	0.0422
		3.6	0.0487						
		7.2	0.0465						
4.92	0.075	1.8	0.0465	3.61	6.89	23	0.4251	Polysulfone	0.0398
		3.6	0.0447						
		7.2	0.0431						
4.93	0.034	1.8	0.0437	2.02	10.34	20	0.4260	C.A.	0.0404
		3.6	0.0430						
		7.2	0.0420						
9.52	0.059	1.8	0.0336	1.80	6.89	22	0.4158	C.A.	0.0264
		3.6	0.0315						
		7.2	0.0300						
9.58	0.038	1.8	0.0275	1.76	10.34	23	0.4094	C.A.	0.0258
		3.6	0.0269						
		7.2	0.0267						

TABLE A-10

BATCH CELL EXPERIMENTS - CARBOWAX 20M (7.5 pH SOLUTION)

c_o (g/100 cc)	c_p (g/100 cc)	T x 10^{-4} (sec)	$\frac{\Delta V_{exp}}{T^{1/2}}$ (mL-sec$^{-1/2}$)	R_m x 10^{-11} (1/cm)	ΔP x 10^{-5} (N/m^2)	Temp. (°C)	$\frac{\Delta V_2 - \Delta V_1}{\Delta V_3 - \Delta V_1}$	Membrane Type	$\left[\frac{\Delta V}{T^{1/2}}\right]_{Lim}$ (mL-sec$^{-1/2}$)
0.260	--	1.08	0.2306	--	3.45	20	0.4111	C.A.	0.2457
		2.16	0.2339						
		4.32	0.2372						
		7.56	0.2407						
0.266	0.029	1.08	0.1704	2.11	3.45	20	0.4079	Abcor WRP	0.1916
		2.16	0.1747						
		4.32	0.1791						
		7.92	0.1851						
0.266	0.056	1.08	0.2152	2.18	6.89	20	0.4081	Abcor WRP	0.2311
		2.16	0.2186						
		4.32	0.2226						
		9.00	0.2260						
0.520	0.096	1.08	0.1419	--	3.45	20	0.4149	C.A.	0.1418
		2.16	0.1424						
		4.32	0.1426						
		8.64	0.1413						
0.531	0.047	1.08	0.1113	2.35	3.45	20	0.4105	Abcor WRP	0.1180
		2.16	0.1129						
		4.32	0.1146						
		8.64	0.1157						
0.531	0.041	1.08	0.1406	3.69	6.89	20	0.4168	Abcor WRP	0.1414
		2.16	0.1410						
		4.32	0.1409						
		7.92	0.1412						

TABLE A-10 (Continued)

BATCH CELL EXPERIMENTS - CARBOWAX 20M (7.5 pH SOLUTION)

c_o (g/100 cc)	c_p (g/100 cc)	$T \times 10^{-4}$ (sec)	$\frac{\Delta V_{exp}}{T^{1/2}}$ (mL-sec$^{-1/2}$)	$R_m \times 10^{-11}$ (1/cm)	$\Delta P \times 10^{-5}$ (N/m^2)	Temp. (°C)	$\frac{\Delta V_2 - \Delta V_1}{\Delta V_3 - \Delta V_1}$	Membrane Type	$\left[\frac{\Delta V}{T^{1/2}}\right]_{Lim}$ (mL-sec$^{-1/2}$)
0.781	0.144	1.08	0.1066	--	3.45	20	0.4180	C.A.	0.1074
		2.14	0.1068						
		4.32	0.1065						
		7.56	0.1074						
0.797	0.060	1.08	0.1103	1.46	3.45	20	0.4121	Abcor WRP	0.0968
		2.16	0.1062						
		4.32	0.1036						
		7.92	0.1018						
0.797	0.54	1.08	0.1068	3.51	6.89	20	0.4126	Abcor WRP	0.1041
		2.16	0.1061						
		4.32	0.1057						
		9.00	0.1049						
1.04	0.165	1.08	0.1025	--	3.45	20	0.4209	C.A.	0.0943
		2.16	0.1005						
		4.32	0.0983						
		8.64	0.0972						
1.06	0.075	1.08	0.0726	2.98	3.45	20	0.4194	Abcor WRP	0.0709
		2.16	0.0724						
		4.32	0.0719						
		8.64	0.0714						
1.06	0.057	1.08	0.0914	4.17	6.89	20	0.4253	Abcor WRP	0.0890
		2.16	0.0911						
		4.32	0.0897						
		7.92	0.0902						

TABLE A-11

BATCH CELL EXPERIMENTS - CMC (7.5 pH SOLUTION), LONG-TERM EXPERIMENTS

c_o (g/100 cc)	c_p (g/100 cc)	$T \times 10^{-4}$ (sec)	$\frac{\Delta V_{exp}}{T^{1/2}}$ (mL-sec$^{-1/2}$)	$R_m \times 10^{-11}$ (1/cm)	$\Delta P \times 10^{-5}$ (N/m^2)	Temp. (°C)	$\frac{\Delta V_2 - \Delta V_1}{\Delta V_3 - \Delta V_1}$	Membrane Type	$\left[\frac{\Delta V}{T^{1/2}}\right]_{Lim}$ (mL-sec$^{-1/2}$)
0.39	0.030	7.2	0.2361	--	11.72	23	--	C.A.	--
0.53	0.025	7.2	0.1681	--	6.89	22	--	C.A.	--
0.53	0.026	7.2	0.2153	--	15.86	20	--	C.A.	--
0.81	0.040	7.2	0.1616	2.31	11.72	24	--	C.A.	--
1.07	0.060	7.2	0.1111	--	6.89	22	--	C.A.	--
1.07	0.064	7.2	0.1457	--	15.86	20	--	C.A.	--
1.49	0.116	7.2	0.1124	3.13	11.72	19	--	C.A.	--
2.06	0.059	7.2	0.0701	--	6.89	20	--	C.A.	--
2.06	0.120	7.2	0.0883	3.33	11.72	23	--	C.A.	--
2.06	0.076	7.2	0.0954	--	15.86	18	--	C.A.	--
2.78	0.091	7.2	0.0790	--	15.86	18	--	C.A.	--
2.97	0.663	7.2	0.0894	--	11.72	23	--	C.A.	--
2.97	0.144	7.2	0.0706	3.32	11.72	14	--	C.A.	--
6.03	0.274	7.2	0.0392	3.33	11.72	22	--	C.A.	--

TABLE A-12

BATCH CELL EXPERIMENTS - CMC (7.5 pH SOLUTION)

c_o (g/100 cc)	c_p (g/100 cc)	T x 10^{-4} (sec)	$\frac{\Delta V_{exp}}{T^{1/2}}$ (mL-$sec^{-1/2}$)	R_m x 10^{-11} (1/cm)	ΔP x 10^{-5} (N/m^2)	Temp. (°C)	$\frac{\Delta V_2 - \Delta V_1}{\Delta V_3 - \Delta V_1}$	Membrane Type	$\left[\frac{\Delta V}{T^{1/2}}\right]_{Lim}$ (mL-$sec^{-1/2}$)
0.53	0.027	1.8	0.1893	2.80	11.72	22	0.4131	C.A.	0.1910
		3.6	0.1896						
		7.2	0.1902						
0.53	0.029	1.8	0.2279	2.19	17.24	21	0.4140	C.A.	0.2207
		3.6	0.2257						
		7.2	0.2243						
1.07	0.050	1.8	0.1225	2.87	11.72	22	0.4130	C.A.	0.1276
		3.6	0.1239						
		7.2	0.1251						
1.07	0.046	1.8	0.1519	2.38	17.24	21	0.4187	C.A.	0.1499
		3.6	0.1517						
		7.2	0.1508						
2.06	0.105	1.8	0.0776	1.60	11.72	19	0.4264	C.A.	0.0826
		3.6	0.0797						
		7.2	0.0799						
2.06	0.094	1.8	0.0997	3.04	17.24	21	0.4135	C.A.	0.0960
		3.6	0.0985						
		7.2	0.0979						

TABLE A-12 (Continued)

BATCH CELL EXPERIMENTS - CMC (7.5 pH SOLUTION)

c_o (g/100 cc)	c_p (g/100 cc)	T x 10^{-4} (sec)	$\frac{\Delta V_{exp}}{T^{1/2}}$ (mL-sec$^{-1/2}$)	R_m x 10^{-11} (1/cm)	ΔP x 10^{-5} (N/m^2)	Temp. (°C)	$\frac{\Delta V_2 - \Delta V_1}{\Delta V_3 - \Delta V_1}$	Membrane Type	$\left[\frac{\Delta V}{T^{1/2}}\right]_{Lim}$ (mL-sec$^{-1/2}$)
2.78	0.233	1.8	0.0675	1.66	11.72	19	0.4206	C.A.	0.0684
		3.6	0.0680						
		7.2	0.0679						
2.78	0.112	1.8	0.0794	4.29	17.24	21	0.4118	C.A.	0.0775
		3.6	0.0787						
		7.2	0.0785						
4.08	0.158	1.8	0.0491	1.77	11.72	22	0.4132	SAN	0.0504
		3.6	0.0494						
		7.2	0.0498						
4.08	0.157	1.8	0.0610	3.28	17.24	22	0.4114	SAN	0.0613
		3.6	0.0610						
		7.2	0.0612						
6.03	0.287	1.8	0.0345	2.66	11.72	22	0.4083	SAN	0.0360
		3.6	0.0348						
		7.2	0.0353						
6.03	0.248	1.8	0.0436	2.02	17.24	22	0.4318	SAN	0.0455
		3.6	0.0446						
		7.2	0.0444						

TABLE A-13

BATCH CELL EXPERIMENTS - PVA (7.5 pH SOLUTION)

c_o (g/100 cc)	c_p (g/100 cc)	$T \times 10^{-4}$ (sec)	$\frac{\Delta V_{exp}}{T^{1/2}}$ (mL-sec$^{-1/2}$)	$R_m \times 10^{-11}$ (1/cm)	$\Delta P \times 10^{-5}$ (N/m^2)	Temp. (°C)	$\frac{\Delta V_2 - \Delta V_1}{\Delta V_3 - \Delta V_1}$	Membrane Type	$\left[\frac{\Delta V}{T^{1/2}}\right]_{Lim}$ (mL-sec$^{-1/2}$)
0.070	0.008	1.08	0.2201	--	1.38	19	0.4037	HFM-180	0.1778
		2.16	0.2063						
		4.32	0.1988						
		7.56	0.1940						
0.070	0.010	1.03	0.2877	--	2.07	19	0.4270	HFM-180	0.1939
		2.16	0.2583						
		4.32	0.2393						
		8.64	0.2266						
0.070	0.002	1.08	0.2271	--	2.76	19	0.4100	HFM-180	0.2038
		2.16	0.2192						
		4.32	0.2146						
		9.00	0.2125						
0.098	0.12	1.08	0.2075	--	3.45	19	0.4123	HFM-180	0.1767
		2.16	0.1981						
		4.32	0.1918						
		8.08	0.1882						
0.098	0.005	1.08	0.2231	0.21	4.14	24-30	0.4140	HFM-180	0.2320
		2.16	0.2266						
		3.24	0.2297						
		4.32	0.2292						
		7.92	0.2266						

TABLE A-13 (Continued)

BATCH CELL EXPERIMENTS - PVA (7.5 pH SOLUTION)

c_o (g/100 cc)	c_p (g/100 cc)	$T \times 10^{-4}$ (sec)	$\frac{\Delta V_{exp}}{T^{1/2}}$ (mL-sec$^{-1/2}$)	$R_m \times 10^{-11}$ (1/cm)	$\Delta P \times 10^{-5}$ (N/m^2)	Temp. (°C)	$\frac{\Delta V_2 - \Delta V_1}{\Delta V_3 - \Delta V_1}$	Membrane Type	$\left[\frac{\Delta V}{T^{1/2}}\right]_{Lim}$ (mL-sec$^{-1/2}$)
0.098	0.004	1.08	0.2264	0.36	5.52	25-29	0.4126	HFM-180	0.2241
		2.16	0.2258						
		3.24	0.2261						
		4.32	0.2259						
		7.92	0.2243						
0.098	0.001	1.08	0.1917	3.45	10.34	24-27	0.4035	HFM-180	0.1985
		2.16	0.1924						
		3.24	0.1943						
		4.32	0.1955						
0.133	0.020	1.08	0.2073	--	1.38	19	0.4170	HFM-180	0.1279
		2.16	0.1843						
		4.32	0.1675						
		7.56	0.1580						
0.133	0.022	1.03	0.1999	--	2.07	19	0.4280	HFM-180	0.1366
		2.16	0.1801						
		4.32	0.1671						
		8.64	0.1587						
0.133	0.11	1.08	0.1873	--	2.76	19	0.4175	HFM-180	0.1470
		2.16	0.1758						
		4.32	0.1671						
		9.00	0.1610						

TABLE A-13 (Continued)

BATCH CELL EXPERIMENTS - PVA (7.5 pH SOLUTION)

C_o (g/100 cc)	C_p (g/100 cc)	$T \times 10^{-4}$ (sec)	$\frac{\Delta V_{exp}}{T^{1/2}}$ (mL-sec$^{-1/2}$)	$R_m \times 10^{-11}$ (1/cm)	$\Delta P \times 10^{-5}$ (N/m^2)	Temp. (°C)	$\frac{\Delta V_2 - \Delta V_1}{\Delta V_3 - \Delta V_1}$	Membrane Type	$\left[\frac{\Delta V}{T^{1/2}}\right]_{Lim}$ (mL-sec$^{-1/2}$)
0.185	0.013	1.08	0.1488	--	3.45	19	0.4201	HFM-180	0.1289
		2.16	0.1433						
		4.32	0.1385						
		8.08	0.1364						
0.185	0.011	1.08	0.1663	0.17	4.14	24-30	0.4183	HFM-180	0.1568
		2.16	0.1645						
		3.24	0.1640						
		4.32	0.1625						
		7.92	0.1591						
0.185	0.014	1.08	0.1693	0.41	5.52	25-29	0.4110	HFM-180	0.1601
		2.16	0.1666						
		3.24	0.1655						
		4.32	0.1654						
		7.92	0.1630						
0.185	0.006	1.08	0.1456	5.61	10.34	24-27	0.4046	HFM-180	0.1401
		2.16	0.1432						
		3.24	0.1431						
		4.32	0.1431						
0.535	0.020	1.08	0.0849	--	3.45	19	0.4180	HFM-180	0.0725
		2.16	0.0817						
		4.32	0.0791						
		7.92	0.0768						

TABLE A-13 (Continued)

BATCH CELL EXPERIMENTS - PVA (7.5 pH SOLUTION)

c_o (g/100 cc)	c_p (g/100 cc)	$T \times 10^{-4}$ (sec)	$\frac{\Delta V_{exp}}{T^{1/2}}$ (mL-sec$^{-1/2}$)	$R_m \times 10^{-11}$ (1/cm)	$\Delta P \times 10^{-5}$ (N/m^2)	Temp. (°C)	$\frac{\Delta V_2 - \Delta V_1}{\Delta V_3 - \Delta V_1}$	Membrane Type	$\left[\frac{\Delta V}{T^{1/2}}\right]_{Lim}$ (mL-sec$^{-1/2}$)
0.535	0.017	1.08	0.0961	--	6.89	19	0.4190	HFM-180	0.0873
		2.16	0.0938						
		4.32	0.0917						
		8.49	0.0904						
0.535	0.019	1.08	0.1017	--	10.34	19	0.4011	HFM-180	0.0938
		2.16	0.0985						
		4.32	0.0978						
		7.56	0.0968						
0.980	0.075	2.16	0.0552	1.81	2.76	24-29	--	HFM-180	0.543
		4.34	0.0557						
		7.92	0.0545						
0.981	0.042	1.08	0.0584	--	3.45	19.	0.4196	HFM-180	0.0504
		2.16	0.0562						
		4.32	0.0543						
		7.92	0.0534						

TABLE A-13 (Continued)

BATCH CELL EXPERIMENTS - PVA (7.5 pH SOLUTION)

c_o (g/100 cc)	c_p (g/100 cc)	$T \times 10^{-4}$ (sec)	$\frac{\Delta V_{exp}}{T^{1/2}}$ (mL-sec$^{-1/2}$)	$R_m \times 10^{-11}$ (1/cm)	$\Delta P \times 10^{-5}$ (N/m^2)	Temp. (°C)	$\frac{\Delta V_2 - \Delta V_1}{\Delta V_3 - \Delta V_1}$	Membrane Type	$\left[\frac{\Delta V}{T^{1/2}}\right]_{Lim}$ (mL-sec$^{-1/2}$)
0.0981	0.032	1.08	0.0684	--	6.89	19	0.4190	HFM-180	0.0609
		2.16	0.0666						
		4.32	0.0650						
		8.49	0.0633						
0.981	0.041	1.08	0.0776	--	10.34	19	0.4187	HFM-180	0.0667
		2.16	0.0747						
		4.32	0.0723						
		7.56	0.0707						
1.85	0.120	2.16	0.0390	1.76	2.76	24-29	--	HFM-180	0.0365
		4.34	0.0386						
		7.92	0.0377						

TABLE A-14

BATCH CELL DATA - STYRENE BUTADIENE LATEX (8.5 pH SOLUTION)

c_o (g/100 cc)	$\Delta P \times 10^{-5}$ (N/m^2)	ΔV (mL)	$T^{1/2}$ ($sec^{1/2}$)	$\mu \times 10^4$ $\frac{(N\text{-}sec)}{m^2}$	$R_m \times 10^{-11}$ (1/cm)
0.01	2.76	7.768	17.32	9.04	2.16
		14.98	24.49		C.A.
		22.27	30.00		
		29.40	34.64		
		43.59	42.43		
		84.64	60.00		
		164.5	84.85		
		310.5	120.0		
		622.5	180.0		
		1123.5	263.2		
0.10	2.76	6.900	17.32	9.14	2.16
		13.36	24.49		C.A.
		19.35	30.00		
		24.86	34.64		
		35.07	42.43		
		61.64	60.00		
		107.5	84.85		
		188.9	120.0		
		261.8	147.0		
		326.3	169.7		
		384.7	189.7		
		437.0	207.8		
		659.0	281.4		
0.10	4.14	9.751	17.32	9.14	2.03
		18.34	24.49		C.A.
		26.25	30.00		
		33.71	34.64		
		47.66	42.43		
		84.25	60.00		
		147.3	84.85		
		256.2	120.0		
		442.3	169.7		
		560.0	199.0		
1.03	5.52	10.62	17.32	9.11	1.57
		18.23	24.49		C.A.
		24.75	30.00		
		30.59	34.64		
		40.88	42.43		
		65.38	60.00		
		101.1	84.85		
		152.1	120.0		
		224.7	169.7		
		279.5	207.8		
		396.3	287.7		

TABLE A-14 (Continued)

BATCH CELL DATA - STYRENE BUTADIENE LATEX (8.5 pH SOLUTION)

c_o (g/100 cc)	$\Delta P \times 10^{-5}$ (N/m^2)	ΔV (mL)	$T^{1/2}$ ($sec^{1/2}$)	$\mu \times 10^4$ $\frac{(N\text{-}sec)}{m^2}$	$R_m \times 10^{-11}$ (1/cm)
1.59	5.52	17.06	30.00	8.74	2.11
		28.53	42.43		C.A.
		46.36	60.00		
		73.15	84.85		
		111.5	120.0		
		164.3	169.7		
		280.3	281.4		
3.24	1.38	4.352	30.00	9.14	1.89
		7.236	42.43		C.A.
		11.57	60.00		
		18.18	84.85		
		28.03	120.0		
		42.89	169.7		
		74.70	261.5		
3.24	2.76	8.746	30.00	9.14	1.65
		14.17	42.43		C.A.
		22.72	60.00		
		35.87	84.85		
		55.39	120.0		
		83.60	169.7		
		136.5	261.5		
3.24	4.14	12.08	30.00	9.14	1.99
		19.54	42.43		C.A.
		31.18	60.00		
		47.83	84.85		
		71.65	120.0		
		97.68	158.7		
		172.0	268.3		
3.18	5.52	13.86	30.00	9.14	1.72
		22.16	42.43		C.A.
		34.86	60.00		
		52.91	84.85		
		78.78	120.0		
		131.1	191.3		
		207.1	290.9		

TABLE A-14 (Continued)

BATCH CELL DATA - STYRENE BUTADIENE LATEX (8.5 pH SOLUTION)

c_o (g/100 cc)	$\Delta P \times 10^{-5}$ (N/m^2)	ΔV (mL)	$T^{1/2}$ ($sec^{1/2}$)	$\mu \times 10^4$ $\frac{(N\text{-}sec)}{m^2}$	$R_m \times 10^{-11}$ (1/cm)
3.24	6.89	15.50	30.00	9.14	1.99
		24.63	42.43		C.A.
		38.53	60.00		
		59.07	84.85		
		87.90	120.0		
		127.8	169.7		
		195.6	258.1		
7.10	5.52	4.592	17.32	8.71	1.71
		7.407	24.49		
		9.534	30.00		
		11.36	34.64		
		14.35	42.43		
		21.05	60.00		
		30.34	84.85		
		48.48	134.2		
		61.89	169.7		
		78.76	216.3		
		105.6	287.7		
9.87	2.76	9.780	17.32	9.14	0.22 μ
		13.96	24.49		Millipore
		17.13	30.00		Filter
		19.91	34.64		
		24.44	42.43		
		34.97	60.00		
		50.81	84.85		
		73.91	120.0		
		116.7	180.0		
		142.1	216.3		
9.87	2.76	3.310	17.32	8.74	0.224
		4.988	24.49		
		6.401	30.00		0.025 μ
		7.649	34.64		Millipore
		9.763	42.43		
		14.74	60.00		
		22.04	84.85		
		33.06	120.0		
		46.61	158.7		
		64.80	207.8		
		97.41	293.9		
14.48	5.52	5.454	30.00	8.33	1.90
		8.005	42.43		C.A.
		11.64	60.00		
		24.15	120.0		
		43.74	207.8		
		64.10	297.0		

TABLE A-15

PARALLEL PLATE EXPERIMENTS - LATEX (8.5 pH SOLUTION)

$\Delta P = 2.76 \times 10^5$ N/m^2 $\quad \overline{R}_m = 4.94 \times 10^{10}$ 1/cm

μ Solvent $= 9.11 \times 10^{-4} \frac{\text{N-sec}}{\text{m}^2}$ $\quad T = 23.9°C$

Axial flow rate = 0.505 liters/sec

c_o Concentration of Feed Tank (g/100 cc)	c_p (g/100 cc)	T x 10^{-3} (seconds)	Port Number	$\lvert v_w \rvert$ x 10^3 (cm/sec)	COMMENTS:
0.432	0.0	0.0	5	6.00	Not all ports measured. Permeate returned to feed tank.
			10	5.98	
			15	6.05	
			20	6.71	
			25	5.86	
			30	6.18	
--	0.0	4.20	5	1.58	
			10	1.22	
			15	1.30	
			20	1.20	
			25	1.25	
			30	1.23	
--	0.0	9.72	5	1.12	
			10	0.862	
			15	0.951	
			20	0.970	
			25	0.943	
			30	0.957	
0.252	0.0	22.5	5	0.844	
			10	0.618	
			15	0.704	
			20	0.731	
			25	0.703	
			30	0.729	
--	0.0	35.7	5	0.775	
			10	0.594	
			15	0.641	
			20	0.655	
			25	0.654	
			30	0.677	
0.253	0.0	42.0	5	0.758	
			10	0.560	
			15	0.632	
			20	0.650	
			25	0.641	
			30	0.660	

TABLE A-16

PARALLEL PLATE EXPERIMENTS - LATEX (8.5 pH SOLUTION)

$\Delta P = 2.76 \times 10^5$ N/m^2 $\quad \overline{R}_m = 4.93 \times 10^{10}$ 1/cm

μ Solvent $= 9.14 \times 10^{-4} \frac{\text{N-sec}}{\text{m}^2}$ $\quad T = 23.9°C$

Axial flow rate = 0.618 liters/sec

c_o Concentration of Feed Tank (g/100 cc)	c_p (g/100 cc)	T x 10^{-3} (seconds)	Port Number	$\lvert v_w \rvert$ x 10^3 (cm/sec)	COMMENTS:
--	0.0	0.0	5	6.00	Not all ports measured. Permeate returned to feed tank
			10	5.98	
			15	6.05	
			20	6.71	
			25	5.86	
			30	6.18	
0.356	0.0	5.40	5	1.75	
			10	1.61	
			15	1.68	
			20	1.59	
			25	1.61	
			30	1.53	
--	0.0	9.00	5	1.20	
			10	1.11	
			15	1.18	
			20	1.17	
			25	1.18	
			30	1.15	
0.340	0.0	17.4	5	1.05	
			10	0.903	
			15	0.942	
			20	0.903	
			25	0.952	
			30	0.962	
0.311	0.0	21.9	5	1.01	
			10	0.805	
			15	0.893	
			20	0.873	
			25	0.913	
			30	0.932	

TABLE A-17

PARALLEL PLATE EXPERIMENTS - LATEX (8.5 pH SOLUTION)

$\Delta P = 3.59 \times 10^5$ N/m^2 $\quad \overline{R}_m = 2.38 \times 10^{11}$ 1/cm

μ Solvent $= 9.88 \times 10^{-4} \frac{\text{N-sec}}{\text{m}^2}$ $\quad$ T = 20.6°C

Axial flow rate = 0.087 liters/sec

c_o Concentration of Feed Tank (g/100 cc)	c_p (g/100 cc)	T x 10^{-3} (seconds)	Port Number	$\lvert v_w \rvert$ x 10^3 (cm/sec)	COMMENTS:
1.09	0.0	0.0	2	1.53	Not all ports measured. Permeate returned to feed tank
			5	1.75	
			8	1.58	
			11	1.37	
			14	1.53	
			17	1.63	
			20	1.43	
			23	1.58	
			26	1.45	
			29	1.46	
			32	1.46	
0.984	0.0	21.6	2	0.460	
			5	0.406	
			8	0.429	
			11	0.360	
			14	0.356	
			17	0.413	
			20	0.368	
			23	0.385	
			26	0.393	
			29	0.360	
			32	0.356	
0.910	0.0	32.4	2	0.294	
			5	0.251	
			8	0.192	
			11	0.215	
			14	0.211	
			17	0.266	
			20	0.242	
			23	0.239	
			26	0.258	
			29	0.225	
			32	0.227	

TABLE A-17 (Continued)

PARALLEL PLATE EXPERIMENTS - LATEX (8.5 pH SOLUTION)

$\Delta P = 3.59 \times 10^5$ N/m^2 $\quad \overline{R_m} = 2.38 \times 10^{11}$ 1/cm

μ Solvent $= 9.88 \times 10^{-4} \frac{\text{N-sec}}{\text{m}^2}$ $\quad T = 20.6°C$

Axial flow rate = 0.087 liters/sec

c_o Concentration of Feed Tank (g/100 cc)	c_p (g/100 cc)	T x 10^{-3} (seconds)	Port Number	$\lvert v_w \rvert$ x 10^3 (cm/sec)	COMMENTS:
0.825	0.0	61.2	2	0.235	
			5	0.142	
			8	0.142	
			11	0.133	
			14	0.139	
			17	0.166	
			20	0.163	
			23	0.143	
			26	0.195	
			29	0.144	
			32	0.152	
0.766	0.0	82.8	2	0.172	
			5	0.083	
			8	0.116	
			11	0.113	
			14	0.123	
			17	0.145	
			20	0.138	
			23	0.112	
			26	0.160	
			29	0.117	
			32	0.131	
0.741	0.0	90.0	2	0.156	
			5	0.082	
			8	0.108	
			11	0.114	
			14	0.112	
			17	0.139	
			20	0.130	
			23	0.099	
			26	0.153	
			29	0.099	
			32	0.124	

TABLE A-17 (Continued)

PARALLEL PLATE EXPERIMENTS - LATEX (8.5 pH SOLUTION)

$\Delta P = 3.59 \times 10^5$ N/m^2 $\quad \overline{R_m} = 2.38 \times 10^{11}$ 1/cm

μ Solvent $= 9.88 \times 10^{-4} \frac{\text{N-sec}}{\text{m}^2}$ $\quad T = 20.6°C$

Axial flow rate = 0.087 liters/sec

c_o Concentration of Feed Tank (g/100 cc)	c_p (g/100 cc)	T x 10^{-3} (seconds)	Port Number	$\lvert v_w \rvert$ x 10^3 (cm/sec)	COMMENTS:
0.836	0.0	120.6	2	0.266	Axial flow rate changed from 0.087 l/sec to 0.199 l/sec at T = 97.2 x 10^3 seconds
			5	0.170	
			8	0.149	
			11	0.200	
			14	0.201	
			17	0.213	
			20	0.205	
			23	0.143	
			26	0.151	
			29	0.150	
			32	0.137	
0.823	0.0	165.6	2	0.206	
			5	0.144	
			8	0.122	
			11	0.141	
			14	0.142	
			17	0.191	
			20	0.150	
			23	0.111	
			26	0.109	
			29	0.093	
			32	0.111	

TABLE A-17 (Continued)

PARALLEL PLATE EXPERIMENTS - LATEX (8.5 pH SOLUTION)

$\Delta P = 3.59 \times 10^5$ N/m^2 $\quad \overline{R_m} = 2.38 \times 10^{11}$ 1/cm

μ Solvent $= 9.88 \times 10^{-4} \frac{\text{N-sec}}{\text{m}^2}$ $\quad T = 20.6°C$

Axial flow rate = 0.087 liters/sec

c_o Concentration of Feed Tank (g/100 cc)	c_p (g/100 cc)	T x 10^{-3} (seconds)	Port Number	$\lvert v_w \rvert$ x 10^3 (cm/sec)	COMMENTS:
0.808	0.0	198.0	2	0.169	
			5	0.140	
			8	0.120	
			11	0.133	
			14	0.127	
			17	0.153	
			20	0.125	
			23	0.097	
			26	0.093	
			29	0.093	
			32	0.109	
0.790	212.4		2	0.161	
			5	0.136	
			8	0.115	
			11	0.116	
			14	0.124	
			17	0.145	
			20	0.118	
			23	0.097	
			26	0.088	
			29	0.090	
			32	0.109	

TABLE A-18

PARALLEL PLATE EXPERIMENTS - LATEX (8.5 pH SOLUTION)

$\Delta P = 3.45 \times 10^5$ N/m^2 $\quad \overline{R_m} = 2.38 \times 10^{11}$ 1/cm

μ Solvent $= 9.95 \times 10^{-4} \frac{\text{N-sec}}{\text{m}^2}$ $\quad T = 20.3°C$

Axial flow rate = 0.198 liters/sec

c_o Concentration of Feed Tank (g/100 cc)	c_p (g/100 cc)	T x 10^{-3} (seconds)	Port Number	$\lvert v_w \rvert$ x 10^3 (cm/sec)	COMMENTS:
1.49	0.0	0.0	Not measured		Not all ports measured. Permeate not returned to feed tank.
1.50	0.0	7.20	2	0.559	
			5	0.446	
			8	0.361	
			11	0.454	
			14	0.439	
			17	0.466	
			20	0.448	
			23	0.440	
			26	0.456	
			29	0.464	
			32	0.328	
1.57	0.0	18.0	2	0.348	
			5	0.274	
			8	0.227	
			11	0.288	
			14	0.270	
			17	0.294	
			20	0.293	
			23	0.276	
			26	0.283	
			29	0.289	
			32	0.189	

TABLE A-18 (Continued)

PARALLEL PLATE EXPERIMENTS - LATEX (8.5 pH SOLUTION)

$\Delta P = 3.45 \times 10^5$ N/m^2 $\quad \overline{R_m} = 2.38 \times 10^{11}$ 1/cm

μ Solvent $= 9.95 \times 10^{-4} \frac{\text{N-sec}}{\text{m}^2}$ $\quad T = 20.3°C$

Axial flow rate = 0.198 liters/sec

c_o Concentration of Feed Tank (g/100 cc)	c_p (g/100 cc)	T x 10^{-3} (seconds)	Port Number	$\lvert v_w \rvert$ x 10^3 (cm/sec)	COMMENTS:
1.52	0.0	28.8	2	0.314	
			5	0.228	
			8	0.168	
			11	0.224	
			14	0.208	
			17	0.244	
			20	0.234	
			23	0.216	
			26	0.222	
			29	0.228	
			32	0.145	
1.53	0.0	39.6	2	0.289	
			5	0.221	
			8	0.151	
			11	0.185	
			14	0.178	
			17	0.218	
			20	0.200	
			23	0.187	
			26	0.185	
			29	0.195	
			32	0.120	

TABLE A-19

PARALLEL PLATE EXPERIMENTS - LATEX (8.5 pH SOLUTION)

$\Delta P = 3.45 \times 10^5$ N/m^2 $\quad \overline{R_m} = 2.38 \times 10^{11}$ 1/cm

μ Solvent $= 9.88 \times 10^{-4} \frac{\text{N-sec}}{\text{m}^2}$ $\quad T = 20.6°C$

Axial flow rate = 0.713 liters/sec

c_o Concentration of Feed Tank (g/100 cc)	c_p (g/100 cc)	T x 10^{-3} (seconds)	Port Number	$\lvert v_w \rvert$ x 10^3 (cm/sec)	COMMENTS:
1.46	0.0	0.0	Not measured		Not all ports measured. Permeate not returned to feed tank.
1.47	0.0	7.20	2	0.828	
			5	0.744	
			8	0.472	
			11	0.433	
			17	0.504	
			20	0.531	
			23	0.492	
			26	0.419	
			29	0.527	
			32	0.339	
1.54	0.0	18.0	2	0.507	
			5	0.646	
			8	0.470	
			11	0.342	
			17	0.441	
			20	0.468	
			23	0.412	
			26	0.313	
			29	0.440	
			32	0.280	
1.65	0.0	28.8	2	0.475	
			5	0.631	
			8	0.451	
			11	0.330	
			17	0.421	
			20	0.447	
			23	0.380	
			26	0.282	
			29	0.419	
			32	0.265	

TABLE A-19 (Continued)

PARALLEL PLATE EXPERIMENTS - LATEX (8.5 pH SOLUTION)

$\Delta P = 3.45 \times 10^5$ N/m^2 $\quad \overline{R_m} = 2.38 \times 10^{11}$ 1/cm

μ Solvent $= 9.88 \times 10^{-4} \frac{\text{N-sec}}{\text{m}^2}$ $\quad T = 20.6°C$

Axial flow rate = 0.713 liters/sec

c_o Concentration of Feed Tank (g/100 cc)	c_p (g/100 cc)	T x 10^{-3} (seconds)	Port Number	$\lvert v_w \rvert$ x 10^3 (cm/sec)	COMMENTS:
1.76	0.0	39.6	2	0.433	
			5	0.549	
			8	0.478	
			11	0.332	
			17	0.459	
			20	0.434	
			23	0.371	
			26	0.273	
			29	0.401	
			32	0.258	
1.76	0.0	79.2	2	0.417	
			5	0.493	
			8	0.435	
			11	0.282	
			17	0.459	
			20	0.433	
			23	0.361	
			26	0.245	
			29	0.395	
			32	0.249	

TABLE A-20

PARALLEL PLATE EXPERIMENTS - LATEX (7.5 pH SOLUTION)

$\Delta P = 3.52 \times 10^5$ N/m^2 $\quad \overline{R}_m = 5.67 \times 10^{10}$ 1/cm

μ Solvent $= 10.10 \times 10^{-4} \frac{\text{N-sec}}{\text{m}^2}$ $\quad$ T = 19.7°C

Axial flow rate = 0.190 liters/sec

c_o Concentration of Feed Tank (g/100 cc)	c_p (g/100 cc)	T x 10^{-3} (seconds)	Port Number	$\lvert v_w \rvert$ x 10^3 (cm/sec)	COMMENTS:
0.595	--	0.0	2	7.97	Permeate returned
			5	6.59	to feed tank.
			8	6.54	
			11	6.11	Membrane blinded
			14	5.09	
			17	6.77	
			21	6.43	
			23	6.11	
			26	4.81	
0.576	0.021	21.3	2	0.0121	
			5	0.0	
			8	0.1280	
			11	0.0385	
			14	0.0	
			17	0.0	
			20	0.489	
			23	0.0087	
			26	0.0169	
			29	0.0233	
			32	0.0100	
0.576	0.022	42.0	2	0.0099	
			5	0.0	
			8	0.1210	
			11	0.0529	
			14	0.0	
			17	0.0	
			20	0.0404	
			23	0.0207	
			26	0.0126	
			29	0.336	
			32	0.0104	

TABLE A-21

PARALLEL PLATE EXPERIMENTS - PVA (7.5 pH SOLUTION)

$\Delta P = 3.45 \times 10^5$ N/m^2 $\quad \overline{R_m} = 2.45 \times 10^{11}$ 1/cm

μ Solvent $= 9.81 \times 10^{-4} \frac{\text{N-sec}}{\text{m}^2}$ $\quad T = 21.1°C$

Axial flow rate = 0.631 liters/sec

c_o Concentration of Feed Tank (g/100 cc)	c_p (g/100 cc)	T x 10^{-3} (seconds)	Port Number	$\lvert v_w \rvert$ x 10^3 (cm/sec)	COMMENTS:
0.092	--	0.0	2	1.37	Not all ports measured.
			5	1.55	
			8	1.24	
			11	1.37	Some ports completely blinded over ($\lvert v_w \rvert$ = 0)
			14	1.36	
			17	1.39	
			20	1.44	
			23	1.46	
			26	1.37	Permeate returned to feed tank
			29	1.50	
			32	1.51	
--	--	3.60	2	0.410	
			5	0.466	
			8	0.267	
			11	0.358	
			14	0.341	
			17	0.349	
			20	0.339	
			23	0.343	
			26	0.294	
			29	0.325	
			32	0.301	
--	--	10.8	2	0.399	
			5	0.450	
			8	0.264	
			11	0.355	
			14	0.340	
			17	0.352	
			20	0.335	
			23	0.291	
			26	0.295	
			29	0.311	
			32	0.303	

TABLE A-21 (Continued)

PARALLEL PLATE EXPERIMENTS - PVA (7.5 pH SOLUTION)

$\Delta P = 3.45 \times 10^5$ N/m^2 $\quad \overline{R_m} = 2.45 \times 10^{11}$ 1/cm

μ Solvent $= 9.81 \times 10^{-4} \frac{\text{N-sec}}{\text{m}^2}$ $\quad$ T = 21.1°C

Axial flow rate = 0.631 liters/sec

c_o Concentration of Feed Tank (g/100 cc)	c_p (g/100 cc)	T x 10^{-3} (seconds)	Port Number	$\lvert v_w \rvert$ x 10^3 (cm/sec)	COMMENTS:
0.073	--	19.8	2	0.392	
			5	0.434	
			8	0.392	
			11	0.343	
			14	0.353	
			17	0.356	
			20	0.344	
			23	0.367	
			26	0.303	
			29	0.320	
			32	0.305	
--	--	25.2	2	0.399	
			5	0.454	
			8	0.368	
			11	0.327	
			14	0.344	
			17	0.330	
			20	0.347	
			23	0.369	
			26	0.302	
			29	0.316	
			32	0.303	

TABLE A-22

PARALLEL PLATE EXPERIMENTS - CARBOWAX 20M (7.5 pH SOLUTION)

$\Delta P = 3.45 \times 10^5$ N/m^2 $\quad \overline{R}_m = 8.11 \times 10^{10}$ 1/cm

μ Solvent $= 10.02 \times 10^{-4} \frac{\text{N-sec}}{\text{m}^2}$ $\quad T = 20°C$

Axial flow rate = 0.039 liters/sec

c_o Concentration of Feed Tank (g/100 cc)	c_p (g/100 cc)	$T \times 10^{-3}$ (seconds)	Port Number	$\lvert v_w \rvert \times 10^3$ (cm/sec)	COMMENTS:
$\approx$ 1.0	--	63.0	4	0.0797	Error in concentration determinations.
			8	0.0032	
			12	0.0447	
			16	0.0641	
			20	0.0405	Permeate returned to feed tank.
			24	0.0304	
			28	0.0313	
			32	0.0213	
$\approx$ 1.0	--	84.9	4	0.0810	
			8	0.0034	
			12	0.0455	
			16	0.0603	
			20	0.0400	
			24	0.0298	
			28	0.0309	
			32	0.0207	

TABLE A-23

PARALLEL PLATE EXPERIMENTS - CARBOWAX 20M (7.5 pH SOLUTION)

$\Delta P = 3.45 \times 10^5$ N/m^2 $\quad \overline{R}_m = 8.11 \times 10^{10}$ 1/cm

μ Solvent $= 10.02 \times 10^{-4} \frac{\text{N-sec}}{\text{m}^2}$ $\quad T = 20°C$

Axial flow rate = 0.039 liters/sec

c_o Concentration of Feed Tank (g/100 cc)	c_p (g/100 cc)	T x 10^{-3} (seconds)	Port Number	$\lvert v_w \rvert$ x 10^3 (cm/sec)	COMMENTS:
0.642	--	0.0	Not Measured		
0.636	0.081	58.1	4	0.0936	Permeate returned
			8	0.0	
			12	0.0621	
			16	0.0676	
			20	0.0497	
			24	0.0421	
			28	0.0416	
			32	0.0261	
0.659	0.079	78.0	4	0.0973	
			8	0.0	
			12	0.0640	
			16	0.0657	
			20	0.0495	
			24	0.0426	
			28	0.0408	
			32	0.0256	

TABLE A-24

PARALLEL PLATE EXPERIMENTS - CARBOWAX 20M (7.5 pH SOLUTION)

$\Delta P = 3.59 \times 10^5$ N/m^2 $\quad \overline{R}_m = 8.11 \times 10^{10}$ 1/cm

μ Solvent $= 10.02 \times 10^{-4} \frac{\text{N-sec}}{\text{m}^2}$ $\quad T = 20°C$

Axial flow rate = 0.097 liters/sec

c_o Concentration of Feed Tank (g/100 cc)	c_p (g/100 cc)	T x 10^{-3} (seconds)	Port Number	$\lvert v_w \rvert$ x 10^3 (cm/sec)	COMMENTS:
≈ 1.0	--	41.4	4	0.1070	Error in concentration determinations.
			8	0.0175	
			12	0.0557	
			16	0.0102	
			20	0.0505	Permeate returned to feed tank.
			24	0.0382	
			28	0.0383	
			32	0.0267	
≈ 1.0	--	57.6	4	0.0111	
			8	0.0201	
			12	0.0571	
			16	0.0921	
			20	0.0500	
			24	0.0380	
			28	0.0391	
			32	0.0272	

TABLE A-25

PARALLEL PLATE EXPERIMENTS - CARBOWAX 20M (7.5 pH SOLUTION)

$\Delta P = 3.45 \times 10^5$ N/m^2 $\quad \overline{R}_m = 8.11 \times 10^{10}$ 1/cm

μ Solvent $= 10.02 \times 10^{-4} \frac{\text{N-sec}}{\text{m}^2}$ $\quad$ T = 20°C

Axial flow rate = 0.097 liters/sec

c_o Concentration of Feed Tank (g/100 cc)	c_p (g/100 cc)	T x 10^{-3} (seconds)	Port Number	$\lvert v_w \rvert$ x 10^3 (cm/sec)	COMMENTS:
0.646	0.075	62.7	4	0.1250	Permeate returned to feed tank.
			8	0.0143	
			12	0.0858	
			16	0.0764	
			20	0.0612	
			24	0.0536	
			28	0.0532	
			32	0.0354	
0.633	0.073	80.1	4	0.1230	
			8	0.0235	
			12	0.0859	
			16	0.0778	
			20	0.0765	
			24	0.0539	
			28	0.0538	
			32	0.0354	

TABLE A-26

PARALLEL PLATE EXPERIMENTS - CARBOWAX 20M (7.5 pH SOLUTION)

$\Delta P = 3.45 \times 10^5$ N/m^2 $\quad \overline{R_m} = 8.11 \times 10^{10}$ 1/cm

μ Solvent $= 10.02 \times 10^{-4} \frac{\text{N-sec}}{\text{m}^2}$ $\quad T = 20°C$

Axial flow rate = 0.190 liters/sec

c_o Concentration of Feed Tank (g/100 cc)	c_p (g/100 cc)	T x 10^{-3} (seconds)	Port Number	$\lvert v_w \rvert$ x 10^3 (cm/sec)	COMMENTS:
≈ 1.0	--	0.0	4	4.59	Permeate returned to feed tank.
			8	4.44	
			12	4.21	
			16	4.64	Membrane blinded over in portions.
			20	4.16	
			24	3.84	
			28	3.91	Error in concentration determinations.
			32	4.18	
		9.6	4	0.1560	
			8	0.0470	
			12	0.1280	
			16	0.2780	
			20	0.0764	
			24	0.0554	
			28	0.0597	
			32	0.0504	
≈ 1.0		20.4	4	0.1410	
			8	0.0360	
			12	0.0655	
			16	0.2230	
			20	0.0644	
			24	0.0437	
			28	0.0481	
			32	0.0399	
≈ 1.0	--	34.8	4	0.1340	
			8	0.0358	
			12	0.0631	
			16	0.1760	
			20	0.0600	
			24	0.0394	
			28	0.0444	
			32	0.0349	

TABLE A-27

PARALLEL PLATE EXPERIMENTS - CARBOWAX 20M (7.5 pH SOLUTION)

$\Delta P = 3.45 \times 10^5$ N/m^2 $\quad \overline{R_m} = 8.11 \times 10^{10}$ 1/cm

μ Solvent $= 10.02 \times 10^{-4} \frac{\text{N-sec}}{\text{m}^2}$ $\quad T = 20°C$

Axial flow rate = 0.193 liters/sec

c_o Concentration of Feed Tank (g/100 cc)	c_p (g/100 cc)	T x 10^{-3} (seconds)	Port Number	$\lvert v_w \rvert$ x 10^3 (cm/sec)	COMMENTS:
0.651	0.080	24.3	4	0.1670	Permeate returned
			8	0.0524	to feed tank.
			12	0.1070	
			16	0.0940	
			20	0.0903	
			24	0.0645	
			28	0.0649	
			32	0.0447	
0.636	0.069	61.2	4	0.1580	
			8	0.0540	
			12	0.1060	
			16	0.0921	
			20	0.0911	
			24	0.0641	
			28	0.0645	
			32	0.0450	

APPENDIX IV

BILL OF MATERIALS

This section consists of a list of materials, or services, which were purchased during the course of the research work. The Institute of Paper Chemistry purchase order numbers are listed along with supplier names in order to facilitate the retrieval of the original information and specifications if desired.

IPC Purchase Order Number	Item	Supplier
B-00124	Porous Kynar	Glasrock-Porex Div., Fairburn, Georgia
B-00141 B-09006	Sundstrand Pump	Valley Pump, Inc. Appleton, Wisconsin
B-02245	DC Ammeter	Consumer Electronics Supply Appleton, Wisconsin
B-02478	Egg Albumin	Sigma Chemical Company, St. Louis, Missouri
B-02893	Pressure gauges - glycerine filled	I. Bahcall, Inc., Appleton, Wisconsin
B-03164 B-05395	Backpressure valve	Reetz Engineering, Inc., Appleton, Wisconsin
B-03610	Carbowax 20M	Union Carbide, Chicago, Illinois
B-05701	Bovine Serum Albumin Fraction 5	Sigma Chemical Company, St. Louis, Missouri
B-07584	HFM-180 Membrane	Abcor, Inc., Wilmington, Massachusetts
B-08201 B-08942	Polyvinyl Alcohol	Aldrich Chemical Co., Milwaukee, Wisconsin
A-10599	Turbine Flowmeters	Fischer & Porter Co., Appleton Wisconsin

Miscellaneous Materials

IPC Purchase Order Number	Item	Supplier
B-02403 B-02599 B-02631 B-03165 B-03364 B-03739 B-04762 B-05493 B-06521	PVC, Plexiglas, Fittings	Eagle Supply & Plastic Appleton, Wisconsin
B-02694 B-02845	Stainless Steel Tubing, Pipe, & Fittings	I. Bahcall, Inc. Appleton, Wisconsin
B-02846 B-03633	Stainless Steel Tubing, Pipe, & Fittings	Schlaefer Supply Co. Appleton, Wisconsin
B-03087	Tube Fittings	Badger Valve & Tube Corp. Wauwatosa, Wisconsin
B-03166	Tube Fittings	W. S. Patterson Co. Appleton, Wisconsin
B-03170 B-05173	Tube Fittings	Kundinger Fluid Power, Inc. Appleton, Wisconsin
B-02900 B-09183	Rubber goods Gaskets, O-rings	C. B. Supply Co. Menasha, Wisconsin
B-02954 B-03066 B-03586	Rubber goods, Gaskets, O-rings	Appleton Packing & Gasket Company Appleton, Wisconsin
B-03330 B-04470	Rubber goods, Gaskets, O-rings	Accurate Gasket & Supply Appleton, Wisconsin
B-03777	Machine work	Van Ryzin Machine Co. Appleton, Wisconsin
A-10820	Machine work	Fox River Tool Co. Menasha, Wisconsin